Morphogenesis of Reovirus as Defined by the Fields Panel of Temperature Sensitive Mutants

By

Paul Russell Hazelton

A Thesis

Submitted to the Faculty of Graduate Studies

University of Manitoba

in Partial Fulfillment of the Requirements

for the Degree of

Doctor of Philosophy

Department of Medical Microbiology and Infectious Diseases

University of Manitoba

Winnipeg, Manitoba, Canada

THE UNIVERSITY OF MANITOBA

FACULTY OF GRADUATE STUDIES

*****

COPYRIGHT PERMISSION PAGE

MORPHOGENESIS OF REOVIRUS AS DEFINED BY THE FIELDS PANEL OF TEMPERATURE SENSITIVE MUTANTS

BY

PAUL RUSSELL HAZELTON

A Thesis/Practicum submitted to the Faculty of Graduate Studies of The University of Manitoba in partial fulfillment of the requirements of the degree of

DOCTOR OF PHILOSOPHY

Acknowledgments

The longest journey begins with the first step. Upon looking back from this nexus of the path it is an honour to note the quality of those who have walked with me: Charles Kuhn III, who introduced me to research and the first love of my professional life, the electron microscope; Bill Davidson and Ian Innes, who kept me in the field of E.M.; Charlie Hannan, who introduced me to virology, the second great love of my research life; Greg Hammond, who gave me the chance to meld those two loves and who often gave me enough rope, just to see if I would hang myself; Allan Ronald, who somehow saw promise in what I did; Gordon Wiseman, who supported my return to school; and Magdy Dawood, who counselled me and then let me when I needed an advisor. Thanks to the office staff: Donna Dorward, Robyn Scott, Carol Sigurdson, Sharon Tardi; and technicians: Joanna Brunka, Gloria Grey, Zeena Mohammed, John Rutherford, Madame Shen, Leslie Slaney, and Barb Urias. Many of my fellow students provided invaluable advice and discussions, particularly Blake Ball, Joe Fan, Karl Fischer, Keith Fowke, Trevor Fyduk,, Karam Ramotar, Dwayne Stupak, Graham Tipples and Guangming Zong. The fellowship of the structural virology group, including Lydia Cox, Natalie Kierstead, and Peng Yin, and of the Virus Detection Unit, Cadham Provincial Laboratory, particularly Paulette Carriere, Richard Drummond, Brian Klisko, Doug Milley, and Barb Wells, was much welcomed in times of good, and of trouble.

Special thanks must be given to my committee for their advice, counsel, and questions; Grant McClarty, Avi Nath, Max Nibert, and Fritz Stevens.

One student must stand separate as my partner in intellectual crime. Thank you Jody Berry, and Tracy, Jordan, and Erin Berry.

Without the active support of my Department Chairman, Dr. Robert C. Brunham, and Administrative Assistant, Theresa Birkholz, the whole dream of returning to school would have been just a dream. Thank you both for all the grief you have put up with from me, and the rest of us, as you have guided the Department through these years of my studies. And thank you Bob for hiring Kevin.

A successful program requires a good mentor. Not many students are also fortunate to have an advisor whom they would have also chosen as their brother if they could. Thank you Kevin Coombs, head of the Structural Virology group, for your time and support.

Dedication

I would like to thank, and dedicate this thesis to the three who have supported me unconditionally through all of this work. Through the good and bad, you have never failed to give me reason to follow the dream, and in spite of our darkest fears, you were all there at the end. Thank you Valerie, Melissa (the Magnificient) and Robert (the Great).

ABSTRACT

The use of amber mutations of bacteriophage have allowed complicated pathways of assembly to be dissected for bacteriophage systems. However, viral assembly continues to be poorly understood with the eucaryotic viruses. Because of the value of amber mutations with bacteriophage the current studies into the assembly pathways of reovirus were initiated using the Fields panel of temperature sensitive *ts* mutants of reovirus.

One problem with investigations involving the Fields panel was the inability to clearly identify the *ts* phenotype in some clones. Increasing restrictive temperature by 0.5 to 1.0 °C effected additional reductions in the titre of infectious progeny obtained at restrictive temperatures, reducing the ratio of infectious progeny between permissive and restrictive cultures by up to three orders of magnitude. Using this data it was possible to clearly identify the *ts* phenotype in a number of clones which were refractive to earlier study. The prototype clones for recombination groups E and I were evaluated. In addition to clearly associating the *ts* lesion to the appropriate gene segment it was possible to confirm that neither clone was able to establish a productive infection at restrictive temperatures. Neither *tsE320*, nor *tsI138* produced dsRNA at restrictive temperature. Further, the clone *tsI138* was identified as having a slow growth phenotype, consistently producing reduced levels of dsRNA and titres of infectious progeny at permissive temperatures than the wild type parent and other mutant clones. Ultrastructural investigations with this clone indicated that the viral inclusions at permissive temperatures were rare and disorganized.

Ts mutations were identified on two separate gene segments with the clone *tsA279*. The M2 gene segment, which encodes the major outer capsid protein $\mu 1$, was associated with a blockade in transmembrane transport of restrictively assembled virions. Four point mutations were identified in the genetic sequence for this segment, each effecting a change in the primary structure of the encoded protein. Two mutations, in proximity with each other, changed prolines to serenes at amino acid residues 306 and 315, and disrupted predicted secondary structure in amphipathic regions by changing proposed α-helices to β-sheets. The other two mutations were also in proximity with each other, effecting primary structure changes from proline to threonine and glutamate to lysine at residues 673 and 687, respectively. These mutations affected predicted positive charge in ϕ, the carboxy terminus proteolytic fragment of $\mu 1$, and may affect the ability of the fragment to interact with host membranes during transmembrane transport.

The second lesion, in the L2 gene segment, was associated with the production of a primary core particle. This core particle was defective for both minor proteins $\mu 2$ and $\lambda 2$. This is the first report of a primary core particle comprised of the core proteins $\lambda 1$, $\lambda 3$, and $\sigma 2$. The existence of this primary core particle has profound implications concerning the assembly processes of reovirus.

Table of Contents

LIST OF ABBREVIATIONS

BSA	bovine serum albumin
cDNA	copy deoxyribonucleic acid
CPE	cytopathic effect
(d)ATP	(deoxy) Adenosine triphosphate
(d)CTP	(deoxy) Cytosine triphosphate
(d)GTP	(deoxy) Guanosine triphosphate
dITP	deoxyInosine triphosphate
(d)TTP	(deoxy) Thymidine triphosphate
DNA	deoxyribonucleic acid
ds	double stranded
EDTA	Ethylenediamine tetraacetic acid
EOP	efficiency of plating
FCS	fetal calf serum
HEPES	N-2-hydroxyethylpiperizine-N-2-ethanesulfonic Acid
IEM	immunoelectron microscopy
IF	immunofluorescent
Ifn	Interferon
IgG	Immunoglobulin fraction G
ISVP	Intermediate subviral particle
mA	milliAmps
MOI	multiplicity of infection
mRNA	messenger RNA
nm	nanometer
NS-TEM	negative stain transmission electron microscopy
ORF	open reading frame
P(x)	Passage (x = passage number)
PBS	phosphate buffered saline
PCR	polymerase chain reaction
PFU	plaque forming units per milliliter
PMSF	Phenylmethylsufonyl Fluoride
PTA	phosphotungstic acid
RDRP	RNA dependent RNA polymerase
RN ase	ribonucleic acid nuclease
RNA	ribonucleic acid
Rnasin	inhibitor of RNase
RT	reverse transcription/ase
S-MEM	Joklik's modified minimum essential medium
SDS-PAGE	sodium dodecyl sulfate-polyacrylamide gel electrophoresis
ss	single stranded
T1L	reovirus Type 1, Lang
T2J	reovirus Type 2, Jones
T3A	reovirus Type 3, Abney
T3D	reovirus Type 3, Dearing
TGU	Tris:Glycine:Urea polyacrylamide gel electrophoresis
TLCK	N-α-p-Tosyl-L-Lysine Chloromethyl Ketone
ts	temperature sensitive
ts^+	non temperature sensitive phenotype
VSP	agammaglobulin-neonate bovine serum VSP

List of Figures

List of Tables

CHAPTER 1

Introduction

1. Introduction.

Viruses exist in two stages, a vegetative and an inanimate stage. During the vegetative stage the virus resides inside a host cell as an obligate parasite, utilizing a combination of host and viral encoded biochemical systems to achieve the goal of reproduction and continuation of the species. In order to survive between replicative cycles the virus must build a package to carry its reproductive information. This package must be able to resist the environment into which the virus will be released. It must also carry the signals necessary for recognition and interaction with target host cells which will be conducive to future growth (Harrison *et al*, 1996; Nibert *et al*, 1991a).

Since the development of negative stain transmission electron microscopy (NS-TEM) (Brenner and Horne, 1959) structural virologists have benefitted from an expanding repertoire of methods to identify and characterize viral structures. X-ray crystallography has allowed the macromolecular resolution of virions such a poliovirus (Hogle *et al.* 1985) and rhinovirus 14 (Rossmann *et al*, 1985). More recently component structures such as the highly immunogenic G-H loop of foot and mouth disease capsid protein VP1 (de Prat-Gay, 1997) and the hemagglutinin of influenza virus expressed in *Escherichia coli* (Hoffman *et al*, 1997) have been the target of high resolution studies. Electron cryomicroscopy has utilized image averaging and multiple images of virions in different

focal planes to provide three dimensional imaging of sindbis virus (Paredes *et al*, 1993) rotavirus (Prasad *et al*, 1996) and aquareovirus (Shaw *et al*, 1996), subviral particles of reovirus (Dryden *et al*, 1993), reassortant rotavirus clones (Shaw *et al*, 1993) and capsids assembled from expressed bluetongue capsid proteins (Hewat *et al*, 1992). More recent electron cryomicroscopy studies have utilized proteolytically degraded reovirus intermediate structures (Luongo *et al.* 1997), expressed rotavirus capsid protein VP2 which was engineered to delete the amino terminus of the protein (Lawton *et al.* 1997), and rotavirus and reovirus virions undergoing *in vitro* transcription (Lawton *et al.* 1997; Yeager *et al*, 1996; Yeager *et al*, in submission) to provide additional structural information. Low temperature, high resolution scanning electron microscopy has also been utilized to visualize reovirus particles (Centonze *et al*, 1995), and atomic force microscopy has been used to visualize double stranded RNA of reovirus (Lyubchenko, *et al*, 1992a, Lyubchenko *et al*, 1992b). These studies allow the visualization of complete structures and some assembly and disassembly intermediate structures, permit the localization of some proteins, and may even identify the regions of interaction between some proteins (Luongo *et al.* 1997) and nucleic acids, (Prasad *et al*, 1996). However, they do not elaborate the temporal pathways and spatial patterns by which viral proteins interact in an additive fashion to assemble the packing crate needed to carry the genomic cargo to its next address through a hostile environment.

Viral assembly is an important late step in replication that is poorly understood in animal viruses. The size and shape of the package which must carry the genome between

replicative cycles is determined by mechanisms involved in assembly, viral release, extracellular transport, attachment, penetration and uncoating (Harrison *et al*, 1996). The assembly pathways of bacteriophage have been studied in detail using conditionally lethal amber mutations of bacteriophage T4 (Berget and King, 1983; Black and Showe, 1983; Wood and Crowther, 1983) and P22 (Prevelige and King, 1993). However, the many different strategies for biochemical regulation and interaction with host cells, genome organization, and assembly and structural designs employed by the eucaryotic viruses have mitigated against similar success in virus:eucaryote systems. These studies are directed toward further elaboration upon the process of viral morphogenesis using reovirus, a small, double shelled agent of intermediate complexity.

2. Reoviruses.

The *Reoviridae* are comprised of seven genera. Three genera (cypovirus, fijivirus, and phytoreovirus) are agents which infect plants and insects. Two genera (coltivirus and orbivirus) infect animals with an insect vector. The remaining genera (reovirus, and rotavirus) contain species which infect animals (Francki *et al*, 1991; Joklik, 1983; Matthews, 1982; Monath and Guirakhoo, 1996). ECHO 10, the original reovirus clone was isolated from stool swabs from a healthy child (Ramos-Alverez *et al*. 1954). In recognition that there had been no pathological syndrome associated with the virus the agent was subsequently redesignated reovirus for Respiratory, Enteric, Orphan virus (Sabin, 1959). Three major serotypes were subsequently isolated from human sources, and prototype clones established: serotypes T1, Lang (T1L) (the original ECHO 10); T2,

Jones (T2J); and T3 Abney (T3A). Another isolate of T3, the Dearing isolate, has also been utilized extensively as a prototype (Sabin, 1959). In addition to the human isolates, a simian source agent was identified from pooled monkey kidney cells (SV12, Hull *et al*, 1956) and from a monkey sick with respiratory illness (SV59, Hull et al, 1958). These isolates were subsequently identified as being T1L and T2J, respectively (Sabin, 1959).

A number of clinical conditions have been associated with reovirus infection. T1L has been associated with viral meningitis in humans (Johansson *et al*, 1996), and acute myocarditis in mice, (Sherry and Blum, 1994, Sherry *et al*, 1996), while T3D has been associated with biliary atresia in mice (Wilson *et al*, 1994) and acute pneumonia (Morin *et al*, 1996). Conversely, probes to the reovirus T3D M3 gene segment identified this agent in only one biopsy from 34 cases of either ideopathic neonatal hepatitis or biliary atresia in infants following reverse transcriptase/polymerase chain reaction amplification, with agarose gel separation and Southern probing (Steele *et al*, 1995). This study suggests reovirus does not play a strong role in human neonatal cholestatic liver disease.

a. <u>Virus structure.</u>

The reovirus virion is a non enveloped double shelled protein structure with a diameter of approximately 85nm (Dryden *et al*, 1993). Controlled degradation studies utilizing proteolytic digestion of the whole particle, heating, or high pH suggest that the virion has at least two intermediate structures (Nibert *et al*. 1996a) (Figure 1.1, Table 1.1). Studies utilizing expressed viral proteins (Xu *et al*, 1993), or digestion after high heat suggest

Figure 1.1 <u>The structure, genome and proteins of reovirus.</u>

A. Polyacrylamide gel electrophoresis of Reovirus Type 1 Lang (V), the Intermediate SubViral Particle (ISVP), and Core Particle (C). The viral genome is shown in the top part of the gel with the three L segments and segments S3 and S4 not separated. The structural proteins present in each structure are resolved in the bottom half of the gel. B. Negative stain electron microscopic preparations of the virion and sub viral particles. C. Cryoelectron microscopic reconstruction of the virion and sub viral particles. D. Cartoon illustrating the proposed location of viral structural proteins and size of the virion. The illustration is provided courtesy of Dr. K.M. Coombs and adapted with addition of panel C, courtesy of Dr. K. Dryden.

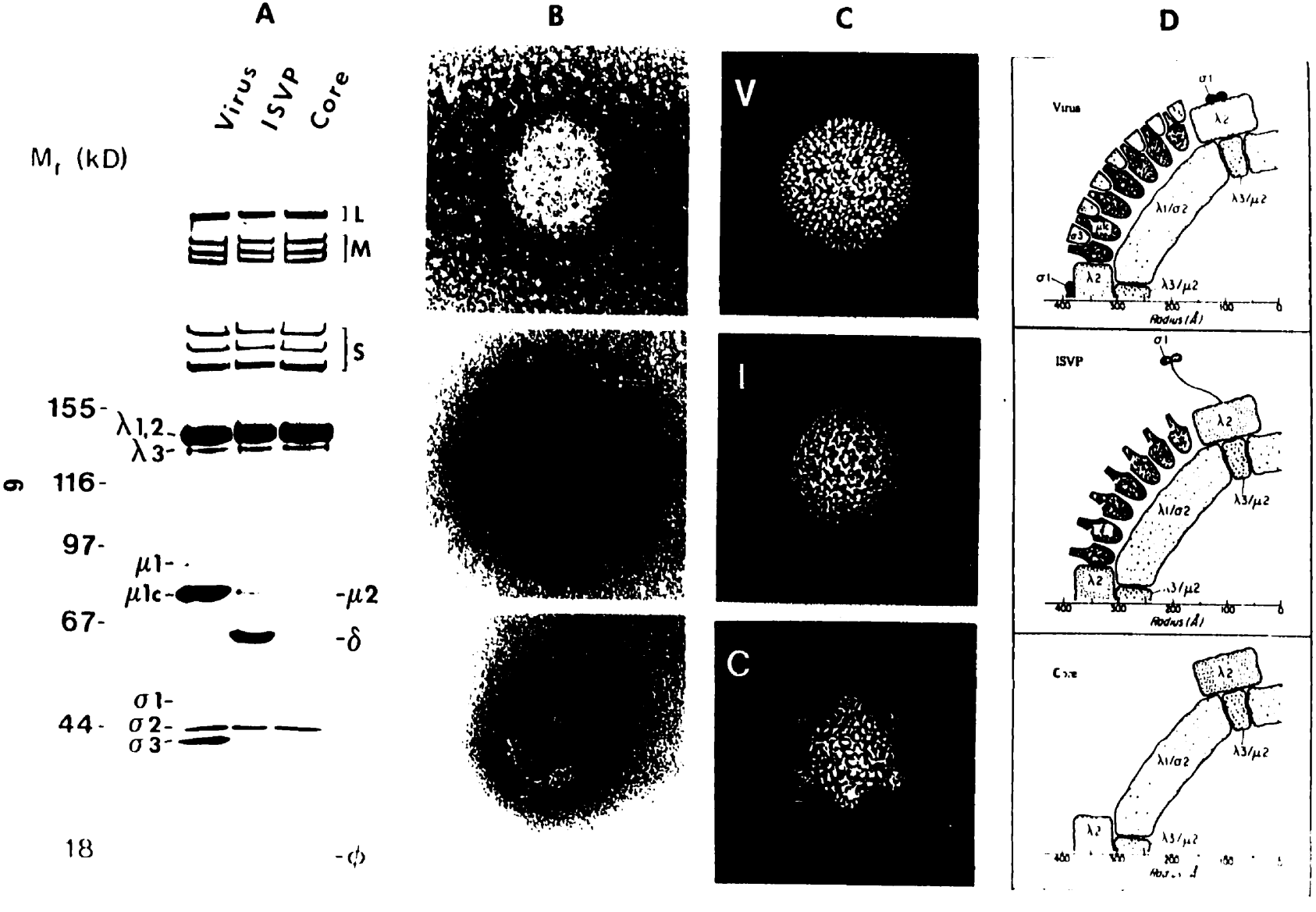
A
B
C
D
Virus
ISVP
Core
M_r (kD)
L
M
S
155-
λ1,2-
λ3-
116-
97-
μ1-
μ1c-
-μ2
67-
-δ
σ1-
44-
σ2-
σ3-
18
-ϕ
V
I
C
Virus
ISVP
Core
σ1
λ2
λ1/σ2
λ3/μ2
σ3
μ2
400
300
200
100
0
Radius (Å)

Table 1.1 **Characteristics of reovirus complete and intermediate particles[a,b]**

Property	Complete Core	ISVP	Virion
Bouyant Density (g/cm^3)	1.43	1.38	1.36
Sedimentation Value (S_{20w})	470	630	730
Diameter (nm)			
NS-TEM	50	65	75
Electron Cryomicroscopy	60	80	85
Outer Capsid Proteins			
λ2	+	+	+
μ1/1c	-	+	+
μ1δ/δ	-	ND	+
φ	-	ND	+
σ1	-	+	+
σ3	-	+	+
Core Capsid Proteins			
λ1	+	+	+
λ3	-*	-*	+
μ2	+	+	+
σ2	+	+	+
Genome			
ssRNA	-	-	-
dsRNA	+	+	+
Infective	No	ND	Yes
Transcription Activity	Yes	Partial§	Partial

a. Adapted from Nibert *et al*, 1996b.
b. Please see text for references
* Not resolved in gel system
§ Initiation and Capping but no elongation

ND Not Done
\+ Present
\- Not Present

that there may be a third dissassembly structure which is similar to the core particle but lacks the minor protein λ2 (White and Zweerink, 1976; Yin *et al.* In submission). The genome is comprised of ten segments of double stranded RNA (Shatkin *et al*, 1968). Most gene segments are monocistronic, with at least one being bicistronic. Please see chapter 1, section 2.c, below, for further information about the genome.

(1.) Core particle

Stoichiometric analysis indicates that the complete core contains 120 copies of both major core proteins, λ1 and σ2 (Coombs *et al*, 1990; Coombs, 1998a), and 12 copies of the minor core protein λ3 (Coombs, 1998a; Dryden *et al*, 1993). In addition, the complete core contains 60 copies of the minor protein λ2 and 21 copies of the minor protein μ2 (Coombs, 1998a). The particle has a buoyant density of 1.43 g/cm^3 in cesium chloride and sedimentation value of $470S_{20w}$ (Joklik, 1983). There is no discernable triangulation lattice structure (Klug and Caspar, 1960; Metcalf et al, 1991). The protein λ2 forms a pentameric spike with a diameter of 18nm, which extends outward from the core for approximately 9nm. The spikes are located at the 12 apical vertices of the core (Dryden *et al*, 1993; Nibert *et al*. 1996b). Electron cryomicroscopic evaluation indicates that the λ2 pentamer also has a central channel of approximately 8.4nm in core particles created *in vitro* (Dryden *et al*, 1993; Yeager *et al*, in preparation) as does low temperature, high resolution scanning electron microscopy (Centonze *et al*, 1995). The core has been identified as the transcriptionally active structure, producing progeny mRNA from the genomic dsRNA (Chang and Zweerink, 1971)(Table 1.1)

(a.) λ1.

The major core protein λ1 is 1233 amino acids long and has a molecular mass of 137.4 kDa for the prototype clone T3D (Bartlett and Joklik, 1988). It is encoded by the gene segment L3 (Ramig *et al*, 1983). The gene segment is 3896 nucleotides in length and contains one translated open reading frame (ORF) of 3699 nucleotides, extending from base 14 through base 3715, and leaving 5' and 3' untranslated regions of 13 and 181 bases, respectively. There are an additional 3 possible ORFs coding for products of 75 amino acids or more. However, there is no evidence that any of these other ORFs are translated (Table 1.2). The protein is slightly acidic and has a predicted alpha-helical content of approximately 24%. The amino terminus is very hydrophilic (Bartlett and Joklik, 1988). Because λ1 can be radio-iodinated in assembled core structures it is hypothesized to reside at least partially on the outer surface of the core (White and Zweerink, 1976). The protein contains a nucleotide binding motif starting at residue 8, and a zinc finger motif starting at residue 194 (Schiff *et al*, 1988; Bartlett and Joklik, 1988). The actual binding of dsRNA has been localized to the site at the amino terminus (Lemay and Danis, 1994). There is latent ATPase activity associated with this protein which is activated with the proteolytic processing associated with penetration and uncoating (Noble and Nibert, 1997a). It has been proposed as the catalytic site of transcription (Morgan and Kingsbury, 1981). While expressed λ1 is incapable of self assembly, the protein can form a core like particle when co-expressed with the other major core protein, σ2 (Xu *et al*, 1993).

Table 1.2 **The gene segments and proteins of reovirus T3D[a]**

Gene Segment	Segment Size (bp)	NTR 5'	NTR 3'	ORF	Protein	Amino Acid Residues	Size (kDa)	Copies per Virion
L1	3854	18	35	3801	λ3	1267	142	12
L2	3916	13	36	3870	λ2	1290	145	60
L3	3896	13	184	3699	λ1	1233	137	120
M1	2304	13	83	2208	μ2	736	83	21
M2	2203	29	50	2124	μ1	708	76	600
M3	2235	18	60	2157	μns	719	80	0
S1	1416	12	39	1365	σ1	455	49	36
		75	435	360	σ1S	120	14	0
S2	1331	18	59	1254	σ2	418	47	120
S3	1198	27	73	1098	σNS	366	41	0
S4	1196	32	69	1095	σ4	365	41	600

a. Please see text for references.

(b.) σ2.

The major core protein σ2 consists of 418 amino acids and has a molecular mass of 47 kDa (Dermody *et al*, 1991; George *et al*, 1987). It is encoded by the S2 gene segment (Ramig *et al*, 1978). The gene segment, which is highly conserved across all three serotypes of reovirus, is 1329-1331 nucleotides in length (Cashdollar *et al*, 1982; Weiner *et al*, 1989; Dermody *et al*, 1991), with one translated ORF extending from base 19 through base 1275, leaving untranslated regions of approximately 18 and 57 nucleotides at the 5' and 3' ends, respectively (Dermody *et al*, 1991). There is no evidence that the two additional ORFs coding potential polypeptides of 75 or more residues are translated (Table 1.2). Sequence analysis suggests two domains, an amino terminal domain spanning three-quarters of the protein, and a hydrophilic carboxy terminus. A 21 residue sequence starting at amino acid 354 has strong similarity to portions of the β subunit for the DNA-dependent RNA polymerase of *Escherichia coli* (Dermody *et al*, 1991). In view of its resistance to radio-iodination in core structures it has been proposed that σ2 resides on the inner face of the core (White and Zweerink, 1976). The protein has been associated with binding dsRNA (Schiff *et al*, 1988). The protein is incapable of assembly into recognizable structures when expressed alone, but will form a core like particle when co-expressed with λ1 (Xu *et al.* 1993).

(c.) λ2.

The λ2 protein is encoded by the single large ORF (Seliger *et al*, 1987) in the gene segment L2 (Mustoe *et al*, 1978). The gene segment is 3916 bases long and contains one

translated ORF 3867 nucleotides in length, encoding 1289 amino acids (Seliger *et al*, 1987). Analysis with Lasergene's EditSeq program (DNAStar, Madison, WI) provides for a predicted molecular mass of 144 kDa (Table 1.2). There is no evidence for translation of the remaining four ORFs which encode polypeptides 70 or more residues long. λ2 was identified as the protein which formed the distinctive core spike by partial disassembly of core particles using high pH (White and Zweerink, 1976). Subsequently, cross linking studies indicated that the spike is a homopentamer (Ralph *et al*, 1980). Antibodies to the λ2 protein react with whole virions and cores (Tyler *et al*, 1993). This, plus the extensive interactions observed between the pentameric spike and the outer shell proteins of the whole virion (Dryden *et al*, 1993) has raised question whether the λ2 pentameric spike protein is, in fact, a core or outer shell protein (Nibert *et al*, 1996b). It has been associated with guanylyltransferase activity (Cleveland *et al*, 1986) and predictive analysis of the sequence suggests methyl transferase activity (Koonin, 1993; Seliger *et al*, 1987). Studies utilizing expressed λ2 proteins indicate that the protein binds GTP in the region localized to the lysine located at amino acid residue 226 (Fausnaugh and Shatkin, 1990). When expressed alone, the λ2 protein does not multimerize (Mao and Joklik, 1991). When co-expressed with the other core proteins λ2 does form multimers which associate with those other core proteins to form core like structures (Xu *et al*, 1993). These studies indicate that λ2 requires the presence of other core proteins to form multimers. Monomeric λ2 can mediate guanine transfer from GTP to 5'pp terminated RNA, producing the GpppG cap structure found with mRNAs. In monomeric form the protein does not synthesize the 5'pp terminated substrate needed to

make the cap structure, nor does it demonstrate methyl transferase activity, suggesting that these properties are the function of either the multimeric λ2 pentamer or some other proteins in the transcription complex (Mao and Joklik, 1991). Finally, studies involving cores from T1L x T3D reassortant clones have associated the L2 gene segment with the ability of T3D cores to form crystals (Coombs *et al*, 1990).

(d.) λ3.

The genetic sequence for the minor core protein λ3 resides on the L1 gene segment (Ramig *et al.* 1978). The gene segment is 3854 nucleotides in length, with one large translated ORF extending from bases 25 through 3828, and coding for a protein of 1267 amino acids with a predicted molecular mass of 142kDa. The sequences of the three serotypic prototypes are highly conserved (98.3% identity between T1L and T3D at the amino acid level) (Wiener and Joklik, 1989). There is no evidence that the other two ORFs coding polypeptides of 75 or more amino acids are translated (Table 1.2). The L1 gene segment has been associated with determination of the pH optimum for transcriptase activity (Drayna and Fields, 1982a). Transcriptionally, the L1 and M1 gene segments have been co-associated with the total amount of transcript made during *in vitro* transcription assay (Yin *et al*, 1996). The expressed protein has specific poly G polymerase activity but does not transcribe dsRNA to ssRNA, nor mRNA to negative sense ssRNA (Starnes and Joklik, 1993). Antibodies to λ3 show that the protein is located in the host cell viral inclusions and is stable in the cytosol of the host cell. During denaturing with urea the protein remains associated with the core even after loss

of the genome and is only removed with the total denaturation of the core particle (Cashdollar, 1994). It has been hypothesized that the protein resides at the base of the λ2 spike and acts as the catalytic site for viral transcriptase activity in conjunction with the λ2 spike (Morgan and Kingsbury, 1981). This proposal is supported by the finding that antibodies to λ3 do not co-precipitate assembled structures nor radio-iodinated surface proteins, suggesting that the protein is located in the inner primary core (Cashdollar, 1994). Sequence analysis has suggested that λ3 has motifs similar to those in the RNA dependent RNA polymerases (RDRP) of other RNA viruses, and is a major component of the reovirus transcriptase complex (Bruen, 1991; Morozov, 1989).

(e.) <u>μ2.</u>

The minor protein μ2 has a molecular mass of 83 kDa. The protein is encoded in the 2304 nucleotide long (Weiner *et al*, 1989) M1 gene segment (Ramig *et al*, 1983) (Table 1.2). There is a long ORF of 2208 nucleotides from base 14 to 2221 which was proposed to encode the μ2 protein (Wiener *et al*, 1989). Later studies suggested that the protein was, in fact, the product of an initiation sequence 147 bases further down stream which is in weak Kozak sequence context (Roner *et al*, 1993). Subsequent work using expressed protein and deletion mutants have confirmed that the sequence is initiated from the first AUG, which is in strong Kozak context (Zou and Brown, 1996a). Sequence analysis indicates that μ2 has a higher α-helical content (36%) than the other inner capsid proteins. Studies involving high passage deletion mutants of M1 indicate that the signal for packaging resides in either the first 135 and/or the last 185 nucleotides of this gene

segment (Zou and Brown, 1992). The gene segment has been associated with the temperature optimum of transcription during *in vitro* assay and co-associated with the L1 gene segment for controlling the total production of transcript produced *in vitro* (Yin *et al*, 1996). Mapping core protein ATPase activity indicates that μ2 and λ1 interact collaterally (Noble and Nibert 1997b). Studies involving the temperature-sensitive mutant *tsH11.2* suggest that the protein μ2 has a role in the viral dsRNA and protein production, without affecting viral ssRNA production (Coombs, 1996). A stably transfected cell line expressing the μ2 protein is able to complement the *ts* mutant during culture at restrictive temperatures (Zou and Brown, 1996b). The protein has been hypothesized to determine tropism for cultured mouse heart and bovine aortic endothelial cells (Matoba *et al*, 1991; Matoba *et al*, 1993). Because the S1 gene segment is also associated with dsRNA production, it has been hypothesized that the actual cause of acute myocarditis associated with reovirus is due to Interferon (Ifn) induction by dsRNA rather than progeny virion synthesis (Sherry *et al*, 1996).

(2.) Intermediate Subviral Particle.

The intermediate, or infectious subviral particle (ISVP) (Figure 1.1, Table 1.1) is the infectious form of the virion which may be transported directly across the target cell cytoplasmic membrane. It is found naturally after passage through the upper gastrointestinal tract of host animals (Amerongen *et al*, 1994; Bass *et al*, 1990; Bodkin *et al*, 1989), and in target cells after attachment and uptake of whole virions (Borsa *et al*, 1979; Borsa *et al*, 1981; Chang and Zweerink, 1971). This intermediate may also

be manufactured *in vitro* by limited proteolytic digestion of whole virions. (Shatkin and LaFiandra, 1972; Spendlove *et al*, 1965). The inhibition of infection by treatment with anisotropic agents in mice intestines (Bass *et al*, 1990) and cell cultures (Canning and Fields, 1983), and by the lysosomal protease inhibitor E64 in cultured cells (Baer and Dermody, 1997) provides further evidence that this particle is the infectious form which transports across the cellular membrane. The ISVP contains 600 copies of the outer capsid protein μ1 (Dryden *et al*, 1993, Coombs, 1998a). However, this protein is cleaved into the large, amino terminal fragment δ/δ1c and the small carboxy terminal fragment ϕ (Nibert *et al*, 1991b). μ1 was originally reported to be present as di-sulfide linked dimers (Huismans and Joklik, 1976; Smith *et al*, 1969). More recent electron cryomicroscopy studies suggest that the protein actually exists as trimers in the outer capsid (Dryden *et al*, 1993). There are variable reports concerning the presence of the attachment protein σ1 in the ISVP. Stoichiometric studies indicate that σ1 exists as 12 homotrimers in the ISVP (Leone *et al*, 1992; Strong *et al*, 1991). ISVPs manufactured from T1L show the presence of σ1 as an extended fibre (Furlong *et al*, 1988; Nibert *et al*, 1991a). Serotype T3D σ1 trimers may be proteolytically digested while those from T1L may not be (Yeung *et al*, 1989). The carboxy terminus, which contains a domain for attachment to sialic acid residues (Yeung *et al*, 1989) is lost from the virion when conversion to the ISVP intermediate occurs (Nibert *et al*, 1995). The ISVP has a buoyant density of 1.38g/cm^3 in cesium chloride and has a sedimentation value of $630S_{20w}$ (Joklik, 1983).

(a.) <u>σ1.</u>

σ1 contains the primary epitopes which determine the serotype-specific humoral response (Weiner and Fields, 1977). Therefore, it should not be surprising that the S1 gene segment, which encodes this protein (Ramig *et al*, 1983) demonstrates the greatest degree of diversity in gene segment size, ORF, and protein encoded. The largest species is found with the T1L serotype, with a total size of 1462-3 nucleotides in length (Duncan *et al*, 1990: Munemitsu *et al*, 1986), has an open reading frame of 1410 bases which encodes a protein which is 470 amino acids long. The S1 gene segment for T2J is 1440 bases long and encodes a protein which is 462 amino acids long in an ORF of 1386 nucleotides (Duncan *et al*, 1990). In contrast, the S1 gene segment for T3D is 1416 nucleotides long and encodes a protein of 455 amino acids in an ORF extending from nucleotide 13 through 1380 (Bassel-Duby *et al*, 1985). The protein has a molecular mass of 49 to 51kDa (Leone *et al*, 1991b; Turner *et al*, 1992)(Table 1.2). The three S1 gene segments have diverged extensively at all three codon positions, but still encode proteins which have functionally retained function, shape and configuration (Duncan *et al*, 1990). There are two domains in the protein, a coiled coil structure at the amino terminus and a hydrophobic carboxy terminus which folds into a globular head domain (Bassel-Duby *et al*, 1985). Studies with monoclonal antibodies suggested that the protein was associated with the apical vertices of the outer capsid (Hayes *et al*, 1981; Lee *et al*, 1981). Mortality studies utilizing monoclonal antibodies and severe, combined immunodeficient (SCID) mice further indicate that the protein resides in an apical complex comprised of σ2, λ2, μ2, and λ3 (Haller *et al.* 1995). Because the location of

λ2 is unequivocally associated with the apices (Dryden *et al*, 1993; Furlong *et al*, 1988), the association of σ1 with the λ2 protein spike secures its location at the apices of the outer capsid.

The σ1 amino terminus domain contains a series of heptad repeats, which suggests coiled- coil structures (Bassal-Duby *et al*, 1985), interspersed with β-sheets (Nibert *et al*, 1990). Trimerization is a two part process (Lee and Leone, 1994). Trimerization of the amino terminal domains occurs cotranslationally through an ATP independent mechanism (Gilmore *et al*, 1996) and adds stability to the attachment fibre (Leone *et al*, 1991b). This domain contains an anchoring sequence of 32 amino acids commencing at residue 3, which interacts with the λ2 pentameric spike (Leone *et al*, 1991c). Protease digestion studies suggest that interaction with the T3D outer capsid is in a 24kDa carboxy terminal segment of λ2 (Luongo *et al*, 1997). The capability of reovirus to hemagglutinate red blood cells has been associated with interactions between σ1 and sialic acid residues on the extracellular domain of cellular plasmalemma proteins (Gentsch and Pacitti, 1985; Gentsch and Pacitti, 1987; Weiner *et al*, 1978). Proteolytic cleavage of the T3D σ1 trimer reduces infectivity by this serotype by 10 fold. However, infection of target cells is still possible due to interactions with the retained amino terminus trimer and sialic acid residues on host ectodomain proteins (Nibert *et al*, 1995). Studies with revertants of mutant clones of T3D which recover the ability to bind sialic acid residues indicate that the β-sheet segments of the coiled coil structure of the amino terminus further mediate interaction with target cells (Chappell *et al*, 1997).

The carboxy terminus domain trimerizes post translationally in an energy dependent fashion, requiring ATP. In addition, the chaperone heat shock protein HSP70 has been associated with the trimerization of the globular head for the attachment fibre (Leone *et al*, 1996). Proteolytic digestion studies and studies on expressed deletion mutants indicate that this domain is protease resistant, and that the intact amino acid sequence is required for proper head folding and formation of the cell binding domains in the globular head region (Duncan *et al*, 1991; Leone *et al*, 1991a).

Tropism to a large variety of cells and tissues has been associated with the S1 gene segment (Bodkin *et al*, 1989; Tyler *et al*, 1986; Wilson *et al*, 1994; Wilson *et al*, 1996), and with induction of apoptosis in cell cultures by the T3D serotype (Rodgers *et al*, 1997; Tyler *et al*, 1995). The role σ1 plays in attachment (Lee *et al*, 1981; Turner *et al*, 1992) may relate to the association of S1 as a determinant of tropism and apoptosis. The S1 gene segment has also been associated with an inhibition of host cell DNA synthesis (Sharpe and Fields, 1981).

(b.) μ1.

The major outer capsid protein μ1 is encoded by the genome segment M2 (Mustoe *et al*, 1978). Prototype clones of all three serotypes have segments with the identical length of 2203 bases (Table 1.2). There is one long ORF starting at nucleotide 30 and continuing to base 2156. There is no evidence for translation of the two other ORFs which code putative proteins greater than 75 amino acids in length. The degree of

identity between the gene segments ranges from 77 to 85%. Because most mismatches are found in third base positions and do not cause changes in the amino acid sequence encoded, there is 97% identity at the amino acid level (Wiener and Joklik, 1988).

The 76kDa μ1 protein is 708 residues long and is myristoylated at the extreme amino terminus (Nibert *et al*, 1991b). The three serotypic μ1 proteins are acidic, low in cysteine, histidine and methionine, and are rich in proline. The predicted α-helical content is 27% (Wiener and Joklik, 1988) . The protein is cleaved between residues 42 and 43 to form the 4.2 kDa μ1N and the 72 kDa μ1C fragments during assembly (Jayasuriya *et al*, 1988; Nibert *et al*, 1991b; Wiener and Joklik, 1988), both of which remain associated with the virion. Co-expression studies involving M2 and S4 indicate that the cleavage between residues 42:43 is dependent upon the presence of the myristate side group at the amino terminus (Tillotson and Shatkin, 1992). The protein is also cleaved during proteolytic processing by chymotrypsin and trypsin at residues 581:582 and 584:585, respectively. The cleavage forms the fragments δ and ϕ, with molecular masses of 59-63 kDa and 13 kDa, respectively (Nibert *et al*, 1991b). This cleavage is similar to that seen in host cell compartments during the replicative cycle (Amerongen, *et al*, 1994; Bass *et al*, 1990; Borsa *et al*, 1981.)

The protein has been associated with virion uptake and transmembrane events (Lucia-Jandris, 1990; Lucia-Jandris *et al*, 1993; Nibert *et al*, 1991b; Nibert and Fields, 1992; Tosteson *et al*, 1993). The gene segments for T2J and T3D have also been associated

with interference with superinfection by T1L (Rozinov and Fields, 1994). This protective action occurs between 8 and 10 hours post infection, a time window posited to fall between uncoating and synthesis of dsRNA (Rozinov and Fields, 1996). Resistance to inactivation by 33% ethanol by mutant clones of T3D has been mapped to the M2 gene segment (Drayna and Fields, 1982b; Hooper and Fields, 1996a; Wessner and Fields, 1993). Ethanol resistant mutants are not as effective as wild type T3D in mediating ^{51}Cr release in cells (Hooper and Fields, 1996a). Monoclonal antibodies to the central region of the $\mu 1$ transcript also block ^{51}Cr release by cells infected with the T3D prototype clone (Hooper and Fields, 1996b). Finally, the temperature sensitive mutant *tsA279* has been shown to have a blockade in transmembrane transport of restrictively assembled virions (Hazelton and Coombs, 1995). These monoclonal antibody and mutant studies further suggest that the $\mu 1$ protein has a role in the membrane:virion interactions of transmembrane transport.

Interactions between $\mu 1$ and the other major outer capsid protein $\sigma 3$ have been associated with a shift from translation control by $\mu 1$ to assembly of progeny virions (Shepard *et al*, 1995). Also, co-precipitation studies indicate that these two major outer capsid proteins must interact in order for them to condense around the $\lambda 2$ pentameric spike protein during the formation of the final progeny virion (Shing and Coombs, 1996). Finally, the M2 gene segment has also been associated with the induction of apoptosis by the prototype clones T3A and T3D (Rodgers *et al*, 1997; Tyler *et al*, 1996).

(3.) Complete virion.

The complete virion is an asymmetric left handed icosahedron with triangulation value of T=13 (Kaustov et al, 1987; Klug and Caspar, 1960). Imaging studies indicate that, in addition to the proteins seen in the intermediate structures, there are 600 copies of the major outer capsid protein σ3 in the complete virion (Dryden *et al*, 1993). Complete infectious particles have a buoyant density which ranges between 1.36 and 1.41 g/cm^3 in cesium chloride, depending on the level of hydration, and a sedimentation value of $730S_{20w}$. The density of genome deficient complete particles (Top Component) is 1.28-1.30 g/cm^3 (Joklik, 1983)(Figure 1.1, Table 1.1).

(a.) σ3.

The S4 gene segment which encodes the major outer capsid protein σ3 (Ramig *et al*, 1983), is 1196 nucleotides in length for each of the three serotype prototypic clones (Seliger *et al*, 1992). The protein is encoded in one long ORF commencing from nucleotide 33 and extending through nucleotide 1130 (Giantini *et al*, 1984; Seliger *et al*, 1992)(Table 1.2). No other ORFs exist in the different prototypic segments which could code proteins of 75 amino acids or more. The non translated leader and trailer sequences are highly conserved between the three serotypes, and most mismatches which occur in the ORFs are in the third codon base position, resulting in 90% or better identity at the amino acid level (Seliger *et al*, 1992).

The 365 amino acid long σ3 protein is a hydrophilic protein (Martin and McCrae, 1993)

with a molecular mass of 41 kDa (Giantini *et al*, 1984). It may be removed from the virion by proteolytic digestion *in vitro* to form the Intermediate Subviral Particle (ISVP) (Borsa et al, 1979; Sturzenbecker *et al*, 1987). The protein has domains homologous to putative zinc binding (zinc finger), dsRNA binding (Schiff *et al*, 1988) and the picorna viral 3C protease (Mabrouk and Lemay, 1994). There are two nucleic acid binding domains resident in the carboxy terminus end, the most terminal of which is required for binding dsRNA, with charge being more important to binding capability than putative α-helical conformation (Wang *et al*, 1996). The zinc binding domain has been implicated in binding with the other major outer capsid protein, μ1 (Shepard *et al*, 1996), an essential step in the condensation of the outer capsid to form a complete virion (Lee *et al*, 1981; Shing and Coombs, 1996). The putative 3C protease like domain is not necessary for the proteolytic conversion of μ1 to μ1C and μ1N (Mabrouk and Lemay, 1994).

The σ3 protein has been associated with host cell RNA synthesis inhibition (Sharpe and Fields, 1982) by binding with dsRNA, thereby preventing Ifn activation of the dsRNA activated Protein Kinase PKR (Imani and Jacobs, 1988), and subsequently blocking phosphorylation and activation of the host cell protein eIF-2α (Lloyd and Shatkin, 1992; Schmeckel *et al*, 1997, Tillotson and Shatkin, 1991). Co-expression of σ3 in cells which have been infected with vaccinia virus mutants defective for the Ifn resistance conferring E3L gene re-establishes Ifn resistance and allows growth by the mutant clones (Beattie *et al*, 1996).

The S4 gene segment has also been associated with the establishment of persistent infections (Ahmed and Fields, 1982; Baer and Dermody, 1997; Dermody *et al*, 1993; Wetzel *et al*, 1997b; Wilson *et al*, 1996).

b. Nonstructural proteins.

(1.) μNS.

The M3 gene segment encodes two versions of the protein μNS, a complete product of approximately 80 kDa mass, and a truncated form, μNSC, with an estimated mass of 75 kDa (Ramig *et al*, 1978; Wiener *et al*. 1989). The truncated form is the result of translation initiation at a downstream, in frame start codon rather than the secondary product of post translational proteolytic processing (Wiener *et al*, 1989). The translated ORF is 2235 nucleotides long and encodes a protein of 719 amino acids. The 5' and 3' non translated regions are 18 and 60 nucleotides, respectively (Table 1.2). The protein encoded has a predicted structure with approximately 50% α-helices and similarities to myosin structure (Wiener *et al*, 1989). The protein has been reported to associate with the cytoskeleton of infected cells (Mora *et al*, 1987). μNS is associated with the replicase particles identified in infected cells, suggesting that the protein may have a role in secondary transcription or assembly of outer capsid (Morgan and Zweerink, 1975). No functional difference has been identified between the two forms of μNS (Nibert et al, 1996b).

(2.) σNS.

The 1198 nucleotide long S3 gene segment (George *et al*, 1987; Richardson and Furuichi, 1983; Wiener and Joklik, 1987) encodes the non-structural protein σNS (Ramig *et al*, 1983). The single translated ORF is 1098 bases long and encodes a protein of 366 amino acids with a predicted molecular mass of 41kDa (Richardson and Furuichi, 1983)(Table 1.2). The three different serotypes code proteins with identity at the amino acid level which ranges between 86 and 97% and are very rich (approximately 50%) in predicted α-helical secondary structure (Wiener and Joklik, 1987). The protein has been reported to bind ssRNA (Huismans and Joklik, 1976).

(3.) <u>σ1s.</u>

The non-structural protein σ1s is the 120 amino acid product of a 360 bases ORF within, and frame shifted from, the large σ1 ORF which is encoded in the S1 gene segment. The predicted molecular mass for the protein is 14kDa (Ceruzzi and Shatkin, 1986; Jacobs and Samuel, 1985; Jacobs *et al*, 1985; Munemitsu *et al*, 1986) (Table 1.2). Studies utilizing expressed σ1s protein indicate that the protein has little effect on cells unless expressed in excess (Fajardo and Shatkin, 1990). It has recently been shown that the protein is capable of eliciting an cytotoxic T lymphocyte response in mice (Hoffman *et al*, 1996).

c. <u>Genome.</u>

The reovirus genome for T3D, the only serotype with a completely published genome, is 23,549 base pairs (Wiener *et al*, 1989) and is comprised of 10 segments; 3 L (large), 3 M (medium) and 4 S (small) segments (Dunnebacke and Kleinschmidt, 1967; Watanabe

and Graham, 1967; Shatkin *et al*, 1968) of double stranded RNA (Gomatos *et al*, 1962; Silverstein and Schur, 1970). With the exception of the bicistronic S1 strand the segments are monocistronic (Ernst and Shatkin, 1985). The gene segments can be resolved on 10% polyacrylamide slab gels (Shatkin *et al*, 1968) and demonstrate unique migration rates associated with each serotype (Sharpe *et al*, 1978). The genome is packed into the core as a nematic liquid crystal, occupying a space estimated to be less than 48nm in diameter, with an average separation of 2.5 to 2.7nm between dsRNA helices (Dryden *et al*, 1993). The genome for rotavirus, another genus of the *Reoviridae* which has 11 gene segments, has also been resolved by electron cryomicroscopy. In this model the dsRNA forms a dodecahedral structure interacting with the inner layer of the inner capsid. Approximately 25% of the rotavirus genome is ordered at the vertices and is packed around the polymerase enzyme complex located there. The rotavirus structure is conducive to movement of dsRNA through the enzyme complex during transcription (Lawton *et al*, 1997; Prasad *et al*, 1996).

To date only one strand of each gene segment has been shown to encode genetic information. These have been designated the positive strands. The 5' end of the positive strands are blocked by a methylated cap with the structure ^{7}mG(5')ppp(5')G^{m}pCpUp... (Chow and Shatkin, 1975; Furuichi *et al*, 1975a; Furuichi *et al*, 1975b; Miura, *et al*, 1974). The 3' termini of all positive strands end with the sequence ...pUpCpApUpC3' (Darzynkiewicz and Shatkin, 1980). The negative sense strands of the different gene segments are not capped. Their terminal sequences are also consensual, with the 5'

sequence being 5'ppGpApUp... and the 3' sequence being ...pApGpC3' (Chow and Shatkin, 1975, Darzynkiewicz and Shatkin, 1980).

The segmented genome and limited number of proteins employed by reovirus have made the agent a useful tool for evaluating eucaryotic regulation systems and have helped identify the cap structure of mRNA (Furuichi *et al*, 1975a; Furuichi *et al*, 1975b); the Kozak sequence, a preferred site for ribosome:mRNA interaction (Kozak and Shatkin, 1976); and the differential ribosomal scanning rates and pausing during translation of nested signals (Doohan and Samuel, 1992; Doohan and Samuel, 1993).

3. Reassortment Mapping.

When host cells are infected with two different serotypes the gene segments may reassort to produce progeny virions with mixed gene complements (Figure 1.2)(Sharpe *et al*, 1978), a phenomenon which may occur both in controlled situations involving tissue culture procedures (Sharpe *et al*, 1978) and in natural settings (Chappell *et al*, 1994). Each viable progeny virion will contain only one copy of each gene segment, regardless of the parentage of that segment. While theory suggests that reassortment will be random, there is some evidence that some genes co-assort (Nibert *et al*, 1996a).

Gene segment reassortment may be utilized to sort large collections of clones with the same parentage and phenotype into classes where phenotype expression is on the same gene segment. This process, which is similar to complementation, is especially effective

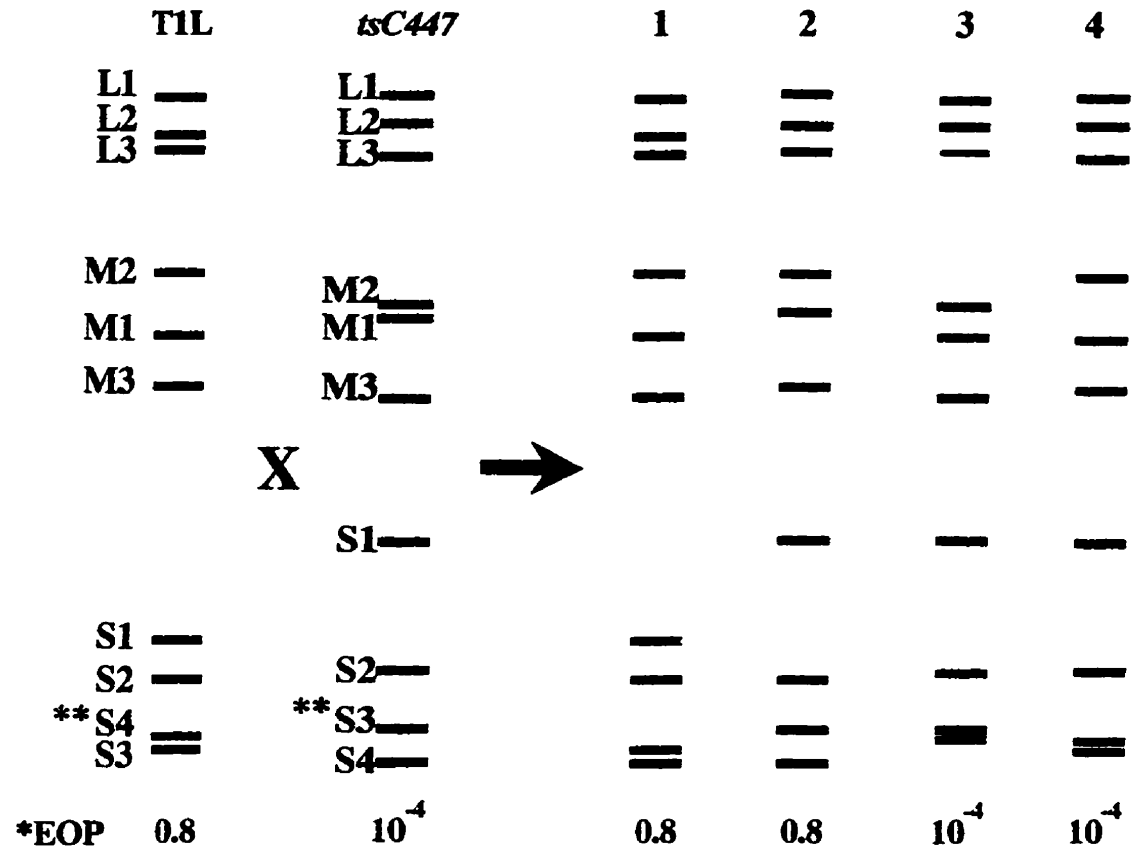

Figure 1.2. Reassortant mapping of a temperature sensitive mutant. Representative electropherogram of T1L (green), the temperature sensitive mutant *tsC447* (purple), and 4 reassortant progeny from a mixed infection, two of which are wild type and two temperature sensitive. The S2 gene segment for *tsC447* (red) contains the lesion responsible for expression of the phenotype. All gene segments except the S2 segment are excluded from the clones expressing their parental phenotype between 1 and 3 times as follows: L1- 2/4; L2 - 1/4; L3 - 2/4; M1 - 3/4; M2 - 1/4; M3 - 2/4; S1 - 1/4; S2 - 0/4; S3 - 2/4; and S4 - 2/4.

*EOP is efficiency of plating, determined by dividing the titre of the clone at 39 degrees C by the titre of the same clone at 32 degrees C. The expression of the temperature sensitive phenotype is demonstrated by a fall in titre of 10,000, or an EOP value of 0.0001 or less.

** The S3 and S4 gene segments migrate differentially in 10% SDS-PAGE for the two serotypes, with the S4 segment of T1L migrating more slowly than the S3 gene segment, while the S3 gene segment of T3D/*tsC447* migrates more slowly than the S4 gene segment.

with conditionally lethal phenotypes. Mixed infections are prepared for sets of two clones and are cultured under permissive conditions. The proportion of progeny expressing the wild type phenotype is determined for each mixed infection. This proportion is compared with the results from unmixed infections of the parental clones. Clones may be grouped as having phenotypic control on the same gene segment when the proportion of progeny expressing the phenotype is similar in both parents and in the mixed infection. Where phenotype control resides on separate gene segments a significant proportion of progeny will be phenotypically wild type (Fields and Joklik, 1969).

The use of individual progeny reassortant clones derived from mixed infections of serotypically diverse parental clones provides additional power to recombination evaluation. In this process clones from separate serotypic parents which have a defined phenotypic difference are co-infected and progeny clones selected by dilution limitation. The electrophoretic pattern of gene segment migration is determined for each reassortant clone, as is the identifying phenotype. The gene segment associated with phenotype expression is determined by analyzing the reassortant panel to determine which gene or group of genes are associated with the phenotype under analysis. Reassortant mapping occurs where the electropherotype of one gene segment or group of segments in the panel, is equivalent to and uniquely associated with the parent which expresses that phenotype, and all remaining gene segments are randomly assorted between the two parental clones (Hazelton and Coombs, 1995; Sharpe *et al*, 1978)(Figure 1.2).

4. Life cycle of reovirus.

The first step in the life cycle occurs when the virion attaches to cell receptors via the $\sigma 1$ trimeric attachment protein (Lee *et al*, 1981; Weiner *et al*, 1980)(Figure 1.3). The attachment process is not cold inhibited, with greater than 50% of available virions adsorbed to the target cell in the first 15 minutes of attachment, whether at 4°C or at 37°C (Dales and Gomatos, 1965; Silverstein and Dales, 1968). There appear to be two domains for attachment with host cell plasmalemmal external proteins, one in the globular head (Duncan *et al*, 1991; Leone *et al*, 1991a), and one in the β-sheet intervening segments of the amino terminal coiled-coil structure (Chappell *et al*, 1997). There appears to be non specific binding with sialic acid residues in sugar side chains of external proteins (Gentsch and Hatfield, 1984; Gentsch and Pacitti, 1985; Gentsch and Pacitti, 1987). This non-specific binding is associated with the interactions in the β-sheet intervening segments (Nibert *et al*, 1995; Chappell *et al*, 1997). More specific binding has been associated with the amino terminus of the Epidermal Growth Factor Receptor (EGFR) (Tang *et al*, 1993) and subsequently confirmed by studies where EGFR was transfected into two non-tropic cell lines which then became tropic targets (Strong *et al*, 1993). Transfection studies utilizing the oncogene *v-erb B* indicate the protein product of this gene also confers tropism for reovirus infection through a proposed mechanism involving opportunistic utilization of an already activated signal transduction pathway. *v-erb B* has ligand independent, constitutive tyrosine kinase activity. Therefore, confirmation that this protein accorded tropism was shown when the transfected cells were treated with the tyrosine kinase inhibitor genistein and cellular susceptibility to the virus

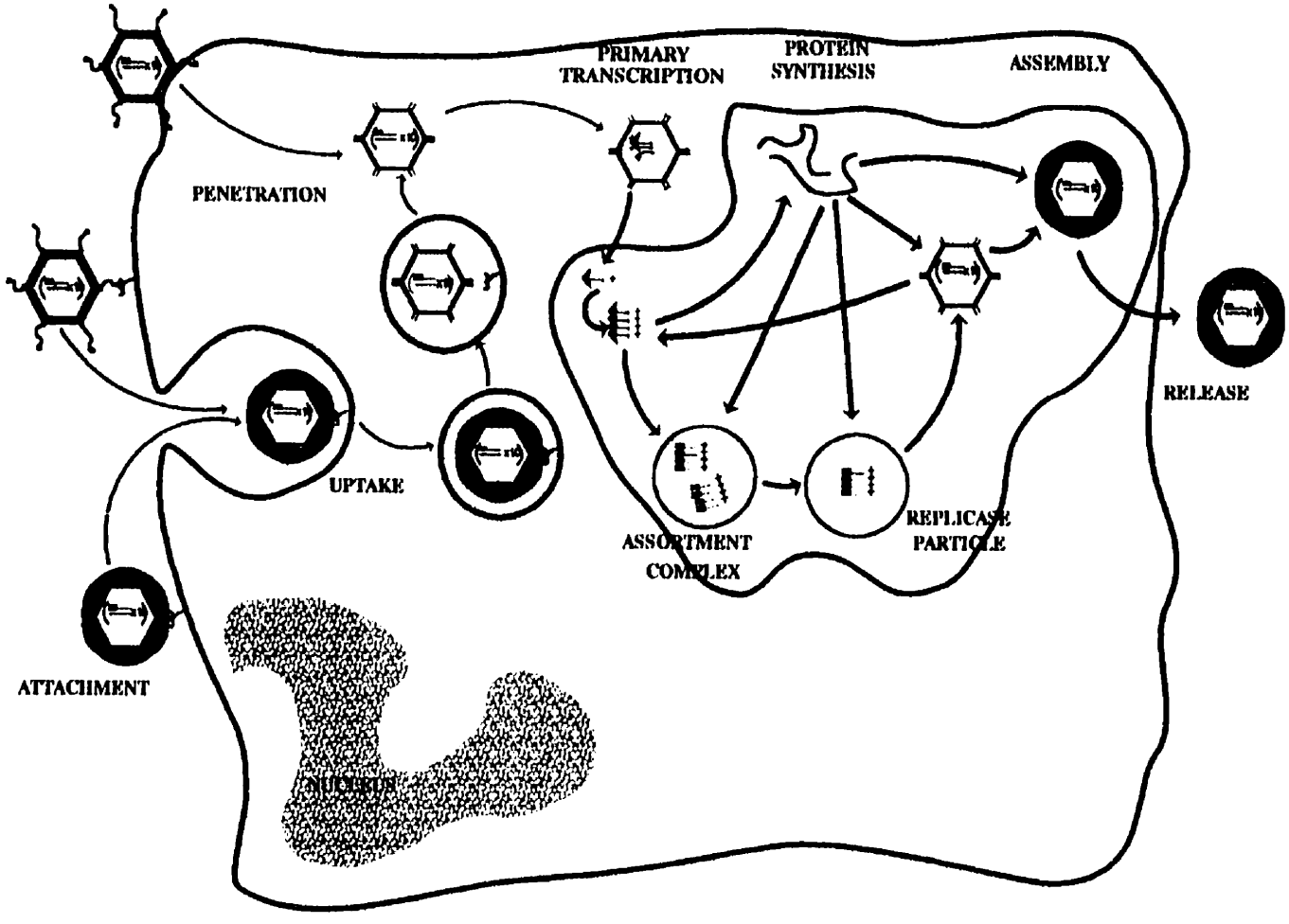

Figure 1.3 The life cycle of reovirus

was lost (Strong and Lee, 1996).

In cell culture systems, when the temperature is elevated above the melting temperature of the cytoplasmic membranes the attached virions are endocytosed via clathrin coated endosomes, with the first virions being endocytosed within 10 to 15 minutes (Silverstein and Dales, 1968; Lucia-Jandris, 1990; Spendlove *et al*, 1963). The endosomes fuse with Golgi transport vesicles containing proteolytic enzymes, the lumen is acidified, and the outer capsid proteins μ1/1c, σ1 and σ3 are digested to produce ISVPs (Borsa et al, 1981). Studies with lysosomotropic agents (Borsa, 1979; Canning and Fields, 1983; Sturzenbecker *et al*, 1989) and the lysosomal protease inhibitor E64 (Baer and Dermody, 1997) indicate this is a critical step in infection.

In the more natural setting of the intestinal tract virions are exposed to reduced pH and various proteolytic processes which cleave the outer capsid proteins μ1/1c, σ1 and σ3 and create a true form of ISVP (Amerongen *et al*, 1994; Bass *et al*, 1990; Bodkin *et al*, 1989). It is hypothesized that these particles are transported across the mucosal tissue of the intestine and released into the submucosal tissue where the particles may then attach to M cells of the Peyer's patch and establish productive infections (Wolf *et al*, 1981). ISVPs may also be created *in vitro* by treatment of virions with either trypsin or chymotrypsin (Borsa *et al*, 1979; Nibert and Fields, 1992; Shatkin and LaFiandra, 1972; Spendlove *et al*, 1970; Spendlove and Schaffer, 1965).

The actual mechanism of transport into the cytosol and uncoating remains unclear. Studies involving both ^{51}Cr release and patch clamp assays on artificial membranes indicate that the ISVP is capable of transport across membranes (Hooper and Fields, 1996a; Tosteson *et al*, 1993). ISVPs have been shown capable of transporting directly across the cytoplasmic membrane and establishing productive infections (viropexis) (Borsa *et al*, 1979). It is generally proposed that some intermediate of the intact structure transports across the membrane. However, one proposal is that the core like structure interacts with the membrane without transport into the cytosol, with viral mRNA production occurring outside the cytoplasmic compartment and collateral extrusion of the viral mRNA into the cytosol (Sturzenbecker *et al*, 1987; Zarbl and Millward, 1983).

The fate of the core particle inside the cytosol, and the ensuing replicative processes, are not well understood (Schiff and Fields, 1990). Host cells have developed strong responses to dsRNA in the cytosol, giving credence to a model in which the replication process occurs inside the protected dominion of the virion core (Jacobs and Langland, 1996; Zweerink *et al*, 1972). There is a preponderance of supporting evidence. Reovirus dsRNA has not been isolated from cells in the absence of viral proteins which would contribute to known viral structures (Schiff and Fields, 1990). It has been demonstrated that the complete viral core particle contains all enzymatic activities necessary for replication (Chang and Zweerink, 1971). It was hypothesized that the virion transcribed mRNA inside the core in a conservative fashion (Bellamy and Joklik,1967; Silverstein *et al*, 1970), extruding the 5' capped transcription product through the λ2 spike either during

or immediately following transcription (Morgan and Zweerink, 1975; Shatkin *et al*, 1983; Vasquez and Kleinschmidt, 1968). Visualization of transcribing viral particles by NS-TEM show apparent single stranded RNA extending from core particles (Bartlett *et al*, 1974; Gillies *et al*, 1971; Yin *et al*, in submission). Recent electron cryomicroscopy of transcribing cores further show densities which are consistent with the passage of single strand RNA from the external end of the λ2 pentameric spike (Yeager *et al*, in preparation). Similar densities have also been identified in transcriptionally active rotavirus particles (Lawton *et al*, 1997). The mechanism is also consistent with the model for conservative transcription of the genome. In this model parental genomic RNA remains in the virion core and the nascent viral ssRNA is extruded during transcription (Bellamy and Joklik, 1967; Silverstein *et al*, 1976). The different segments are transcribed independently by core particles *in vitro*, with the relative proportion of transcripts being inversely proportional to the gene segment length (Spandidos *et al*, 1976).

As with transcribing core particles *in vitro*, the mRNA produced from the S4 gene segment is the most abundant viral mRNA found in the infected cell. The relative proportion of mRNAs produced by the other gene segments *in vivo* differs from the *in vitro* experience. The relative proportions of transcripts seen in cells, standardized to the S4 segment, are; S4 (1.0), M2 (0.7), S2 & S3 (0.5), L2, L3, & M3 (0.25-0.3), S2 (0.05-0.1) and L1 &M1 (<0.01) (Gaillard and Joklik, 1985). The first mRNAs identified in infected cells are transcribed from the L3, M3, S3 and S4 gene segments (Lau *et al*,

1975). σ3, the product of the S4 gene has been shown to localize in and around the nucleus during the initial replicative stages (Yue and Shatkin, 1996). The proteins from three of these segments, μNS, σNS and σ3, have been shown to associate with ssRNA early in the infectious cycle (Antczak and Joklik, 1992).

λ2 is added to the μNS, σNS and σ3 complexes (Antczak and Joklik, 1992), and dsRNA transcription occurs in early replicase particles which are found soon after association of viral proteins with ssRNA (Acs *et al*, 1971; Antczak and Joklik, 1992). The next particle identified is a complete replicase particle. This particle has a putative diameter of approximately 40nm and contains the proteins λ1, λ2, μ1/1c, μ2, σ1, σ2, and σ3 (Morgan and Zweerink, 1975; Zweerink *et al*, 1976). The absence of the minor core structural protein λ3 noted in this structure may be due to the relative proportion of the protein and the fact that it co-migrated with other proteins in the gel system used.

The actual process of virion assembly occurs in perinuclear cytoplasmic inclusions, with progeny virions forming large paracrystaline arrays. These inclusions are not membrane bound (Fields *et al*, 1971). Progeny are released into the environment through lytic cell death. Many of the assembly processes inside the host cell are poorly understood (Schiff and Fields, 1990).

5. Genetic engineering in reovirus.

Reovirus is generally refractive to genetic engineering procedures. A system has been

reported which requires the addition of all ten gene segments, the *in vitro* translation product for all ssRNA species of the same serotype, and a helper virus. Usually the helper virus is a different serotype of reovirus (Roner *et al*, 1990). Recently a system has been reported where this system was used to combine the M2 gene segment of the mutant *tsA201* and the S2 gene segment from the mutant *tsC447* to obtain a double mutant progeny (Roner *et al*, 1997). While this system shows promise, successful recovery of engineered progeny into which designed mutations have been introduced has not been reported.

6. The Fields panel of temperature sensitive mutants.

Conditionally lethal phenotypes simplify the analysis of morphogenic processes. Two panels of temperature sensitive mutants were developed from the reovirus Type 3, Dearing strain in order to dissect the assembly pathways of eukaryotic viruses (Ikegami and Gomatos,1968; Fields and Joklik, 1969). The property of the segmented genome was utilized to sort one panel into recombination groups. The members of each group were postulated to contain lesions in common gene segments. Briefly, mixed infections were prepared using two mutant clones, and the infections were incubated at permissive temperature. After incubation the cultures were harvested, the infectious titres of progeny virions were determined at both the permissive and restrictive temperatures by standard plaque assay, and the following formula was used to determine the proportion of recombination:

$$\{[(\text{Yield A x B})^{R} - (\text{Yield A}^{R} + \text{Yield B}^{R})] \div [\text{Yield A x B})^{P}\} \times 100;$$

where R was the infectious titre of progeny when titred at the restrictive temperature and P was the infectious titre of progeny when titred at the permissive temperature. Restrictive yields (the numerator) which were a relatively high proportion of the permissive yield (the denominator) suggested that the control of the ts phenotype for the two clones resided on separate gene segments, and that the gene segments from the two clones could recombine to produce a significant proportion of wild type (ts^+) progeny. Restrictive yields which were significantly reduced from the permissive yields indicated that gene segments from the two clones could not recombine to produce a proportion of ts^+ progeny. In this latter case the control of the *ts* phenotype for in the two clones resided on the same gene segment. (Fields and Joklik, 1969) (Table 1.3). During early studies it was determined that one clone, *tsG453* had been mis-classed. This clone became the prototype clone for a seventh recombination group (Cross and Fields, 1972). Some prototype mutants were selected and examined by thin section electron microscopy for the effect of their mutations on morphogenesis (Fields *et al*, 1971). Purified fractions from cytoplasmic extracts have been evaluated by negative stain electron microscopy for the recombination groups C (Matsuhisa and Joklik, 1974), and B and G (Morgan and Zweerink, 1974; Danis *et al*, 1992).

Prototype clones from the Fields panel were analyzed for protein (Fields *et al,* 1972; Cross and Fields, 1976b) and ssRNA and dsRNA synthesis (Cross and Fields, 1976a; Cross and Fields, 1976b). The clones were used to establish persistent infections (Ahmed and Graham, 1977) and to identify mechanisms of extragenic reversion (McPhillips and

Table 1.3 Characteristics of the Fields panel of temperature sensitive mutants of reovirus.§

Reassortment Group	Prototype Mutants	Gene Segment	Protein	dsRNA	EOP† 37°C	EOP† 39°C	Morphology
A	*tsA201*	M2	μ1	+	0.33	0.02	Normal
	tsA279			?	0.58	0.11	
	tsA329			?		0.053	
	tsA340			?		0.019	
B	*tsB271*	L2	λ2	+		0.005	Core Like
	tsB352					0.00025	
	tsB405					0.001	
C	*tsC447*	S2	σ2	-		0.0004	Empty Outer Shell
D	*tsD357*	L1	λ3			0.001	Empty Whole
E	*tsE320*	S3	σNS	-	0.53	0.21	?
F	*tsF557*	(M3)	μNS	+		0.02	Normal
G	*tsG453*	S4	σ3	+		0.0002	Core Like
H	*tsH26/8*	M1	μ2	?	0.29	0.000028	?
I	*tsI138*	L3	λ1	?	0.079	<0.0021	?
J	*tsJ128*	S1	σ1, σ1bNS	?		0.046	?

§ Adapted from Fields and Joklik, 1969; and Schiff and Fields, 1990.

† EOP : $(Titre_R) \div$ (Titre 32°C).

Ramig, 1984 Ramig and Fields, 1977; Ramig *et al*, 1977; Ramig and Fields, 1979). Recent investigations with *tsC447* revertants have identified point mutation back to parental nucleotide sequences at one mutation site in ten wild type phenotype (ts^+) revertant clones studied (Coombs *et al*, 1994). There was a concomitant reversion in morphogenesis of the revertant clones at restrictive temperature (Coombs *et al*, 1994).

Pseudorevertant clones were back crossed to wild type T3D and additional *ts* mutants identified. The rescued mutants were assayed against the original panel and prototype clones for recombination groups representing the remaining gene segments were identified (Ahmed *et al*, 1980a; Ahmed *et al*, 1980b; Ramig *et al*, 1983). Prototype clones from nine recombination groups were tested by reassortant analysis and the *ts* phenotype associated to the responsible gene segments (Mustoe *et al*, 1978; Ramig *et al*, 1978; Ramig *et al*, 1983). There has been no further characterization of the rescued pseudorevertants.

Reassortant analysis of revertant clones generated from *tsC447* revealed a spontaneous temperature sensitive mutation in the T1L M1 gene segment of a reassortant progeny clone, *tsH11.2*. Due to it's reassortant electropherotype this clone is perhaps not a true member of the Fields panel. Characterization of this clone has indicated that, while it produces ssRNA and normal levels of protein at early time points, it is defective for dsRNA and viral protein production at later time points (Coombs, 1996). There has been no further characterization of this clone. For a more complete review of the temperature

sensitive mutants of reovirus please see Coombs, 1998b.

7. Evaluation of viral assembly.

The electron microscope has been a valuable tool for the examination of viral structure and assembly processes (Harrison, 1990). The use of thin section electron microscopy allows observation of the interactions which occur during morphogenesis. Unfortunately section thickness and stain granularity limits the resolution of this method to between 5 and 7.5nm. Negative stain electron microscopy provides better resolving power, achieving levels of less than 2nm under ideal conditions. However, while negative stain electron microscopy allows resolution of isolated or extended proteins or nucleic acids, the procedure is limited since upper and lower surface structures may be visualized at the same time (Hayat and Miller, 1990; Miller, 1995)

As stated in Chapter 1.1, recent studies involving either X-ray crystallography or electron cryomicroscopy have provided valuable insight into the overall structure and putative protein interactions for a number of viruses at the macromolecular level. (For examples see: Hogle *et al*, 1985; Paredes *et al*; 1993, Rossmann *et al;* 1985). Most studies have focused upon complete virions, a limited number of naturally occurring subviral particles, and the products of digestion and disassembly processes to create subviral components (Dryden *et al.*, 1993; Luongo *et al*, 1997; Yeager *et al*, 1994); reassortant viruses (Shaw *et al.*, 1993); or capsids assembled from expressed proteins (Montrose *et al*, 1991; Hewat *et al.*, 1992). Recent electron cryomicroscope studies have visualized the extruding

nascent viral ssRNA from transcriptionally active reovirions and the related rotavirions (Lawton *et al*, 1997; Yeager *et al*, in press). X-ray diffraction studies show the interactions between structures on an atomic level. However, the need for crystalline aggregates of biological units has restricted investigation by this technique to simple protein systems ranging from single proteins to small viruses. More complicated structures, such as the different reovirus structures, exceed the current limitations of X Ray diffraction (Coombs *et al*, 1990; Dryden *et al*, 1993). These structures are limited to examination by the relatively lower resolution of electron cryomicroscopy (Harrison *et al*, 1996).

While X Ray diffraction and electron cryomicroscopic studies show complete structures and some assembly intermediate structures, and permit the localization of some proteins, they do not show the processes and interactions involved in viral assembly. The existence of conditionally lethal, assembly defective mutants is a powerful tool for dissection of viral assembly.

The success in using conditionally lethal amber mutations of bacteriophage mutants to deduce procaryotic virus assembly pathways (Fane and King, 1987; Fane *et al.*, 1991; Gordon and King, 1993) suggests that the conditionally lethal reovirus *ts* mutants from the Fields panel may be elegant tools for delineating the assembly pathways of a eucaryotic virus. The recombination groups which were obtained from rescued pseudorevertants have not been characterized (recombination groups H, I, and J: representing gene

segments M1, L3, and S1; and proteins μ2, λ1, and σ1, respectively). Further, no morphological variants have been demonstrated for recombination groups A (gene segment M2, protein μ1) nor E (gene segment S3, protein σNS). With the exception of the non structural protein σNS these recombination groups represent structural entities whose disruption or faulty folding could interfere with assembly (Figure 1.4). The initial goal of this study was to characterize recombination groups A, E, H, I, and J from the Fields panel and investigate the possible roles of the proteins involved in viral morphogenesis. Once this initial characterization was completed, the double mutant clone *tsA279*, which demonstrates multiple *ts* lesions and mechanisms for their expression, became the subject of more complete characterization.

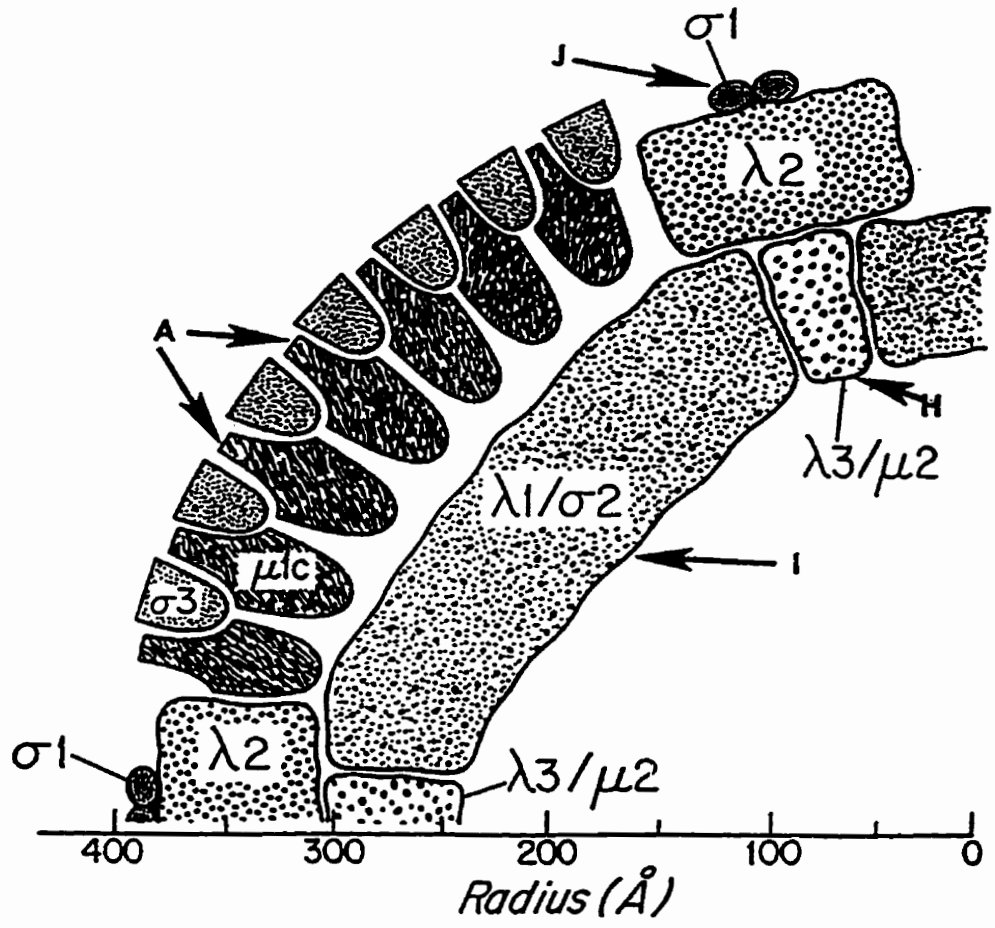

Figure 1.4 **The proteins of the uncharacterized *ts* mutant recombination groups of reovirus.**

Viral structural proteins identified for characterization are from reassortment groups A, Major outer capsid protein μ1; H, minor core protein μ2; I major core protein λ1; and J, minor outer capsid (attachment) protein σ1.Non structural proteins are represented by reassortment groups E, μNS, and J, σ1S. Illustration adapted from Figure 1.1.

CHAPTER 2

Materials and Methods

1. Solutions and media.

L929 cells are a transformed mouse connective tissue cell line (Earle, 1943) (ATCC CCL 1) which has reverse transcriptase activity and expresses type A retrovirus particles. Joklik's modified minimum essential medium (S-MEM) and Medium 199 were purchased from Gibco BRL (Gaithersburg, MD) and were prepared in accordance with the manufacturer's instructions as 1x and 2x solutions, respectively, with sterilization by filtration through 0.2μ pore membranes. Phosphate free S-MEM was made in accordance with the S-MEM formulation provided by Gibco BRL, with 5% the prescribed amount of monobasic Sodium Phosphate and sterilized as mentioned above. Fetal Calf Serum (FCS) was obtained from Intergen (Purchase, NY) and agammaglobulin-neonate bovine serum VSP (VSP) was supplied by Biocell Laboratories, Inc. (Carson, CA). $^{32}PO_4^{-3}$ organophosphate (1mCi/ml and 2mCi/ml), ^{32}P-ATP (10mCi/ml) and ^{35}S-Methionine:Cysteine (7.9mCi/ml) were obtained from New England Nuclear (DuPont, Wilmington, DE). Electrophoresis quality reagents for Sodium Dodecyl Sulfate-Polyacrylamide Gel Electrophoresis (SDS-PAGE) were obtained from Bio-Rad (Richmond, VA) and Boerhinger Mannheim (Indianapolis, IN). Polyclonal rabbit anti-whole reovirus T3D and anti-reovirus T3D σ2 and λ1 proteins were prepared by National Diagnostic Labs (Dugald, MB) and rhodamine and horseradish peroxidase conjugated goat anti-rabbit Immunoglobulin G was obtained from Chemicon (Temecula,

CA). Electron Microscopy reagents and media were obtained exclusively from Electron Microscope Sciences (EM Sciences, Fort Washington, PA.) except where otherwise noted. All other chemicals were routinely purchased from Sigma Chemical Company (Saint Louis, MO) and Fisher Scientific (Fair Lawn, N.J.). All reagents were initially prepared in fresh glass redistilled water, and latterly in reverse osmosis purified water which was then glass distilled. All solutions were passed through 0.2μM pore filters to sterilize the reagents and remove particulate material. Abbreviations are provided in the List of Abbreviations and solutions are listed in Appendix A.

2. Cells and viruses.

a. Stock cells and viruses.

Mouse L929 cells and reovirus Type 1 Lang (T1L), Type 3 Dearing (T3D) and temperature sensitive (*ts*) mutant clones derived from reovirus T3D representing recombination groups A (gene segment M2, μ1 protein, clones *tsA201, tsA279, tsA329.r117* and *tsA340*), B (gene segment L2, λ2 protein, clones *tsB271, tsB352,* and *tsB405.F54*), C (gene segment S2, σ2 protein, clone *tsC447*), D (gene segment L1, protein λ3, clone *tsD357.F25*), E (gene segment S3, σNS protein, clone *tsE320*), F (reputed gene segment M3, μNS protein, clone *tsF556*) G (gene segment S4, protein σ3, clone *tsG453c*), H (gene segment M1, μ2 protein, clone *tsH26/8*), I (gene segment L3, λ1 protein, clone *tsI138*), and J (gene segment S1, σ1 and σ1S proteins, clone *tsJ128*) are laboratory stocks which were kindly provided by the late Dr. B. N. Fields (Table 2.1)

Table 2.1 **Stock clones of the Fields panel of temperature sensitive mutants of reovirus.**[a]

Recombination Group	Gene Segment	Protein	Clones	Source of Isolation	Reference[b]
A	M2	μ1	*tsA201*	Proflavin	Fields and Joklik, 1969
			tsA279	Proflavin	Fields and Joklik, 1969
			tsA329.r117	Nitrous Acid	Fields and Joklik, 1969
			tsA340	Nitrous Acid	Fields and Joklik, 1969
B	L2	λ2	*tsB271*	Proflavin	Fields and Joklik, 1969
			tsB352	Nitrous Acid	Fields and Joklik, 1969
			tsB405	Nitrous Acid	Fields and Joklik, 1969
C	S2	σ2	*tsC447*	Nitrosoguanidine	Fields and Joklik, 1969
D	L1	λ3	*tsD357.f25*	Nitrous Acid	Fields and Joklik, 1969
E	S3	σNS	*tsE320*	Nitrous Acid	Fields and Joklik, 1969
F	M3	μNS	*tsF556*	Nitrosoguanidine	Fields and Joklik, 1969
G	S4	σ3	*tsG453*	Nitrous Acid	Fields and Joklik, 1969, Cross and Fields, 1972[c]
H	M1	μ2	*tsH26/8*	Rescued Pseudorev.	Ahmed *et al*, 1980b
I	L3	λ1	*tsI138*	Rescued Pseudorev.	Ramig and Fields, 1979
J	S1	σ1,σ1S	*tsJ128*	Rescued Pseudorev.	Ramig and Fields, 1979

a. Laboratory stocks kindly provided by the late Dr. Bernard N. Fields.
b. Original report of isolation.
c. Classification changed from recombination group B.

b. Culture and maintenance of stock cells.

L929 cells were routinely maintained in suspension culture as 500ml volumes in 1 litre Florence flasks. Cell concentrations were determined daily by direct count using a haemocytometer, and the cells were diluted to a concentration of $5x10^5$cells/ml by removing stock cell suspension and replenishing the volume with fresh MEM supplemented with 2.5% FCS, 2.5% VSP, and 2mM Glutamine (supplemented S-MEM). Monolayers were prepared by inoculation into indicated flasks or dishes with cells at a concentration of $4.0x10^5$ cells/ml and the cells allowed to attach and grow to near confluence overnight at 37°C in 5% CO_2 controlled atmosphere incubators. The volume seeded was 2.5ml/well in 6 well plates, 5.0ml/P60 or T25 culture vessel, 12.5ml/P100 culture dish, 15ml/T75 culture flask, and 30ml/P150 culture flask. Where necessary, cells were detached by washing monolayers twice with fresh, sterile Phosphate Buffered Saline (PBS) followed by incubation for 5 minutes in PBS containing 0.05mM EDTA at 37°C. Stock cells were routinely maintained in the absence of antibiotics.

c. Plaque assay of virus stocks.

Plaque assays were conducted as previously described (Fields and Joklik, 1969). Briefly, sequential 10-fold dilutions of virus stocks were prepared in gel/saline. Near-confluent L929 monolayers were infected with aliquots of sequentially diluted stock viral preparations after withdrawing the overlaying supplemented S-MEM. After attachment for 1hr at either 4°C or 20°C the infections were overlayed with fresh Medium 199 in 1% agar and supplemented with 1.25%FCS, 1.25% VSP, 2mM Glutamine, 100U

penicillin/ml, 100μg streptomycin sulfate/ml and 1μg amphotericin B/ml (agar/medium 199). The infections were incubated at the temperatures and for the times indicated. Infections were fed by overlaying fresh agar/medium 199 between 12 and 24 hours prior to the mid point of the incubation, and were overlayed initially with medium 199 in 1% agar containing 0.004% filtered neutral red stain (neutral red staining overlayment) between 12 and 24 hours prior to the termination of the incubation. In later experiments PBS was substituted for medium 199 in the neutral red staining overlayment.

d. <u>Plaque purification of virus stocks.</u>

Virus stocks were plaque purified by standard plaque assay as above with the following modifications. After attachment of virus for 1 hour at 32°C excess inoculum was withdrawn, and the monolayers were overlayed with agar/medium 199 and incubated at 32°C. After staining with neutral red staining overlayment individual plaques which were separated by at least 0.5 cm were identified and plugs of overlayment which contained clonal progeny virions from the plaques were collected in sterile pasteur pipettes. The plugs were placed in supplemented S-MEM and virus allowed to diffuse from the plugs.

e. <u>Amplification of isolated plaques.</u>

Selected clones were amplified through first passage (P1) on monolayers in T25 tissue culture flasks. After adsorption with infecting virus as in section 2.2.c, above, the monolayers were overlayed with supplemented S-MEM and cultured at 32°C until ≥

75% of the cells demonstrated cytopathic effects (CPE) unless otherwise indicated. Viral lysate stocks were created by subjecting cultures to three cycles of freezing to -80°C followed by slow thawing to room temperature (freeze/thaw cycles). Selected clones were amplified through subsequent passages on L929 cells as indicated. Experimental procedures were performed using second passage amplifications (P2) unless otherwise noted.

f. Virus titrations, identification of expression of temperature sensitivity, and efficiency of plating (EOP) determinations.

Parallel L929 monolayers in 6-well cluster dishes were infected with sequential 10-fold dilutions of viral lysate stocks as described in 2.2.c, above (Fields and Joklik, 1969; Sharpe *et al*, 1978; Hazelton and Coombs, 1995). Attachment was performed at 4°C and the infections were incubated at 32°C (permissive temperature) and at 0.5° increments from 37°C through 40.5°C (restrictive temperatures) as indicated. Incubation temperatures were monitored using immersion mercury thermometers and fluctuations of less than 0.25°C were confirmed by using a Fluke Model 52 recording thermocouple probe (J. Fluke Mfg. Co., Inc., Everett, WASH) (Hazelton and Coombs, 1995). The infectious titre for each virus stock was determined by the relationship:

{[plaques in the infection]x[volume inoculum (in ml)]} ÷ {dilution factor of inoculum},

with the result expressed in plaque forming units/ml (PFU/ml). Efficiency of plating (EOP) values for each temperature were determined by dividing the infectious titre for

the clone at the indicated restrictive temperature by the infectious titre for the parallel infection of that clone at 32°C (Fields and Joklik, 1969). EOP values $\leq$ 0.05 of the EOP value for parallel control T3D cultures were considered temperature sensitive (*ts*) while EOP values $\geq$ 0.1 of the EOP values for the parallel control T3D cultures were considered wild type (ts^+) (Hazelton and Coombs, 1995).

g. Generation of T1L x *ts* reassortants.

Mixed infections and all subsequent plaque purifications and amplifications of candidate reassortant clones were incubated at 32°C to ensure there was no selection against either *ts* or ts^+ progeny. L929 cell monolayers were co-infected with T1L and either *tsA201*, *tsA279*, *tsB405*, *tsE320*, *tsH26/8*, *tsI138*, or *tsJ128* at a multiplicity of infection (MOI) of 5 PFU of each clone per cell (total MOI = 10 PFU/cell). Infections were incubated for 33 hours to generate reassortants (approximately one replicative cycle at 32°C). Viral lysates were prepared by three freeze/thaw cycles, candidate reassortant clones isolated by plaque purification, and placed in supplemented S-MEM (Chapter 2.2.c, above). L929 cells in suspension were added to each plaque suspension and the cells and inoculum cultured between 3 and 7 days to obtain P1 stocks.

h. Suspension cultures of *ts* clones and T3D control infections.

L929 cell pellets were suspended in supplemented S-MEM containing stock P2 lysates of either T3D or the selected *ts* clone at an MOI of 5 PFU/cell. Virus was allowed to attach for one hour at 4°C. After attachment the cells were diluted into pre-warmed,

supplemented S-MEM and were incubated in suspension culture at either 32°C, 39°C, 39.5°C, or 40°C. Aliquots were taken from each culture at various times post attachment and treated as follows:

(1.) Frozen for later titration for yield of infectious virus. Titration was done by plaque assay at 32°C (Chapter 2.2.f);

(2.) The proportion of viable cells determined by trypan blue stain exclusion; and

(3.) Combined directly with freshly purified 50% aqueous glutaraldehyde (final concentration glutaraldehyde = 2%), fixed, and stored at 4°C for later processing for thin section transmission electron microscopy (TS-TEM).

3. Isolation of viral RNA and electropherotyping of viral stocks.

a. Preparation of cytoplasmic extracts.

Cytoplasmic extracts were prepared from P3 stocks as described (Sherry and Fields, 1989; Hazelton and Coombs, 1995). Briefly, L929 monolayers were infected with P2 stocks of individual reassortant clones. Infections were harvested by scraping the monolayer from the surface of the infection vessel when they demonstrated ≥ 75% CPE. Infections which showed no CPE were harvested after seven days culture. The cells were pelleted by centrifugation, the pellet lysed with Nonidet P-40, the nuclei and cellular organelles removed by centrifugation, and the cytosolic fractions were extracted with phenol/chloroform. The dsRNA was precipitated at -20°C in ethanol with sodium

acetate, resuspended in electrophoresis sample buffer (Laemmli, 1970), and stored at -20°C until subjected to electrophoresis.

b. Identification of reassortant progeny clones by sodium dodecyl sulfate - polyacrylamide gel electrophoresis.

Gene segments of candidate reassortant clones were resolved by sodium dodecyl sulfate-polyacrylamide gel electrophoresis (SDS-PAGE) with 10% polyacrylamide slab gels (16.0 x 16.0 x 0.15cm) (Laemmli, 1970) at 18mA per slab for 45 hours. The gels were stained with ethidium bromide, and dsRNA visualized and photographed under ultraviolet irradiation. Electropherograms were recorded on Polaroid positive print film and Polaroid positive/negative print film. Gene segment identities were determined for each candidate clone from their electrophoretic mobilities and reassortant clones identified as described (Mustoe *et al*, 1978; Ramig *et al*, 1978; Sharpe *et al*, 1978; Hazelton and Coombs, 1995; Coombs et al, 1996).

4. Electron microscopy.

a. Thin section transmission electron microscopy.

All fixation and buffer washing steps were carried out at 4°C, buffer wash steps were for 10 minutes each, and the pelleting of cell suspensions was done at approximately 1000xg for 10 minutes. Fixed cells were pelleted and washed three times in 100mM sodium cacodylate, 10mM magnesium chloride, pH 7.4 (SC-Mg Buffer), post fixed in 1% osmium tetroxide in SC-Mg buffer, washed two times in fresh SC-Mg buffer, and

resuspended in low melting point agarose at 30°C (Yuan and Gulyas, 1981). The agarose/cell blocks were diced and dehydrated through a graded series of acetone, infiltrated, and embedded in medium DER 332-732 with a hard plastic composition (Hayat, 1985). Silver sections were cut on a diamond knife (Microstar, Huntsville, Texas) using an LKB Ultratome III ultramicrotome (LKB, Upsalla), mounted on uncoated copper grids (Maravac, Ltd, Halifax, NS), stained with ethanolic uranyl acetate, followed by lead citrate in 0.1M Sodium Hydroxide (Stempek and Ward, 1964; Venable and Coggeshell, 1965), and viewed at machine magnifications ranging from 4,500 to 100,000x in a Philips model 201 Electron Microscope (Philips Electron Optics, Eindhoven, Netherlands) at an acceleration voltage of 60KeV. Images were recorded on Kodak Direct Release Positive film 5302 (Kodak, Toronto, Ontario) and were printed on Kodak Polycontrast III paper using a Kodak Ektomatic print processing system.

b. Negative stain transmission electron microscopy (NS-TEM).

(1.) Determination of ideal staining conditions.

A panel of negative stains were tested both separately and in combination, and under different conditions in order to determine the best conditions for staining reovirus as previously described (Hazelton and Hammond, 1983). Blind review indicated that 2.5 mM Phosphotungstic Acid, pH 7.0 (PTA) provided the best overall staining medium.

(2.) Preparation and evaluation of cultures.

Monolayers were infected with T1L, T3D, *tsA279, tsE320,* or *tsI138* at MOIs of either

5 or 50 PFU/cell, allowed to attach, and incubated at permissive and restrictive temperatures for either 36 or 72 hours. In addition, T1L x *tsA279* reassortant clones LA279.08, LA279.10, LA279.11, LA279.15, LA279.56, and LA279.76 were cultured at 40°C for 72 hours. The isolation and identity of these reassortant clones is discussed in Chapter 4, and their examination is discussed in Chapter 6. After three freeze/thaw cycles the crude cell debris was cleared by centrifugation as described (Hammond *et al*, 1981), and viral and subviral particles separated from tissue culture debris by pelleting the cleared lysates through 30% potassium tartrate cushions, pH 7.2, in an Airfuge® (Beckman Instruments, Palo Alto, C) (A100 Rotor, 26psi, 1 hour). Pellets were resuspended in 0.1% glutaraldehyde in S-MEM, pH 7.2, fixed, viral materials centrifuged directly to carbon stabilized 400 mesh grids (Beckman Airfuge®, EM-90 Rotor, 26psi, 30 minutes) as previously described (Hammond *et al*, 1981), and stained with PTA. Samples were viewed and photographed at machine magnifications of 30,000x and 70,000x as described above. The relative proportion and type of particles produced in each infection was determined by directly counting the total number of particles in each of five randomly selected, non adjacent grid squares from the four outer quadrants and the central portion of the grid (Hammond *et al*, 1981, Hazelton and Coombs, in preparation). The infectious titer of each infection was determined as described (Chapter 2.2.f, above).

c. Immunoelectron microscopy (IEM).

(1.) Preparation of colloidal gold suspensions.

Gold probes were prepared from chloroauric acid by reduction with aleppo nutgall tannin (Mallinckrodt Chemicals) and filtered as described (Slot and Geuze, 1985).

(2.) Protein A affinity column purification of Immunoglobulin fraction G.

Hyperimmune whole rabbit anti-sera were preabsorbed against L929 monolayers. Immunoglobulin fraction G (IgG) fractions were prepared using a protein A:sepharose affinity column as described (Peeling *et al*, 1984). Briefly, heat inactivated antiserum was passed through a bed of protein A:sepharose (Sigma Chemical Co., St. Louis), washed with 50mM Tris, pH 8.0, 150mM sodium chloride (Running Buffer) and bound IgG was eluted directly into 0.5M Phosphate Buffer, pH 8.0 with 100mM sodium acetate, pH 4.0, 150mM sodium chloride (Elution Buffer). Ultraviolet absorbance at λ280 was determined and peak fractions pooled. The pooled fractions were dialyzed against 2mM sodium borate, pH 8.0, concentrated with a Minicon B-15 Concentrator (Millipore, Bedford, MA), ultraviolet absorbance measured at λ280, and the concentration of protein determined.

(3.) Adsorption isotherm assay to determine correct concentration of protein required to stabilize gold probe.

The concentration of IgG needed to stabilize the gold probe was determined by adsorption isotherm assay essentially as described (Geoghagen and Ackerman, 1977). Briefly, antibody in 2mM sodium borate was combined with gold probe at pH 8.0 and

incubated at room temperature. Sterile, filtered 10% sodium chloride was added and the absorbance measured at λ520. The concentration of IgG required to stabilize the aliquot of gold was determined as that concentration preceding a change of absorbance of greater than 10%. To ensure sufficient protein for complete conjugation the concentration calculated in the adsorption isotherm was doubled for the conjugation step (Geoghagen and Ackerman, 1977; Horisberger, 1989; Lucocq and Baschong, 1986; Vreeswijk *et al*, 1988).

(4.) Conjugation of colloidal gold and protein.

Except where otherwise indicated all conjugation steps were conducted at 20°C. Briefly, 10 parts gold probe, pH 8.0, was combined with the required amount of IgG in 4 parts sterile, filtered, glass redistilled water. After incubating for 5 minutes, Carbowax M20 (polyethylene glycol MW20,000, Sigma, Saint Louis, MO) was added to the reaction and it was allowed to stabilize. IgG:Gold was sedimented by centrifugation. The soft pellet was resuspended in 200mM Tris base, pH 8.0, 150mM sodium chloride, 0.05% Carbowax M20, 10% glycerol, (Stabilizing Buffer 1), and sonicated for 5 seconds with a Vibra Cell sonicator mini probe (Branson, Danbury, CONN) at 10% duty cycle, 35% output, to disrupt loose aggregates. The conjugates were washed 2 times by repelleting the gold:IgG conjugates, the soft pellet was resuspended in Stabilizing Buffer 1 with 0.2% (wt/vol) low bloom gelatin (Sigma, Saint Louis)(Stabilization Buffer 2)(Behnke *et al*, 1986), and sonicated as described.

(5.) Immunogold labeling of viral product.

Viral lysates from permissive and restrictive temperature cultures prepared at an MOI of 5 PFU/ml were prepared, cleared through 30% potassium tartrate, pH 7.2, and pelleted directly to 400 mesh formvar-carbon nickel Hex grids. The grids were washed by floating on drops of S-MEM, pH 8.0, buffered with N-2-hydroxyethylpiperizine-N-2-ethanesulfonic Acid (HEPES buffered S-MEM), pH 8.0, followed by HEPES buffered S-MEM with 1% bovine serum albumin (BSA), and then floated on a drop of Stabilization Buffer 2. The grids were immune reacted with the gold:IgG probes by incubation on 5μl aliquots of IgG labeled gold probes at 20°C for 30 minutes in a humid chamber. The grids were washed with successive changes of 10mM Phosphate Buffer, pH 8.0, 750mM sodium chloride (Gold-PBS) and the IgG:gold immune complexes were stabilized by floating the grids on a drop of fresh 0.1% glutaraldehyde in Gold-PBS. The grids were then washed briefly on 3 drops of Gold-PBS and stained with PTA. The samples were evaluated and photographed as described above.

5. Immunofluorescent Microscopy.

Immunofluorescent microscopy (IF) was performed essentially as described (Fields *et al*, 1971; Hazelton and Coombs, 1995; Illa *et al*, 1991). Briefly, cells grown on glass coverslips were infected with virus (T3D or the selected *ts* clone) at an MOI of 10 PFU/cell. After attachment at 4°C the infections were overlayed with pre-warmed, supplemented MEM and incubated at either 32°C or 40°C. Parallel infections were removed at set intervals, washed briefly in cold PBS that contained 1% BSA (PBS-BSA)

and fixed at -20°C with freshly prepared acetone:methanol (1:1). After further washing in cold PBS-BSA, nonspecific reactivity was blocked by incubation in PBS-BSA with 5% FCS (Blocking Buffer). The samples were incubated in a humid chamber in blocking buffer that contained preabsorbed 2% rabbit polyclonal anti-reovirus T3D antisera (primary antibody), washed in PBS-BSA and developed with rhodamine conjugated goat anti-rabbit IgG in blocking buffer (secondary antibody) in a light-safe humid chamber. The infections were examined in a fluorescent microscope, the infection level graded in accordance with the system described by Rhim (Rhim *et al*, 1962), and parallel IF and phase contrast exposures were made for each field using Fuji color slide film, ASA 1600. The proportion of infected cells in each field was determined from photographs by dividing the number fluorescing cells by the total number cells observed in the same field by phase microscopy.

6. Radiolabeling of viral encoded biomolecules

a. $^{32}PO_4^{-3}$ Organophosphate labeling of dsRNA.

Phosphate-containing biomolecules were labeled with $^{32}PO_4^{-3}$ during viral infection. Briefly, monolayers in six well cluster dishes were infected at predetermined MOIs, the virus allowed to attach at 4°C, washed, and overlayed with phosphate free S-MEM and incubated at permissive and restrictive temperatures to exhaust residual organophosphate. After 45 minutes incubation, sufficient labeled $^{32}PO_4^{-3}$ was added to provide for an activity level of 16.5μCi/ml of medium. The infections were incubated for equivalent replication cycles at each temperature.

b. ^{35}S-Methionine labeling of viral proteins.

Suspension cultures were prepared at an MOI of 5 PFU/cell as described. After attachment at 4°C for 45 minutes the infected cells were added to supplemented S-MEM pre-warmed to either 32°C (permissive) or 40°C (restrictive). The infections were incubated for an equivalent number of replication cycles at each temperature (36 hours for restrictive cultures and 54 hours for permissive cultures). Three hours post attachment sufficient ^{35}S-Methionine:Cysteine was added each culture to provide for an activity level of 25μCi/ml culture.

7. Isolation and characterization of viral dsRNA and assembly structures from labeled cultures.

a. Isolation of $^{32}PO_4^{-3}$ labeled dsRNA.

Crude cytoplasmic extracts were prepared from infections radiolabelled with ^{32}P essentially as described (Chapter 2.3.a). Briefly, cell monolayers were lysed with 0.5% NP-40, nuclei and cellular organelles sedimented, crude extracts of the supernatents treated with 250 μg/ml Proteinase K and 1% SDS (final concentrations), and extracted one time with phenol/chloroform. The dsRNA fraction was precipitated at -20°C in ethanol with sodium acetate, resuspended in electrophoresis sample buffer, and stored at -20°C until electrophoresed. Electrophoresis was conducted as described in Chapter 2.3.b.

b. Separation of assembly structures by isopycnic gradient centrifugation.

Infected cultures which contained labeled viral proteins were pelleted at 1200xg for 40 minutes, the pellets resuspended in cold 10mM Tris Base, pH 7.4, 250mM sodium chloride, 9.25μM 2-mercaptoethanol (BioRad, Richmond, VA) (HO Buffer) containing 0.2% desoxycholate and incubated for 30 minutes at 4°C. The incubations were sonicated for 20 seconds every 10 minutes with a Vibra Cell sonicator mini-probe (Branson, Danbury, CONN) at a duty cycle of 40% and with 35% output. The crude cytoplasmic fraction was extracted two times at 4°C with Genetron (1,1,2-trichloro-1,2,2-trifluoroethane).

The Genetron extracted material was separated on 1.2-1.55gm/ml CsCl gradients for 7½ to 16 hours at 35,000rpm in an SW41 rotor (Beckman Instruments, Inc., Palo Alto, CA), and 300μl fractions collected by bottom puncture. The refractive index for each fraction was determined with a Bosch and Lomb Abbe 3-L refractometer (Bosch and Lomb, Rochester, NY) and the density for each fraction calculated from standard CsCl refractive index:density tables (Sober, 1970). The profile of radiolabelled material in each gradient was determined by scintillation counting 10μl aliquots in a model LS 5000CE scintillation counter (Beckman Instruments, Palo Alto, CA).

c. <u>Separation of assembly structures by rate zonal gradient centrifugation.</u>

Aliquots from selected CsCl gradient fractions were slowly diluted 3 fold by sequentially adding 10% volume aliquots of 10mM Tris, 1mM ethylenediamine tetraacetic acid (EDTA), pH 8.0, and were layered over either 15 to 30% sucrose or 10 to 50% sucrose

gradients in 10mM Tris Base, pH 7.4, 1mM EDTA. Viral structures were separated by centrifugation for 2½ hours at 25,000 rpm at 4°C in an SW41 Rotor, and 300μl fractions collected by bottom puncture. The profile of radiolabelled material was determined by scintillation counting 20μl aliquots as described above.

d. Protease digestion evaluation of complete virions.

Permissively and restrictively assembled virions purified by isopycnic gradient centrifugation were dialyzed against 10mM Tris Base, pH 7.4, 150mM sodium chloride, 15mM magnesium chloride (dialysis buffer) and subjected to protease digestion at 37°C with either 200μg/ml α-chymotrypsin or trypsin, or 100μ/ml proteinase K or V8 Protease as described (Bass *et al*, 1990; Cleveland *et al*, 1986; Spendlove *et al*, 1963; Spendlove *et al*, 1965; Spendlove *et al*, 1970). Aliquots were taken at selected time intervals. The digestions were stopped by addition of protease inhibitor N-α-p-tosyl-L-lysine chloromethyl ketone (TLCK) for trypsin, or phenylmethylsufonyl fluoride (PMSF) for the remaining proteases (2.5mM final concentration inhibitor), and plunging into wet ice. The proteins were cold precipitated at -20°C by ethanol with sodium acetate. The precipitated proteins were dried, resuspended in electrophoresis sample buffer and stored at -20°C until electrophoresis.

e. Immunoprecipitation of viral assembly structures.

Aliquots from selected CsCl isopycnic gradient fractions of ^{35}S-Methionine:Cysteine radiolabelled cultures were slowly diluted three fold by sequentially adding 10% volume

aliquots of 50mM Tris Base pH8.0, 100mM sodium chloride. 0.5% NP-40 (lysis buffer) and viral structures were immunoprecipitated overnight, all at 4°C, using polyclonal anti-reovirus λ1 conjugated to *S. aureus* protein A:sepharose beads (Sigma Chemical, Saint Louis, MO) as described (Hazelton and Coombs, 1995, Hazelton and Coombs, in preparation). After washing to remove unbound material the beads were resuspended in electrophoresis buffer and stored at -20°C until electrophoresis.

f. Identification of labeled viral proteins by Polyacrylamide Gel Electrophoresis.

30μl aliquots of each CsCl fraction were diluted to 100μl with sterile distilled water and the proteins were precipitated at -20°C in ethanol with sodium acetate. 150μl aliquots of each sucrose fraction were diluted to 500μl with sterile distilled water and proteins precipitated at -20°C in ethanol with sodium acetate. The pellets were re-suspended in electrophoresis sample buffer (Laemmli, 1970) and stored at -20°C until electrophoresed.

(1.) Tris:glycine gradient gel SDS-PAGE.

Proteins were separated on 5-15% polyacrylamide gradient slab mini-gels (7 x 8 x 0.075cm) using a Mini-Protean II electrophoresis apparatus (BioRad, Richmond, VA) at 180 Volts for 45 minutes.

(2.) Tris:Glycine/Urea SDS-PAGE.

Proteins were separated on 0.1 x 16 x 20 cm slab gels using a tris:glycine/urea gradient

gel system (TGU) as described (Coombs, 1998a; Hazelton and Coombs, in preparation). A 16 to 5% polyacrylamide:5 to 2.5% glycerol exponential gradient was covered by a continuously poured 5 to 4% polyacrylamide:2.5 to 2% glycerol linear gradient. Both linear and exponential gradients contained 43% urea. A 4% polyacrylamide:2% glycerol step without urea was poured over the gradient. The whole system was in 375mM Tris base, pH 8.8. Gels were polymerized for 6 to 10 hours, a 3.75% polyacrylamide discontinuous stacking gel in 125mM Tris base, pH 6.0 was layered over the resolving gel (Laemmli, 1970) and the proteins were separated by electrophoresis at either 9mA for 9½ hours or 7½mA for 16 hours.

g. <u>Western blot analysis of the protein composition of viral assembly structures.</u>

Proteins separated on unfixed TGU and tris-glycine SDS-PAGE gels were transferred to nylon membranes (Immobilon, Millipore, Bedford, MA) using a Semi-Dry Transblot Transfer system (BioRad, Richmond, VA) and stained lightly with Ponceau Stain to confirm protein transfer. The membranes were blocked with skim milk proteins in 10mM Tris base, pH 7.5, 100mM sodium chloride containing 0.1% Tween 20 (TBS-T). The membranes were probed with polyvalent rabbit anti-whole reovirus antiserum pooled with rabbit polyclonal anti-reovirus μ2 antiserum. After probing the membranes were washed with TBS-T and probed with horseradish peroxidase (Jackson ImmunoResearch Labs, West Grove, PA) conjugated goat anti-rabbit IgG. Immune complexes were detected with diamino benzoate (DAB) as described (Hazelton and Coombs, in

preparation).

h. Autoradiography of labeled viral products in SDS-PAGE.

(1.) Autoradiography of $^{32}PO_4^{-3}$ labeled viral products.

Radiolabelled dsRNA segments were resolved by polyacrylamide gel electrophoresis as described above. After ethidium bromide staining to confirm the presence of dsRNA the gels were dried and developed by exposure to Kodak X-AR X-Ray film.

(2.) Fluorography of ^{35}S-Methionine/Cysteine Labeled viral products.

Viral proteins were radiolabelled and resolved in either TGU or tris-glycine SDS-PAGE gel systems as described above. After fixing in acetic acid:methanol the gels were impregnated with Enlightening (Dupont, Boston, MA), dried and fluorographed by exposure to Kodak X-AR sheet film (Kodak, Rochester, NY).

8. Sequencing the Reovirus T3D and *tsA279* temperature sensitive mutant M2 gene segment.

The procedures for cycle sequencing were conducted in accordance with the protocol provided for the Gibco BRL Life Sciences dsDNA Cycle Sequencing System (Gibco BRL) except as noted.

a. Primer design for Reverse Transcriptase copying and Polymerase Chain Reaction amplification of the M2 gene segment.

A panel of 12 primers were designed using the published sequence for the Reovirus T3D M2 gene segment (Jayasuriya et al, 1988, Wiener et al 1988). Primers T3M2-01 through T3M2-06 were complementary to the positive sense strand, while primers T3M2-07 through T3M2-12 were complementary to the negative strand. Primer T3M2-01, and T3M2-07 were complimentary to sequences which were upstream of the open reading frame boundaries for μ1, thereby allowing the entire open reading frame to be amplified and sequenced. The melting temperature for each primer was calculated from the formula:

Melting Temperature = $\{4x(nC+nG) + 2x(nA+nT)\}°C$ (Itakura *et al*, 1984).

The primers, their location in the genome segment and their melting temperatures are given in Table 2.2. The primers were initially synthesized on an Oligo 1000 DNA Synthesizer (Beckman Instruments, Palo Alto, CA) or latterly obtained from Gibco BRL.

b. <u>Preparation of gene segment template.</u>

Cytoplasmic extracts were prepared from infected cultures of T3D or the mutant *tsA279* essentially as already described. The extracts were treated two times with phenol/chloroform, followed by an extraction with chloroform only, precipitated at -20°C in ethanol with Sodium Acetate, the precipitated nucleic acids dried, resuspended in RNase free 90% Dimethyl Sulfoxide, 1mM Tris Base, pH 6.8, and stored at -20°C until use (Bassel-Duby *et al*, 1986).

Table 2.2 **Primers for Reverse transcriptase and polymerase chain reaction amplification and sequencing of the M2 gene segment of tsA279.§**

Primer	Strand	First Base	Last Base	Sequence	Total Bases	% GC	Melting Temperature (°C)
M2-01	+	7	24	CTG CTG ACC GTT ACT CTG	18	55	56
M2-02	+	393	407	CGT GAG TTC CTT GAC	15	53	46
M2-03	+	789	803	GAA GGC ACC GTG ATG	15	60	48
M2-04	+	1194	1209	GAG ACG ACG TGG GAT C	16	62	52
M2-05	+	1592	1606	CTA CAC TCC AGA ATC C	16	50	48
M2-06	+	1985	2000	CTC ATC TGA GTC TAT C	16	44	46
M2-06a	+	1984	2001	GCT CAT CTG AGT CTA TCC	18	50	54
M2-07	-	8	25	TGC CTG CAT CCC TTA ACC	18	55	56
M2-08	-	366	380	GAA AGC CTG CAT TGC	15	53	46
M2-09	-	804	818	CAA CTG CTC AGG CTC	15	60	48
M2-10	-	1206	1220	CAC ATT ATA ATC TGC	15	33	40
M2-10a	-	1235	1248	TGG CAA ACA CGG GTG	15	60	48
M2-11	-	1598	1614	GAG ATC AAT CTC CCA C	16	50	48
M2-12	-	2031	2045	CCA TGG TA CCC TCC	15	60	48

§ Primers derived from sequence data by Jayasuriya *et al*, 1988.

c. **Reverse transcriptase preparation of T3D and *tsA279* M2 gene segment cDNA.**

Aliquots of the gene template preparations to be copied and amplified were melted at 50°C and snap cooled by plunging into wet ice with simultaneous addition of cold RNase free sterile water. A final reaction mix was prepared containing 32 units RNasin, 100μM each of primers #1 and #7, 500μM each of dATP, dCTP, dGTP, and dTTP, 50mM Tris base, pH8.0, 2.5mM potassium chloride, mM magnesium chloride, 0.01% BSA, 0.01% dithiothreitol, and 160 Units Superscript II® reverse transcriptase enzyme (Gibco BRL) in 100 μl reaction mix volume, and the reaction mix incubated for 1 hour at 42°C. The reactions were placed in wet ice and immediately amplified by polymerase chain reaction (PCR).

d. **Polymerase Chain Reaction amplification of reoviral M2 cDNA.**

A PCR reaction mix was prepared containing the cDNA preparations, and 10mM Tris base, pH 8.3, 50mM potassium chloride, 2.75mM magnesium chloride, 0.001% gelatin, 1.0mM each of primers #1 and #7, 500μM each of dATP, dCTP, dGTP, and dTTP, and 20 Units AmpliTaq DNA polymerase (F. Hoffmann - La Roche, Basel, Switzerland), the mix was diluted to 600μl reaction mix final volume. The reaction mix was divided into 100μl aliquots for incubation. The cDNA was amplified by thermal cycling through the following conditions: pre-heating to 95°C for 3 minutes; five cycles of 1½ minutes at 95°C, 1½ minutes at 44°C and 3 minutes at 72°C; 35 cycles of 1½ minutes at 92°C, 1½ minutes at 44°C, and 3 minutes at 72°C; and 10 minutes at 72°C.

e. **Purification, quantification and identification, of polymerase chain reaction product.**

Reovirus T3D and *tsA279* M2 gene segment cDNA PCR product was originally precipitated in ethanol with Sodium Acetate, the precipitated nucleic acids dried and resuspended in sterile distilled water. Later preparations were purified using the QIAquick PCR Purification Kit (QIAGEN, Hilden, Germany) in accordance with the manufacturer's instructions, with the PCR cDNA product eluted into 10mM Tris base, pH8.5. PCR products were separated at 115 Volts for approximately 1 hour in 9 x 11 cm 0.9% agarose horizontal slab gels in 45mM Tris Base, 45mM boric acid, 1mM EDTA, pH 8.0 (0.5x TBE), containing 1μl/ml ethidium bromide. The gels were exposed to ultraviolet irradiation and the bands of fluorescing nucleic acids at approximately 2.2Kbp in length were excised. The cDNA product was purified with silica matrix, initially using the Prep-A-Gene system (BioRad, Richmond, VA) with elution into the manufacturer's elution buffer, and latterly the QIAquick Gel Extraction Kit spin columns (QIAGEN, Hilden, Germany) with elution into 10mM Tris base, pH 8.5. Silica matrix purifications were done in accordance with the respective manufacturer's protocols. The concentration of cDNA in each preparation was determined by running cDNA aliquots parallel to 100 and 1000 bp dsDNA ladder markers of known concentration (Gibco BRL). The identity of the M2 cDNA was confirmed by reviewing the endonuclease digestion fragment pattern obtained when aliquots from each cDNA amplification were digested with the restriction endonucleases Bam HI, Eco RI, Hind III, and Pst I with the expected pattern.

f. **Polymerase Chain Reaction cycle sequencing of the T3D and tsA279 M2 gene segment cDNA.**

Cycle sequencing was conducted using the protocol provided for the Gibco BRL Life Sciences dsDNA Cycle Sequencing System (Gibco BRL; Murray, 1989; Craxton, 1991). Briefly, primers were ^{32}P end labeled using ^{32}P-γATP and T4 Polynucleotide Kinase at 37°C. Termination mixes containing 100μM each dATP, dCTP, dGTP, and dTTP and containing either 2mM ddATP (Mix A), 1mM ddCTP (Mix C), 0.2mM ddGTP (Mix G), or 2mM ddTTP (Mix T) were utilized for the dideoxy sequencing reactions. Alternatively, 100μM dITP was substituted for dGTP in the termination mixes used in some sequencing reactions to accommodate reading problems caused by possible G:C compressions in the sequencing gels (Barnes *et al*, 1983, Gough and Murray, 1983). The sequencing reactions were conducted in reaction mixes containing 10mM Tris base, pH 8.3, 50mM potassium chloride, 5mM magnesium chloride, 0.001% gelatin, 66ng cDNA (30ng cDNA/Kb template length) and 2.5Units AmpliTaq® DNA. Cycle sequencing was done in accordance with the following schedule: pre-heating to 95°C for 3 minutes; 20 cycles of 30 seconds at 95°C, 30 seconds at 53°C and 60 seconds at 70°C; 10 cycles of 30 seconds at 92°C, 1½ minutes at 53°C, and 60 seconds at 70°C. After addition of formamide/dye stop solution the sequencing reactions were stored at -20°C.

g. **Polyacrylamide gel electrophoresis separation of sequencing products.**

Reaction products were heated to 95°C and snap cooled by immersion into wet ice, and were resolved on 8% and 6% polyacrylamide sequencing gels containing

0.5x TBE with 65-70mA per gel constant current. The mutant and wild type reactions for each primer were run next to each other to assist in identification of mutation events. Gels were dried and autoradiographs were prepared by exposure to Kodak X-Omat AR x-ray film.

CHAPTER 3

Mapping the Temperature Sensitive Lesions of the Study Clones

1. Introduction.

Reovirus has several unique biophysical and genetic properties which make it well suited for mapping phenotypic traits. First, the genome is divided into ten segments. These segments may be thought of in a similar manner as eukaryotic chromosomes, with the exception that most reoviral segments are monocistronic. One segment, the S1 segment, is bicistronic. Second, the gene segments are double stranded RNA (dsRNA). Therefore, they are resistant to degradation during processing. Third, the gene segments may be readily resolved on 10% polyacrylamide gels, stained with ethidium bromide and visualized under ultraviolet irradiation. Fourth, the reovirus family has at least three distinct serotypes, each having unique migration rates for their compliment of genome segments. Fifth, the serotypes are able to interact in mixed infections and produce progeny with a mixed genomic compliment (Figure 3.1). Finally, infectious progeny virions contain only one copy of each gene segment. For recent reviews see Nibert *et al*, 1996b, and Coombs, 1998b.

The ability to reassort during mixed infections may be used to sort large panels of mutants into recombination groups on the assumption that mutants which do not recombine to produce wild type progeny must contain a lesion in the same gene segment(s) (Fields and Joklik, 1969; Ramig, 1983). Where a distinct phenotype may be

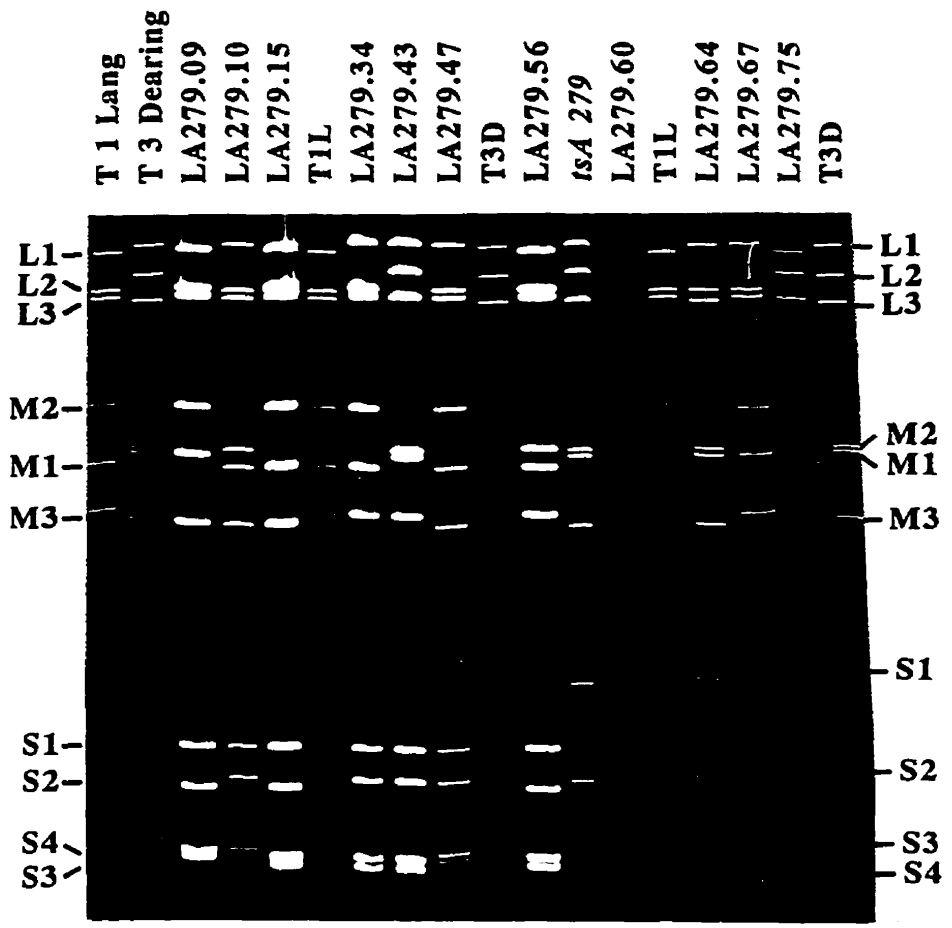

Figure 3.1. Sodium Dodecyl Sulfate Polyacrylamide Gel Electropherogram of dsRNA from T1 Lang, T3 Dearing, Mutant *tsA279*, and T1L x *tsA279* Reassortant Progeny Clones.

Gene segments from approximately 4 x 10^6 cells infected with the indicated clones were resolved in a 10% slab gel (16.0 x 16.0 x 0.15cm) at a constant current of 18mA for 46 hours, stained with ethidium bromide and photographed under ultraviolet irradiation. Positions and identites of the T1L and T3D genes are located on the left and right sides, respectively.

identified with one reovirus serotype it is possible to use the genetic properties to create reassortants, the biophysical properties to identify the parentage of each gene segment, and analyze a reassortant panel for the presence or absence of the phenotypic trait. Reassortant analysis provides a finer level of resolution which may associate the phenotype with one gene segment.

Recombination mapping had been utilized to sort the previously isolated *ts* mutants of the Fields' panel into recombination groups (Fields and Joklik, 1969; Cross and Fields, 1972; Ramig *et al*, 1983), and the *ts* lesion had been mapped to specific gene segments for prototype mutants from nine out of ten recombination groups by reassortant analysis (Mustoe et al, 1978; Ramig et al, 1978; Ramig et al, 1983; Coombs, 1996). Candidate *ts* clones were isolated during initial studies (Appendix B). Modified assay methods made it possible to clearly confirm that the mutants identified for investigation were all temperature sensitive (Appendix B.2). It was, however, necessary to confirm that the clones were as reported (Appendix B.1). Further, the genetic composition of the isolated mutants in the study had not been verified. Therefore, confirmatory mapping was undertaken for the mutants in the study.

2. <u>Confirmation of the recombination grouping of the test clones.</u>

Recombination grouping was performed as described (Fields and Joklik, 1969). Essentially, sub-confluent L929 monolayers were infected at an MOI of 5 PFU/cell with each of: 1. the clones under evaluation (*tsA201, tsA279, tsA340, tsE320, tsH26/8-3,*

tsI138 (1/80), tsI138 (12/82), and *tsJ128-1,*); and 2. a panel of mutants from the remaining Reassortment Groups. Excess inoculum was removed after one hour adsorption at 4°C, supplemented S-MEM with antibiotics was added, and the infections were incubated at 32°C for 33 hours. Viral lysates were prepared by freeze/thaw followed by a brief burst of sonication with a Branson Vibra Cell mini probe sonicator. Lysates were titred at 32°C, 39°C and 40°C and the proportion of reassortment was determined from the relationship:

$$\{[(Yield\ A \times B)^R - (Yield\ A^R + Yield\ B^R)] \div [Yield\ A \times B)^P\} \times 100$$

where (A x B) represents the mutants crossed in the particular infection, yield is the infectious titre of the infection at the indicated temperature, and R and P are the restrictive and permissive temperatures, respectively, used for titration (Fields and Joklik, 1969).

3. Reassortant mapping of the *ts* lesions.

The *ts* lesions were mapped for each mutant in the study using reassortants generated at 32°C. Except where noted, between 72 and 82 plaques were isolated from each mixed infection lysate, amplified through two passages, cytoplasmic extracts prepared from each second passage stock, the dsRNA resolved in polyacrylamide slab gels, and gene segments identified by electrophoretic migration as described above (Chapter 2.2, 2.3). Infections which showed no CPE were harvested after seven days culture and extracts were prepared. Gene segment identities were determined from their electrophoretic mobilities as described (Mustoe *et al*, 1978; Ramig *et al*, 1978; Sharpe *et al*, 1978;

Hazelton and Coombs, 1995) and EOP values determined for reassortant clones. The electropherotypes for panel members were analyzed collaterally with EOP values for the reassortant clones to determine which gene segment(s), if any, were associated with expression of the *ts* phenotype for each parent clone examined.

4. Results of recombination grouping of the test clones.

Where two clones have lesions in different gene segments, the restrictive titre of progeny in the mixed infection culture will be similar to the permissive titre of progeny. Recombination assay values for such situations generally range upwards of 10% (eg. Fields and Joklik, 1969, Ramig *et al*, 1983). Where the lesions are on the same gene segment the restrictive titre of progeny in the mixed infection culture will be similar to the restrictive titre for each parental clone parallel condition. Theoretically such values would approach 0.00. For example, mutant clone *tsA340* does not recombine with the clone *tsA279*, as indicated by the recombination value of -0.01, but does recombine with the mutant clone *tsE320*, as indicated by the recombination value of 0.74 (Table 3.1). The results of the recombination assay at 40°C are shown in Table 3.1. The three recombination group A clones did not recombine with each other, nor with the clone *tsH26/8-3* (recombination values ranging from negative to 0.00%). The recombination values also indicate the *tsA201* and *tsA340* clones did not recombine with the *tsB352* nor the *tsF556* clones, and the *tsA340* clone also failed to recombine with the *tsB271* clone. The *tsE320* clone, with recombination values from 0.84 to 9.27%, recombined with all other clones in the panel. In addition to not recombining with the group A clones, the

Table 3.1. **Recombination[a,b] testing of *tsA201, tsA279, tsE320, tsH26/8-3, ts138,* and *tsJ128* against prototype clones from the Fields' panel of temperature sensitive mutants of reovirus.**

Clone	*tsA201*	*tsA279*	*tsA340*	*tsE320*	*tsH26/8-3*	*I138*	*tsJ128*	*tsB271*	*tsB352*	*tsB405*	*tsC447*	*tsD357*	*tsF556*	*tsG453*
tsA201	--	-0.06	-0.06	0.62	-0.035	0.66	1.055	1.00	0.00	0.27	0.07	2.33	-1.265	0995
tsA279		--	-0.01	1.66	1.07	0.08	1.68	ND	0.18	0.93	0.29	2.99	0.16	1.53
tsA340			--	0.74	0.00	0.00	0.03	-0.02	0.015	0.195	0.195	0.90	0.01	0.03
tsE320				--	0.84	ND	4.10	3.32	1.135	2.44	1.475	3.535	0.93	9.27
tsH26/8-3					--	0.00	3.25	0.00	0.00	0.00	0.775	1.93	0.125	0.02
tsI138						--	0.00	0.00	0.44	ND	0.81	1.41	0.20	0.00
tsJ128							--	0.00	1.14	0.70	0.74	5.77	0.80	ND

a. Recombination determined by the formula $\left\{ [\text{titre } (AxB)_R - \text{titre } A_R - \text{titre } B_R] \div \text{titre } (AxB)_{32} \right\} \times 100$.

b. Restrictive temperature = 40°C.

tsH26/8-3 clone did not recombine with any of the group B or group I clones (recombination value 0.00%). The *tsI138* clone recombined variably with clones from recombination groups A, and B, and did not react with clones from groups G, H and J. Finally, the clone *tsJ128* failed to recombine with *tsB271* (Table 3.1).

5. Results of electropherotype mapping of the *ts* lesions.

a. Mapping the *tsA279* double *ts* lesion.

A total of 78 clones from the mixed infection were selected, amplified and electropherotyped. Four clones provided no growth and 34 had reassortant electropherotypes (reassortant efficiency = 45.9%), of which 30 were unique. There were seven monoreassortants portraying five unique reassortant patterns. One monoreassortant, *LA279.56*, had a *tsA279* M2 gene segment in a background of T1L gene segments (Figure 3.1, Table 3.2). Initial examination of *tsA279* x T1L reassortants provided contradictory interpretations. No gene segment was associated with the *ts* lesion at 39°C. However the L2 and M2 gene segments from the wild type T1L parent uniquely assorted to the ts^+ phenotype. When the panel was sorted by degree of temperature sensitivity at 40°C two classes of *ts* reassortants emerged, a strong *ts* phenotype associated with the *ts* parental M2 gene (reassortant clone LA279.43, Figure 3.2, Table 3.2) and a weak *ts* phenotype associated with the *ts* parental L2 gene segment (reassortant clone LA279.11, Figure 3.2, Table 3.2). Review of the EOP values obtained at 39°C and 39.5°C with the sorted values obtained at 40°C showed that all clones in the set of mild *ts* reassortants at 40°C were mildly *ts* at 39°C and 39.5°C. In

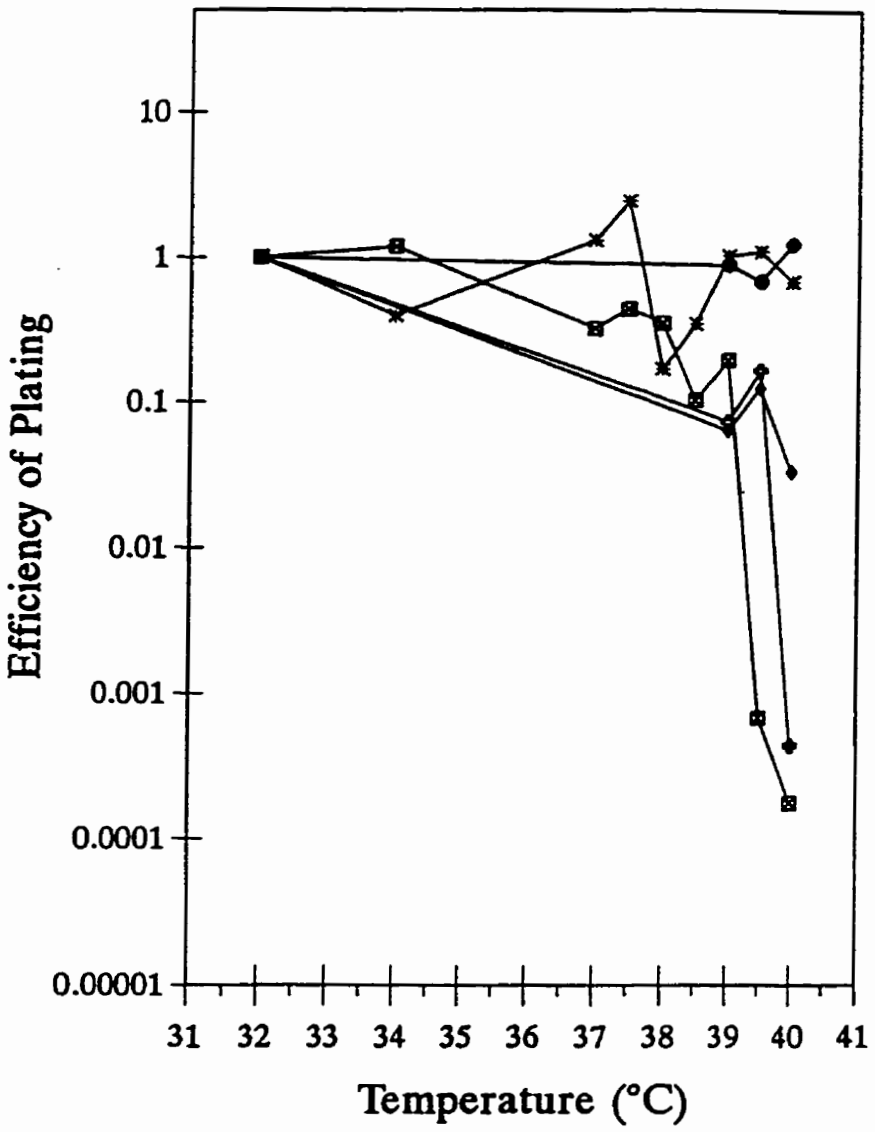

Figure 3.2 **Temperature profile of efficiency of plating (EOP) values for T1 Lang, *tsA279*, and wild type, mild *ts* and strong *ts* phenotype T1L x *tsA279* reassortants.**

EOP values of T1L (*), *tsA279* (⊗), and selected T1L x *tsA279* reassortants {LA279.09 (●), LA279.11 (◆), and LA279.43 (+)}, determined as described (Chapter 2.2, 2.3)

Table 3.2. Electropherotypes and EOP†s of T1 Lang/tsA279 reassortants

	Gene Segment										EOP†	
CLONE	L1	L2	L3	M1	M2	M3	S1	S2	S3	S4	39/32	40/32
LA279.08	1§	A	1	A	A	A	A	A	A	A	0.000139	0.000002
LA279.77	1	A	1	A	A	A	A	A	A	A	0.000057	0.000011
LA279.64	A	1	1	A	A	A	A	A	1	A	0.000557	0.000032
LA279.75	1	A	1	1	A	A	A	1	A	1	0.00338	0.000072
LA279.20	A	A	1	1	A	A	1	A	A	1	0.00568	0.000142
LA279.53	A	A	1	A	A	A	A	A	A	1	0.0802	0.000158
LA279.28	A	A	A	1	A	A	1	A	1	1	0.000019	0.000195
LA279.43	A	A	1	A	A	1	1	A	1	1	0.0156	0.000218
LA279.10	A	1	1	1	A	A	1	A	A	A	0.024	0.000441
LA279.60	1	1	A	1	A	A	1	A	1	1	0.0735	0.000507
LA279.55	1	A	A	A	A	A	A	A	A	A	0.000035	0.00073
tsA279	A	A	A	A	A	A	A	A	A	A	0.045	0.000933
LA279.56	1	1	1	1	A	1	1	1	1	1	0.171	0.00406
tsA279/T1	6/6	8/4	3/9	6/6	12/0	10/2	6/6	10/2	7/5	5/7		
LA279.41	1	A	1	1	1	A	A	A	A	A	0.0197	0.00296
LA279.76	A	A	1	1	1	1	1	1	A	A	0.0199	0.0199
LA279.11	A	A	A	A	1	A	A	A	A	1	0.063	0.0331
LA279.45	A	A	1	A	1	A	A	A	A	1	0.0395	0.0362
LA279.39	A	A	1	1	1	A	1	1	1	1	0.105	0.0432
LA279.31	1	A	1	1	1	A	1	A	A	1	0.382	0.0465
LA279.42	1	A	1	1	1	A	1	A	A	1	0.0589	0.0472
tsA279/T1	4/3	7/0	1/6	2/5	0/7	6/1	3/4	5/2	1/6	2/5		
LA279.05	A	1	1	1	1	1	1	1	A	A	0.647	0.314
LA279.12	1	1	1	A	1	1	1	1	1	1	0.728	0.369
LA279.15	1	1	1	1	1	A	1	1	1	1	0.465	0.392
LA279.46	1	1	1	1	1	A	1	1	1	1	0.82	0.447
LA279.06	1	1	1	1	1	A	1	A	1	1	0.933	0.505
LA279.47	A	1	1	1	1	A	1	A	A	1	1.92	0.708
LA279.63	1	1	A	1	1	1	1	A	1	1	1.24	0.713
T1L	1	1	1	1	1	1	1	1	1	1	2.8	0.748
LA279.67	A	1	1	A	1	1	1	A	1	A	1.52	0.913
LA279.16	A	1	1	1	1	1	A	A	A	1	0.852	0.974
LA279.33	1	1	1	1	1	1	1	1	A	1	0.197	1.03
LA279.09	1	1	1	A	1	A	1	1	A	1	0.885	1.23
LA279.48	1	1	1	A	1	1	1	A	1	1	0.701	1.31
LA279.34	A	1	1	1	1	1	1	A	1	1	0.524	1.42
LA279.73	1	1	1	A	1	1	1	1	A	1	0.834	1.49
LA279.21	1	1	1	1	1	A	1	1	1	1	0.741	3.99
tsA279/T1	5/10	0/15	1/14	5/10	0/15	6/9	1/14	7/8	6/9	2/13		

†: EOP : Efficiency of Plating (titre @ 39°C or 40°C) ÷ (titre @ 32°C). Ranked by EOP at 40°C.
§: Denotes parental origin of gene; 1: T1Lang; A: *tsA279*

most cases increasing the restrictive temperature improved *ts* expression by less than 3 fold. The class of strong *ts* mutants provided a range of ts^+ and *ts* EOP values at 39°C. The level of temperature sensitivity increased gradually by 3 or more orders of magnitude as the temperature was increased in steps to 40°C (Figure 3.2, Table 3.2). The mono-reassortant *LA279.56* was a member of the strong *ts* panel. The remaining 8 gene segments were randomly distributed between the parental genotypes.

b. Mapping the *tsA201 ts* lesion.

A total of 78 candidate reassortant clones were selected to map the lesion for *tsA201*. Four clones provided no growth, 3 clones were of mixed electropherotypes and 3 clones were not available for testing due to insufficient sample. There were 25 clones with reassortant electropherotypes (reassortant efficiency = 35.2%), with 5 mono-reassortants demonstrating 4 unique reassortant patterns, for a total of 24 unique electropherotypes. One monoreassortant, *LA201.69*, had a *tsA201* M2 gene segment in a background of T1L gene segments. The mutant M2 gene segment was associated with the panel of *ts* clones, and the T1L M2 gene segment was associated with the panel of ts^+ clones. The M2 monoreassortant clone *LA201.69* was a member of the *ts* panel. All other 9 gene segments were randomly assorted between the different serotypes. This confirms the previously reported mapping for the mutant lesion (Mustoe *et al*, 1978)(Table 3.3).

c. Mapping the *tsE320 ts* lesion.

A total of 164 clones were selected in two series of experiments. In the first experiment

Table 3.3. Electropherotypes and EOP†s of T1 Lang/*tsA201* reassortants.

	Gene Segment										EOP†	
CLONE	L1	L2	L3	M1	M2	M3	S1	S2	S3	S4	39/32	40/32
LA201.05	A§	A	A	1	A	A	A	A	A	A	0.000041	0.000001
LA201.39	A	A	A	A	A	1	A	A	1	A	0.000120	0.000005
LA201.48	A	A	A	A	A	A	A	1	A	A	0.000272	0.000006
LA201.59	A	A	A	A	A	1	1	A	1	1	0.000474	0.000046
LA201.51	1	1	1	1	A	A	A	1	A	A	0.000498	0.000133
LA201.36	A	A	1	1	A	1	1	A	A	A	0.001460	0.000870
LA201.65	1	A	A	A	A	A	1	A	1	A	0.001580	0.000160
LA201.04	A	1	A	A	A	A	A	A	A	A	0.001620	0.000148
LA201.69	1	1	1	1	A	1	1	1	1	1	0.002170	0.000355
LA201.44	1	A	A	A	A	1	1	1	A	A	0.002210	0.000065
LA201.47	1	1	1	A	A	A	A	1	A	A	0.003030	0.000402
tsA201	**A**	**A**	**A**	**A**	**A**	**A**	**A**	**A**	**A**	**A**	**0.00714**	**0.000714**
LA201.74	A	A	A	A	A	A	A	1	A	1	0.010400	0.000183
LA201.30	1	1	1	1	A	A	1	A	1	1	0.024100	0.000577
LA201.22	A	1	A	A	A	A	A	1	A	A	0.026700	0.003370
tsA201/T1	8/6	8/6	9/5	9/5	14/0	9/5	8/6	7/7	9/5	10/4		
LA201.34	1	A	1	A	1	1	1	A	A	1	0.41	0.57
LA201.12	1	A	1	1	1	1	A	A	A	1	0.58	0.12
LA201.46	A	A	1	A	1	A	A	A	A	A	0.86	1.21
LA201.35	A	1	A	1	1	A	A	1	A	1	1.00	1.23
LA201.52	1	1	1	A	1	1	1	1	1	1	1.28	2.00
LA201.43	A	1	1	1	1	1	1	1	1	1	1.65	0.94
LA201.26	1	A	1	1	1	1	A	1	A	1	2.12	0.74
LA201.28	A	1	1	1	1	1	1	1	1	1	2.71	2.23
T1L	**1**	**1**	**1**	**1**	**1**	**1**	**1**	**1**	**1**	**1**	**2.91**	**1.47**
LA201.33	1	1	1	A	1	1	1	1	A	A	2.97	3.52
LA201.16	1	1	1	1	1	1	1	1	A	A	10.40	10.70
LA201.58	A	1	1	1	1	1	1	A	1	1	27.80	12.80
tsA201/T1	5/6	4/7	1/10	4/7	0/11	2/9	4/7	4/7	7/4	3/8		

†: EOP : Efficiency of Plating (titre @ 39°C or 40°C) ÷ (Titre @ 32°C). Ranked by EOP at 40°C.
§: Denotes parental origin of gene; 1: T1Lang; A: *tsA201*.

81 clones were selected, of which 2 showed no growth and 75 were parental T1L. Due to the low success in manufacture of reassortants a fresh panel was prepared with freshly titred parental stocks. 83 candidate reassortant clones were selected. One clone showed no growth and 5 were of mixed electropherotype. A total of 35 reassortant clones, representing 31 unique gene patterns, were identified from the second panel (reassortant efficiency = 45.5%). Eight monoreassortants with 4 different genotypes were identified. One monoreassortant, clone *LE320.158*, contained a T1L S3 gene segment in a field of *tsE320* gene segments. Three clones were not available for further testing. The mutant S3 gene segment was associated solely with the panel of *ts* clones, and the T1L S3 gene was assorted to the ts^+ set of clones. The T1L S3 mono-reassortant *LE320.158* was a member of the ts^+ panel. All other 9 gene segments were randomly assorted. This confirms the previously reported mapping (Ramig *et al*, 1978)(Table 3.4).

d. Mapping the *tsH26/8-3 ts* lesion.

Two panels with 80 candidate reassortant clones were generated from two different stocks of clone 26/8-3 (total reassortant candidate clones tested = 160). The first panel (parental clone *tsH26/8-3*, P4c) contained 2 clones with no growth, 1 clone of mixed parentage, and 28 reassortants with 26 unique electropherotypes (reassortant efficiency = 35.9%). Six reassortant clones were monoreassortants. The mutant L2 gene segment was associated with the *ts* set of clones while the T1L L2 gene segment assorted uniquely to the ts^+ set of reassortants. The *tsH26/8-3* M1 gene segment was present in 15 of 17 *ts* phenotype clones and the T1L M1 segment was present 9 of 11 ts^+ clones All other

Table 3.4. Electropherotypes and EOP†s of T1 Lang/*tsE320* reassortants.

	Gene Segment										EOP†
CLONE	L1	L2	L3	M1	M2	M3	S1	S2	S3	S4	39/32
LE320.29	E	E	E	E	E	E	1	E	E	1	ND[a]
LE320.66	1	1	1	E	1	E	1	1	E	1	ND[a]
LE320.115	1	E	1	1	E	1	1	E	E	1	0.000068
LE320.87	1	1	1	1	E	1	1	1	E	1	0.000377
LE320.140	E	E	E	E	E	E	1	E	E	E	0.001514
LE320.141	1	E	1	E	E	1	E	E	E	1	0.001630
LE320.137	E	1	1	1	E	1	1	1	E	1	0.001788
LE320.101	E	E	E	E	E	1	1	1	E	E	0.002000
LE320.162	E	E	E	E	E	1	E	E	E	E	0.003561
LE320.142	E	E	E	E	E	E	1	E	E	E	0.007692
LE320.161	1	E	E	E	E	E	E	E	E	E	0.008571
LE320.106	E	E	E	E	E	E	1	E	E	E	0.010710
LE320.86	E	1	E	E	E	E	1	E	E	1	0.015200
LE320.114	1	E	1	E	E	E	E	1	E	1	0.015330
LE320.129	1	E	E	E	E	E	E	E	E	E	0.016030
LE320.104	1	E	E	E	E	E	E	E	E	1	0.016430
LE320.139	E	E	1	1	1	1	E	E	E	E	0.017580
LE320.121	1	E	1	1	E	1	E	1	E	E	0.018570
LE320.112	1	1	1	E	1	E	E	E	E	1	0.020530
LE320.152	E	E	E	E	E	E	E	E	E	1	0.020910
LE320.111	E	1	1	E	E	E	E	E	E	E	0.021460
LE320.159	1	E	E	E	E	E	E	E	E	E	0.025000
tsE320	**E**	**E**	**E**	**E**	**E**	**E**	**E**	**E**	**E**	**E**	**0.076**
tsE320/T1L	11/11	16/5	12/10	17/5	19/3	14/8	12/10	16/6	21/0	11/11	
LE320.123	E	E	E	1	E	1	1	1	1	1	0.2308
LE320.164	E	1	E	E	E	E	1	E	1	1	0.4080
LE320.144	1	E	1	E	E	E	E	E	1	E	0.4754
LE320.132	E	1	1	E	E	E	1	1	1	E	0.5258
LE320.85	E	1	1	E	E	E	1	E	1	E	0.5565
LE320.109	E	E	1	E	E	E	E	E	1	1	0.5972
LE320.158	E	E	E	E	E	E	E	E	1	E	0.6111
LE320.92	1	E	1	E	1	E	1	E	1	1	0.6364
LE320.118	E	E	E	1	1	1	1	1	1	1	0.7917
LE320.105	1	1	E	1	E	1	1	E	1	1	0.8000
LE320.149	1	1	1	1	1	1	1	1	1	1	0.9000
LE320.113	1	E	1	1	E	1	1	E	1	1	1.9000
LE320.156	E	E	E	1	1	E	1	E	1	1	2.0770
T1L	**1**	**1**	**1**	**1**	**1**	**1**	**1**	**1**	**1**	**1**	**2.800**
LE320.97	1	1	1	1	1	E	E	E	1	1	3.2291
tsE320/T1L	8/6	8/6	6/8	7/7	9/5	9/5	4/10	10/4	0/14	4/10	

a. EOP not done @ 39°C. EOP_{40} : LE320.29 = 0.0000355; LE320.66 = 0.0750

†: EOP : Efficiency of Plating (titre @ 39°C) ÷ (titre @ 32°C). Ranked by EOP at 40°C.

§: Denotes parental origin of gene; 1: T1Lang; E: *tsE320*

8 gene segments were randomly assorted between the different serotypes.

The lesion for mutant clone *tsH26/8-3* had been previously mapped to the M1 gene segment (Ramig *et al*, 1983). Because the mapping for this clone did not confirm the previous results the mapping was repeated using a different clone. A second panel of 80 candidate reassortants was generated from the stock clone *tsH26/8-3*, P4a. The panel contained 3 clones which showed no growth, 3 of mixed genetic composition and 15 reassortant clones (2 monoreassortants), each with a unique gene pattern (reassortment efficiency = 19.5%). As before, all clones in the *ts* set contained the L2 gene segment from the *tsH26/8-3* parent, while all 3 clones in the ts^+ panel derived their L2 gene segment from the T1L parent. The M1 gene was randomly assorted between the two sets of clones. The remaining 8 gene segments were also randomly selected in each phenotypic group. This confirms that the clone of mutant *tsH26/8-3* which is included in this study has a *ts* lesion in gene segment L2, rather than M1 (Table 3.5).

e. <u>Mapping the *tsI138 ts* lesion.</u>

A panel of 75 candidate reassortant clones were selected from the cross infection between *tsI138* and T1L. The clones were selected during several different isolation procedures, with evidence that the first 20 clones may have been mis-identified during isolation. Therefore, those clones were not analyzed. Three of the remaining clones showed no growth, 1 was of mixed parentage, and 21 were reassortant clones (4 monoreassortants), representing 21 unique gene patterns (reassortment efficiency = 40.4%). A strong *ts*

Table 3.5. Electropherotypes and EOP†s of T1 Lang/*tsH26/8-3* Reassortants.

	Gene Segment										EOP†
CLONE	L1	L2	L3	M1	M2	M3	S1	S2	S3	S4	39/32
LH26/8.146	1	H	1	H	H	1	1	1	H	H	0.0000000
LH26/8.148	H	H	H	H	H	H	H	H	H	1	0.0000002
LH26/8.129	1	H	1	1	H	H	1	H	H	H	0.0000002
LH26/8.80	H	H	1	H	1	H	1	H	1	H	0.0000004
LH26/8.160	1	H	1	H	H	H	H	1	H	H	0.0000004
LH26/8.29	1	H	1	H	1	H	H	H	1	H	0.0000013
LH26/8.61	H	H	1	H	1	H	H	H	H	H	0.0000022
LH26/8.45	H	H	1	H	H	H	H	H	H	H	0.0000026
LH26/8.56	H	H	H	H	1	H	H	H	H	H	0.0000033
LH26/8.79	1	H	1	1	H	1	H	H	H	H	0.0000042
LH26/8.153	1	H	1	H	1	1	1	H	H	1	0.0000042
LH26/8.92	H	H	H	H	H	H	1	H	H	H	0.0000046
LH26/8.76	1	H	1	H	1	1	H	H	H	1	0.0000056
LH26/8.73	H	H	1	H	H	1	1	1	H	H	0.0000063
LH26/8.88	1	H	1	1	1	1	1	H	1	1	0.0000070
LH26/8.11	1	H	1	H	1	1	H	H	H	H	0.0000083
LH26/8.62	H	H	1	H	H	1	H	1	H	H	0.0000083
LH26/8.132	1	H	1	H	1	H	H	H	H	H	0.0000093
LH26/8.55	1	H	1	H	H	1	H	1	H	H	0.0000100
LH26/8.18	H	H	H	H	1	1	1	1	1	H	0.0000179
LH26/8.127	H	H	1	H	H	H	1	H	1	H	0.0000200
LH26/8.34	1	H	H	H	H	H	H	H	H	H	0.0000222
LH26/8.99	H	H	H	1	H	H	H	H	1	H	0.0000286
LH26/8.37	H	H	H	1	H	1	H	H	H	H	0.0000476
tsH26/8	H	H	H	H	H	H	H	H	H	H	**0.000090**
LH26/8.93	1	H	1	1	H	1	1	1	1	1	0.0001170
LH26/8.19	H	H	1	H	H	1	H	H	H	1	0.0001330
LH26/8.101	H	H	1	1	H	H	H	H	1	H	0.0001520
LH26/8.16	H	H	1	H	1	1	1	1	1	H	0.0008620
LH26/8.23	1	H	1	H	1	1	1	H	H	H	0.0074100
tsH26/8/T1L	15/14	29/0	7/22	22/7	17/12	14/15	17/12	21/8	20/9	23/6	
LH26/8.72	1	1	1	1	H	H	1	1	1	1	0.148
LH26/8.28	1	1	1	1	1	1	1	1	1	H	0.270
LH26/8.113	H	1	H	H	H	H	H	H	1	H	0.334
LH26/8.01	H	1	H	H	1	1	H	1	H	H	0.381
LH26/8.57	H	1	1	1	H	1	1	1	1	1	0.410
LH26/8.77	1	1	1	1	H	H	1	1	1	1	0.465
LH26/8.17	1	1	1	1	1	1	1	H	1	H	0.558
LH26/8.106	1	1	H	H	H	H	H	H	1	H	0.644
LH26/8.63	1	1	1	H	1	1	H	H	H	1	0.755
LH26/8.52	1	1	1	1	1	1	H	1	1	1	1.000
LH26/8.02	H	1	H	1	1	1	1	1	1	H	1.257
LH26/8.09	1	1	1	1	1	1	H	1	1	1	2.470
LH26/8.84	1	1	1	1	1	H	1	H	1	1	2.780
T1L	1	1	1	1	1	1	1	1	1	1	2.800
LH26/8.07	1	1	1	1	1	1	H	H	H	1	3.330
tsH26/8/T1L	4/10	0/14	4/10	4/10	5/9	5/9	7/7	6/8	3/11	6/8	

†: EOP : Efficiency of Plating (titre @ 39°C) ÷ (titre @ 32°C). Ranked by EOP at 40°C.
§: Denotes parental origin of gene; 1: T1Lang; H: *tsH26/8*

phenotype was associated with 8 clones at 39°C. These clones all derived their L3 gene segments from the *tsI138* parent. All other clones were ts^+, with the exception of one which repeat tested as indeterminate (EOP values between 0.05 and 0.1) (Ramig *et al*, 1983, Hazelton and Coombs, 1995). All clones in this group had an L3 gene segment donated from the T1L parent. The other 9 gene segments showed random distribution of genetic derivation in both groups of this panel (Table 3.6). This confirms that the *tsI138* clone included in this study has a *ts* lesion in the same gene segment as previously reported (Ramig *et al*, 1983).

f. Mapping the *tsI128 ts* lesion.

A total of 75 candidate reassortant clones were isolated. One represented mixed genomic complement, and 15 were reassortant clones (reassortment efficiency = 20.0%). Twelve of the clones represented identical monoreassortants, leaving only 4 unique gene patterns available for analysis. No gene segment showed selective distribution of parental genotype when all four clones were considered as a whole. The mapping of the *ts* lesion for this clone was not pursued further.

6. Discussion

a. Recombination grouping of test clones.

For viruses with segmented genomes, recombination mapping is a powerful tool for rapidly sorting large panels of clones with a common phenotype into subsets in which phenotype expression resides on a common gene segment. The problem experienced

Table 3.6. Electropherotypes and EOP†s of T1 Lang/*tsI138* Reassortants.

	Gene Segment										EOP†
CLONE	L1	L2	L3	M1	M2	M3	S1	S2	S3	S4	39/32
LI138.21	3§	3	3	1	3	3	3	3	3	3	0.0001053
LI138.29	3	3	3	1	3	3	1	1	1	3	0.0000125
LI138.32	3	3	3	1	3	1	1	3	3	1	0.0000089
LI138.34	3	3	3	3	3	1	3	1	3	3	0.0000050
LI138.52	3	3	3	3	1	3	1	3	3	3	0.0000132
LI138.55	1	3	3	3	3	3	3	3	3	3	0.0000007
LI138.58	3	1	3	3	3	3	1	3	1	3	0.0001130
tsI138	**3**	**3**	**3**	**3**	**3**	**3**	**3**	**3**	**3**	**3**	**0.000470**
LI138.39	1	3	3	3	1	1	1	3	3	3	0.0067000
tsI138/T1L	6/2	7/1	8/0	5/3	6/2	5/3	3/5	6/2	6/2	7/1	
LI138.56	3	3	1	1	3	3	3	3	3	1	0.0439
LI138.43	1	1	1	1	1	1	1	3	3	3	0.1756
LI138.61	3	3	1	1	1	1	1	3	1	1	0.2083
LI138.50	1	1	1	1	1	1	1	1	3	3	0.3001
LI138.38	3	3	1	3	1	3	1	3	1	1	0.5070
LI138.23	3	3	1	1	3	3	1	1	3	1	0.6551
LI138.47	1	1	1	1	1	1	1	3	3	1	0.6592
LI138.51	3	3	1	1	1	3	1	3	1	1	0.8495
LI138.46	1	3	1	1	1	1	1	3	1	1	0.9065
LI138.65	1	3	1	1	1	1	3	3	1	1	0.9520
LI138.36	3	3	1	3	1	1	3	1	3	1	0.9845
LI138.26	1	1	1	1	3	1	1	1	1	1	1.3103
T1L	**1**	**1**	**1**	**1**	**1**	**1**	**1**	**1**	**1**	**1**	**2.800**
tsI138/T1L	6/6	8/4	0/12	2/10	3/9	4/8	3/9	8/4	6/6	2/10	

†: EOP : Efficiency of Plating (titre @ 39°C) ÷ (titre @ 32°C). Ranked by EOP at 40°C.
§: Denotes parental origin of gene; 1: T1Lang; 3: *tsI138*

with the mapping of the *tsH26/8* clone dictated re-examining the recombination group placement for all study clones (Fields and Joklik, 1969; Ramig *et al*, 1983). The restrictive temperatures utilized in these recombination infections were 39°C and 40°C, with the best separation into recombination groups occurring at 40°C. In this reassessment the group B and H mutants did not appear to recombine. This is consistent with the observation that the tsH clone used contains a lesion in gene segment L2. In addition, the group G clone *tsG453* did not recombine with the tsB and tsH mutants. This is also consistent with previous reports for *tsG453*, which was originally grouped in recombination group B (Fields and Joklik, 1969) and reclassified at a later time based on additional characteristics (Cross and Fields, 1972).

There were discrepancies surrounding the interactions of the clones from reassortment groups B, G, and H with the group I mutant. As indicated in Appendix B, the *tsI138* clone generally grows very poorly. The failure to recombine may be explained by the clone's slow growth phenotype. It had previously been reported that recombination is not efficient at restrictive temperatures when members of the recombination groups D and E are involved (Chakraborty *et al*, 1979), the group D and E clones both recombined with clones from other recombination groups in these studies (Table 3.1).

Finally, while recombination is potentially a very valuable tool for screening, it must be noted that the experience with the recombination assay done in these studies was not good in comparison to the results reported elsewhere (Fields and Joklik, 1979; Ramig

et al, 1983). In some cases the degree of reassortment is in fractions of percent, even between mutants with lesions clearly isolated and identified as in different groups. These results indicate that the degree of recombination was between 10^{-1} and 10^{-3}. While the poor results obtained here parallel those reported for *tsI138* (Ramig *et al*, 1983), confirmation of recombination groupings from these studies is dubious.

b. <u>Reassortant mapping studies.</u>

There are a number of reasons which justify re-mapping the *ts* lesions in the mutant clones before further work. Identification of gene segment parentage can be highly subjective. It is easy to misinterpret gene segment serotype where assay conditions do not allow clear definition of unique gene migration rates for each serotypic segment. This is a serious consideration when determining the pedigree of T1L versus T3D L3 segments, or M1 segments from all three reovirus serotypes. Previously gene segments were resolved for relatively short times (24 hours) and with relatively low current (110V, or approximately 14mA) (Sharpe *et al*, 1978). This study utilized bigger polyacrylamide gels, thereby increasing the length of the lanes in which each sample could be run. The gels were also electrophoresed for longer times (45 hours) at higher currents (18mA). The technical changes amplify the differences in migration rates between the serotypic gene segments and facilitates their identification.

The procedures previously utilized for generating reassortant progeny may also present a number of theoretical and practical technical concerns:

1. In some instances multiple serotypes were used as non T3D parents (Mustoe *et al*, 1978; Ramig *et al*, 1978; Ramig *et al*, 1983). The control problem introduced by multiple parents is difficult but not insurmountable. However, an additional problem is that the T2J parent grows more slowly than the other serotypes. This complicates the problem of establishing controls and appraising the *ts* phenotype. Finally, many of the T1L and T2J parents were derived from high passage laboratory stock clones (Ramig *et al*, 1978). High passage stocks may include gene segments with altered migration patterns, deletion mutations in gene segments (Zou and Brown, 1992) or contain additional lesions which would confound data analysis. This concern is amplified by the technical problems introduced by short gel paths in those earlier studies;

2. Temperature sensitive clones of T1L and T2J were used as parents for generating reassortant progeny (Mustoe *et al*, 1978; Ramig *et al*, 1978; Ramig *et al*, 1983). In some instances the non T3D serotype parent contained more than one *ts* lesion (Ramig *et al*, 1978; Ramig *et al*, 1983), including one example where the second lesion became known during data analysis (Ramig *et al*, 1978). In addition to problems in controlling interpretation of data there is theoretical concern over fitness of fit between the non-parental gene segments under these conditions. Recent examination of T1LxT3D reassortants generated from wild type parents has suggested selective interactions encourage parental pairing with the L1-L2, L1-M1, L1-S1 and L3-S1 gene segments and/or their products (Nibert *et al*, 1996a). One

explanation for those findings is non-permissive interactions between segments of different parentage. Such interactions could lead to potential progeny which may not fully assemble, or replicate poorly if assembly does occur. The question of fitness of interaction between non serotypic gene segments is compounded when the parents have known mutations affecting their fitness to replicate;

3. For some mapping experiments the generation of recombinants was done at 39°C with *ts* parents. This was to encourage the generation of ts^+ reassortants over *ts* parental progeny (Ramig *et al*, 1978; Ramig *et al*, 1983). Because a number of mutants are only mildly *ts* at 39°C there is no guarantee there will be significant selection for ts^+ reassortant progeny. It has been reported that culture at elevated temperature encourages selection of intra- and/or extra-genic revertants, clones with compensatory mutations which suppress the *ts* phenotype under restrictive conditions (Ramig *et al*, 1977). The observation that a significant number of suppressed lesions were observed during the mapping for the *tsI138* lesion (Ramig *et al*, 1983) is consistent with these concerns. The use of a panel with predominantly ts^+ reassortants with few, if any *ts* reassortant clones, could lead to mis-interpretation of results. The mapping of the double *ts* mutant *tsA279*, which has been conducted in the studies reported here, would be difficult if only one phenotypic panel had been used. One possible interpretation could have been that the lesion in the L2 segment represents a compensatory reversion mutation rather than a separate *ts* mutation. This could have led to different directions in

the supplemental studies done with this clone (see Chapter 5, below);

4. In previous studies reassortant panels which were mildly *ts* were also isolated under culture conditions which discouraged selection for *ts* phenotypic reassortants (Ramig et al, 1983). The prototypic parental clones selected to represent these recombination groups (groups H, I, and J) are all strongly temperature sensitive (Ahmed and Graham, 1977; Ramig and Fields, 1979; Ahmed *et al*, 1980b). In consideration of the variance between the mild EOPs obtained with the *ts* reassortant panels and the previously reported EOPs for the *ts* parents, the mapping of a strong *ts* lesion with mildly *ts* reassortant clones generated at restrictive temperatures must be questioned. This concern is especially important considering reports of selection for reversion and suppression mutations at elevated temperature and the observation of suppressed lesions observed during the mapping *tsI138* (Ramig *et al*, 1983); and

5. Suppression, and frequently degree of *ts* expression, by at least some reassortant clones, was determined with an assay referred to as the lytic/leaky plaque assay (Ramig and Fields, 1977; Ramig *et al*, 1983). This assay is conducted at 39°C, and uses the size and appearance of plaques to determine whether a clone is *ts* or not (Ramig and Fields, 1977). The interpretation of 'lytic' and 'leaky' plaques is subject to bias, whether intentional or not. Further, in this instance the *ts* parental clones were all strongly *ts*, thereby challenging the validity of any test conducted

at a single temperature which is purported to identify expression of the *ts* lethal phenotype.

In consideration of potential problems with previous mapping exercises, the mapping was reviewed using large panels of *ts* and ts^+ clones which had been generated at 32°C. One clone of T1L was used as the wild type parent for all mapping studies reported here. This clone did not contain any known *ts* lesions. The temperatures at which each clone expressed the *ts* phenotype were determined. The clones were then tested at both permissive and restrictive temperatures, and true EOP values established. Where appropriate, elevated temperatures were used during plaque assays to improve identification of the *ts* phenotype.

Finally, the conditions for electrophoresis utilized here were optimized to demonstrate differences in the migration rates of gene segments from different parents. Improved identification of the gene segments makes reassortant identification more reliable, thereby ensuring inclusion of clones which may otherwise have been discarded through the failure to discriminate gene segment parentage (eg. between the L3 gene segments if T1L and T3D, or with the M1 segment for all three serotypes).

The theoretical proportion of reassortants has been predicted to be 25% (Nibert et al, 1996a). While previous reports of reassortant efficiency achieved from mixed infections

have ranged as high as 20%, the general level is at or below 3%. Poor performance in obtaining reassortants could be due to interference between segments from specific recombination groups (eg. groups D and E)(Chakraborty *et al*, 1979). The aforementioned use of *ts* parents multiple serotypes, and culture conditions which select for wild type progeny could contribute to poor reassortant efficiency (Ramig *et al*, 1977), as could the concept of non-permissive gene segment pairings (Nibert *et al*, 1996a). It is theoretically possible that non permissive recombinations would be amplified in progeny clones with multiple *ts* lesions derived from parents of different serotypes.

The levels of reassortant efficiency noted in these studies generally ranged between 36% and 46%. There was initially poor performance in generating reassortants with the mutant *tsE320*. However, when freshly titred stocks were used for the mapping of *tsE320* the reassortant efficiency increased dramatically, from 4.9% to 45.5%. The proportion of reassortants obtained in the first mapping experiment for the mutant *tsH26/8-3* was 35.9%. This efficiency fell to 19.5% when the same wild type parental stock lysate was in a subsequent experiment. In the latter case the parental clones had not been freshly titred. The generally high efficiency with which reassortants were generated in this study indicates that the ratio between MOIs provided by each parent and permissive growth conditions are important considerations in the successful generation of reassortants. It should be noted that *tsJ128*, had an efficiency of 20.0% for the single reassortant generation procedure conducted.

The use of multiple, and elevated temperatures allowed the identification of two *ts* lesions with the clone *tsA279*; a mild lesion in the L2 segment expressed equally at all elevated temperatures, and a dominant lesion in the M2 segment which is expressed mildly at 39°C, but which increases in expression as temperature is raised to 40°C (Table 3.2, Figure 3.2). The presence of two lesions in this clone led to a review of the prototype clone *tsA201* to confirm that the procedures as used in this study were correct. The use of double mutants and multiple parents, with progeny generated at elevated temperature could have mitigated against success in the identification of double lesions such as seen with clone *tsA279*.

The *ts* lesions for the group E clone *tsE320* and the group I clone *tsI138* both mapped cleanly to the gene segments which were previously identified. The clone *tsI138* had proven difficult to map in previous study. In fact, the best mapping was to the M2 gene segment. However, considering the apparent ability to recombine with the Group A prototype clones and the fact that the lesion for that group was shown to be in the M2 gene segment, a lot of effort was made to identify suppressed expression of the phenotype so that the L3 segment could be identified with the lesion (Ramig *et al*, 1983). The use of permissive temperatures to generate reassortants allowed many earlier problems to be avoided. There was no selection towards revertants, and no problem with suppression was observed.

The clone tsH26/8-3 presented the most serious problem of the study clones. The results

of these studies showed that the laboratory copy of this clone contains a lesion in the L2 gene segment, not the M1 segment, as previously reported. To confirm the location of the *ts* lesion a different parental *tsH26/8-3* clone was tested. The possible selection for revertants by high temperature culture condition, the use of double mutants of high passage stock, and similarity in M1 gene segment migration rates for all three reovirus serotypes under electrophoresis conditions used in previous studies make it possible to mis-interpret the identification of gene segments. Further, the L2 gene segment was ruled out in only one of three panels identified for the mapping, the ts^+ panel (Ramig *et al*, 1983).

Another observation which may be of import is that mutant *tsH26/8* was rescued from the pseudorevertant clone 26. Clone 26 was itself isolated from a long term persistent culture of *tsC447* (Ahmed and Graham, 1977; Ahmed *et al*, 1979). *Ts* clones with lesions in the L2 (Group B) and S4 (Group G) gene segments were also rescued from clone 26. This questions whether the vial containing the clone used in this study had been properly labeled, or had been mis-read or mis-labeled during previous amplifications. Considering the advances in gene segment resolution, the mapping of the lesion to the L2 gene segment does not conflict with previously reported data. Examination of all the data suggests that the laboratory stock clone *tsH26/8-3* is either not the original clone as reported, or that there was a mistake in the previous mapping.

The *tsJ128* clone did not generate a sufficient number of reassortants to permit mapping.

This is similar to the previous study results (Ramig *et al*, 1983). Since only four reassortment patterns had been identified, with no clear suggestion of mapping, further work with this clone was limited.

CHAPTER 4

Examination of the *ts* mutants *tsE320, tsH26/8,* and *tsI138,*

1. Introduction

Morphogenesis has been reviewed by thin section electron microscopy for prototype clones from recombinant groups A, B, C, D, E, and F (Fields *et al*, 1971) and G (Danis *et al*, 1992) of the Fields panel. As noted in Chapter 1, there has been no reported morphogenetic evaluation of mutants from the remaining three groups; H, I, and J. Further, as with the prototype mutant *tsA201*, study involving the prototype *tsE320* used a restrictive temperature of 39°C and demonstrated no effect upon the infection process (Fields *et al*, 1971). The prototype *tsE320* has variably been reported to produce no infection (Cross and Fields, 1972). Therefore, thin section electron microscopic investigation into the morphogenesis of the mutant clones *tsE320, tsH26/8,*and *tsI138,* was initiated. Growth curves were also established in conjunction with the morphogenetic studies. Because the lesion for the study clone of *tsH26/8* was identified in the L2 gene segment no work beyond thin section electron microscopy was done with that clone. The production of dsRNA was examined for the remaining two clones, and the course of infection was noted by immunofluorescent microscopy for the clone *tsE320.* It was not possible to obtain sufficient titres for the clone *tsI138* to allow examination by immunofluorescent microscopy. Assembly intermediate structures produced by these mutants were not identified by direct particle counting, as was performed with the mutant *tsA279* (Chapter 5).

a. Electron microscopy.

For thin section electron microscopy suspension cultures of cells were prepared with the mutant clone *tsE320*, *tsH26/8*, and *tsI138*, at a multiplicity of infection (MOI) of 5 PFU/cell as describe (Chapter 2.2.h). All infections were cultured at a permissive temperature of 32°C. The restrictive temperature used for *tsH26/8* was 39°C. The restrictive temperature used for all other mutants was 39.5°C. Ultrastructurally, parallel mock infection control cells appeared normal for both permissive and restrictive temperatures.

b. Labelling and purification of dsRNA.

To examine synthesis of dsRNA L929 cell monolayers in 6 well cluster dishes were infected with T3D, *tsA201*, *tsA279*, *tsB405*, *tsE320*, and *tsI138*, labeled with $^{32}PO_4^{-3}$, the gene segments resolved by SDS-PAGE, and the gels autoradiographed as described (Chapter 2.6a,2.7a, h).

c. Immunofluorescent microscopy.

L929 monolayers were infected, fixed, reacted against rabbit anti-whole reovirus polyclonal antibody, and developed with rhodamine conjugated goat anti-rabbit IgG as described (Chapter 2.5). The monolayers were examined by immunofluorescent microscopy (IF) and evaluated in accordance with the 4 stage system described by Rhim (Rhim *et al*, 1962): stage 1, fine granular points of fluorescence; stage 2, coalescence of fluorescence into larger inclusions and some reticulate fluorescence; stage 3,

perinuclear condensation of fluorescence; and stage 4, a general diffuse fluorescence throughout the cytoplasm. Parallel IF and phase contrast exposures were made for each field using Fuji color slide film, ASA 1600. The proportion of infected cells in each field was calculated as per:

(No. cells fluorescing by IF) ÷ (Total No. cells in field (Phase Microscopy)) x 100.

2. Uninfected L929 control cells

Ultrastructurally, uninfected control cells appeared normal at both permissive and restrictive temperatures. During a typical 72 hour infection the cell density in the cultures would increase 2 to 3 fold, with approximately 70% viability (Figure 4.1A). The only significant observation was that uninfected control cells expressed a type A retrovirus particle into the lumen of the rough endoplasmic reticulum.

3. The morphogenesis of wild type T3D at permissive and restrictive temperatures.

Generally, T3D infections showed the same pattern of morphogenesis at both permissive and restrictive temperatures as permissive cultures of the *ts* mutants. Cytoskeletal elements were associated with the inclusions of permissive temperature cultures but not of restrictive temperature cultures. The progress of infection did not differ from previous reports concerning wild type reovirus (Borsa *et al*, 1979; Chaly *et al*, 1980; Dales *et al*, 1965; Fields *et al*, 1971; Silverstein and Dales, 1968; Silverstein, 1976; and Wolf *et al*, 1981). The first viral inclusions appeared between 12 and 24 hours post

Figure 4.1 **Growth curves of T3D, *tsE320*, *tsH26/8-3*, and *tsI138* and electron microscopic evidence of infection at permissive and restrictive temperature.**

L929 cells were infected and incubated at permissive and restrictive temperatures. Aliquots were taken at indicated times, titered, and examined for evidence of infection by thin-section electron microscopy (Chapters 2.2, 2.4.a). Infected cells are expressed as the proportion of cells showing infection in the plane of section; virus titre is corrected to an input value of 1 unit per cell. Infected cells (○) and infectious titre (▲) at 32°C; and infected cells (■) and infectious titre (+) at 39°C for T3D and *tsH26/8-3*, or 39.5°C for *tsE320* and *tsI138*. Viability (+) and growth(○) of control uninfected L929 cells in suspension culture culture and incubated at 39°C is shown in panel A.

A. Uninfected Control Cell Viability

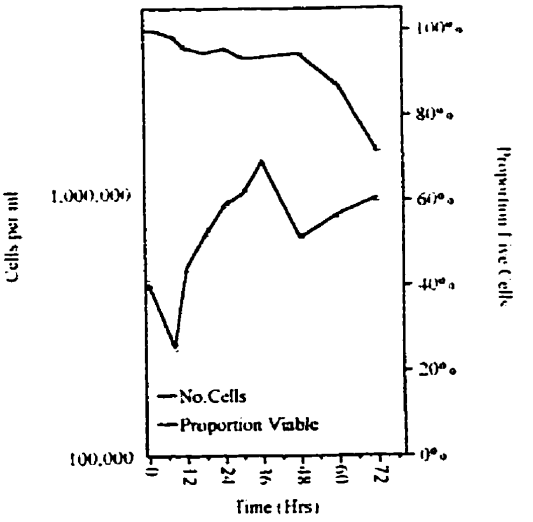

B. T3D

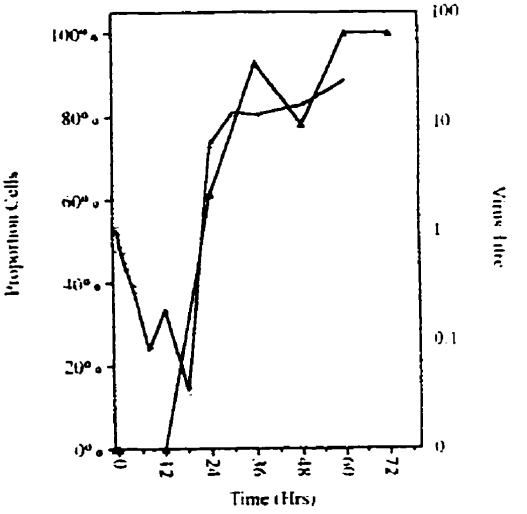

C. *tsE320*

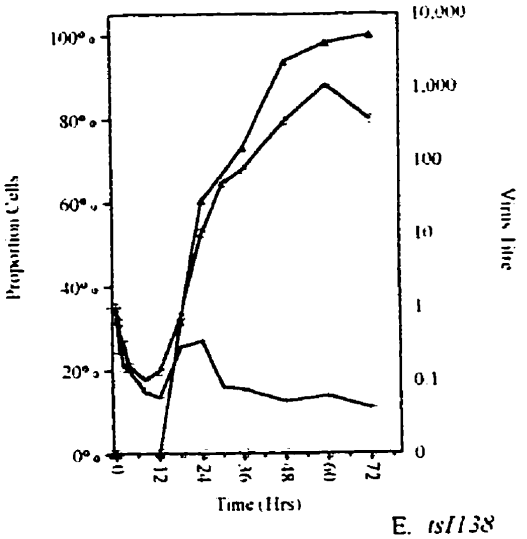

D. *tsH26.8*

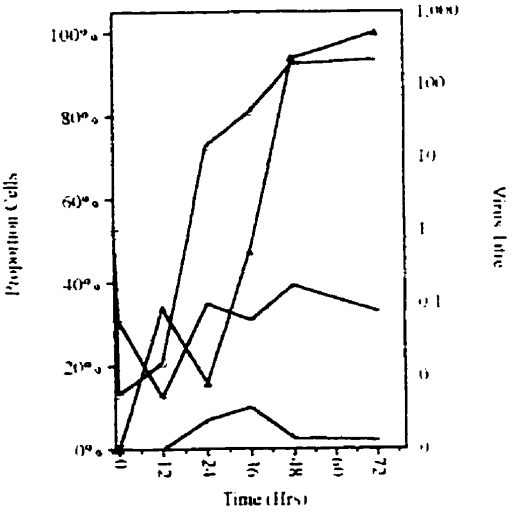

E. *tsI138*

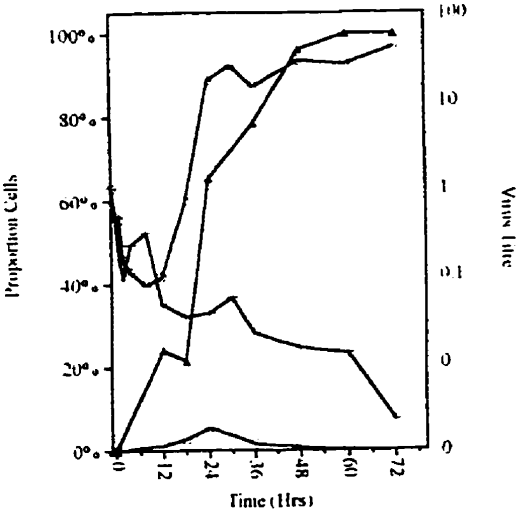

attachment, and by 60 hours post attachment all cells would be infected, both at permissive and restrictive temperatures (Figure 4.1B). The infections were not very cytopathic until late in infection. While there was some vacuolization of the cytosol, the infections did not demonstrate the ultrastructural characteristics associated with apoptotic cell death (condensation of nucleoplasm and cytoplasm; ruffling or rupture of nuclear or cytoplasmic membranes). Cultures were not evaluated for the characteristic chromosomal degradation associated with apoptosis (Lu *et al*, 1994). Swelling of the cytosol and the appearance of electron dense material in the mitochondria late in infection further indicated that cellular membranes were no longer integral. After infection there was a brief lag phase, where the titre of recoverable infectious virus declined to less than 10% of the input titre, followed by a rapid increase to values typically between 100x and 1000x the input infectious titre (Figure 4.1B)

4. Studies into the life cycle of *tsE320.*

a. The morphogenesis of *tsE320* at permissive temperatures.

Permissive infections with *tsE320* showed a delayed appearance of virus, with the first small inclusions appearing 18 hours post attachment. These viral foci developed into well defined cytoplasmic inclusions which displaced the nucleus and provided a eucentric appearance to the cells by 36 hours. The inclusions were smaller than those observed with the permissive temperature cultures of T3D (Chapter 4.3), *tsA279*, (Chapter 5.3) and *tsH26/8-3* (Chapter 4.5.a, below). Ultrastructurally, the early inclusions were

disorganized aggregations of viral product around cytoskeletal tubules (Figure 4.2A, inset). Later in the course of infection the expected paracrystaline arrays of assembling virions associated with cytoskeletal elements developed (Figure 4.2B). The cells maintained a healthy appearance until late in the infection. There was no apparent condensation of the nucleoplasm or cytosol and no changes to the endoplasmic reticulum until 60 hours post infection, at which time the mitochondria also began to display some distension. The nuclear and cytoplasmic membranes remained unbroken and showed no ruffling. There was reduced expression of the transforming Type A retrovirus.

b. The morphogenesis of *tsE320* at restrictive temperatures.

Parallel restrictive infections with *tsE320* did not demonstrate evidence of infection in any cells examined at every time point between 12 and 48 hours. Neither was there any evidence of viral material accumulating nor digesting in lysosomes (Figure 4.1C). Due to the failure to observe evidence of infection, no samples were evaluated for later times in the infection. The cells remained relatively healthy through the duration of culture. There was reduced expression of the transforming Type A retrovirus.

c. Growth curves for *tsE320*.

Permissive infections showed a brief lag phase of 12 hours followed by rapid rise in titre which peaked at three orders of magnitude over input after 60 hours post infection (Figure 4.1C). Restrictive cultures for *tsE320* had a slightly longer lag phase, followed by a brief rise in recoverable infectious titre which peaked below the input values at 24

Figure 4.2. Thin sections of permissive and restrictive infections of L929 cells by *tsE320.*

Thin-section electron micrographs of permissive infections with *tsE320.* L929 cells were infected at an MOI of 10 PFU per cell and incubated in suspension at 32°C. After 18 hours nascent inclusions are observed which are disorganized aggregations of viral material (A). By 36 hours post infection the inclusions show a paracrystalline array of virions (B). Parallel restrictive temperature cultures showed no evidence of infection. Bars represent 1.0μm (200nm for insets).

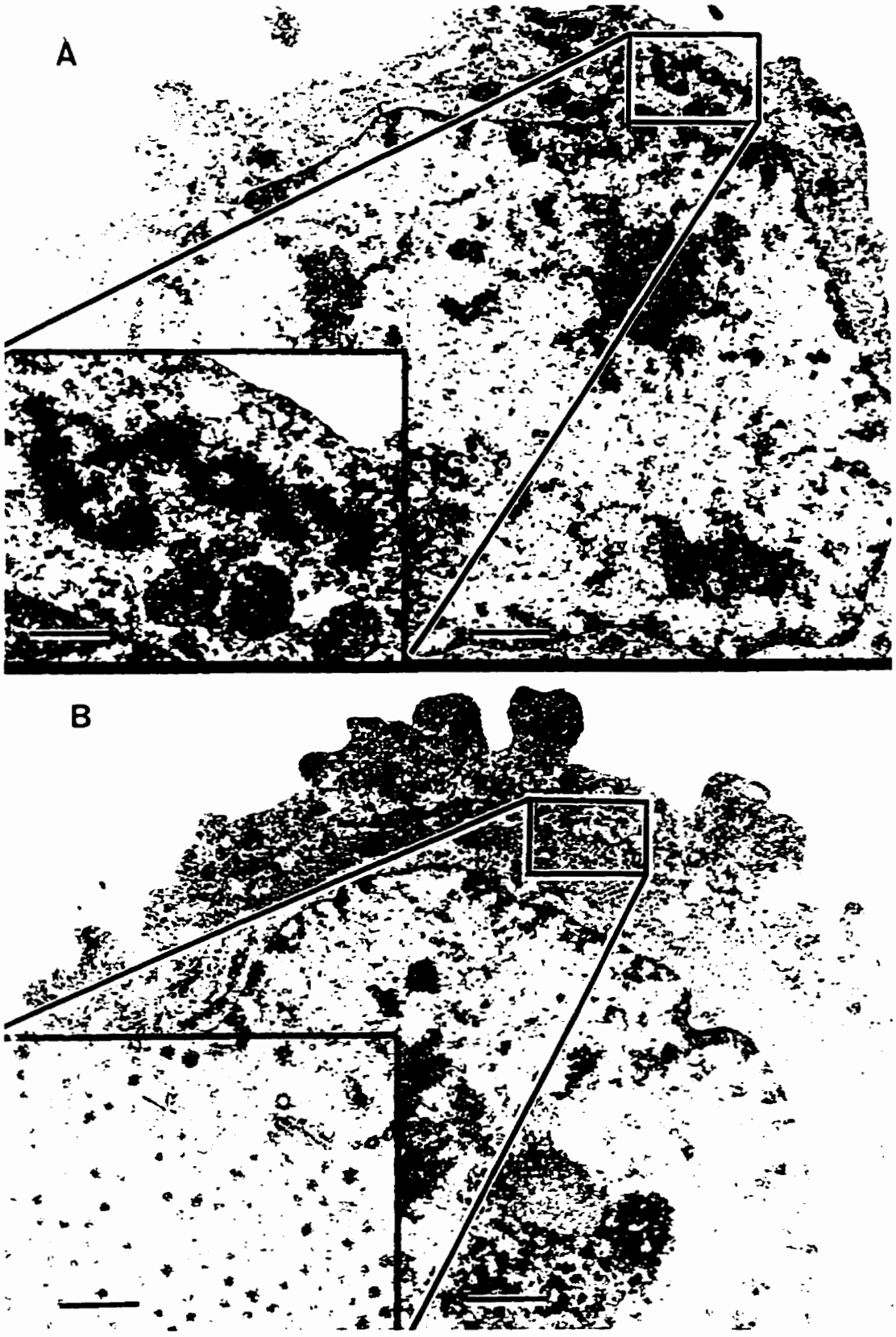
A
B

hours post infection. The recoverable infectious titre then declined two orders of magnitude below the input levels (Figure 4.1C).

d. Production of dsRNA by *tsE320.*

The mutant clone *tsE320* was positive for dsRNA production under permissive growth conditions and negative at all restrictive temperatures (Figure 4.3). This result is consistent with previous reports for this clone (Cross and Fields, 1972).

e. Immunofluorescent determination of protein production by *tsE320.*

Permissive infections displayed early stage 1 levels of infection in a small proportion of cells at 6 hours post infection. Photographic evaluation showed that 53.2% of the cells examined were infected at 48 hours post infection, the majority at stages 3 to 4 (Figure 4.4A).

There was no strong cytopathic effect demonstrated in restrictive infections by this clone. The monolayers remained confluent and showed little immunofluorescence beyond background during the course of infection at restrictive temperature. Evidence of infection was displayed in 3.4% of the cells examined photographically at 48 hours, with most of the infected cells demonstrating stage 1 levels of infection. The occasional cell showed stage 2 levels of infection (Figure 4.4B).

Figure 4.3 **Production of dsRNA by *tsA279*, *tsE320*, and *tsI138* at permissive and restrictive temperatures.**

$^{34}PO_4^{-3}$ labelled cytoplasmic extracts were prepared from monolayers infected with T3 Dearing and *ts* Mutants *tsA201*, *tsA279*, *tsB405*, *tsE320*, and *tsI138* and electrophoresed as described (Chapters 2.6a, 2.7a,h, 5.1.c). A: 32°C; B: 39°C; C: 39.5°C; and D: 40°C . The gels were autoradiographed for 24 hours at room temperature (A) or 4 days at -70°C with an intensifier screen (B, C, D).

A.
32°C
T3D
tsA201
tsA279
tsB405
tsE320
ts1138
Control
B.
39°C
T3D
tsA201
tsA279
tsB405
tsE320
ts1138
Control
C.
39.5°C
T3D
tsA201
tsA279
tsB405
tsE320
ts1138
Control
D.
40°C
T3D
tsA201
tsA279
tsB405
tsE320
ts1138
Control
L1
L2
L3
M2
M1
M3
S1
S2
S3
S4

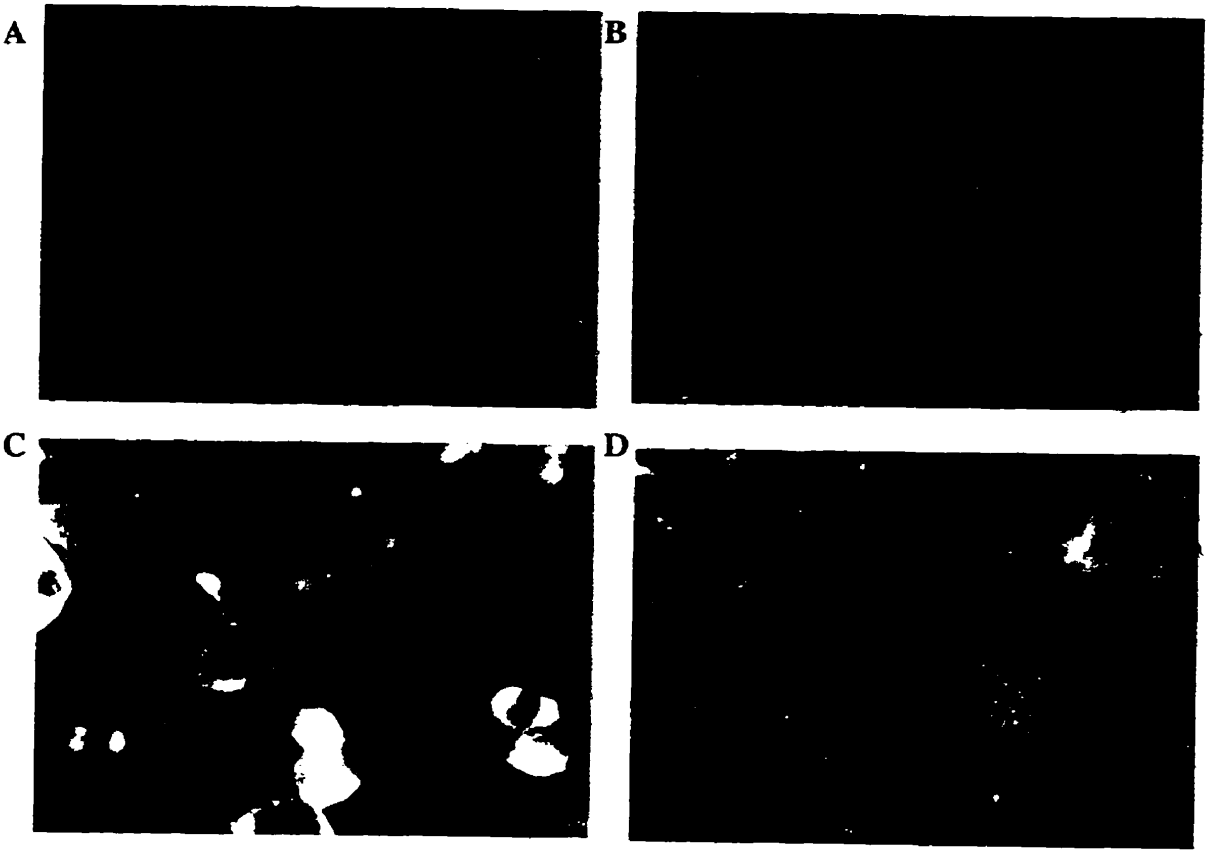

Figure 4.4. Immunofluorescent microscopy of uninfected control, and permissive and restrictive infections with *tsE320*.

Subconfluent monolayers were infected at an MOI of 10 PFU per cell with *tsE320* (C,D) and incubated at 32°C (A,B,C) and 40°C (D) for 48 hours. Control cells (A,B) were treated with rabbit anti-reovirus hyperimmune serum (primary antibody (A)), developed with rhodamine-conjugated anti-rabbit serum (secondary antibody (B)), and viewed and photographed with fluorescent and phase contrast microscopy (Chapters 2.5, 5.1.c).

f. Discussion, *tsE320.*

Characteristics for the *tsE320* mutant clone had been previously reported, with the initial report stating that incubation at the restrictive temperature did not result in discernable differences from the permissive cultures by electron microscopy and immunofluorescent microscopy (Fields *et al*, 1971). Subsequently the clone was reported to have not provided any ultrastructural evidence of infection in the earlier study at a restrictive temperature of 39°C (Cross and Fields, 1972). Preliminary work in the current study indicated that the expression of the conditionally lethal phenotype was increased by elevating the restrictive temperature for *tsE320,* which is only marginally *ts* at 39°C (Appendix B, Table B.2). Because the phenotype could be turned on more effectively at elevated restrictive temperatures, and because of the variable nature of previous reports, this mutant was re-examined. The results of this study indicate that the mutation interferes with the early appearance of virus at the permissive temperature, with the first small inclusions not showing up until 18 hours post infection. This does not prevent the course of infection from proceeding to all cells infected, and a yield in recoverable infectious virus similar to that seen with control cells and other permissive cultures (Figures 4.1, 4.3A, 5.9). There was no evidence of infection observed at any time during the experiment when the restrictive temperature of 39.5°C was used. Previous reports had indicated evidence of infection by immunofluorescent microscopy at 39°C. Use of the elevated restrictive temperature of 40°C resulted in severely reduced evidence of infection after 48 hours (3.4% at the restrictive temperature versus 53.2% at permissive temperature). Further, the degree of infection as demonstrated by

immunofluorescence was changed from stages 3 to 4 at permissive temperatures to very weak stage 1 levels of infection. The immunofluorescence results are consistent with reduced protein production at the restrictive temperature.

As observed in earlier work there was no evidence for production of dsRNA under restrictive conditions (Cross and Fields, 1972). Failure to produce dsRNA is consistent with reduced viral protein production. In addition, no assembly intermediate stage has been identified as being produced by this mutant at restrictive temperatures in either earlier studies (Fields *et al*, 1971) nor in this study. The results of ultrastructural examination, protein production as determined by IF microscopy, dsRNA production and failure to identify intermediate structures suggest expression of the *ts* phenotype is the result of early intervention in the replicative process.

5. Studies into the life cycle of *tsH26/8-3.*

a. The morphogenesis of *tsH26/8-3* at permissive temperatures.

As with the mutant clone *tsE320*, permissive infections with the putative mutant clone *tsH26/8-3* did not produce viral inclusions in the host cell until relatively late in infection, with the first small inclusions not being visualized until 24 hours post infection (Figure 4.5.1). Other than the time until the first appearance of inclusions, the infection did not differ from the results observed with mutants *tsA279* (Chapter 5.3) and *tsE320* (Chapter 4.4.a) (Figure 4.5.3).

Figure 4.5. **Thin sections of permissive and restrictive infections of L929 cells by *tsH26/8-3.***

Thin-section electron micrographs of permissive (1,3) and restrictive (2,4) infections with *tsH26/8-3*. L929 cells were infected at an MOI of 10 PFU per cell, incubated in suspension at 32°C and 39°C, and examined at 24 hours (1,2) and 48 hours (3,4) post infection. (1) Nascent inclusions are first seen 24 hours post infection, with progeny virons assembling around condensed genomic material at 32°C. (2) The early inclusions appear as more disorganized aggregates of viral material at 39°C. (3) After 48 hours incubation inclusions at 32°C fill the cytoplasm in paracrystalline arrays. (4) The inclusions at 39°C remain as small diffuse areas of viral product. Bars represent 1.0μm (200nm for insets).

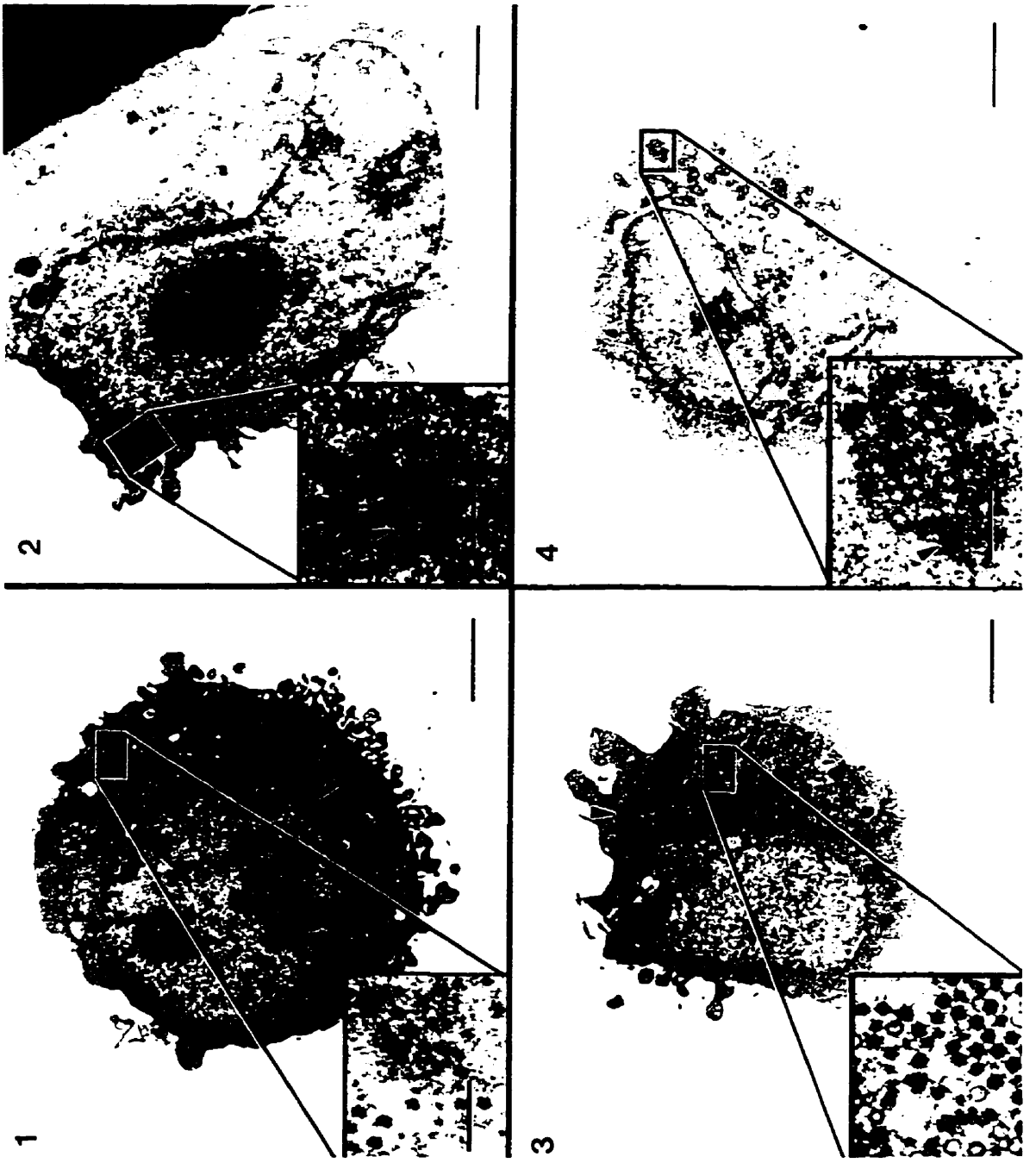
2
4
1
3

b. The morphogenesis of *tsH26/8-3* at restrictive temperatures.

As with the permissive temperature infections, there was no evidence of productive infection prior to 24 hours post attachment. All inclusions observed during the course of the infection were small diffuse masses of viral product. Ultrastructurally, the inclusions contained rare foci of genomic material in loose aggregates of viral material. There was no accumulation of digesting virions in transport vesicles or lysosomes (Figure 4.5.2, 4). The cells remained relatively healthy in appearance during the course of the experiment. Evaluation of inclusions from dead cells suggests that there is an accumulation of empty core particles in the restrictive cultures (Figure 4.6). These results are consistent with previous reports concerning *tsB352* (Fields *et al*, 1971).

c. Growth curves for *tsH26/8-3.*

The profile for recoverable infectious titre during permissive infection with *tsH26/8-3* was similar to that for *tsE320* (Figure 4.1C). Restrictive cultures of *tsH26/8* showed a gradual rise in ultrastructural evidence of infection which peaked at 10.0% of all cells examined after 36 hours post infection, and then declined to 2.0% of all cells examined after 72 hours incubation (Figure 4.1D).

d. Discussion, *tsH26/8-3.*

As noted in Chapter 3, the laboratory copy of *tsH26/8-3* does not contain a lesion in the M1 gene segment. Rather, this clone contains a lesion in the L2 gene segment, coding for the major core protein λ2. For this reason, this clone was not evaluated past the

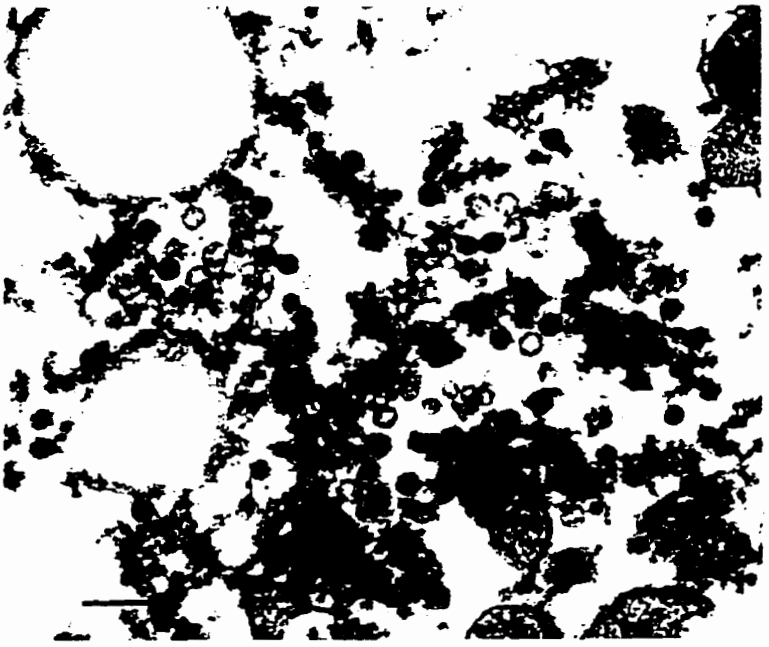

Figure 4.6. Thin section evidence of restrictively produced assembly intermediate core particles by *tsH26/8-3.*

Thin-section electron micrograph of an inclusion found 48 hours after infection in a dead cell from a restrictive infection with *tsH26/8-3*. Samples were prepared as for Figure 4.5. Bar represents 200nm.

work done with thin section microscopy and growth curves. Thin section electron microscopy noted an apparent accumulation of empty core particles in this study (Figure 4.6). The product reported by thin section electron microscopy for *tsB352*, the prototype group B clone, was a core like particle (Fields *et al*, 1971). Negative stain examination of gradient materials from restrictive temperature cultures with *tsB405* also identified core like particles (Morgan and Zweerink, 1974). No information was provided concerning whether the core like particles observed with the group B mutants contained genomic material (Fields *et al*, 1971; Morgan and Zweerink, 1974). Therefore, the ultrastructural findings from this study do not conflict with previous findings for mutants which contain a lesion in the L2 gene segment. The accumulation of empty core particles is also similar to the product reported for the Group D mutant *tsD357* (Fields *et al*, 1971) and for the group G mutant *tsG453* (Morgan and Zweerink, 1974).

6. Studies into the life cycle of *tsI138.*

a. The morphogenesis of clone *tsI138* at permissive temperatures.

Gross evaluation of permissive infections by *tsI138* shows nascent inclusions first appearing at 18 hours post infection. With this exception, ultrastructural examination provides a very different result than noted with the other mutants in this study. The inclusions progress to small, disorganized foci of viral product in the host cell cytoplasm. Ultrastructurally the inclusions are comprised of occasional foci of condensed genomic material in loose aggregates of viral protein. This appearance remained throughout the course of the infections. In the few examples of larger inclusions which were observed

the inclusions remained loose and disorganized, and did not display the paracrystalline arrays of virions normally seen in permissive temperature cultures (Figure 4.7.3, 4). The cells remained relatively healthy until 48 hours post infection, when the culture began to die off quite rapidly.

b. The morphogenesis of clone *tsI138* at restrictive temperature.

At the restrictive temperature there was little evidence that the cells had been infected. There was transient appearance of small, diffuse inclusions in a small proportion of cells sampled 18 hours post attachment. There was no evidence of infection observed in cells sampled commencing at 36 hours post infection. On rare occasion the inclusions showed clear foci of genomic material with no assembly of viral proteins. The most striking characteristic was the appearance of large, electron dense concentric condensates in the inclusions (Figure 4.7.2). There was no evidence of accumulation and digestion of viral product in lysosomes. As with the permissive infection, the cells remained relatively healthy until 48 hours post infection. There was no evidence that the death of the culture was caused by the effects of the infection. Evaluation of inclusions found in the one infected dead cell identified in the latter stages of the infection suggested that there was an accumulation of genome complete core particles (Figure 4.8).

c. Growth curves *tsI138*.

Permissive infections showed a brief lag phase of 12 hours followed by rapid rise in titre which peaked below two orders of magnitude over input after 72 hours post infection.

Figure 4.7. Thin sections of permissive and restrictive temperatures of L929 cells by *tsI138*.

Thin-section electron micrographs of permissive (1,3,4) and restrictive (2) infections with *tsI138*. L929 cells were infected at an MOI of 10 PFU per cell, incubated in suspension at 32°C and 39°C, and examined at 18 hours (1,2) and 36 hours (3,4) post infection. (1) Nascent inclusions observed 18 hours post infection at 32°C are small but contain assembling virions. (2) After 18 hours incubation at 39.5°C the inclusions are diffuse and disorganized with no evidence of assembly. Electron dense concentric sworls of viral product may be seen in larger inclusions. (3)At 32°C the inclusions continue to be seen as small diffuse masses of viral product with little assembly. (4)Large inclusions remain disorganized and do not assume the paracrystalline array normally observed (Figure 4.2C). Bars represent 1.0μm (200nm for insets).

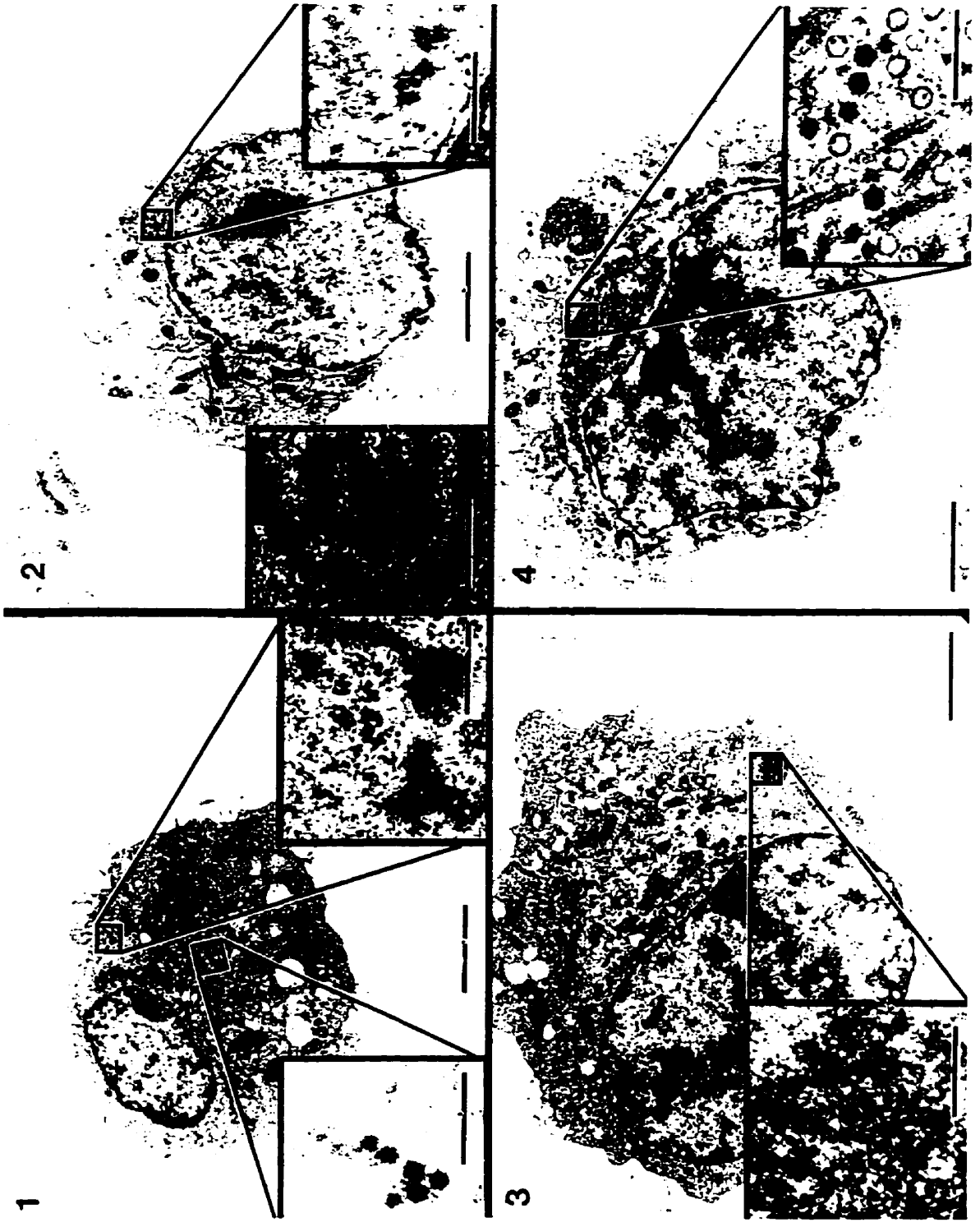
1
2
3
4

Figure 4.8. Thin section evidence of restrictively produced assembly intermediate core particles by *tsI138.*

Thin-section electron micrographs from an inclusion found 48 hours after infection in a dead cell from a restrictive infection with *tsI138.* Samples were prepared as for Figure 4.7. The inclusions are loose unassembled foci of genomic material (large arrowhead) with some complete particles (large arrows). Some top component is produced (small arrows). Bar represents 1 μm.

The first appearance of inclusions coincided with the end of the lag phase, and showed gradual increase, culminating with all cells examined being infected at 72 hours post infection (Figure 4.1B, C, D, E).

Restrictive cultures of *tsI138* demonstrated a brief lag and rise in recoverable infectious titre, peaking at just below input values after 8 hours incubation. This was followed by a slow decline of greater than two orders of magnitude in recoverable infectious virus through the time course of the study (Figure 4.1E).

d. Production of dsRNA by *tsI138.*

All mutants produced dsRNA at permissive temperature. However, the mutant *tsI138* produced reduced levels of dsRNA compared to other permissive cultures (Figure 4.3A). There was no evidence that dsRNA was produced by *tsI138* at 39°C. The dsRNA positive mutant cultures of *tsA201*, *tsA279*, and *tsB405* produced detectable levels of dsRNA at restrictive temperatures (Figure 4.1B,C, D).

e. Discussion *tsI138.*

The inability to culture *tsI138* to high titre presented numerous problems throughout the course of these studies. The results of the characterization provides insight into the reasons. The clone did not produce noticeable levels of infection at permissive temperatures as observed in thin section electron microscopy. Further, those inclusions observed never assumed the paracrystalline array anticipated in permissive infections.

Rather, the inclusions were usually disorganized masses of viral product with rare foci of genomic materials (Figure 4.7). At restrictive temperatures the infections failed to generate any distinct progeny. Rather, there were concentric sworls of electron dense material observed in small cytoplasmic inclusions. This structure is similar to those observed in the published electron micrographs of *tsC447* restrictive inclusions (Fields *et al*, 1971). Growth curves for permissive cultures show levels of recoverable infectious titre between one and two orders of magnitude below those obtained for permissive infections with other mutants (Figure 4.1E). The evidence of this study also shows that there is severely reduced production of dsRNA by the mutant at permissive temperature (Figure 4.3). These data support the findings in Appendix B which showed the clone required prolonged culture periods to reach maximum titres. The results from restrictive temperature cultures indicate that there is limited production of viral material with little or no assembly of progeny.

These studies provide preliminary evidence that there may be more than one mechanism of action by which the mutant *tsI138* demonstrates its conditionally lethal phenotype. First, that there is a defect in the replication cycle, as demonstrated by the reduced production of dsRNA by this clone. This defect occurs with the permissive temperature cultures. Second, there is the apparent failure to assemble into progeny virions. Further insight into these mechanisms may be extrapolated from future studies into the production of ssRNA and proteins by this clone under permissive and restrictive growth conditions, and by direct particle counts of intermediate assembly structures which may accumulate.

All the data for permissive cultures suggest that the mutant clone *tsI138* would be useful for examining the phenomenon of persistent infections by lytic viruses. This is consistent with the history of this clone, which is a rescued pseudorevertant clone obtained from a persistent culture of the L2 mutant *tsB352* (Ramig *et al*, 1979; Ramig *et al*, 1983). Detailed examination and correlated comparison of the mutant *tsB352* with *tsI128* may also prove valuable.

CHAPTER 5

Evaluation of the mutant clone *tsA279*

1. Introduction.

The process of infection involves a number of steps; attachment, uptake, transmembrane transport, uncoating, replication and synthesis of proteins, assembly, and, lastly, release (Lucia-Jandris, 1990). Temperature sensitive lesions may affect any one, or more, of these steps. Ultrastructural examination of the course of infection is a non-specific test which allows the impact of the *ts* lesion upon the whole process to be observed. Once the process of morphogenesis has been reviewed it may be possible to identify specific steps affected by the lesion, and thereby direct further studies.

The impact of temperature upon morphogenesis has been examined by thin section electron microscopy for the group A prototype clone *tsA201* at a restrictive temperature of 39°C. No effect upon the infection process was observed (Fields *et al*, 1971). Preliminary results in the current study indicate that some of the mutants, including the mutant *tsA279*, become more temperature sensitive as temperature is increased (Appendix B.2). In addition, *tsA279* has been shown to contain *ts* lesions in both the L2 and M2 gene segments, both of which code for significant structures in the fully assembled virion (L2 coding the λ2 core spike; M2 coding the major outer capsid protein μ1) (Table 3.2). Therefore, ultrastructural examination was undertaken to ascertain the impact of temperature sensitivity upon the morphogenesis of the mutant clone *tsA279*.

2. **Batch cultures of infections and sampling for evaluation.**

Parallel suspension cultures of cells were prepared for the reovirus parental wild type T3D serotype and the mutant clone *tsA279* at a multiplicity of infection (MOI) of 5 PFU/cell as described (Chapter 2.2.h). The infections were cultured in suspension at a permissive temperature of 32°C and a restrictive temperature of 39.5°C. Parallel uninfected control cells were also cultured in suspension cultures. Aliquots were collected at intervals from 0 to 72 hours post attachment, or until fewer than 20% of the cells in the culture were viable. The cultures were not fed nor otherwise treated during the course of infection.

In order to map and define specific mechanisms for expressing the *ts* phenotype to the appropriate *ts* gene segment, restrictive temperature cultures were also prepared using T1L and the T1L x *tsA279* reassortant clones LA279.11, LA279.39, and LA279.56 (Table 3.2). Samples were collected for these studies at 24, 36, and 48 hours post attachment. In addition, restrictive and permissive infections of T1L and *tsA279* were prepared using an MOI of 15,000 virions/cell to determine whether the *ts* phenotype was expressed by virions assembled at both permissive and restrictive temperatures, or assembled at the restrictive temperature only. Aliquots were collected 0, ½, 1, and 4 hours post attachment and viewed by thin section electron microscopy. Finally, an antibody blocking experiment was conducted to confirm that material observed in cytoplasmic vesicles was the result of heterophagic degradation of nascent virions that had been endocytosed by the host cell, rather than autophagic digestion of abortive viral

infections in the host cell cytoplasm. Samples were collected at time points between 18 and 48 hours for the antibody blocking experiments.

Selected samples were subject to assessment for: 1.) proportion of viable cells by trypan blue stain exclusion; 2.) yield in recoverable infectious virus. Yield of infectious virus was determined at a permissive temperature of 32°C as described (Chapter 2.2.f); and 3.) thin section electron microscopic evaluation. Culture aliquots were processed at 4°C, infiltrated, embedded, sectioned, and evaluated as described (Chapter 2.4a). Restrictive temperature cultures of T1L and the reassortant T1L x *tsA279* clones were evaluated by vital staining and thin section electron microscopy, and high MOI infections were evaluated by thin section electron microscopy only.

3. Ultrastructural evaluation of *tsA279* by thin section electron microscopy.

a. The morphogenesis of *tsA279* at permissive temperatures.

The overall progress of infection in cells infected with the mutant *tsA279* and cultured at a permissive temperature of 32°C was similar to that seen with the wild type parental T3D. Gross evaluation of the infections showed early appearance of small inclusions, with the first clear inclusions evident by 12 hours post infection. By 24 hours post infection large inclusions displaced the cell nuclei, giving a characteristic eucentric appearance.

Ultrastructurally, nascent virions were associated with microtubules by 12 hours post

infection. By 18 hours post infection the cells were filled with large aggregates of complete virions in dense networks of viral products (Figure 5.1A), and 36 hours after infection the inclusions existed as paracrystaline arrays of complete virions. In addition, genome deficient virions (top component) and outer shell structures were also observed (Figure 5.1C). The cells remained relatively healthy during the course of infection, with no evidence of cell death occurring until the latter stages of infection.

b. The morphogenesis of *tsA279* at restrictive temperatures.

Gross examination of cells infected with *tsA279* and cultured at 39.5°C showed small inclusions after 12 hours. However, in contrast to permissive infections, the inclusions in the restrictive infections did not progress to a further stage of development (Figure 5.1B,D).

Ultrastructural examination of infected cells suggested two pathways for the expression of temperature sensitivity evolving by 18 hours post infection; failure to produce and assemble viral product in the first round of replication, and an apparent blockade in transmembrane transport of restrictively assembled virions in subsequent rounds of infection.

(1.) Reduced production and assembly of viral progeny at restrictive temperature.

The small cytoplasmic inclusions contained foci of genomic material in loose networks of viral proteins, with little or no assembly into mature virions (Figure 5.1B). There was

Figure 5.1 **Thin sections of permissive and restrictive infections of L929 cells by *tsA279.***

Thin-section electron micrographs of permissive (A,C) and restrictive (B,D) infections with *tsA279*. L929 cells were infected at an MOI of 10 PFU per cell, incubated in suspension at 32°C and 39.5°C, and examined at 18 hours (A,B) and 36 hours (C,D) post infection. Bars represent 1.0μm (200nm for insets). Degraded virions in lysosomes are indicated by arrows.

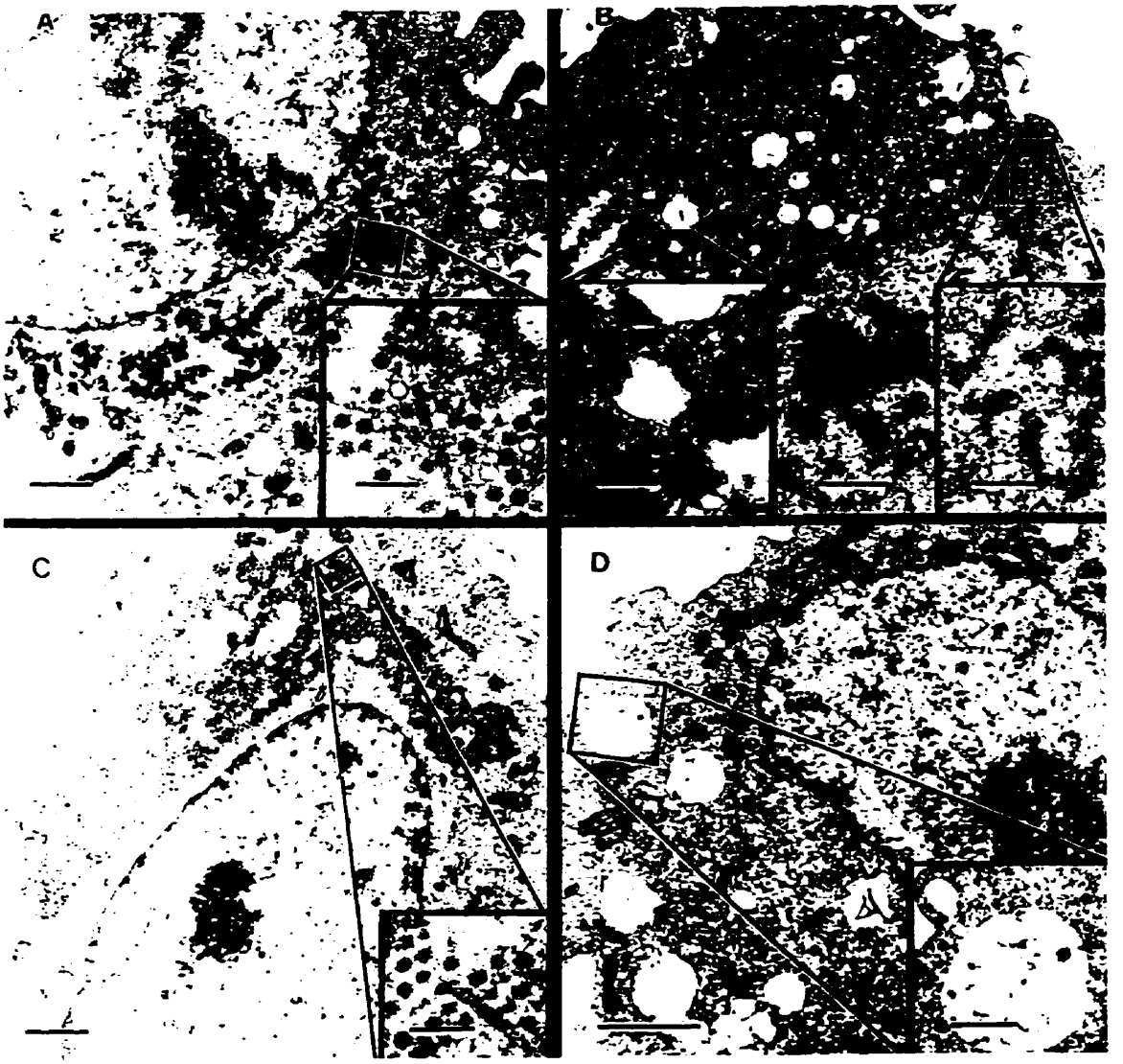
A
B
C
D

no evidence of infection observed in thin sections of cells after 36 hours post attachment (Table 5.1). The cells did not demonstrate evidence of necrotic nor apoptotic cell death until late in the experiment, when the culture started to die. The apparent level of production of the transforming Type A retrovirus was reduced during the earlier stages of infection.

(2.) Accumulation and degradation of *tsA279* mutant virions in lysosomes.

There was an apparent blockade in transmembrane transport of virus in restrictive cultures. The virions accumulated and were degraded in lysosomes (Figure 5.1B,D). The proportion of cells showing cytoplasmic inclusions and degrading virions in lysosomes at both permissive and restrictive temperatures is shown in Table 5.1 At permissive temperature there was no appreciable accumulation of virus in lysosomes at any time point. At the restrictive temperature virions first appeared to be accumulating and degrading in lysosomes at 18 hours post attachment. The presence of virions degrading in lysosomes increased to over 50% of cells viewed at 36 hours and then declined to approximately 25% of cells at 72 hours post attachment (Figure 5.1B, Table 5.1).

4. The blockade in transmembrane transport.

a. Mapping the blockade in transmembrane transport.

Restrictive temperature infections were prepared from a panel of T1L x *tsA279*

Table 5.1 Characteristics of *tsA279* batch infections.

	32°C			39.5°C		
Time[a]	Titre[b]	infected[c]	Lysosomes[d]	Titre	infected	Lysosomes
0	$1.2x10^6$	ND	ND	$9.0x10^5$	ND	ND
1	$9.7x10^5$	ND	ND	$9.0x10^5$	ND	ND
2	$1.6x10^6$	ND	ND	ND	ND	ND
4	$2.0x10^6$	ND	ND	$5.0x10^5$	ND	ND
8	$7.8x10^5$	ND	ND	$3.3x10^5$	ND	ND
12	$6.1x10^5$	43.40	0.0	$4.0x10^5$	11.9	9.3
18	$1.8x10^7$	35.7	0.0	$2.7x10^6$	10.9	15.2
24	$5.1x10^8$	68.8	0.0	$4.5x10^6$	5.0	17.0
30	$3.6x10^8$	ND	ND	$1.1x10^6$	ND	ND
36	$6.0x10^8$	76.5	0.0	$5.0x10^5$	1.25	58.8
48	$9.1x10^8$	80.3	0.0	$5.5x10^5$	0.0	36.23
60	$4.3x10^9$	100	0.0	$6.4x10^5$	0.0	35.05
72	$3.5x10^9$	100	0.0	$3.9x10^5$	0.0	25.9

a. Time : Hours after attachment at 4°C.

b. Titre in Plaque Forming Units per ml

c. Infected : Proportion of cells examined which demonstrated viral inclusions in the plane of section.

d. Lysosomes : Proportion of cells examined which contained viral particles being digested in lysosomes.

ND. Not Done

reassortants to confirm the existence of and map the apparent blockade in transmembrane transport. The infections were examined at various time frames between 24 and 48 hours. Infections with the wild type parent T1L and the mutant L2/wild type M2 reassortants LA279.11 and LA279.39 showed most cells infected by 24 hours. The infections progressed to lytic cell death in essentially all cells by 36 hours post infection with the three clones. There was limited evidence of virions in transport vesicles/lysosomes at 24 hours post attachment (Figure 5.2A). However, none of the vesicles contained degraded virions. There was clear evidence of virion transport into the cytosol at 24 hours post attachment (Figure 5.3A, Table 5.2).

The mutant M2 monoreassortant clone LA279.56 showed reduced evidence of infection, with small inclusions in approximately 1% of all cells examined at 36 hours, and no ultrastructural evidence of infection after that time. Lysosomes which contained degrading virions were clearly evident in almost 50% of the cell sections evaluated 36 hours post infection. The proportion of cells demonstrating the presence of digesting virions in lysosomes declined to approximately 30% after 48 hours, with no evidence of productive infection being observed in the cytosol of any cells by that time point. (Figure 5.2B, Figure 5.3B, Table 5.2). Review of the electropherotypes for the panel examined for transmembrane transport shows the M2 gene segment associated with the phenotype, and that all other gene segments are randomly assorted (Table 5.3).

Figure 5.2 **Evidence of infection and blockade of transmembrane transport with the *tsA279* L2 and M2 gene segments.**

L929 cells were infected at an MOI of 5 PFU per cell, incubated in suspension at 39.5°C, and sampled for electron microscopic examination at 24, 36, and 48 hours. (A) Reassortant clones LA279.11 and LA279.39 (mutant L2; T1L M2) demonstrated no accumulation and degradation of virions in lysosomes. (B) The mutant M2 monoreassortant clone LA279.56 demonstrated little evidence of infection in the cytoplasm of infected cells while there was an accumulation of virions digesting in lysosomes which fell off after 36 hours.

A.

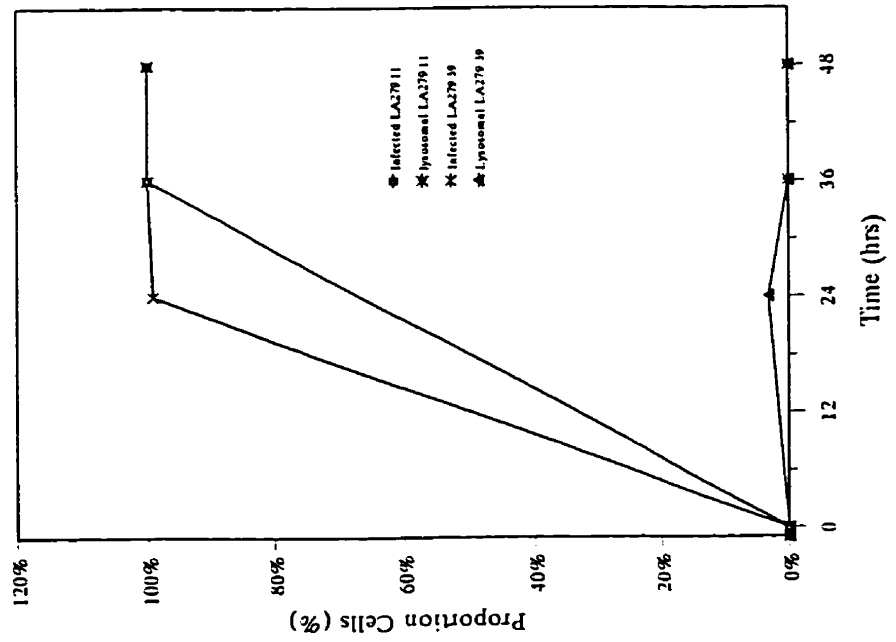
Proportion Cells (%)
120%
100%
80%
60%
40%
20%
0%
0
12
24
36
48
Time (hrs)
Infected LA279 11
Lysosomal LA279 11
Infected LA279 39
Lysosomal LA279 39

B.

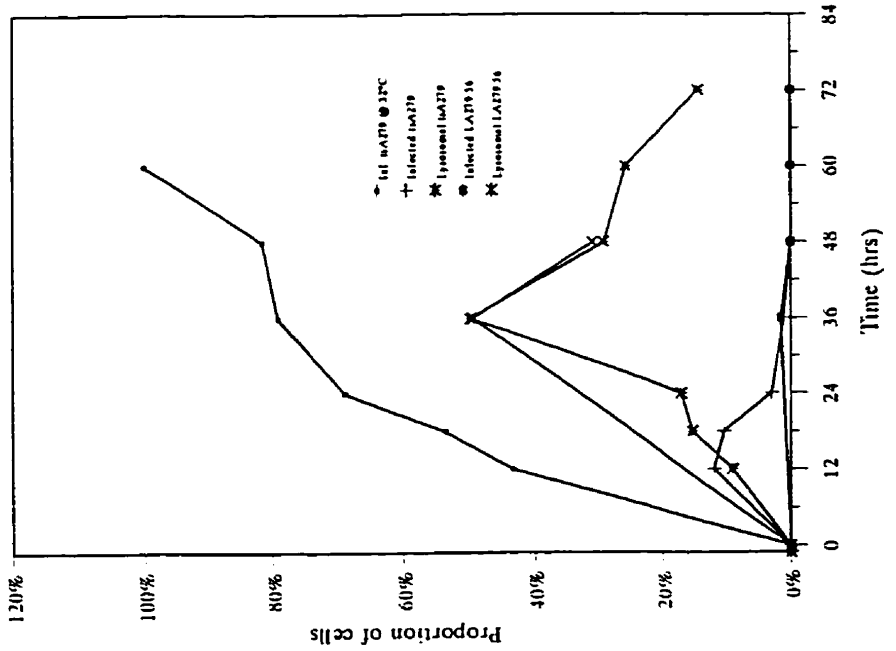
Proportion of cells
120%
100%
80%
60%
40%
20%
0%
0
12
24
36
48
60
72
84
Time (hrs)

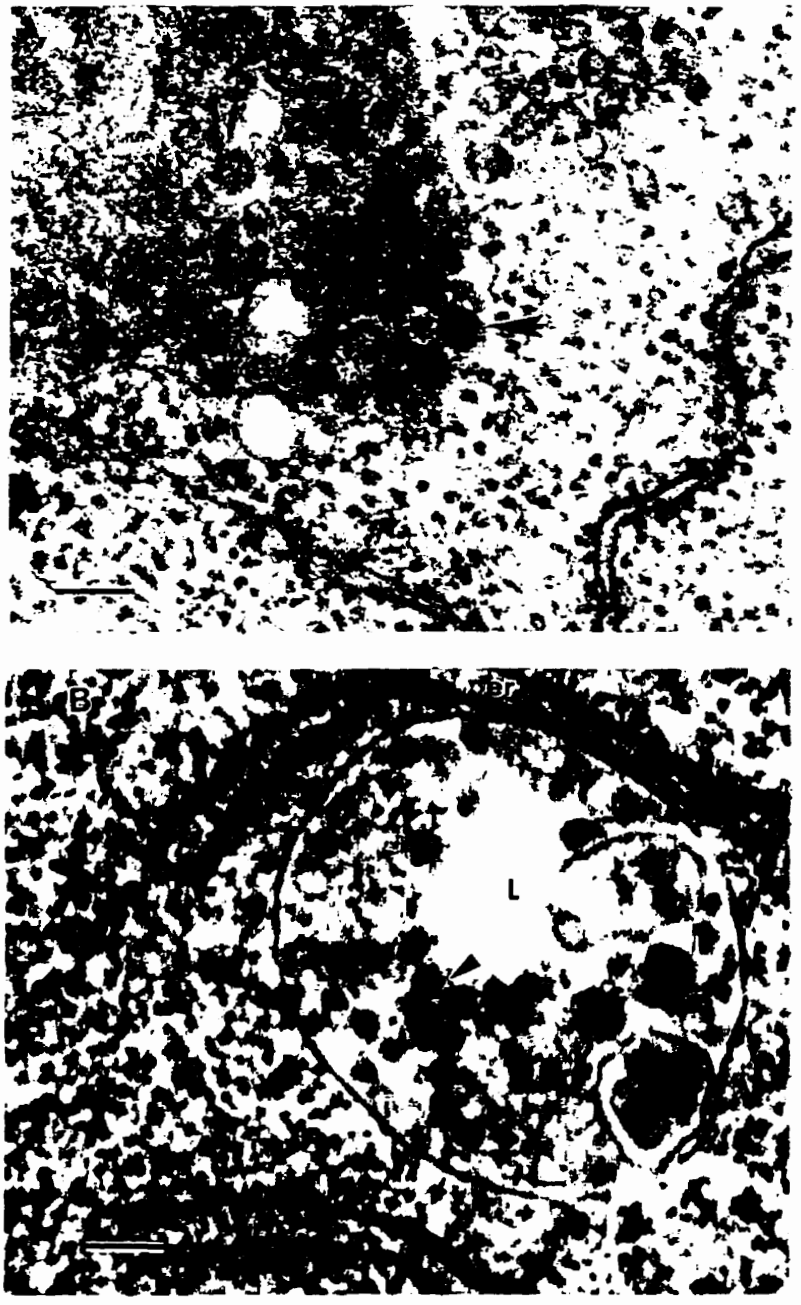

Figure 5.3 Thin section examination of transmembrane transport with the *tsA279* L2 and M2 gene segments.

L929 cells were infected at an MOI of 5 PFU per cell and incubated in suspension 39.5°C, and examined at 24 hours (A) and 36 hours (B) post infection. Magnification, 50,000x; bars represent 200nm. A: Mutant L2 reassortant LA279.39. Virions in cytosol indicated by large arrowhead. B: Mutant M2 reassortant LA279.56. Degraded virions in Lysosome (L) indicated by arrowhead.

Table 5.2 Infection and presence of virus in lysosomes in T1L/*tsA279* reassortants.

Gene Pattern	Time[a]	Viable[b]	Infected[c]	Lysosomes[d]
Mutant L2:	24 Hr	19.4%	2.97	17.0
Mutant M2	36 Hr	<10.0%	1.06	58.8
	48 Hr	0.0%	0.0	29.4
T1L L2:	24 Hr	70.0%	ND	ND
Mutant M2	36 Hr	72.6%	1.53	49.6
	48 Hr	68.5%	0.00	31.2
Mutant L2:	24 Hr	70.0%	99.2	3.13
T1L M2	36 Hr	72.6%	100	0
	48 Hr	68.5%	ND	ND
T1L L2:	24 Hr	10.0%	87.0	7.61
T1L M2	36 Hr	5.0%	100	0.00
	48 Hr	ND	ND	ND

a. Time : Duration of incubation after attachment at 4°C.
b. Viable : Proportion of cells in culture viable by Trypan Blue dye exclusion.
c. Infected : Proportion of cell sections containing viral inclusions.
d. Lysosomes: Proportion of cell sections in which viral material is being digested in lysosomes.
ND Not Done

Table 5.3. **Electropherotypes and transmembrane transport capability of T1 Lang/tsA279 reassortants at the restrictive temperature.**

	Gene Segment§									
CLONE	L1	L2	L3	M1	M2	M3	S1	S2	S3	S4
A. No transmembrane transport.										
tsA279	A	A	A	A	A	A	A	A	A	A
LA279.56	1	1	1	1	A	1	1	1	1	1
tsA279/T1	1/1	1/1	1/1	1/1	2/0	1/1	1/1	1/1	1/1	1/1
B. Transport across lysosomal membranes										
T1L	1	1	1	1	1	1	1	1	1	1
LA279.11	A	A	A	A	1	A	A	A	A	1
LA279.39	A	A	1	1	1	A	1	1	1	1
tsA279/T1	2/1	2/1	1/2	1/2	0/3	2/1	1/2	1/2	1/2	0/3
C. Phenotypic/nonphenotypic†										
	2/3	2/3	3/2	3/2	5/0	2/3	3/2	3/2	3/2	4/1

§: Denotes parental origin of gene; 1: T1Lang; A: *tsA279*

†: Phenotypic / nonphenotypic = number of gene segments donated by the phenotypic parent / gene segments donated by the non phenotypic parent

b. Confirming the blockade in transmembrane transport.

An excess of neutralizing antibody was added to restrictive temperature cultures of the *ts* M2 monoreassortant LA279.56 at 6 hours post attachment to confirm that viral product observed in cytoplasmic vesicles late in infection was the result of a defect in transmembrane transport of restrictively assembled particles during a secondary round of infection. Aliquots were collected at 18, 24, 36 and 48 hours post infection and processed for thin section electron microscopy as already described. Virions were observed in endosomes in 2.5% of all cell sections examined at 18 hours post infection. No virions were observed in endosomes at later times post infection. There was no evidence of degrading viral product in cytoplasmic vesicles in cell sections from the antibody treated restrictive cultures of LA279.56 (Figure 5.4).

c. Transmembrane transport of tsA279 virions produced at permissive temperature.

Infections conducted at restrictive temperatures with permissively assembled T1L and *tsA279* at an MOI of 15,000 particles/cell showed normal attachment and uptake of virus. Virions were observed in the cytosol of infected cells within 30 minutes post attachment with both wild type and *ts* clones. There was no evidence of digestion of virions in lysosomal bodies with either the T1L or the *tsA279* infections after 4 hours post infection at restrictive temperature (Figure 5.5).

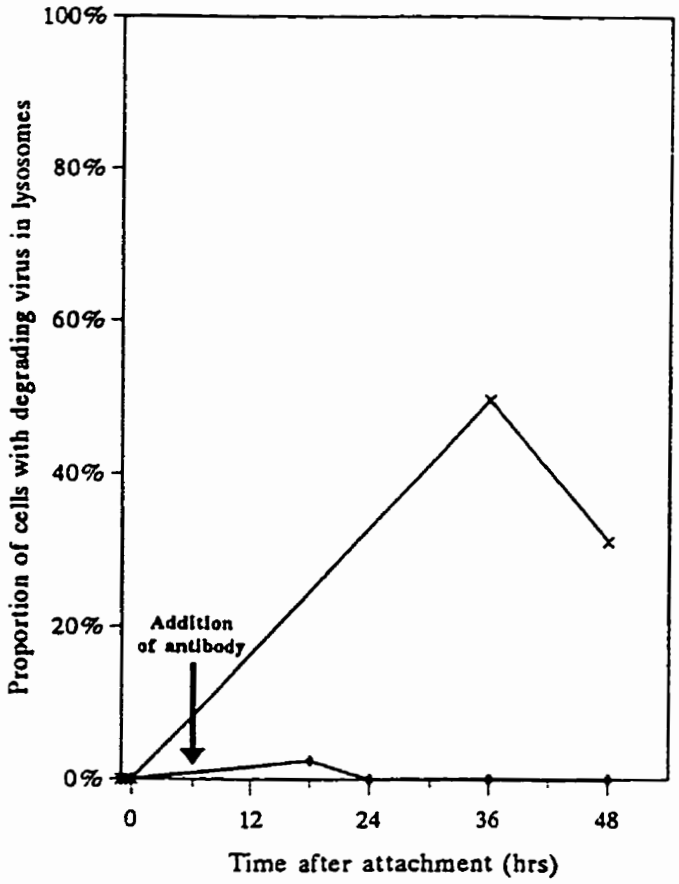

Figure 5.4. Examination for accumulation of virions in endocytotic vesicles after treatment of restrictive cultures with antiserum to whole reovirus.

L929 cells were infected with the monoreassortant mutant M2 clone LA279.56 and incubated at 40°C. Anti-whole reovirus antiserum was added 6 hours after attachment to prevent attachment and uptake of progeny assembled under restrictive conditions. Samples were collected and evaluated by thin section microscopy as described (Chapter 5.4.b). (+), LA279.56 cultures not treated with antiserum; (◆), LA279.56 cultures treated with antiserum 6 hours after attachment.

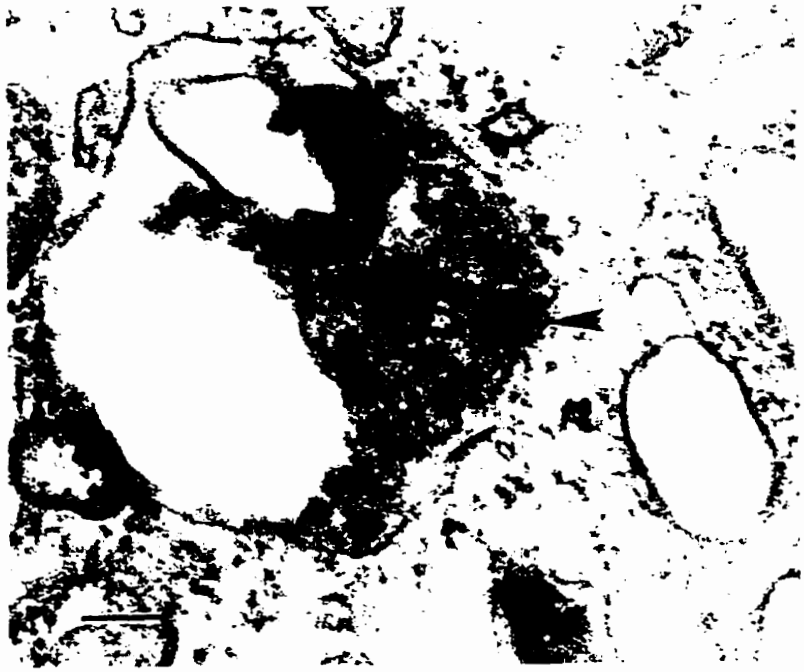

Figure 5.5 Thin section restrictive temperature transmembrane transport of *tsA279* assembled at 32°C.

L929 cells were infected at an MOI of 15,000 permissively assembled virions per cell from a *tsA279* P3 culture incubated at 32°C, and incubated in suspension at 39.5°C. At 4 hours post infection the infecting permissively assembled virus (Arrow) is seen in the cytosol (C) after transport across the lysosomal membrane (m). Magnification, 100,000x; bar represents 100nm.

5. Identification of the lesions associated with the *ts* phenotype in the M2 gene segment of *tsA279*.

RT-PCR preparation and amplification of M2 cDNA from both T3D and *tsA279* provided a cDNA fragment of approximately 2200 base pairs. Endonuclease digestions of the product with Bam HI, Eco RI, Hind III , and Pst I provided cleavage products of the predicted sizes for the M2 cDNA prepared from both T3D and *tsA279*. Analysis of the sequence for the *tsA279* M2 gene segment identified 4 point mutations as compared to the T3D sequence: $C_{945} \rightarrow T_{945}$; $C_{972} \rightarrow T_{972}$; $C_{2046} \rightarrow A_{2046}$; and $G_{2088} \rightarrow A_{2088}$ (Figure 5.6). These result in changes in the amino acid sequence from $P_{306} \rightarrow S_{306}$, $P_{315} \rightarrow S_{315}$, $P_{673} \rightarrow T_{673}$, and $E_{687} \rightarrow K_{687}$. In addition, the clone of T3D used in these studies differed from the reported sequence (Jayasuriya *et al*, 1988, Wiener and Joklik, 1988) with $T_{2067} \rightarrow C_{2067}$, resulting in a change of $P_{680} \rightarrow S_{680}$. (Figure 5.7). The clone of *tsA279* which was sequenced contained a C at base 2067, making its amino acid sequence at that base a proline, the same as reported for the wild type parent T3D (Jayasuriya *et al*, 1988, Wiener and Joklik, 1988).

6. Proteolytic cleavage of restrictively assembled *tsA279* virions.

Kinetic studies of proteolytic digestion with trypsin showed no change in the rate at which $\sigma 3$ was totally removed and $\mu 1$ was cleaved to δ and ϕ for permissive and restrictive mutant virions and permissive T3D. In all cases the total removal of $\sigma 3$ and initial appearance of δ and ϕ was virtually instantaneous. When the different types of virions were subjected to chymotrypsin digestion at 32°C the kinetics of loss for $\sigma 3$ was

Figure 5.6. **cDNA sequence for the M2 gene segment of reovirus T3D and temperature sensitive mutant *tsA279.***

The cDNA nucleotide sequence of the M2 gene segment of reovirus serotype 3 as determined by RT-PCR sequencing is listed. The sequence for the temperature sensitive mutant *tsA279* is shown below, with identical nucleotides shown as dashes (-). The sequence of the mutant is shown starting and ending with the bases for the primers used in the initial reverse transcriptase copying of the genomic dsRNA.

Figure 5.6. **cDNA sequence for the M2 gene segment of reovirus T3D and temperature sensitive mutant tsA279.**

Clone	Base	Sequence
T3D	1	gctaatctgc tgaccgttac tctgcaaaga tggggaacgc ttcctctatc gttcagacga
tsA279		------ ---------- ---------- ----------
T3D	61	tcaacgtcac tggagatggc aatgtattta aaccatcagc tgaaacttca tctaccgctg
tsA279		---------- ---------- ---------- ---------- ---------- ----------
T3D	121	taccatcgtt aagcttatca cctggaatgc tgaatcccgg aggggtacca tggattgctg
tsA279		---------- ---------- ---------- ---------- ---------- ----------
T3D	181	ttggagatga gacatctgtg acttcaccag gcgcattacg tcgaatgacg tcaaaggaca
tsA279		---------- ---------- ---------- ---------- ---------- ----------
T3D	241	tcccggaaac ggcaataatc aacacagaca attcatcagg cgccgtgcca agcgaatcag
tsA279		---------- ---------- ---------- ---------- ---------- ----------
T3D	301	cgcttgtgcc ctacatcgat gagccgctgg tagtggttac agagcatgct attaccaact
tsA279		---------- ---------- ---------- ---------- ---------- ----------
T3D	361	tcaccaaagc tgagatggca cttgaattca atcgtgagtt ccttgacaag atgcgtgtgc
tsA279		---------- ---------- ---------- ---------- ---------- ----------
T3D	421	tgtcagtgtc accaaaatat tcggatcttc tgacctatgt tgactgctac gtcggtgtgt
tsA279		---------- ---------- ---------- ---------- ---------- ----------
T3D	481	ctgctcgtca ggctttaaac aattttcaga aacaagtgcc tgtgattaca cctactaggc
tsA279		---------- ---------- ---------- ---------- ---------- ----------
T3D	541	agacgatgta tgtcgactcg atacaagcgg ccttgaaagc tttagaaaag tgggagattg
tsA279		---------- ---------- ---------- ---------- ---------- ----------
T3D	601	atctgagagt ggctcaaacg ttgctgccta cgaacgttcc gattggagaa gtctcttgtc
tsA279		---------- ---------- ---------- ---------- ---------- ----------
T3D	661	caatgcagtc ggtagtgaaa ctgctggatg atcagctgcc agatgacacg ctgatacgga
tsA279		---------- ---------- ---------- ---------- ---------- ----------
T3D	721	ggtatcccaa ggaagccgcc gtcgctttgg ctaaacgaaa cgggggaata caatggatgg
tsA279		---------- ---------- ---------- ---------- ---------- ----------
T3D	781	acgtatcaga aggcaccgtg atgaacgagg ctgtcaacgc tgttgcagct agtgcactgg
tsA279		---------- ---------- ---------- ---------- ---------- ----------
T3D	841	caccttcagc atcagcccca cccttagaag agaagtcaaa gttaaccgaa caagcgatgg
tsA279		---------- ---------- ---------- ---------- ---------- ----------
T3D	901	atctcgtgac cgcggctgag cctgagataa ttgcctcact cgcgccagtt cccgcacccg
tsA279		---------- ---------- ---------- ---------- ----t----- ----------
T3D	961	tgtttgccat accacctaaa ccagcagatt ataatgtgcg tactctgagg atcgacgagg
tsA279		---------- -t-------- ---------- ---------- ---------- ----------

Continued 145/

Figure 5.6 (continued)

Clone	Base	Sequence
T3D	1021	ccacttggct gcgaatgatt ccaaaatcaa tgaacacacc ttttcaaatc caggtgactg
tsA279		---------- ---------- ---------- ---------- ---------- ----------
T3D	1081	ataacacagg aactaattgg catctcaatt tgagggggag gactcgtgta gtgaatctgg
tsA279		---------- ---------- ---------- ---------- ---------- ----------
T3D	1141	accaaatcgc tccgatgcgg tttgtattag atttaggggg aaagagttat aaagagacga
tsA279		---------- ---------- ---------- ---------- ---------- ----------
T3D	1201	gctgggatcc aaacggcaag aaggtcggat tcatcgtttt tcaatcgaag ataccattcg
tsA279		---------- ---------- ---------- ---------- ---------- ----------
T3D	1261	aactttggac tgctgcttca cagatcggtc aagccacggt ggttaactat gtccaactat
tsA279		---------- ---------- ---------- ---------- ---------- ----------
T3D	1321	acgctgaaga cagctcattt accgcgcagt ctatcattgc tactacctct ttggcttata
tsA279		---------- ---------- ---------- ---------- ---------- ----------
T3D	1381	actatgagcc tgagcagttg aataagactg accctgagat gaattattat cttttggcga
tsA279		---------- ---------- ---------- ---------- ---------- ----------
T3D	1441	cctttataga ctcagccgct ataacgccaa cgaatatgac acagcctgat gtttgggatg
tsA279		---------- ---------- ---------- ---------- ---------- ----------
T3D	1501	ccttgctgac gatgtcccca ctatcagctg gcgaggtgac agtgaagggt gcggtagtga
tsA279		---------- ---------- ---------- ---------- ---------- ----------
T3D	1561	gtgaagtagt ccctgcagac ttgataggta gctacactcc agaatcccta aacgcctcac
tsA279		---------- ---------- ---------- ---------- ---------- ----------
T3D	1621	ttccgaatga tgctgctaga tgcatgatcg atagagcttc gaagatagcc gaagcaatca
tsA279		---------- ---------- ---------- ---------- ---------- ----------
T3D	1681	agattgatga tgatgctgga ccagatgaat attccccaaa ctctgtacca attcaaggtc
tsA279		---------- ---------- ---------- ---------- ---------- ----------
T3D	1741	agcttgctat ctcgcaactc gaaactggat atggtgtgcg aatattcaac cctaaaggga
tsA279		---------- ---------- ---------- ---------- ---------- ----------
T3D	1801	tcctttctaa aattgcatct agggcaatgc aggctttcat tggtgacccg agcacaatca
tsA279		---------- ---------- ---------- ---------- ---------- ----------
T3D	1861	tcacgcaggc ggcgccagtg ttatcagaca agaataattg gattgcattg gcacagggag
tsA279		---------- ---------- ---------- ---------- ---------- ----------
T3D	1921	tgaaaactag tctgcgtact aaaagtctat cagcgggagt gaagactgca gtgagtaagc
tsA279		---------- ---------- ---------- ---------- ---------- ----------
T3D	1981	tgagctcatc tgagtctatc cagaattgga ctcaaggatt cttggataaa gtgtcagcgc
tsA279		---------- ---------- ---------- ---------- ---------- ----------
T3D	2041	attttccagc accaaagccc gattgttcga ctagcggaga tagtggtgaa tcgtctaatc
tsA279		-----a---- ---------- ------c--- ---------- -------a-- ----------

Continued 146/

Figure 5.6 (continued)

Clone	Base	Sequence
T3D	2101	gccgagtgaa gcgcgactca tacgcaggag tggtcaaacg tgggtacaca cgttaggccg
tsA279		---------- ---------- ---------- ---------- ---------- ----------
T3D	2161	ctcgccctgg tgacgcgggg ttaagggatg caggcaaatc atc
tsA279		---------- ---------

Figure 5.7. Amino acid sequence for the μ1 protein of reovirus T3D and *tsA279.*

The amino acid sequence of the major outer capsid protein μ1 of reovirus serotype 3 generated by translation of the RT-PCR sequence with the program EditSeq (DNAStar). The sequence for the μ1 protein of the temperature sensitive mutant *tsA279* is shown below, with identical amino acids shown as dashes (-).

Figure 5.7. Amino acid sequence for the μ1 protein of Reovirus T3D and *tsA279*.

Clone	Residue	Sequence
T3D	1	MGNASSIVQT INVTGDGNVF KPSAETSSTA VPSLSLSPGM LNPGGVPWIA VGDETSVTSP
tsA279		---------- ---------- ---------- ---------- ---------- ----------
T3D	61	GALRRMTSKD IPETAIINTD NSSGAVPSES ALVPYIDEPL ...TEHAITN FTKAEMALEF
tsA279		---------- ---------- ---------- ---------- ---------- ----------
T3D	121	NREFLDKMRV LSVSPKYSDL LTYVDCYVGV SARQALNNFQ KQVPVITPTR QTMYVDSIQA
tsA279		---------- ---------- ---------- ---------- ---------- ----------
T3D	181	ALKALEKWEI QLRVAQTLLP TNVPIGEVSC PMQSVVKLLD QQLPDDTLIR RYPKEAAVAL
tsA279		---------- ---------- ---------- ---------- ---------- ----------
T3D	241	AKRNGGIQWM QVSEGTVMNE AVNAVAASAL APSASAPPLE EKSKLTEQAM QLVTAAEPEI
tsA279		---------- ---------- ---------- ---------- ---------- ----------
T3D	301	IASLAPVPAP VFAIPPKPAD VNVRTLRIDE ATWLRMIPKS MNTPFQIQVT QNTGTNWHLN
tsA279		-----S---- ----S----- ---------- ---------- ---------- ----------
T3D	361	LRGGTRVVNL QQIAPMRFVL QLGGKSYKET SWQPNGKKVG FIVFQSKIPF ELWTAASQIG
tsA279		---------- ---------- ---------- ---------- ---------- ----------
T3D	421	QATVVNYVQL YAEQSSFTAQ SIIATTSLAY NYEPEQLNKT QPEMNYYLLA TFIDSAAITP
tsA279		---------- ---------- ---------- ---------- ---------- ----------
T3D	481	TNMTQPQVWQ ALLTMSPLSA GEVTVKGAVV SEVVPAQLIG SYTPESLNAS LPNDAARCMI
tsA279		---------- ---------- ---------- ---------- ---------- ----------
T3D	541	QRASKIAEAI KIQQQAGPQE YSPNSVPIQG QLAISQLETG YGVPIFNPKG ILSKIASRAM
tsA279		---------- ---------- ---------- ---------- ---------- ----------
T3D	601	QAFIGQPSTI ITQAAPVLSQ KNNWIALAQG VKTSLRTKSL SAGVKTAVSK LSSSESIQNW
tsA279		---------- ---------- ---------- ---------- ---------- ----------
T3D	661	TQGFLQKVSA HFPAPKPQCS TSGQSGESSN RRVKRQSYAG VVKPGYTR
tsA279		---------- --T------P ------K--- ---------- --------

shifted from 1.25 minutes with T3D to 2.17 and 1.67 minutes for permissive and restrictive *tsA279* virions, respectively. There was a trend towards later initial cleavage of μ1 to δ and ϕ with both permissive and restrictive mutant virions (Table 5.4). There appeared to be residual levels of μ1 which were not cleaved to δ and ϕ even after one hour of digestion (Figure 5.8).

7. Growth curves for infection with the mutant *tsA279* clone at permissive and restrictive temperatures.

Evaluation of 32°C cultures showed a brief lag phase of approximately 12 hours, followed by exponential increase in the amount of recoverable infective virus until 48 hours post infection, after which time the rate of increase in viral titre declined. Electron microscopic evaluation demonstrated cytoplasmic inclusions in more than 40% of the cells at the end of the lag phase. The proportion of cells with viral inclusions increased gradually until 60 hours post infection, at which time every cell was infected and maximal titres achieved (Figure 5.9, Table 5.1).

In contrast, restrictive temperature infections showed a brief lag phase followed by a slight increase in recoverable infectious virus to just above the input load. The titre of recoverable infective virus attained a peak below input at 24 hours and then declined by up to one order of magnitude at 72 hours post infection. Thin section electron microscopy demonstrated infections in approximately 12% of cells viewed at 12 hours post infection. The presence of cytoplasmic inclusions decreased to 1% of cells

Table 5.4 **Proteolytic digestion kinetics[a] of *tsA279*.**

		Chymotrypsin		Trypsin	
	Assembly Conditions[b]	Removal of $\sigma 3$	Appearance of δ	Removal of $\sigma 3$	Appearance of δ
T3D	Permissive	1.25(0.54)[c,d]	1.42(0.66)	0.00[e]	0.00
tsA279	Permissive	2.17(0.24)	1.58(0.12)	0.00	0.00
tsA279	Restrictive	1.67(0.12)	1.83(0.47)	0.00	0.00

a. Digestions done at 32°C.
b. Assembly conditions: Permissive = culture and assembly at 32°C, Restrictive = culture and assembly at 40°C.
c. Time in Minutes, Standard deviation in parentheses.
d. Chymotrypsin data the results of three separate experiments.
e. Trypsin data the results of two separate experiments.

A. T3D permissively assembled virions

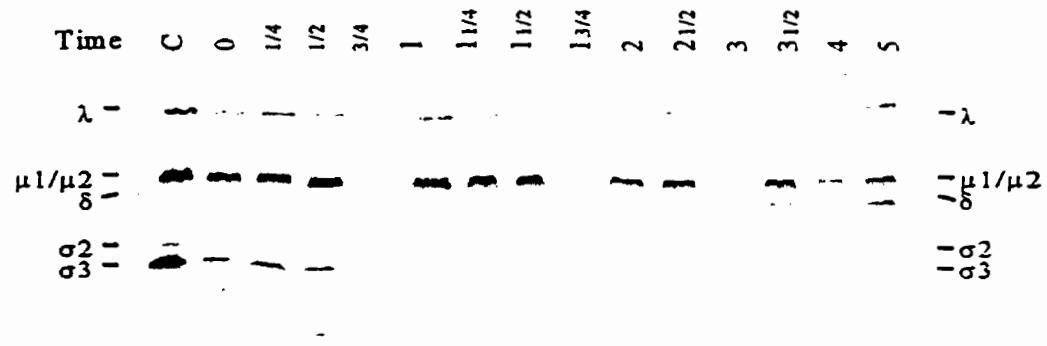

B. *tsA279* permissively assembled virions

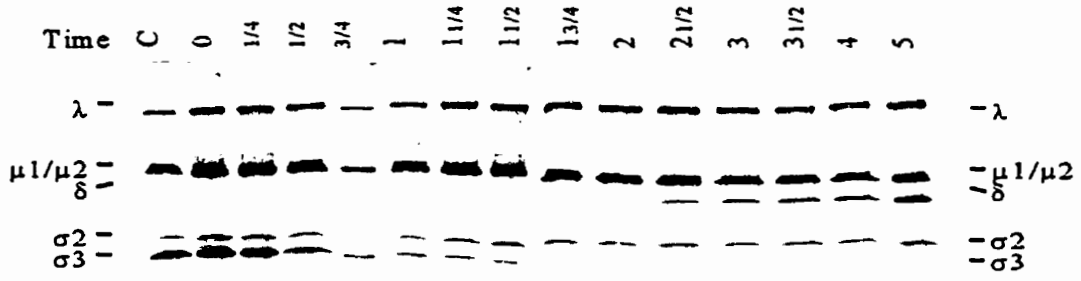

C. *tsA279* restrictively assembled virions

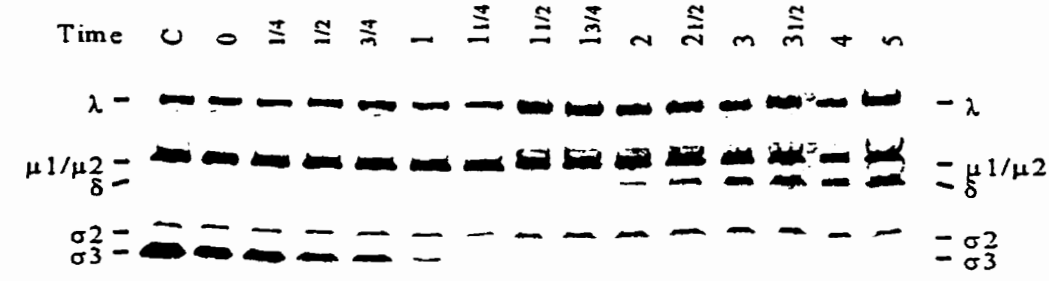

Figure 5.8. <u>Chymotrypsin digests of T3D, permissively assembled *tsA279* and restrictively assembled *tsA279*.</u>

T3D virions assembled at permissive temperature and *tsA279* mutant virions assembled at both permissive and restrictive temperatures were digested at 32°C with α-chymotrypsin, sampled as indicated and the digestion process stopped by simultaneous addition of PMSF and immersion into wet ice bath. The proteins were suspended in electrophoresis buffer and separated by SDS-PAGE as indicated (Chapter 2.7.d, & f). Control samples (C) were treated the same as the 0 time samples with the exception that no α-chymotrypsin was added.

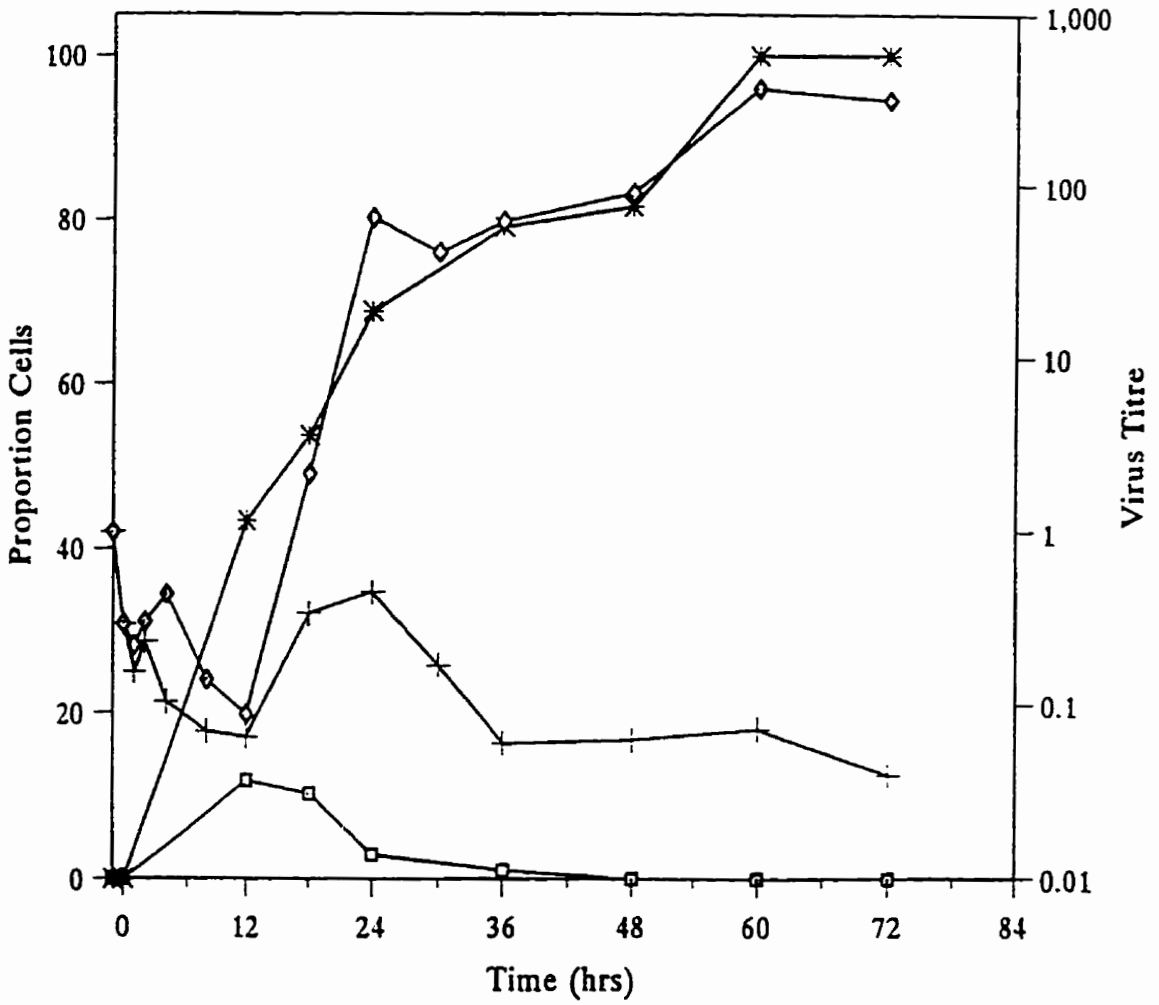

Figure 5.9 Growth curve of *tsA279* and electron microscopic evidence of infection at permissive and restrictive temperatures.

L929 cells were infected and incubated as described in Figure 5.1. Aliquots were taken at indicated times, titered, and examined for evidence of infection by thin-section electron microscopy. Infected cells are expressed as the proportion of cells showing infection in the plane of section; virus titre is expressed as PFU/cell. Infected cells (*) and infectious titre (◆) at 32°C; infected cells (□) and infectious titre (+) at 39.5°C.

examined by 36 hours post infection, after which there was no evidence of cytoplasmic inclusions (Table 5.1).

8. Identification of assembly intermediate structures produced by *tsA279*.

a. Culture of monolayers and preparation for evaluation.

Cell monolayers were prepared in 24 well cluster dishes, infected at MOIs of 5 and 50 PFU/cell with T1L or *tsA279*, and incubated at a restrictive temperature of 40°C as described in Chapter 2, Materials and Methods. Alternatively, infections were prepared at an MOI of 5 PFU/cell with a panel of T1L x *tsA279* reassortant clones containing only the mutant L2 gene, only the mutant M2 gene, both mutant L2 and M2 genes, or neither of the mutant L2 or M2 genes, and incubated at a restrictive temperature of 40°C. Lysates were prepared by freeze/thaw, the crude cellular debris cleared, the particles stabilized with glutaraldehyde, and centrifuged directly to formvar-carbon coated grids and stained with PTA as described in Chapter 2.10. The pelleted material was evaluated in a Philips model 201 electron microscope at a machine magnification of 20,000x using a binocular focusing scope (final magnification of evaluation 95,000x), and the proportion of particles determined by direct count as described (Hammond *et al*, 1981; Chapter 2.4.b, above). Statistical evaluation of the production of the assembly intermediates was performed using a standard χ^2 test with Yate's correction.

b. The assembly intermediates produced at restrictive temperatures.

Preliminary evaluation from direct particle counts of whole cell lysates indicated that

there was essentially no difference in the distribution of particles produced at MOIs of 5 or 50 PFU/cell at either permissive or restrictive temperature. Therefore, the analyses were done using infections with an MOI of 5 PFU/cell. The predominant structural form produced at 32°C by both *tsA279* and T3D was the genome complete whole virus particle (whole particles) (diameter approximately 80nm) after both 36 and 72 hours, followed by top component (diameter approximately 80nm). For *tsA279* the next most common structures produced by all but one infection at both time frames were outer shell structures (outer shells) (diameter approximately 90nm) followed by core particles (diameter approximately 50nm), both with and without the λ2 pentameric spikes. One 36 hour infection produced a relatively high proportion of core particles (sample 3, 3.35%), raising the overall proportion of this class of particles for this time frame. T3D produced a lesser proportion of shells at 36 hours than at 72 hours and a higher proportion of core particles, complete with λ2 pentameric spikes, at 36 hours than was evident at 72 hours. As with *tsA279*, the higher values at 36 hours post infection were attributable to one sample with a high proportion of cores relative to the other species of assembly intermediates visualized (Table 5.5).

The distribution of whole virions and assembly intermediates produced in infections of both *tsA279* and T3D which were incubated at a restrictive temperature of 40°C differed from that seen at the permissive temperature. The most common component was still whole virus after both 36 and 72 hours. The proportion of top component remained relatively stable with *tsA279* at the restrictive temperature as compared to permissive

Table 5.5. Distribution of species of particles produced by T3D and *tsA279* at permissive and restrictive temperatures[a].

Clone	°C	Time	Total Particles[b]	Total Particles/ml[c]	Proportion of Particle[d]			
					Virion	Top Component	Outer Shell	Core
T3D	32	36	1773	1.69×10^8	85.70 (4.30)	6.45 (0.73)[f]	2.65 (0.84)	5.23 (2.95)
		72	24682	2.94×10^9	78.60 (<0.1)	15.37 (0.29)	5.93 (0.29)	0.10 (<0.1)
	40	36	1632	1.32×10^8	64.08 (2.38)	22.36 (2.84)	9.10 (1.47)	1.68 (0.28)
		72	4904	4.39×10^8	56.05 (8.54)	22.48 (5.43)	9.88 (0.66)	11.55 (4.02)
tsA279	32	36	12546	1.33×10^9	76.88 (3.83)	18.98 (3.17)	2.13 (0.55)	1.88 (1.05)
		72	31659	3.82×10^9	79.00 (1.02)	18.80 (1.74)	2.03 (1.78)	0.23 (0.16)
	40	36	3401	3.17×10^7	60.60 (2.66)	19.63 (3.87)	0.98 (0.35)	18.80 (5.94)
		72	1209	3.56×10^7	50.23 (7.51)	18.60 (7.34)	0.73 (0.67)	30.47 (15.12)

a. Calculated from 3 to 4 separate experiments.
b. Total number of viral and subviral particles counted.
c. Total particles in the cell lysates, calculated as previously described (Hammond *et al*, 1981).
d. Proportions of indicated particles, expressed as percentages of the total number of particles produced, with standard error of the mean of replicate experiments shown in parenthesis.

temperature. T3D showed a relatively large increase in this structure at both times. The proportion of outer shell structures decreased slightly for *tsA279* at both 36 and 72 hours but increased in all samples of T3D. The proportion of core particles produced by *tsA279* at the restrictive temperature increased one to two orders of magnitude at both 36 and 72 hours. The proportion of core particles produced for parental T3D was slightly reduced at 36 hours but increased by 72 hours (Table 5.5).

A new species of particle, a core particle which appeared deficient in the λ2 pentameric spikes, was observed in cultures of tsA279 at 40°C (Figure 5.10A). Core particles produced under permissive growth conditions for both T3D and *tsA279*, and at restrictive temperature for T3D clearly demonstrated the presence of λ2 pentameric spikes. Core particles produced at restrictive temperature conditions by *tsA279* appeared to have fewer, if any λ2 pentameric spikes (Figure 5.10A). To confirm the identity of the λ2 pentameric spike deficient particles polyclonal rabbit anti-reovirus IgG was conjugated to a 12nm colloidal gold probe as described in Chapter 2. Whole cell fractions which had been cleared of cell debris, fixed with 0.1% glutaraldehyde in MEM, and centrifuged directly to 400 mesh formvar-carbon grids, were reacted with the gold labeled antibody preparation, stained with PTA and evaluated electron microscopically. The gold:anti reovirus probe showed clear reaction with all species of subviral and viral structures previously identified, including the λ2 spike deficient core particles (Figure 5.10B).

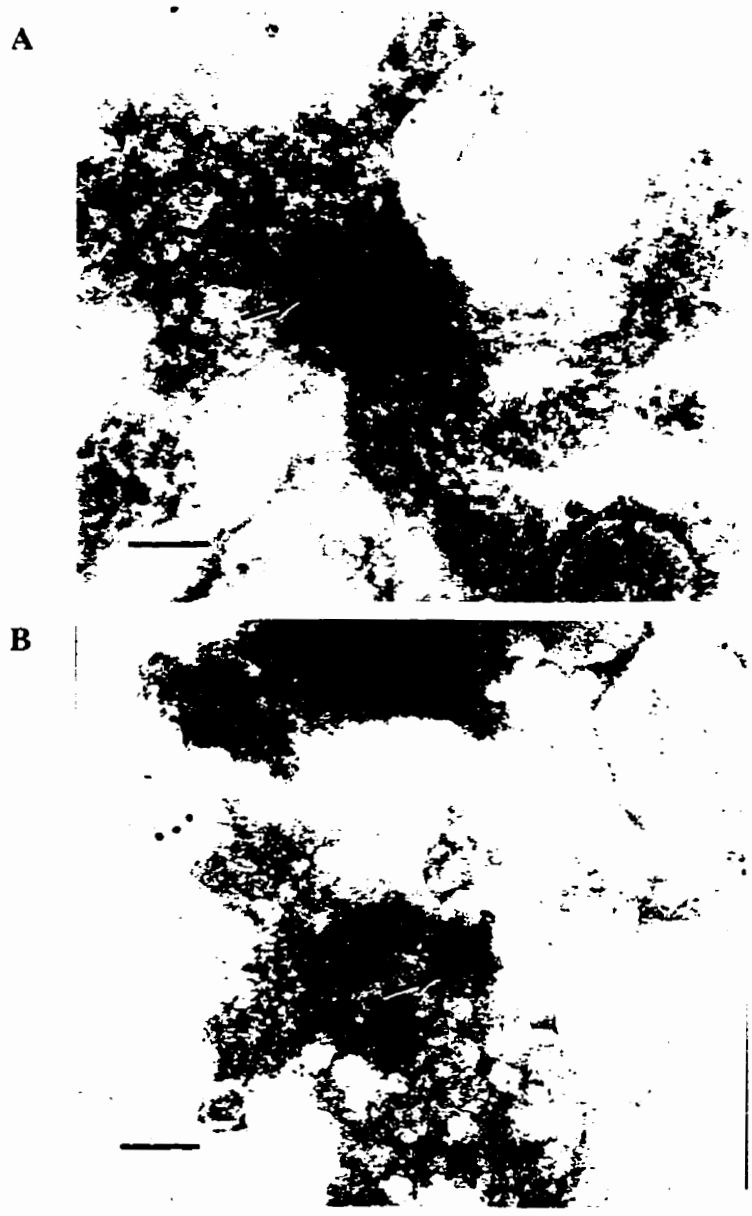

Figure 5.10 Negative stain and immunogold labelled λ2 spike deficient core particles produced at restrictive temperature.

(A) Restrictive temperature cytoplasmic extracts were centrifuged directly to electron microscope grids and negatively stained with PTA as described (Chapters 2.4b,c, 6.8) (B) Same as (A) except grid samples were immuno-labelled (12nm gold) before negative staining. Arrows indicate core particles. Magnification 100,000x; bars represent 100nm.

9. Protein composition of the assembly intermediates produced at restrictive temperatures.

Scintillation count data from radiolabelled cultures of permissive and restrictive radiolabelled cultures showed single clear peaks of radioactivity at a density of 1.33-1.35gm/ml CsCl. No individual peaks of activity could be identified in fractions of lower density (Figure 5.11). Negative stain electron microscopic examination of fractions after direct centrifugation to carbon-formvar coated copper grids revealed complete virions in the peaks (Figure 5.12.A.1). Intermediate assembly structures were identified in fractions of lower densities, with the λ2 spike deficient core like particles, and outer shells being found at densities ranging between 1.26 and 1.29gm/ml. These structures were genome deficient and were usually isolated in fractions which contained minimal amounts of top component structures (Figure 5.12.A.2 and 3). The spike deficient core particle also demonstrated the characteristic apical cavity reported in earlier structures (Figure 5.12.A.2) (Yin *et al*, in submission). No core like structures containing genome were found in higher density fractions.

Protein analysis of the fractions by SDS-PAGE using the TGU gel system(Chapter 2.7.f) indicated that both the λ2 spike deficient cores and the outer shells were deficient for the λ2 protein. In addition, the minor core protein μ2 was either missing or had an altered rate of electrophoretic migration (Figure 5.12.B). Western blot analysis of parallel electrophoretic separations using high titre polyclonal antibody specific to the μ2 protein, in combination with high titre polyclonal antiserum to reovirus T3D, indicated that levels

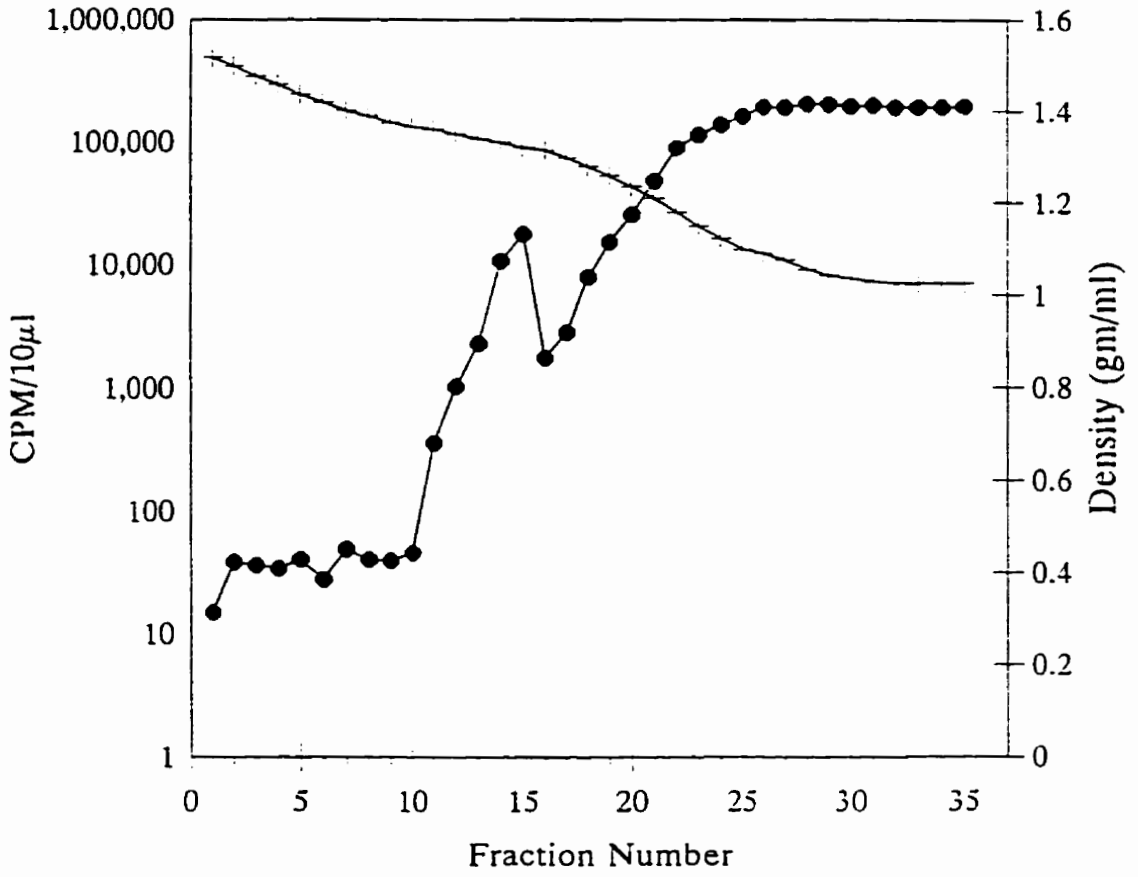

Figure 5.11 Cesium chloride fractionation of restrictive temperature cultures for *tsA279.*

L929 cells were infected, and viral proteins labeled with ^{35}S-Methionine during culture at 40°C. Cell pellet membranes were solubilized with desoxycholate, the samples extracted two times with genetron, the viral components separated on preformed CsCl gradients, and fractionated. The density of each fraction was determined from the refractive index and aliquots were counted for radioactivity as described (Chapters 2.2h, 2.6.b, 2.7b). (●), Radioactivity in cpm/10μl; (+), Fraction density in gm/cm^3.

Figure 5.12. **Analysis of the protein composition of assembly structures produced by *tsA279* at restrictive temperature.**

L929 cells were infected with *tsA279* and incubated in suspension culture in the presence of ^{35}S-Methionine at 40°C. The cell pellets were extracted with Genetron, the viral structures separated by CsCl buoyant density centrifugation, and the CsCl gradients fractionated, all as described (Chapter 5.9).

A. Electron micrographs of representative particles found in: (1.) gradient fraction 15, whole virus; (2.) gradient fraction 18, λ2 spike deficient core particles; and (3.) Gradient fraction 19, outer shell structures. Note the apical cavity present in the spike defective core (arrow)(5.12.A.2). Magnification = 100,000x, bar = 100nm.

B. Fluorogram of TGU polyacrylamide electrophoresis gel which was loaded with gradient fraction volumes adjusted to provide 15,000cpm per lane (Chapter 2.7.f.2). The gel was prepared from the same samples shown in 5.12.A. Note the absence of λ2 in fractions 18 and 19, which are composed primarily of core particles (Fraction 18) and outer shells (Fraction 19), with a small amount of top component (5.12.A.3). T3: permissively assembled CsCl purified virions of T3Dearing. A: Permissively assembled, CsCl purified virions of *tsA279*.

C. Immunoblot of a TGU gel run in parallel with and using the same samples as the gel shown in 5.12.B. The gel was probed by both whole antireovirus antiserum and high titre anti μ2. Note the intense reaction of anti μ2 in the permissively assembled *tsA279*, and absence of reaction in the remaining lanes. The anti whole reovirus shows weak reaction to λ2 in the control lane, but no reaction to λ2 in the remaining lanes. Anti whole reovirus antiserum reacts to μ1 and σ3 in both fractions 18 and 19. M: marker lane.

A. Reovirus structures produced by *tsA279* at restrictive temperatures

1. Fraction 15, whole virus **2. Fraction 18, spikeless cores** **3. Fraction 19, outer shells**

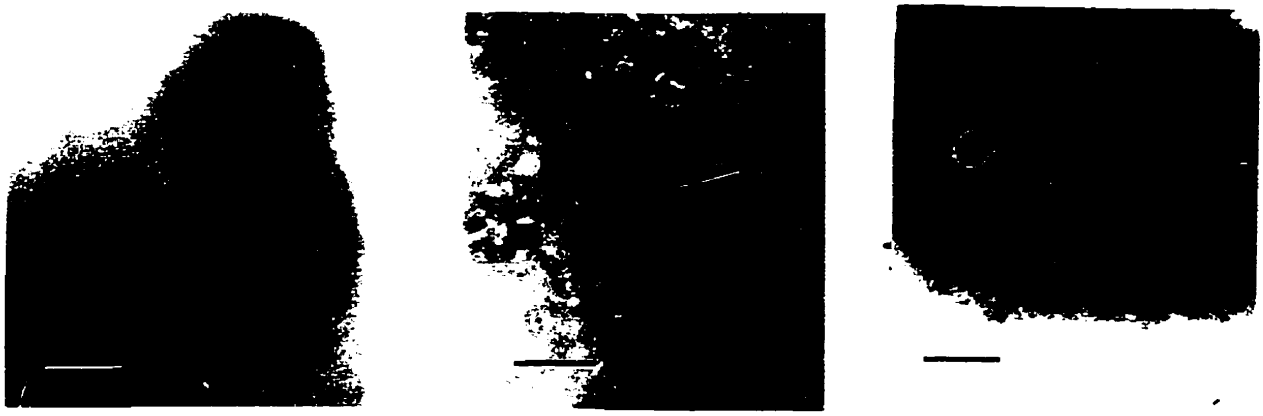

B. Protein composition of restrictive intermediates produced by *tsA279*

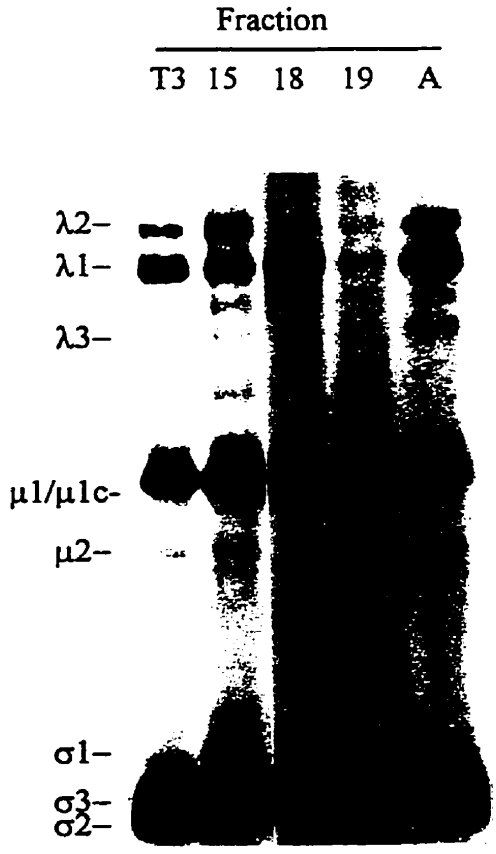

C. Immunoblot analysis of restrictive intermediates produced by *tsA279*.

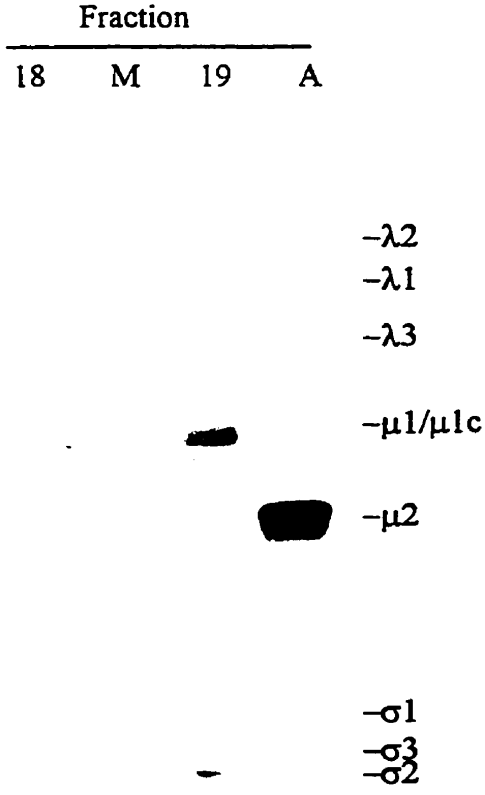

of μ2, were negligible (Figure 5.12.C). Attempts to further separate outer shells from spike defective cores by rate zonal centrifugation experienced marginal success. To confirm the reduction in copy numbers of λ2 and μ2 present in the core like particles, laser densitometric scans of fluorograms were analyzed. The number of cysteines and methionines contributed by each structural protein to whole virions, intermediate subviral particles and core particles was determined by multiplying the copy number of the protein in the structure by the number of cysteines and methionines present in one copy of the relevant protein. The copy number of residues contributed by each protein was then standardized to the proportion of residues contributed by the major core protein λ1 (Table 5.6). The signal for l1 was determined for each fraction and used to determine the predicted signal for the remaining structural proteins in that fraction. The actual signal for each protein was then expressed as a proportion of the predicted signal (Table 5.7). There was no significant difference between permissively assembled T3D and both permissively and restrictively assembled *tsA279* whole virions. However, the levels of λ2 and μ2 present in the fractions containing core structures was reduced to approximately 2% and 5%, respectively, of the levels of these proteins anticipated to be found in complete core particles (Table 5.7). These values represent approximately one copy of each protein per spike defective core. The amount of these proteins may be attributed to the low levels of contaminating top component found in the fractions of some cultures.

Table 5.6 **Relative copy numbers, and cysteine and methionine content of the structural proteins in reovirus virions and core particles.**

Protein	MW	Copies Protein[a]		Copies Cysteine and Methionine			Relative Proportion Cysteine and Methionine[b]	
		Virus	Core	Molecule[c]	Virion[d]	Core	Virion	Core
λ1	137.4	120	120	55	6600	6600	1.00	1.00
λ2	144.0	60	60	43	2580	2580	0.39	0.39
λ3	142.4	12	12	65	780	780	0.11	0.11
μ1/1c	76.3	600	600	22	13200	13200	2.0	2.0
μ2	83.3	21[e]	14	39	819	546	0.12	0.08
σ1	51.4	36	-	9	324	-	0.05	-
σ2	47.1	120	120	18	2160	2160	0.33	0.33
σ3	41.2	600	-	27	16200	-	2.45	-

a. From Dryden *et al*, 1993.
b. Relative proportion cysteine and methionine in each structure is normalized to the total copy number of cysteine and methionine in the λ1 protein by the following formula: {(copies C and M for the protein)x(copies of the protein)}÷{(copies C and M in λ1)x(Copies λ1)}.
c. From published sequence data as per: λ1, Bartlett and Joklik, 1988; λ2. Seleger *et al*, 1987; λ3, Weiner and Joklik, 1988,; μ1, Jayasuriya *et al*, 1988; μ2, Weiner *et al*, 1989; σ1, Bassel-Duby *et al*, 1985; σ2, Dermody *et al*, 1991; and σ3, Giantini *et al*, 1984.
d. Total cysteine and methionine in the structure for each protein obtained by the following formula (total C and M in the protein)x(Copies protein).
e. Copy numbers of μ2 from Coombs, 1998a.

Table 5.7 Relative Amounts of Proteins Present in Permissively and Restrictively Assembled *tsA279* Virions and Intermediate Structures.[a]

	Permissive			
	T3D	*tsA279*	Restrictively Assembled *tsA279*	
Protein	Virions	Virions	Virions	Core Fractions
λ1	100.0(0.0)	100.0(0.0)[b,c]	100.0(0.0)	100.0(0.0)
λ2	111.5(11.3)	107.3(6.9)	108.7(7.8)	2.1(1.5)
λ3	92.8(15.2)	284.4(267.4)	97.8(15.5)	91.1(24.8)
μ1/1c	127.5(48.6)	131.3(49.0)	160.6(64.6)	59.3(49.4)
μ2	100.0(12.5)	79.1(17.5)	96.8(9.0)	5.4(5.4)
σ1	ND[d]	ND	ND	ND
σ2/3[e]	156.1(43.2)	123.8(17.2)	201.3(81.3)	109.0(65.5)

a. All values calculated from 3 to 4 separate infections.

b. All values expressed as percent of predicted quantity with the standard deviation of the mean of replicate cultures shown in parenthesis.

c. Integration values for λ1 expressed as 100% of expected value. Values for other proteins scaled to the λ1 values.

d. Values for σ1 were not determined.

e. σ2 and σ3 were analysed jointly due to insufficient resolution in the TGU gel system for scan analysis.

10. Mapping the gene lesions associated with the assembly intermediates produced at restrictive temperatures.

Particle counts for the panel of reassortant clones segregating the mutant L2 and M2 gene segments showed that the L2 gene segment was responsible for the blockade in assembly resulting in the λ2 spike deficient core particle. This blockade occurred both in the presence and the absence of the mutant M2 gene segment. Cultures of reassortant clones with the mutant M2 gene segment, in the absence of the mutant L2 gene segment, demonstrated an accumulation of top component. These clones contained a negligible proportion of core particles, both with and deficient for the λ2 spike. The clones with both the L2 and M2 gene segments from the wild type parent T1L showed a distribution of particle species similar to that seen with T3D and permissive cultures of *tsA279*, (Table 5.2, Table 5.8). Analysis of the electropherotypes for the panel of reassortant clones analyzed associates the production of the λ2 spike deficient core particle with the L2 and S3 gene segments. The S3 segment codes for the non-structural protein μNS. The possible role of the non structural protein μNS in assembly of a λ2 spike deficient core particle cannot be completely discounted since it is synthesized in relatively large amounts during the viral life cycle (Schiff and Fields, 1990). Further, this protein has been associated with the cytoskeleton of infected cells and may play a role in anchoring viral structures to the cell matrix during assembly (Mora *et al*, 1987). Finally, co-precipitation studies have indicated that μNS interacts with σNS and viral ssRNA early in the replication cycle (Antczak and Joklik, 1992). The production of top component was associated with the mutant M2 gene (Table 5.9). Conversely, the reassortant clone

Table 5.8. Mapping the assembly intermediate particles produced by T1Lang/*tsA279* reassortants at the restrictive temperatures.

Gene Segments Clone	Total Particles[a]	Total Particles/ml[b]	Proportion of Particle[c] Virion	Top Component	Outer Shell	Core Particles With λ2	Core Particles No λ2
Mutant L2 & M2							
tsA279	1209	5.6×10^7	50.23	18.60	0.73	0.10	30.47
LA279.08	5768	2.06×10^8	50.92	20.06	1.60	0.05	27.38
Mutant L2, T1L M2							
LA279.11	6415	2.30×10^8	56.15	27.06	0.12	1.71	14.95
LA279.76	1144	4.03×10^7	15.03	38.90	0.00	0.00	46.07
T1L L2, Mutant M2							
LA279.10	1603	5.74×10^7	26.51	67.37	1.06	3.93	1.12
LA279.56	2689	9.62×10^7	38.56	53.85	1.49	5.76	0.33
T1L L2, T1L M2							
LA279.15	10554	3.78×10^9	82.80	11.65	1.28	4.06	0.21
T1L	4965	1.78×10^9	72.00	23.16	1.89	0.56	2.38

a. Total number of viral and subviral particles counted.
b. Total particles in the cell lysates, calculated as previously described (Hammond *et al*, 1981).
c. Proportions of indicated particles, expressed as percentages of the total number of particles produced.

Table 5.9. **Electropherotypes and assembly intermediate particles produced by T1Lang x *tsA279* reassortants at the restrictive temperature.**

	Gene Segment§									
CLONE	L1	L2	L3	M1	M2	M3	S1	S2	S3	S4
A. λ2 spike deficient core particle										
tsA279	A	A	A	A	A	A	A	A	A	A
LA279.08	1	A	1	A	A	A	A	A	A	A
LA279.76	A	A	1	1	1	1	1	1	A	A
LA279.11	A	A	A	A	1	A	A	A	A	1
tsA279/T1L	3/1	4/0	2/2	3/1	2/2	3/1	3/1	3/1	4/0	3/1
B. Top Component										
LA279.10	A	1	1	1	A	A	1	A	A	A
LA279.56	1	1	1	1	A	1	1	1	1	1
tsA279/T1L	1/1	0/2	0/2	0/2	2/0	1/1	0/2	1/1	1/1	1/1

§: Denotes parental origin of gene; 1: T1Lang; A: *tsA279*

LA279.10, which contains a mutant S3 but wild type L2 gene segment, does not make spike defective cores, suggesting that the gene segment is not associated with this phenotype.

11. Immunofluorescent microscopy of permissive and restrictive temperature cultures.

In order to determine the production of viral proteins at permissive and restrictive temperatures monolayers were infected, fixed, reacted against rabbit anti-whole reovirus polyclonal antibody, and developed with rhodamine conjugated goat anti-rabbit IgG. The monolayers were examined by immunofluorescent microscope and evaluated in accordance with the 4 stage system described (Chapter 2.5, 4.1.c).

T3D infections showed little evidence of infection after incubation at 32°C for 6 hours. Those cells which demonstrated evidence of infection had fine granular points of fluorescence in the cytoplasm (Stage 1). By 12 hours fluorescing viral inclusions were larger, with some reticulate appearance (Stage 2). Some cells showed perinuclear condensation of fluorescence (Stage 3) and a few cells gave no appearance of infection. By 48 hours essentially all cells were infected with most showing diffuse fluorescence throughout the cytoplasm (Stage 4) (Figure 5.13.A). At 40°C most cells infected with T3D initially progressed more rapidly than the parallel permissive infections, with most cells attaining an advanced stage 1 after 6 hours. The infection progressed rapidly to stage 3 in most cells by 12 hours. After 12 hours the progress of infection to stage 4

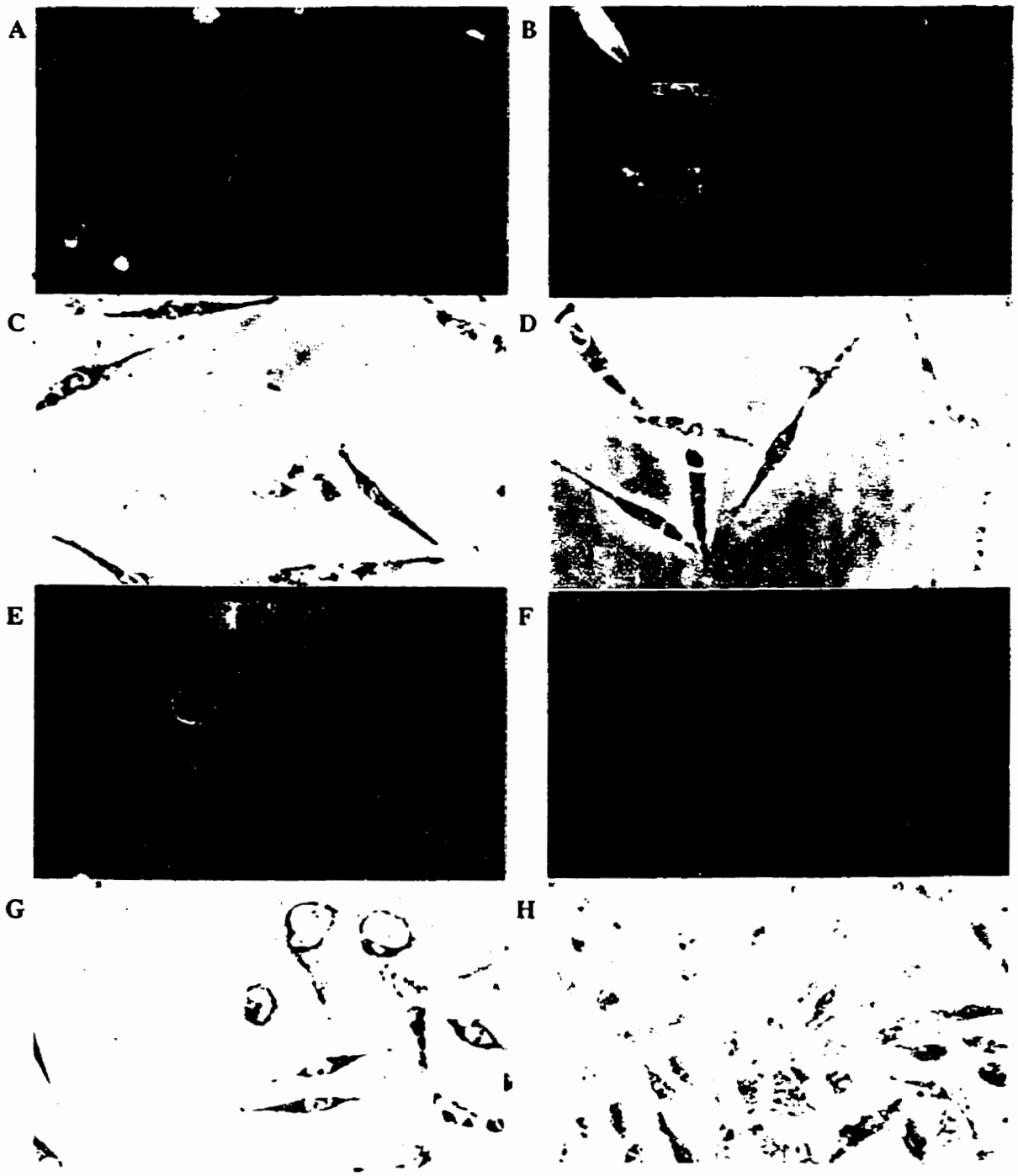

Figure 5.13. Immunofluorescent and phase contrast microscopy of permissive and restrictive temperature infections of wild-type T3D (A-D) and *tsA279* (E-H).

Subconfluent monolayers were infected at an MOI of 10 PFU per cell and incubated at 32°C (A,C,E,G) and 40°C (B,D,F,H) for 48 hours. Cells were treated with rabbit anti-reovirus hyperimmune serum, developed with rhodamine-conjugated anti-rabbit serum, and viewed and photographed with fluorescent and phase contrast microscopy.

was slower than at 32°C, and fewer cells reached stage 4 level of infection after 48 hours (Figure 5.13B). Parallel phase contrast micrographs showed most cells were no longer viable (Figure 5.13.C, D).

Cells which were infected with *tsA279* progressed through the stages of infection more slowly at 32°C than did those which were infected with T3D. After 6 hours most cells showed no sign of infection, those that did showed pinpoints of fluorescence, as would be expected at an early stage 1 level of infection. By 18 hours the majority of cells were infected and had advanced to either stage 2 or 3. The infections rarely progressed past the third stage of infection even after 48 hours. However, every cell examined displayed evidence of infection by that time (Figure 5.13.E). At a restrictive temperature of 40°C parallel infections with mutant *tsA279* showed pinpoint levels of fluorescence after 6 hours (early stage 1). Most cells showed no evidence of fluorescence above background. A few cells were at a late stage 2 level after 24 hours, but most cells were still uninfected. By 48 hours most cells demonstrated background levels of staining. A small proportion of cells (10.62%) demonstrated weak stage 1 or stage 2 levels of fluorescence (Figure 5.13.F).

12. <u>Evaluation of the production of dsRNA.</u>

L929 monolayers were infected with T3D, *tsA201*, *tsA279*, *tsB405*, and *tsE320*, labeled with $^{32}PO_4^{-3}$, and the dsRNA segments were resolved by SDS-PAGE (Chapters 2.6a, 2.7a, h, 5.1.b). After ethidium bromide staining to confirm the presence of dsRNA the

gels were dried and autoradiographed using Kodak X-Ray film.

Infections with the parental T3D clone showed production of dsRNA at the permissive temperature of 32°C and at all restrictive temperatures. The mutant clone *tsA279* also demonstrated the production of dsRNA at all temperatures tested. The mutant clone repeatedly produced more dsRNA than did the parental wild type T3D clone at each restrictive temperature (Figure 4.2). At restrictive temperatures the previously identified dsRNA positive control mutants *tsA201* and *tsB405* produced reduced levels of dsRNA relative to the levels attained by the parental T3D clone. The dsRNA negative mutant *tsE320* produced no dsRNA at restrictive temperatures, as previously reported (Cross and Fields, 1972).

13. Discussion

Ultrastructural examination of infected cells grown at the restrictive temperature suggested restrictive cultures of *tsA279* were rapidly cleared of infection (Table 5.1). If each cell contained one small cytoplasmic inclusion with a diameter as little as 1μm, the thickness of a thin section is assumed to be 60nm, and the average diameter of an L929 cell is approximately 10μm, as measured in thin sections, then at least 6% of the cells viewed would show evidence of infection in the plane of section. Approximately 12% of all cell sections examined showed inclusions at 12 hours post attachment, suggesting that every cell was infected and contained at least one inclusion per cell. Cell culture populations increased almost threefold over 72 hours incubation at both

permissive and restrictive temperatures, with 70% viability retained in the cultures (Figure 5.9). These characteristics are comparable to those of uninfected control cultures. Vertical transmission of infection by reovirus in L929 cells has been previously reported (Spendlove *et al*, 1963). Therefore, it is reasonable to expect that daughter cells in the expanding culture would show the presence of infection over the passage of time. However, by 48 hours incubation at restrictive temperatures no evidence of productive infection was found, suggesting that many cells may have cleared their infections. Three different mechanisms appeared to be responsible for the clearing phenomenon: 1.) reduced production of viral encoded product; 2.) blockade in transmembrane transport; and 3.) the production of assembly intermediates.

a. **Reduced production of virally encoded product.**

Evidence for reduced production of viral product was first identified ultrastructurally by inclusions observed in restrictively cultured infections. These inclusions were small, loose, amorphous masses of viral product surrounding foci of condensed genomic material (Figure 5.1.B) which never developed into the large ordered inclusions seen in permissive infections (Figure 5.1.C). Immunofluorescent microscopy provided additional support for this conclusion (Figure 5.13). While there was early evidence of infection in a small number of cells after 12 hours under restrictive conditions, by 48 hours post attachment the cells showed predominately small, pin point foci of fluorescence (Figure 5.13.F), which was only marginally different from the appearance of uninfected control cells. This differed from previous reports for prototype group A clone *tsA201*, using a

restrictive temperature of 39°C. Those reports showed perinuclear to diffuse whole cell fluorescence similar to the pattern observed with wild type and permissive temperature infections (Fields *et al.*, 1971).

Two additional avenues of investigation provided evidence that viral product was reduced: 1.) the reduction in recoverable infectious virus over the time course of restrictive temperature cultures (Table 5.1); and 2.) calculation of total particles/ml produced from direct particle counting of viral lysates (Miller *et al.*, 1979, Hammond *et al.*, 1981). The reduction in total particles produced by the mutant at restrictive temperatures is approximately two orders of magnitude (Table 5.5).

The production of dsRNA provided conflicting evidence for reduced manufacture of viral encoded product. Previous studies indicated that the *ts* prototype mutants which produce dsRNA do so in quantities which are reduced relative to the levels seen with the wild type parental T3D strain (Cross and Fields, 1972). There was an apparent reduction in the overall amount of dsRNA produced by all clones cultured at non permissive temperatures, as indicated by the longer exposure times necessary for the fluorograms (Figure 4.3). At the same time, these studies demonstrated increased production of dsRNA by the mutant tsA279 relative to the production levels observed with parallel wild type clones. Since the production of dsRNA is a positive marker for the production of ssRNA, these results indicated that the failure to produce progeny or viral product must reside in functions other than the replicase and polymerase activities of the mutant.

Mapping of the gene segment responsible for this phenomenon has not been done as a part of these studies.

b. <u>The blockade in transmembrane transport of restrictively assembled virions.</u>

The accumulation of virus in lysosomes, where it was digested (Figure 5.1B,D, Figure 5.3B) was evidence that the mutant *tsA279* has a blockade in transmembrane transport at the restrictive temperature. During the course of infection progeny were produced by a small number of breakthrough infections which appeared normal electron microscopically. These progeny were released into the cultures, attached to available cells and were endocytosed. However, rather than transport across the reticulate membranes, these progeny remained in the lysosomal compartments, where they were degraded. The appearance of a very weak stage 1 level of infection by immunofluorescent microscopic evaluation of restrictive infections after 48 hours incubation is consistent with the accumulation of virus in lysosomal compartments.

High MOI infections made with permissively assembled progeny and incubated at the restrictive temperature were examined to determine whether the blockade in transport was a defect of progeny produced at any temperature and induced by the elevated temperature or was a defect of folding and assembly of progeny produced at the restricted temperature. There was evidence of transport across the membrane, and no evidence of accumulation and degradation of virus in lysosomes 4 hours after infection (Figure 5.5). This supported the hypothesis that the blockade was effected by the temperature at which

folding of the mutant μ1 protein occurred. The ability of permissively assembled mutant virions to transport across the cytoplasmic membrane suggested that the simple act of increasing the temperature of infection did not affect the ability of the μ1 protein to unfold and interact with the host cell cytoplasmic membrane. Conversely, the modifications in folding inhibited the ability of restrictively produced μ1 protein to unfold and interact with the cytoplasmic membrane. This is consistent with reports by King and co-workers that P22 tailspike mutations were affected by the temperature at which the proteins originally fold, and that once folded the proteins were resistant to elevations in temperature (Sturtevant *et al*, 1989; Thomas *et al*, 1990; Yu and King, 1988).

Elevated temperatures allowed *ts* lesions to be identified in the L2 and M2 gene segments of *tsA279*. Infections prepared and incubated at restrictive temperature from a panel of T1L x *tsA279* reassortants which segregated the mutant L2 and M2 gene segments provided evidence that transport across the lysosomal membranes in the clones associated with the wild type M2 segment, and accumulation and degradation in lysosomes associated with the mutant M2 segment (Figure 5.3), thereby mapping the blockade in transmembrane transport to the lesion in gene segment M2 and its protein product, μ1 (Table 5.3).

Reports have identified putative membrane insertion structures in the outer capsid protein μ1: 1.) the myristate side chain at the amino terminus of μ1N, the 42 residue product of cleavage during assembly (Nibert *et al*, 1991b); 2.) the paired amphipathic α-helices

from residues 534 to 551 and 591 through 604, which flank the chymotrypsin and trypsin cleavage sites at residues 581/582 and 584/585, respectively (Nibert and Fields, 1992); and 3.) the focus of net negative charge in ϕ, the carboxy terminus fragment generated by chymotrypsin and trypsin proteolysis (Nibert and Fields, 1992; Hooper and Fields, 1996b). The M2 gene segment has also been associated with transmembrane events (Lucia-Jandris *et al*, 1993, Tosteson *et al*, 1993). Finally, the M2 gene of two ethanol resistant mutants, one of reovirus type 3 Abney (T3A) and one of T3D has been associated with reduced release of ^{51}Cr during infection. The reduction in release of ^{51}Cr has been attributed to increased stability of the major outer capsid protein $\mu 1$, resulting in greater resistance to inactivation by ethanol treatment (Hooper and Fields, 1996a). The first mutation region in the $\mu 1$ capsid protein of *tsA279* falls within the early part of the central region identified by Hooper and Fields (Hooper and Fields, 1996a). This region contains the sites of point mutations identified in the two ethanol resistant mutants whose resistance has been mapped to the M2 gene segment. The second region is in the highly charged ϕ fragment identified by Nibert and co-workers (Nibert and Fields, 1992).

Sequence analysis of the parental M2 genome indicates that the wild type $\mu 1$ protein contains a high proportion of proline residues (50 of 708 residues, or approximately 7.1%) and that its net charge at pH 7.0 is -13.65. The protein has a predicted α-helical content of 27% (Wiener and Joklik, 1988). Analysis of the *tsA279* $\mu 1$ protein and comparison to the reported wild type protein using the EditSeq program in Lasergene

(DNASTAR) showed a change in net proline and serine residues (50 to 48, and 67 to 68, respectively). There was also a change in both isoelectric point of the protein (4.91 to 5.00) and net charge at pH 7.0 (-13.65 to -11.66).

The five mutations in the *tsA279* μ2 protein were localized in two areas. The first area involved residues P306 and P315, and the second involved P673 and E687. Predictive analysis using Lasergene's Protean program proposes changes in secondary structure in both locales. The fifth difference in sequence, U2067→C2067, resulting in alteration of amino acid S680 to P680, represented a difference in the sequence of the laboratory clone for T3D used in these studies and the previously reported sequence for T3D for this site (Jayasuriya *et al*, 1988, Wiener and Joklik, 1988). The coding for the *tsA279* M2 gene for C2067 is consistent with those previous reports. Predictive analysis predicts no differences in protein secondary structure between two sequences whose only difference is the observed change at base 2067. The potential effect of these changes upon membrane interactions is further discussed in Chapter 6.

c. <u>The accumulation of a λ2 and μ2 deficient core-like particle.</u>

Finally, ultrastructural evaluation suggested a blockade in assembly resulting in an accumulation of both core-like particles and genome deficient whole virions (top component) produced at restrictive temperature. Thin section electron microscopy provides insufficient resolution to distinguish between structures with subtle differences. The application of negative stain electron microscopy combined with direct particle

counting of whole cell cytoplasmic extracts after centrifugation onto an electron microscope grid confirmed, and provided further insight into the nature of the particles observed in thin sections. Direct particle count data did not support all ultrastructural observations. While there was an accumulation of core particles there was no apparent accumulation of top component intermediate structures with the parental mutant *tsA279*.

The proportion of core particles defective for λ2 spike structures which were produced by *tsA279* under restrictive culture conditions increased 10 to 20 fold ($p<0.0001$, as evaluated by a χ^2 test with Yates' correction (Hassard, 1991) (Table 5.8). More importantly, the core particles produced were also deficient for the λ2 protein, the minor core protein μ2, and genomic material (Figures 5.10, and 5.12B&C, and Tables 5.5, 5.6, 5.8, and 5.9). Production of the λ2 spike deficient core particle was a dominant phenotype which mapped to the L2 gene segment (Tables 5.8 and 5.9). When the mutant M2 gene segment was segregated from the mutant L2 gene segment the result was an increase of 2 to 3 fold in the proportion of top component produced (Tables 5.8, 5.9). This association was also significant ($p<0.001$) by a χ^2 test with Yates' correction (Hassard, 1991). The role of this structure is further discussed in Chapter 6.

CHAPTER 6

Discussion

1. Introduction.

The use of temperature sensitive mutants provides a precise method for dissecting the mechanisms involved in viral replication. The panel of reovirus temperature sensitive mutants isolated by Fields and co-workers (Fields and Joklik, 1969; Ramig *et al*, 1979) is a significant but as yet largely untapped resource for the elaboration of the biochemical and biophysical processes which are involved in the viral life cycle. The initial purpose of this project was to review morphogenetic characteristics of clones from the Fields panel representing reassortment groups for which no altered life cycle had been reported. Once the morphogenetic properties were noted, clones could be selected to further elaborate the mechanisms involved in the expression of the *ts* phenotype.

2. Mapping temperature sensitivity in reoviruses.

The previous mapping of the prototypic reovirus temperature sensitive mutants was done with a small panel of ts^+ reassortants at a restrictive temperature of 39°C (Mustoe *et al*, 1978; Ramig *et al*, 1978; Ramig *et al*, 1983). These conditions may not provide sufficient power to resolve fine differences such as the existence of multiple *ts* lesions with mild phenotype (Hazelton and Coombs, 1995). A reassessment of the mapping of the *ts* lesions contained in the mutants which were candidates for this study was undertaken once the conditions which maximized the expression of the *ts* phenotype were

established for each clone to be tested. Idealizing those conditions led to clear cut identification of the *ts* phenotype for those clones previously identified as mildly *ts* at 39°C (Appendix B, Table B.2). The presence of single *ts* lesions associated with previously reported gene segments for the clones *tsA201, tsE320* and *tsI138* (Mustoe *et al*, 1978; Ramig *et al*, 1978; Ramig *et al*, 1983) were readily confirmed using the maximized conditions (Tables 3.3, 3.4, and 3.6, respectively). However, the study also indicated that the laboratory copy of the mutant *tsH26/8-3* contained a lesion in the L2 gene segment (Table 3.5), rather the M1 gene segment, as previously reported (Ramig *et al*, 1983). This reduced the value of the mutant *tsH26/8* in this study of the morphogenetic processes of reovirus. The mapping for the clone *tsJ128* was inconclusive regardless of the conditions used and this mutant was not further examined as a part of these studies.

The mutant clone *tsA279* is an excellent example of the potential value of the Fields panel. Reassortment analysis to associate the *ts* lesion to a gene segment provided a number of valuable insights. First, polyacrylamide gel electrophoresis of the clone demonstrated differences in electrophoretic migration rates for gene segments, L2, M2, M3 and S1 (Figure 3.1). Temperature sensitive lesions were associated with two segments, a mild lesion with the L2 segment, and a dominant lesion with the M2 segment (Table 3.2) (Hazelton and Coombs, 1995). No unique phenotype has as yet been associated with the mutations in the M3 and S1 segments of this clone. Recombination testing had previously classed the mutant *tsA279* in recombination group A with no

indication of the lesion in the L2 gene segment (Fields and Joklik, 1969). In consideration of the mapping of the lab clone for *tsH26/8* to the L2 gene segment, the inability to easily map the lesion in the clone *tsJ128*, and the double gene segment mapping observed with clone *tsA279*, confirmatory classification of the group A prototype clone *tsA201* was reviewed both by recombination assay (Table 3.1) and reassortant analysis (Table 3.3) to confirm that results observed at elevated temperatures for well characterized mutants were consistent with previous reports (Mustoe *et al*, 1978).

A review of the profile of expression of temperature sensitivity at different temperatures explains the failure to identify the anomaly presented by multiple lesions in earlier studies. Recombination testing and reassortant mapping assays were done at a restrictive temperature of 39°C. Clones for recombination groups A, D, and E, and some recombination group B clones have been reported to exhibit mild levels of temperature sensitivity at that temperature (Tables 1.3, 3.2) (Fields and Joklik, 1969). The normal experimental deviations of plaque assays make it possible for expression of the *ts* and wild type phenotypes to overlap. This could allow what erroneously appears to be a sufficient percentage of recombination to occur to cause faulty sorting of clones into recombination groups.

Focused use of ts^+ phenotype progeny clones from reassortment cultures, where both reassortment culture and plaque assay have been conducted under conditions marginally

sufficient to ensure phenotypic expression, may also provide for faulty association of phenotype to specific gene segments. Both lesions in the mutant *tsA279* exhibit mild temperature sensitivity at a restrictive temperature of 39°C. Therefore, electropherotyping the clone at this temperature with reassortant progeny clones from cross infections with reovirus T1L did not allow association of the *ts* phenotype with any individual gene segment. The existence of more than one lesion was first suggested by the mild and strong expressions of temperature sensitivity at 40°C.

The presence of a characteristic pattern of expression for the phenotype with increasing temperature allowed two lesions to be identified, a mild lesion in L2 which maintained a mild expression pattern as temperature was increased, and a stronger, dominant lesion in the M2 gene segment which provided for increased expression of the phenotype as the temperature was elevated. The results from these studies demonstrate the necessity of using large reassortant panels of both *ts* and ts^+ phenotypes, and assaying phenotypic expression over a range of temperatures which allow for clear differentiation between the *ts* and ts^+ phenotypes.

A vast number of interactions occur in the cell during the replicative cycle. When rates of mutation are experimentally accelerated it is possible that more than one mutated genome segment may be included in a proportion of progeny clones. Therefore, the existence of multiple gene lesions in some mutants is not surprising given the harsh and non-selective mutagenesis procedures used to generate the mutants (Fields and Joklik,

1969). Some of the other reovirus *ts* mutants contain lesions in multiple genes, as demonstrated by altered mobilities of proteins and gene segments in SDS-PAGE (Cross and Fields, 1976a; Cross and Fields, 1976b; Coombs *et al*, 1994). Clone *tsA279* was generated from proflavin treated reovirus infections (Fields and Joklik, 1969). This agent causes skips in genetic reading during transcription and replication, resulting in frame shift mutations in the progeny genome (Bermann *et al*, 1992; Revich and Ripley, 1990). In keeping with this mechanism, proflavin mutagenesis was the most lethal of the processes used in the original report (Fields and Joklik, 1969).

The mutant clone *tsB271* was also created by mutagenesis with proflavin at the same time that clone *tsA279* was created. That clone was also reported to have mild levels of temperature sensitivity (Fields and Joklik, 1969). Reassortant analysis maps the lesion for the recombination group B prototype clone *tsB352* to genome segment L2 (Mustoe *et al*, 1978), the segment with the previously unsuspected temperature sensitive lesion in clone *tsA279*. The ability of the segmented genome of reovirus to reassort in mixed infections creates the possibility of the same mutant genome segment being present in more than one selected progeny clone. The dominant intermediate assembly structure produced by the mutant *tsA279* has been mapped using reassortant analysis with direct particle counting to the L2 gene segment. As noted, the group B mutant clone *tsB405* accumulates core particles which have the λ2 spike (Morgan and Zweerink, 1974). The group B clone *tsB271* has not been analyzed. If assembly intermediate blockade and sequence data are similar for the L2 gene segments of both *tsA279* and *tsB271* it may be

possible to confirm the mapping of the dominant structural defect, the λ2 spike deficient core, with a separate *ts* mutant without the contributions of other mutations. This would confirm and elaborate further on the assembly processes occurring within the cell.

3. Mechanisms for expressing temperature sensitivity.

Electron microscopy is an effective tool for initial evaluation of morphogenetic pathways. The morphogenetic process has been well defined by previous investigators for the wild type parent T3D clone (Bodkin *et al*, 1989; Borsa *et al*, 1979; Chaly *et al*, 1980; Dales and Gomatos, 1965; Fields *et al*, 1971; Silverstein and Dales, 1968; Silverstein *et al*, 1976; Wolf *et al*, 1981). Infections of L929 cells with reovirus suggest a replication cycle of approximately 24 hours at 37°C (Rhim *et al*, 1961). The virus does not induce rapid cell death, rather there is a prolonged, relatively healthy cycle culminating in cell death due to lysis of the infected cell (Silverstein *et al*, 1976) or, alternatively, apoptosis (Rodgers *et al*, 1997; Tyler *et al*, 1995) . In this study cell death appeared to be necrotic rather than apoptotic. Cellular organelles did not demonstrate any outward signs of damage until late in the life cycle, when the mitochondria were alternatively swollen or electron dense and some vacuolization appeared in the cytoplasm. Nuclear and cytoplasmic membranes appeared to be uninterrupted and did not display ruffling. The nuclear chromatin and cytosol were not condensed. This last observation is consistent with previous reports that nuclear processes are retarded but not shut down, and that there is no fragmentation of the genetic material of the host cell (Chaly *et al*, 1980). The major effect of the infection process prior to lytic release of progeny was the evident

reduction in expression of the transforming Type A retrovirus. Cells from the permissive and restrictive infections from the mutant clones used in this study demonstrated the same appearance. These results are not consistent with cell death through the process of apoptosis, or programmed cell death, which has been posited to be a defense mechanism induced by some other viral agents (Esolin *et al*, 1994; Lu *et al*, 1994; Rodgers *et al*, 1997; Tyler *et al*, 1995)

Testing cells infected with different *ts* mutants and cultured at restrictive temperatures suggests multiple ways in which temperature sensitivity is expressed. The first is reduced production of viable progeny clones, as revealed by the decline in infectious virus recovered from cultures. The decline ranged from just below the input values to greater than two orders of magnitude below the original input titer (Figures 4.1, 5.9). Immunofluorescent studies supported this observation. Each evaluated clone demonstrated reduced labeling by rhodamine labeled anti-antibody (Figure 4.4, 5.13). Restrictive cultures for the mutants *tsE320*, and the group A prototype mutant *tsA201* were previously reported to react with rhodamine labeled antibodies to a similar degree as permissive cultures (Fields *et al*, 1971). However, those tests were performed using a restrictive temperature of 39°C, while the studies reported here used the more effective restrictive temperature of 40°C. Finally, direct particle counting of infections from T3D and *tsA279* confirmed reduced production of progeny at restrictive temperature for this *ts* mutant (Table 5.5)

Ultrastructural examination supported the observation that progeny production was reduced by demonstrating small disorganized viral inclusions in most restrictive infections. Further, with the exception of the infections with the mutant *tsH26/8-3*, restrictive infections for the remaining mutants appeared to clear the infections by the end of each experiment. Persistent cultures have been established with the mutant clone *tsC447* (Ahmed and Graham, 1977; Ahmed *et al*, 1980), and wild type serotypes Type 2 Jones (T2J) and T3D (Ahmed *et al*, 1983; Baer and Dermody, 1997; Dermody *et al*, 1993; Wetzel *et al*, 1997a; Wetzel *et al*, 1997b). Persistent cultures were not established, maintained, and tested at restrictive temperatures in this study. The low levels of recoverable infectious virus present at the end of each infection suggests that there was residual viral activity after three days culture at restrictive temperatures. The apparent ability to clear infection by *tsA279*, *tsH26/8*, and *tsI138*, along with the origin of the group H and I clones, suggests these would be good candidates for future study of this phenomenon.

A second mechanism for the expression of the *ts* phenotype is interference with the transcription, translation and replication processes. This was observed with restrictive cultures for the mutant *tsE320*, which showed no clear evidence of infection other than a gradual decline in titre of recoverable infectious virus (Figure 4.1), and with the mutant *tsI138*, which demonstrated reduced levels of production of dsRNA at permissive temperature, along with no production of dsRNA in restrictive cultures (Figures 4.1, 4.3). The mutant *tsE320* was previously reported to produce both ssRNA (Cross and

Fields, 1972) and viral proteins (Fields *et al*, 1972) at a restrictive temperature of 39°C.

A third mechanism for the expression of the *ts* phenotype is interference with folding and assembly of viral proteins into progeny virions. As noted in Chapter 1, bacteriophage assembly pathways have been well elaborated using conditionally lethal amber mutations (Black and Showe, 1983, Privelege and King, 1983). With *ts* mutants the focus of mechanisms relate to induced thermodynamic stability or instability which results in the inability to fold properly and, therefore, form ideal tertiary and quaternary structures at elevated temperatures. The result may be to interfere with assembly, disassembly, or with other biological properties such as enzymatic function. Tailspike *ts* mutations with P22 irreversibly form stable structures at elevated temperatures which do not interact to form tailspikes (Fane and King, 1987; Sturtevant *et al*, 1989). *Ts* mutants affecting the capsid protein for the same bacteriophage form stable crystals which do not fold properly nor assemble into capsid structures when incubated at elevated temperatures (Gordon and King, 1993). The result of these interactions is to prevent formation of multimeric structures due to the thermodynamically induced distortion of some or all of the proteins.

4. *TsA279* produces a core particle deficient in λ2 and μ2.

Variant morphological structures were identified by ultrastructural evaluation in the *ts* mutants *tsA279* and *tsI138*. As noted above, however, the available resolution of thin section electron microscopy is insufficient to resolve subtle structural differences. In addition, a misinterpretation of ultrastructure due to unintentional bias and the random

selection of sections may lead to erroneous evaluations of change in the proportions of different species of viral particles and intermediate assembly structures present in an infection (Sjöstrand, 1962). It is possible to miss the existence of entire populations of sub viral structures when evaluations are made from thin sections or from gradient purified fractions. When the production of viral encoded products is reduced the problem is magnified further. To overcome these difficulties, particle counting of whole cell cytoplasmic fractions from permissive and restrictive cultures was utilized with the double *ts* mutant *tsA279* to elaborate upon the assembly intermediates produced. Thin section electron microscopy had suggested that there was an accumulation of top component in restrictive cultures from this system. However, the result of the particle counts revealed an accumulation of core like particles without accumulation of top component (Tables 5.5, 5.8). Production of top component was subsequently associated with the mutant M2 gene segment during reassortment mapping of the intermediate assembly core particles to the mutant L2 gene segment (Table 5.8).

Restrictively grown core particles from the mutant *tsA279* appeared to be defective for the λ2 pentameric spike structure (Figure 5.10, Table 5.8). Spikeless core particles have been prepared from top component (Smith *et al.*, 1969) and whole virus (White and Zweerink, 1976; Yin *et al*, in submission). However, the inability to isolate spike deficient core-like particles from cell extracts, coupled with the ability to readily disassemble virions and create spiked core-like particles (Dryden *et al*, 1993; Luftig *et al*, 1972; Nibert *et al.*, 1991a), has led to the supposition that the core particles usually

seen in infected cells are complete core particles. Further support for this theory was derived from the observation that the blockade in assembly which occurs at restrictive temperature with the reovirus recombination groups B and G temperature sensitive mutants is a core particle complete with the λ2 pentameric spike (Danis *et al*, 1992; Morgan and Zweerink, 1974).

The core-like particles reported by White and Zweerink demonstrate cavities at the apices of cores produced by removal of the λ2 spikes at high pH (White and Zweerink, 1976). Investigations into the mechanisms of reovirus transcription have produced spike defective core particles with a similar, pitted appearance (Yin *et al*, in submission). The core particles produced by the mutant *tsA279* also exhibited such divots (Figure 5.10). Similarities in particle morphology, combined with previous reports concerning protein contents of artificially produced spikeless cores indicated that the λ2 proteins were not present in the structure but that all other apical core proteins are present (White and Zweerink, 1976; Yin *et al*, in submission). TGU polyacrylamide gel analysis of the products of restrictive cultures of *tsA279* confirmed the absence of λ2 in the spike defective core particles. Perhaps of greater interest was the unexpected finding that the minor core protein μ2 is also missing from these structures, as was genomic material (Figures 5.10, 5.12A, 5.12B, Tables 5.5, 5.7).

5. <u>The assembly pathway of reovirus.</u>

The accumulation of spike deficient core-like particles in restrictive infections and

subsequent mapping of the phenotype suggests that the assembly pathway is blocked as a result of the mutated product λ2. The identification of this structure *in vivo* suggests a capsid assembly pathway evolving around interactions of proteins λ1, λ3, and σ2, but not λ2 nor μ2, to form a primary core structure (Figure 6.1, Table 6.1). The apparent inability of the λ1 mutant *tsI138* to form complete cores is consistent with this model. This conclusion is further supported by the observed assembly of core like structures in expression systems involving proteins VP2, VP5, and VP7 of Bluetongue virus (Hewat *et al*, 1992). Reports involving co-expressed λ1 and σ2 indicate that these two proteins together contain sufficient structural information to assemble into core like particles. Neither protein was capable of assembly into such structures when expressed alone (Xu *et al.*, 1993).

The presence of genomic material in the primary core is preferred but not essential for assembly, as indicated by assembly of viral encoded structures from expression systems (Xu *et al*, 1993) and the isolation of top component as a naturally occurring assembly intermediate (Tables 5.5, 5.8). Disassembly intermediate structures which are defective for the λ2 pentameric spike but contain μ2 may contain genomic material in 60% or better of the particles present (Yin *et al*, in submission). It is easy to speculate that the posited apical locus of incorporation of μ2 is such that it acts to stereologically hinder leakage of genomic material which may have been previously incorporated into primary cores. Such a location would be consistent with a number of hypotheses concerning the location of μ2 (Coombs, 1996; Coombs, 1998a; Dryden *et al*, 1993; Sherry and Blum,

Figure 6.1. **The assembly pathways of reovirus.**

Stage 1: The major core proteins λ1 and σ2 co-condense to form the primary core particle, along with the minor core protein λ3.

Stage 2: During assembly of the complete core particle, the minor core protein μ2 assembles at the apices of the primary core. The minor outer capsid protein λ2 also assembles at the apices either collateral to or immediately following the assembly of μ2. The minor outer capsid attachment protein σ1 associates with the outermost portions of the λ2 pentameric spike. This may occur simultaneously or immediately subsequent to the condensation of the λ2 pentameric spike at the apices of the core particle.

Stage 3: The major outer capsid proteins μ1 and σ3 condense and assemble around the λ2 pentameric spikes to form the complete virion.

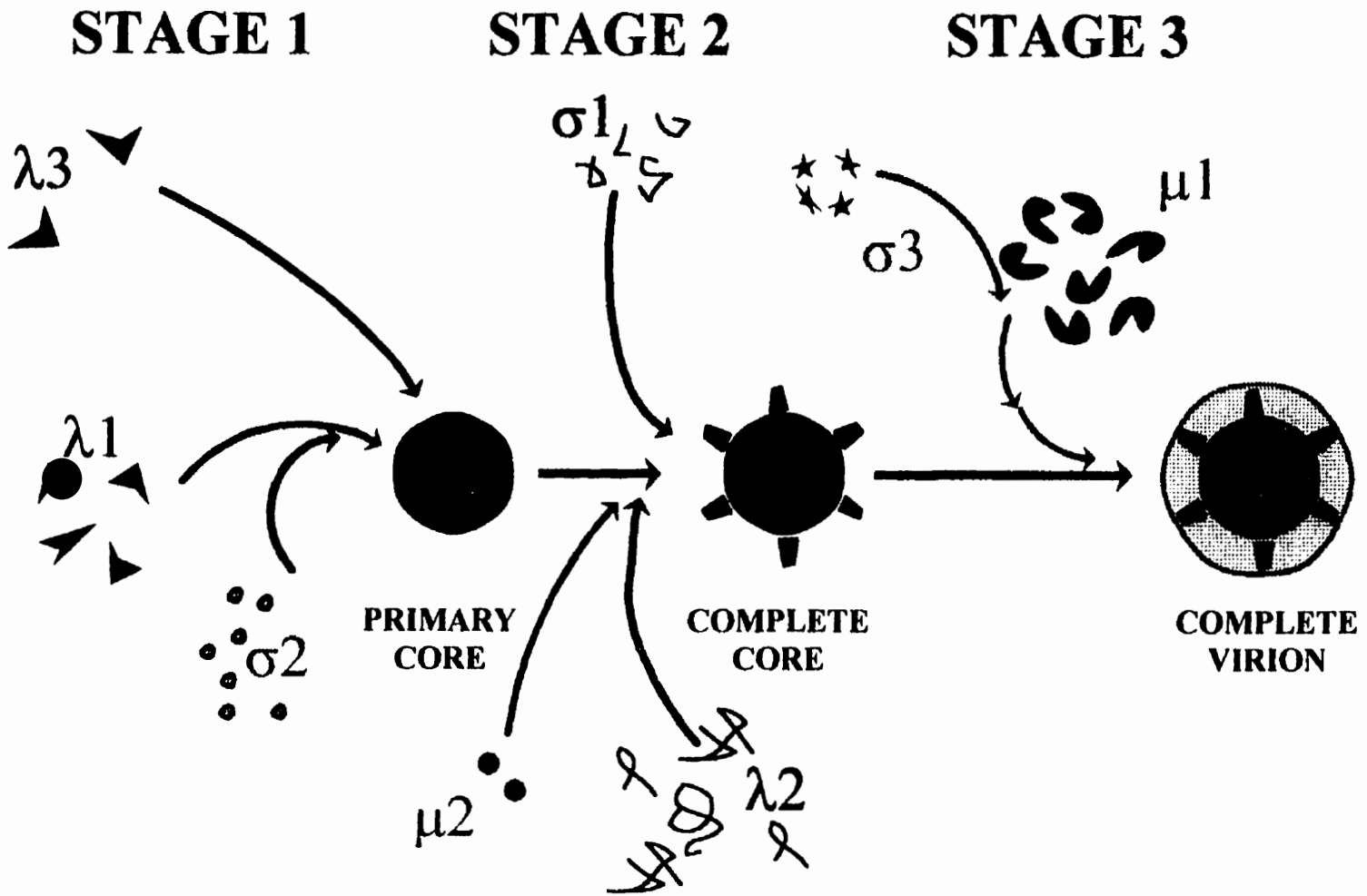

Figure 6.1. The assembly pathways of reovirus.

Table 6.1. Characteristics of reovirus complete and intermediate particles[a,b].

Property	Primary Core	Complete Core	ISVP	Virion
Bouyant Density (gm/cm^3)	ND	1.43	1.38	1.36
Sedimentation Value (S_{20w})	ND	470	630	730
Diameter (nm)				
NS-TEM	50	50	65	75
Electron Cryomicroscopy	ND	60	80	85
Outer Capsid Proteins				
λ2	-	+	+	+
μ1/1c	-	-	+	+
μ1δ/δ	-	-	+	+
ϕ	-	-	+	+
σ1	-	-	+	+
σ3	-	-	+	+
Core Capsid Proteins				
λ1	+	+	+	+
λ3	+	+	+	+
μ2	-	+	+	
σ2	+	+	+	+
Genome				
ssRNA	?	-	+	-
dsRNA	?	-	+	+
Infective	ND	No	Yes	Yes
Transcription Activity	ND	Yes	Partial§	Partial

a. Adapted from Table 1.1.
b. See text for details.
ND Not done
§ Initiation and Capping but no elongation

\+ Present
\- Not Present

01994, Yin *et al*, 1996).

In the second step of assembly, μ2 may then associate with the apices of the core particle either immediately prior to or collaterally with λ2 to form the complete core particle (Figure 6.1, Table 6.1). The lack of evidence that λ2 pentamerizes prior to attachment to the primary core suggests that the λ2 monomers condense into pentamers during association with the primary core. The incorporation of the trimeric σ1 attachment fibre with the λ2 pentameric spike most likely occurs at this stage, with the amino terminus of the fibre interacting with the carboxy terminus of the λ2 proteins in their pentameric spike structure (Leone *et al*, 1991c; Luongo *et al*, 1997).

The altered migration rate of the *tsA279* S1 gene segment in SDS-PAGE (Figure 3.1), while not conclusive, suggests that its product may contain a compensatory mutation to reinforce assembly of viable, infectious progeny in the presence of the mutation to the λ2 protein. *Ts* mutant reversion analysis (McPhillips and Ramig, 1984) suggests that systems containing multiple mutations may be the result of compensatory mutagenesis in closely interacting regions of proteins. Such mutations would enhance the capability of assembly into complete structures. Evidence that both the λ2 and μ1 proteins contain temperature sensitive mutations in the mutant clone *tsA279*, provides further support for the concept of compensatory mutagenesis.

The final stage of assembly is condensation of the outer capsid around the core structure

(Figure 6.1, Table 6.1). The presence of λ2/μ1/σ3 outer shell complexes in *tsC447*-infected cells (Matsuhisa and Joklik, 1974) suggest that pentamerized λ2 contains sufficient information for this condensation. Mutations in σ3 (*tsG453*) also lead to the generation of core particles which lack the outer shell (Danis *et al*, 1992). These, and data concerning co-precipitation studies have led to the proposal that proteins μ1 and σ3 complex with each other before associating with the core (Lee *et al.*, 1981; Joklik, 1983; Shing and Coombs, 1996). These combined observations imply important λ2, μ1, and σ3 interactions for outer shell assembly.

The assembly interactions involved with the mutant gene segment M2 are more difficult to interpret. The protein encoded by this gene segment is a major outer capsid protein. Reassortant analysis indicates that there is a strong preponderance of top component produced by this mutation when it is segregated from the mutant L2 segment. This supports the proposal that inclusion of genomic material is essential for the production of infectious progeny, but not for assembly of the packing crate which transports that genomic material.

The implication drawn from the accumulation of top component is that the M2 gene segment either has a role in the replication of genomic material, is involved in packaging by binding the dsRNA so that it may be incorporated into the final structure, or interacts with some other viral protein(s) in a manner which empowers packaging. In the first instance, the functions involved in genomic replication reside in the proteins of the core

particle. There has been no evidence that μ1 has binding capacity for either single or double stranded RNA, suggesting the second hypothesis is not likely.

A number of reovirus proteins have been implicated in binding dsRNA, including the major outer capsid protein σ3 (Schiff *et al*, 1988). Association of μ1 with σ3 has been implicated as an early (Lee *et al*, 1981) and essential step in assembly (Shing and Coombs, 1996), with the interaction resulting in a shift from transcription control by σ3 to assembly of progeny virions (Shepard *et al*, 1995). The mutant μ1 protein may be effecting deficient packaging of genomic material by interfering with the interactions of other dsRNA binding proteins. If the mutant μ1 protein were not capable of interacting with σ3 the posited switch of σ3 from transcription control to assembly would be disrupted.

The presence of top component is further compounded by the observation that the mutant *tsA279* produces elevated levels of dsRNA relative to the wild type parent when cultured at restrictive temperatures. The gene segment associated with this phenotype has not been mapped. However, this phenotype would be consistent with a model in which defective μ1 is unable to interact with σ3, resulting in failure of the transition to viral assembly. The resultant run away transcription would result in increased levels of viral encoded RNA.

6. Restrictively assembled *tsA279* virions are defective for transmembrane transport.

Infection is initiated by attachment and uptake of the virion. An additional mechanism for expression of the temperature sensitive phenotype which involved these stages was noted with the mutant *tsA279*. Progeny virions produced by breakthrough infections at restrictive temperature appeared able to attach to and be endocytosed by host cells. However, accumulation of virions in transport vesicles and subsequent virion degradation in lysosomes indicated that the progeny produced at restrictive temperature were not able to be transported across the lysosomal membrane to the cytoplasm (Figure 5.2). The small, pin point foci of fluorescence observed at restrictive temperature (Figure 5.13F) are also consistent with the accumulation of virions in endosomes. These data suggest there is a blockade in transmembrane transport of the virion in clone *tsA279*. High MOI infections indicated that the virions produced at permissive temperature were able to transport across the cytoplasmic membrane under restrictive culture conditions (Figure 5.3). This is evidence that the mutation affected the folding process at the restrictive temperature but not at the permissive temperature. Similar observations concerning protein folding have been made in the P22 bacteriophage system (Yu and King, 1988; Sturtevant *et al*, 1989; Thomas *et al*, 1990, Gordon and King, 1993).

Several reports have associated transmembrane transport with gene segment M2 or its product, the major outer capsid protein μ1 (Hooper *et al*, 1996a; Hooper *et al*, 1996b; Lucia-Jandris, 1990; Lucia-Jandris *et al.*, 1993; Tosteson *et al*, 1993; Wessner *et al*,

1993). The presence of a *ts* lesion in the *tsA279* μ1 protein, coupled with accumulation of virions in transport vesicles and lysosomes is consistent with the observation that the M2 segment is associated with transmembrane transport.

It has been suggested that the process of membrane insertion by proteins requires proteolytic processing and exposure to lowered pH in the reticulo-endothelial compartments to allow exposure of hydrophobic moieties which may then insert into the cytoplasmic membrane (Gaudin *et al*, 1993; Hoffman *et al*. 1997; Nibert *et al*, 1991b; Sturzenbecker *et al*, 1987). With reovirus exposure to lowered pH and proteolytic processing of the outer capsid protein μ1 may occur in either passage through the intestinal tract (Bodkin *et al*, 1989; Wolf *et al*, 1982) or the lysosomal compartments of the cell (Nibert *et al*, 1991a). Treatment of virions with proteolytic enzymes *in vitro* creates infectious subviral particles, which are capable of transport across the cytoplasmic membrane without entering the endosomal compartments (Borsa *et al*, 1979). The effect of proteolytic processing could be to release constraints which hold the insertion or fusion elements in place. This would allow the hydrophobic moieties to become exposed and make insertion into the cytoplasmic membrane thermodynamically stable (Parker *et al*, 1990).

As previously noted, proflavin was the chemical agent used in the mutagenesis experiment from which the mutant *tsA279* was obtained (Fields and Joklik, 1969). Studies in bacteriophage systems indicated that this agent causes skips in reading the

template segment during replication of the genome (Berman *et al*, 1992; Revich and Ripley, 1990). It should be expected that many of the skips in reading frame would result in dead end mutations due to the resultant nonsense coding. However, where the skip is late enough in an open reading frame, or where there are sufficient skips to re-establish a protein product relatively close to the original parental protein it should be possible to get viable progeny clones. Therefore, the original hypothesis was that the mutation event which resulted in the expression of a temperature sensitive phenotype was due to a sequence of three deletions of sufficient proximity that the protein would not be perturbed extensively. These deletions were not found. Instead, five point mutations were observed, each resulting in a change in the primary structure of μ1.

Changes in primary structure resulting in apparently minute secondary structural changes may affect the stability of proteins produced at elevated temperatures (Jaenicki, 1991). Correct folding requires properly formed β-turns (Stroup *et al.* 1990). Proline residues induce bends in secondary structure. Mutation of the proline residues in the short β-turns preceding an α-helix in the penicillinase repressor protein introduces a temperature sensitive structure, with folding at the elevated temperature irreversibly creating an inactive repressor (Imanaka *et al*, 1992). Similar results have been shown with point mutations of proline residues in the nucleoside diphosphate kinase of *D. melanogaster* (Lascu *et al*, 1992). The role of several proline residues in ensuring folding sufficiently proper for the production of active porcine pancreatic ribonuclease at elevated temperature has also been investigated (Lang and Schmid, 1990). Three of the observed

deviations in the *tsA279* μ1 protein involved mutations of proline residues to either serine or threonine.

The five mutations were grouped in two regions, the central portion of the protein and the carboxy terminal region. Predictive analysis of secondary structure in the first region, from amino acid residues 296 through 325, using the Chou-Fasman secondary structure prediction algorithm (α region threshold 103, β region threshold 105), the Eisenberg hydropathic moment algorithm (α angle 100, β angle 170, with averaging over 11 residues), the Emani surface probability algorithm (surface decision threshold 0.600), and the Karplus-Schulz chain flexibility algorithm (flexibility threshold 1.000). The charge average parameters of Lasergene's Protean program are 9 residues at a pH of 7.0. These analyses indicate that a stretch of predicted amphipathic α-helical structure from residues 309 to 314 is disrupted, with a predicted shift to β-sheet structure. A short stretch of β-turn is also predicted to be replaced by a long stretch of β-turn. There is also a reduction in the probability of surface exposure and flexibility in this region (Figure 6.2).

Predictive analysis of secondary structure in the second region, from amino acid residue 666 through 695 shows a slight shift in hydrophobicity and an increase in probability of surface exposure of the protein in this locale. There is no apparent disruption in predicted secondary structure. However, there is a predicted change in charge in the charged stretch between residues 679 through 696, with changes of two negative charged

Figure 6.2. **Predicted secondary structure[a], mutation region #1 [b]**

aa	296										306										316									
Sequence	A	E	P	E	I	I	A	S	L	A	P/S	V	P	A	P	V	F	A	I	P/S	P	K	P	A	D	Y	N	V	R	T
T3D	α	α	α	α	α	α	α	α	α	α	α	-	-	α	α	α	α	α	α	-	-	-	βT	βT	βT	βT	β	β	β	β
tsA279	α	α	α	α	α	α	α	α	α	α	α	-	-	β	β	β	β	β	β	βT	βT	βT	βT	-	βT	βT	βT	βT	β	β

a. Predictions of secondary structure by Protean (DNASTAR) using the Chou-Fasman algorithm for secondary structure, Eisenberg algorithm for amphipacity, and Ermani algorithm for surface probability. Please see Chapter 6.6 for details

b. Two mutations exist in the locus: P306→S306; P315→S315.

c. There is a slight shift to lower probability of surface location around each site of mutation.

d. There is a slight reduction in predicted flexability from residues 312-317.

e. The sequence between 315 and 325 is predicted to be amphipathic.

residues to neutral, one negative charge to positive, and two neutral charges to positive (Figure 6.3). Changes in this locale are associated with the change in the net charge of the protein.

Structural features of the μ1 protein have been proposed to support a role in membrane insertion. A number of factors which may contribute to the interference in transmembrane transport due to faulty folding of the μ1 protein and thereby affect these structural features can be identified. First, the protein is myristoylated near its amino terminus (Nibert *et al.*, 1991b). Second, structural models extrapolated from sequence data for the μ1 protein suggest the existence of two adjacent amphipathic α-helices which flank trypsin and chymotrypsin cleavage sites (Nibert and Fields, 1992). The presence of a cleavage site between amphipathic α-helices and a proximal myristate side group constitute membrane insertion motifs in non viral proteins (Kanellis *et al.*, 1980; Moe and Kaiser, 1985; Parker *et al.*, 1990). Neither of these two features appear to be affected by the mutations identified in the μ1 protein of *tsA279*.

The third structural feature which has been identified is the Trypsin Stable Fragment (TSF) of μ1 which remains associated with core particles during their generation by trypsin proteolysis (Hooper and Fields, 1996a). The first region of mutation in μ1 of *tsA279*, from residues 295 through 325, is in the TSF. Lasergene analysis using the Chou-Fasman and Eisenberg algorithms predicts the loss of an amphipathic α-helix and its replacement with a β-sheet. In addition there is an increase in the length of β-turn

Figure 6.3 **Predicted secondary structure[a], mutation region #2 [b]**

aa	666										676										686									
Sequence	D	K	V	S	A	H	F	P/T	A	P	K	P	D	C	S/P[c]	T	S	G	D	S	G	E/K	S	S	N	R	R	V	K	R
T3D	⊙	⊙	⊙	⊙	⊙	⊙	⊙	⊙	⊙	⊙	⊙	⊙	⊙	⊖	⊖	⊙	⊖	⊖	⊖	⊖	⊖	⊖	⊖	⊙	⊕	⊕	⊕	⊕	⊕	⊕
tsA279	⊙	⊙	⊙	⊙	⊙	⊙	⊙	⊙	⊙	⊙	⊙	⊙	⊙	⊖	⊖	⊙	⊖	⊖	⊖	⊙	⊙	⊕	⊕	⊕	⊕	⊕	⊕	⊕	⊕	⊕

a. Predictions of secondary structure by Lasergene (DNASTAR) as with Figure 6.2. Please refer to Chapter 6.6 for details.

b. Three mutations exist in the locus, P673→T673, S680→P680, and E687→K687.

c. There is a shift to hydrophobic characteristics for residues 670, 671, and 672.

d. There is a shift in probability of surface exposure, to less probable in the vicinity of residue P673, and to more probable from residues 677 through 689.

⊙, predicted neutral charge; ⊕, predicted positive charge; ⊖, predicted negative charge.

structure which precedes the subsequent β-sheet found in both wild type and mutant proteins (Figure 5.14). Analysis of the effects of each mutation separately and in sets predicts that the mutations in this location are not affected by those in the second region. While both the mutations at this locale slightly affect predictions of surface probability, the proposed change in secondary structure, the replacement of an amphipathic α-helix with a β-sheet and lengthening of the β-turn, is effected by the mutation P315→S315. The predicted locale would not be surface exposed, reducing it's possible interactions with other virion proteins.

It has been suggested that amphipathic α-helices have a role in membrane penetration by fusion proteins of many enveloped viruses (reviewed in White, 1990). The hydrophobic faces of the amphipathic double helices may be arranged to allow hydrophobic interactions between the helices (Branden and Tooze, 1991; Creighton, 1993). Mutations which affect the secondary structure and effect loss of the α-helices could effect folding at elevated temperature which strengthens hydrophobic interactions, thereby preventing the exposure of the hydrophobic insertion sequences after exposure to low pH and proteolytic digestion. Alternatively, mutation of the prolines involved in the β-turn sequences, could limit exposure of the amphipathic structures, whether α-helix or β-sheet, and disrupt the subsequent exposure of the hydrophobic moieties after proteolytic processing of the capsid proteins. The mutations identified in the first region with *tsA279*, and their predicted effect upon secondary structure further strengthen the observed role of proline residues in short β-turns which are proximal to amphipathic α-

helices (Imanaka *et al*, 1992; Lang and Schmid, 1990; Lascu *et al*, 1992; and Stroup *et al*, 1990).

Ethanol resistant mutants of T3A and T3D which have had their phenotype mapped to the M2 gene segment contain lesions in this region (Hooper and Fields, 1996a; Wessner and Fields, 1993). The T3D derived ethanol resistant mutant 3a9 contains a lesion resulting in the mutation $K_{459} \rightarrow Q_{459}$ (Wessner and Fields, 1993). It has been suggested that this mutation may have strengthened the interactions of the protein and made it more resistant to denaturation by ethanol (Hooper and Fields, 1996a). Predictive analysis of this mutation using the Protean program of Lasergene suggests the loss of a focus of positive charge at position 457. The predicted result is the insertion of an α-helical structure from residues 454 through 459. The overall local structure is predicted to be slightly less flexible. The changes in 3a9, with the predicted insertion of an α-helix in surface exposed regions appear to be antithetical to the changes observed here.

The T3A derived ethanol resistant mutant JH4 contains a lesion within the TSF which results in the mutation $P_{497} \rightarrow S_{497}$. As with the mutant 3a9 it has been predicted that the result of this mutation is increased stability of the fragment, resulting in reduced susceptibility to ethanol denaturation and reduced membrane interactions as evidenced by release of ^{51}Cr (Hooper and Fields, 1996). Predictive analysis of the changes which may be effected by this mutation utilizing the Chou-Fasman and Eisenberg algorithms show loss of an amphipathic α-helix, with commensurate insertion of a non-amphipathic β-

sheet structure. In addition the β-turn present is also shortened. It is predicted that this location would not be surface exposed. The change from α-helix to β-sheet is similar to the prediction for the ethanol resistant mutant JH4.

The fourth structural feature which may play a role in transmembrane events is ϕ, the carboxy terminus proteolytic fragment of μ1 which results from proteolytic cleavage of μ1 both *in vivo* (Bass *et al*, 1990) and *in vitro* (Nibert and Fields, 1992). Interactions between the high positive charge of this fragment and negative charge within the plasmalemma have been proposed to have a role in insertion into membranes (Nibert and Fields, 1992).

The second mutation region, between residues 666 and 695, is in ϕ. The region has a very strong probability of surface exposure. Both mutations in this region are implicated in effecting an increase in surface probability and disruption of predicted coil structure in their immediate vicinity. The predicted effects of these mutations are not influenced by those occurring in the first region. Analyses of the two mutations separately and in tandem indicate that the mutation at P673 is responsible for the predicted increase in hydrophobicity which occurs from residues 666 through 672. The mutation at residue E687 is uniquely associated with the change in charge which extends from residues 679 through 696. This mutation is also solely responsible for the predicted change in net charge of the protein from -13.65 to -11.66 at pH 7.0, and the change in pI from 4.91 to 5.00. The change in charge to a more acidic fragment suggests a decrease in the

ability of the protein to interact with host cell plasma membranes. This is consistent with reduced transmembrane transport.

The changes this study have identified in ϕ include an increase in hydrophobicity. Studies with mutants of Bovine pancreatic trypsin inhibitor show increased hydrophobic interactions and more compact structures are formed at elevated temperatures (Gottfried and Haas, 1992). The added hydrophobic interactions, and the increase in these interactions and compactness of structure seen in the Bovine pancreatic trypsin model at elevated temperature suggests that the change in residue P673→S673 stabilizes inter- and intra-protein hydrophobic interactions so that exposure of hydrophobic faces after proteolysis is reduced, resulting in reduced transport across the cell membrane. The increase in charge focused between residues 679 and 696 could alleviate the effects of the increased hydrophobic interactions when translation and assembly occur at permissive temperatures.

An alternative model for reovirus penetration and uncoating has been proposed based upon the altered appearance of the λ2 spike which occurs as a result of the processing which creates the core particle. This model suggests that the ISVP is inserted into but does not cross the cytoplasmic membrane. The model proposes that the virion then transcribes viral mRNA through the λ2 spike as through a porin (Sturzenbecker *et al*, 1987). Porin insertion motifs have been identified with the B chain of cholera toxin. Upon exposure to low pH and proteolytic processing B chain proteins insert into the

cytoplasmic membrane to form a porin and allow the toxic A chain to pass into the cytosol of the target cell (Middlebrook and Dorland, 1984; Steven and Pietrowski, 1986; Lubran, 1988). Similar systems have been proposed for transmembrane transport of colicins (Parker *et al*, 1990). The mutations identified in *tsA279* affect two regions which could mediate the Sturzenbecker porin model, ϕ and the TSF. The mutations affecting the highly charged sequence between residues 679 and 696 could reduce the ability of ϕ to mediate interaction with the cytoplasmic membrane. The predicted local increase in hydrophobicity, while minor, could limit the effect of the change in charge in this region. Increased stability of the hydrophobic interactions within the TSF which occur at elevated temperatures could prevent exposure of amphipathic structures which are necessary for interaction of the processed capsid with cytoplasmic membranes.

7. Future directions.

The results of these studies are shown in the modified listing of characteristics of the clones of the Fields panel of *ts* mutants of reovirus (Table 6.2). These studies have provided insights into mechanisms of virus assembly and uptake. They have also suggested a number of additional areas of investigation which deserve to be pursued. The role of the mutant μ1 protein of *tsA279* provides insight into the mechanisms of membrane insertion and transmembrane transport in biological systems. Visualization of restrictively and permissively assembled *tsA279* progeny, coupled with comparisons to wild type parental virions could provide information concerning the location of different amino acid sequences within the protein in the assembled virion. Comparative

Table 6.2 **Characteristics of the Fields' panel of temperature sensitive mutants of reovirus.[a]**

Reassortment Group	Prototype Mutant	Gene Segment	Protein	dsRNA[c]	EOP[b] 39°C	EOP[b] 40°C	Morphology
A	*tsA201*	M2	μ1	+	0.073	0.0025	Normal
	tsA279	M2	μ1	+	0.11	0.00019	Empty Whole Virus
		L2	λ2				Spike Deficient Core
	tsA329			?	0.0969	0.00044	
	tsA340			?	0.0019	0.0000064	
B	*tsB271*	L2	λ2	+	0.003	0.000015	Core Like
	tsB352				0.000011	0.0000051	
	tsB405				0.00016	0.000025	
C	*tsC447*	S2	σ2	-	0.00078	0.00078	Empty Outer Shell
D	*tsD357*	L1	λ3		0.00025	0.0000071	Empty Whole
E	*tsE320*	S3	σNS	-	0.076	0.001	No Assembly
F	*tsF557*	(M3)	μNS	+	0.0023	0.0.0006	Normal
G	*tsG453*	S4	σ3	+	0.000016	0.000016	Core Like
H	*tsH26/8*	M1	μ2	?	0.00009	0.000097	?
I	*tsI138*	L3	λ1	-	0.00047	0.0034	No Assembly
J	*tsJ128*	S1	σ1	?	0.000029	0.00000028	?

a. Adapted from Table 1.3.
b. EOP : $(Titre_R) \div$ (Titre 32°C).
c. Synthesis of dsRNA at restrictive temperature

studies using permissively versus restrictively assembled virions could elucidate the interactions with the host cell plasmalemma, and establish the fate of outer capsid proteins during transport and uncoating and their role in transcriptional activation.

The possibility of similar ultrastructural characteristics in the restrictively grown inclusions of *tsC447* and *tsI138*, both of which are major core proteins, suggest that the interactions of these two proteins could be dissected further with comparative studies. The concentric sworls of electron dense material noted in inclusions of *tsI138*, and suggested in printed micrographs of *tsC447*, suggests the production of irreversibleaggregates at elevated temperature similar to those seen with the P22 capsid protein (Gordon and King, 1977). Investigation into this possibility could provide insight into assembly of the core capsid.

The different mechanisms involved in expression of temperature sensitivity make the Fields panel of temperature sensitive mutants an excellent, and, as yet under utilized tool for studying viral:host interactions and the viral life cycle. The multifaceted nature of the mutant clone *tsA279* and the possible mechanisms involved in assembly and reduced replication activity of *tsI138* provides for investigation of an exquisite complexity of protein interactions and is an example of the many possible avenues of analysis that the clones in the Fields panel may provide.

CHAPTER 7

References

Acs, G., Klett, H., Schonberg, M., Christman, J., Levin, D.H., Silverstein, J.C. (1971). Mechanism of reovirus double-stranded RNA synthesis in vivo and in vitro. J. Virol. 8:684-689.

Ahmed, R., Chakraborty, P.R., and Fields, B.N. (1980a). Genetic variation during lytic reovirus infection: High passage stocks of wild-type reovirus contain temperature-sensitive mutants. J. Virol. 34:285-287.

Ahmed, R. Chakraborty, P.R., Graham, A.F., Ramig, R.F., and Fields, B.N. (1980b) Genetic variation during persistent reovirus infection: Presence of extragenically suppressed temperature-sensitive lesions in wild type virus isolated from persistently infected L cells. J. Virol. 34:383-389.

Ahmed, R. and Fields, B.N. (1982). Role of the S4 gene in the establishment of persistent reovirus infection in L cells. Cell. 28:605-612.

Ahmed, R., and Graham, A.F. (1977). Persistent infections in L cells with temperature-sensitive mutants of reovirus. J. Virol. 23:250-262.

Ahmed, R., Kauffman, R.S. and Fields, B.N. (1983). Genetic variation during persistent reovirus infection: isolation of cold-sensitive and temperature sensitive mutants from persistently infected L cells. Virology 131:71-78.

Amerongen, H.M., Wilson, G.A., Fields, B.N. and Neutra, M.R.. (1994). Proteolytic processing of reovirus is required for adherence to intestinal M cells. J. Virol. 68:8428-8432.

Antczak, J.B, and Joklik, W.K. (1992). Reovirus genome segment assortment into progeny genomes studied by the use of monoclonal antibodies directed against reovirus proteins. Virology, 187:760-776.

Baer, G.S. and Dermody, T.S. (1997). Mutations in reovirus outer-capsid protein F3 selected during persistent infections of L cells confer resistance to protease inhibitor E64. J. Virol. 71:4921-4928.

Barnes, W.M., Bevan, M. and Son, P.H. (1983). Kilo-sequencing: creation of an ordered nest of asymmetric deletions across a large target sequence carried on phage M13. Methods in Enzymology 101:98-122.

Bartlett, J.A., and Joklik, W.K. (1988). The sequence of the reovirus Serotype 3 L3 genome segment which encodes the major core protein 81. Virology 167:31-37.

Bartlett, N.M., Gillies, S.C., Bullivant, S., and Bellamy, A.R. (1974). Electron microscope study of reovirus reaction cores. J. Virol. 14:315-326.

Barton, D.J., Morasco, B.J., Eisner-Smerage, L., Collis, P.S., Diamond, S.E., Hewlett, M.J., Merchant, M.A., O'Donnell, B.J. and Flanegan, J.B. (1996). Poliovirus RNA polymerase mutation 3D-M394T results in a temperature-sensitive defect in RNA synthesis. Virology. 217:459-469.

Bass, D.M., Bodkin, D., Dambrauskas, R., Trier, J.S., Fields, B.N., Wolf, J.L.(1990). Intraluminal proteolytic activation plays an important role in replication of Type 1 reovirus in the intestines of neonatal mice. J. Virol. 64:1830-1833.

Bassel-Duby, R., Jayasuriya, A. Chatterjee. D., Sonenberg, N., Maizel, J.V. Jr., and Fields, B.N. (1985). Sequence of the reovirus haemagglutinin predicts a coiled-coil structure. Nature 315:421-423.

Bassel-Duby, R., Spriggs, D.R., Tyler, K.L. and Fields, B.N. (1986). Identification of attenuating mutations on the reovirus type 3 S1 double stranded RNA segment with a rapid sequencing technique. J. Virol. 60:64-67.

Beattie, E., Kauffman, E.B., Martinez, H., Perkus, M.E., Jacobs, B.L., Paoletti, E., Tartaglia, J. (1966). Host range restriction of vaccinia virus E3L-specific deletion mutants. Virus Genes. 12:89-94.

Behnke, O., Ammitzbøll, T., Jessen, H., Klokker, M., Nilausen, K., Tranum-Jensen, J., and Olsson, L. (1986). Non-specific binding of protein-stabilized gold sols as a source of error in immunocytochemistry. Eur. J. Cell Biol. 41:326-338.

Bellamy, A.R. and Joklik, W.K. (1967). Studies on Reovirus RNA. II. Characterization of reovirus messenger RNA and of the genome RNA segments from which it is transcribed. J. Mol. Biol. 29:19-26.

Bellamy, A.R.,Shapiro, L., August, J.T. and Joklik, W.K. (1967). Studies on Reovirus RNA. I. Characterization of reovirus genome RNA. J. Mol. Biol. 29:1-17.

Berget, P.B., and King, J. (1983) T4 tail morphogenesis. p246-258. *In* C. Mathews, E.M. Kutter, G. Mosig, and P.B. Berget (eds.), Bacteriophage T4. American Society for Microbiology, Washington, D.C.

Berman, H.M., Sussman, J.L., Joshua-Tor, L., Revich, G.G., and Ripley, L.S. (1992). A structural model for sequence specified proflavin DNA interactions during in vitro

frameshift mutagenesis. J. Biomol. Struct. Dyn. (10-317-331).

Black, L.W., and Showe, M.K. (1983). Morphogenesis of the T4 head, p. 219-245. *In* C. Mathews, E.M. Kutter, G. Mosig, and P.B. Berget (eds.), Bacteriophage T4. American Society for Microbiology, Washington, D.C.

Bodkin, D.K., Nibert, M.L., and Fields, B.N. (1989). Proteolytic digestion of reovirus in the intestinal lumens of neonatal mice. J. Virol. 63:4676-4681.

Borsa, J., Morash, B.D., Sargent, M.D., Copps, T.P., Lievaart, P.A. and Szekely, J.G. (1979). Two modes of entry of reovirus particles into L cells. J. Gen. Virol. 45:161-170.

Borsa, J., Sargent, M.C., Lievaart, P.A., and Copps, P.A. (1981). Reovirus: Evidence for a second step in the intracellular uncoating and transcriptase activation process. Virology 111:191-200.

Brandon, C. and Tooze, J. (1993). Introduction to protein structure. Garland Publishing, New York.

Brenner, S., and Horne, R.W. (1959). Negative staining method for high resolution electron microscopy of viruses. Biochemica et Biophysica Acta 34:103-110.

Bruen, J.A. (1991). Relationships among the positive strand and double stranded RNA viruses as viewed through their RNA dependent RNA polymerases. Nucleic Acids Res. 19:217-226.

Canning, W.M. and Fields, B.N. (1983). Ammonium chloride prevents lytic growth of reovirus and helps to establish persistent infection in mouse L cells. Science. 219:987-988

Cashdollar, S.E. (1994). Characterization and structural localization of the reovirus λ3 protein. Res. Virol. 148:191-206.

Cashdollar, L.W., Esparza, J., Hudson, G.R., Chmelo, R., Lee, P.W.K. and Joklik, W.K. (1982). Cloning the double-stranded RNA genes of reovirus: sequence of the cloned S2 gene.Proc. Natl. Acad. Sci. USA. 79:7644-7648.

Centonze. V.E., Chen, Y., Severson, T.F., Borisy, G.G. and Nibert, M.L. (1995). Visualization of individual reovirus particles by low-temperature, high-resolution scanning electron microscopy. J. Struct. Biol. 115:215-225.

Ceruzzi, M. and Shatkin, A.J. (1986). Expression of reovirus p14 in bacteria and identification in the cytoplasm of infected mouse L cells. Virology. 153:35-45.

Chakraborty, P.R., Ahmed, R., and Fields, B.N. (1979). Genetics of reovirus: The relationship of interference to complementation and reassortment of temperature-sensitive mutants at non-permissive temperatures. Virology. 94: 119-127.

Chaly, N., Johnstone, M., and Hand, R. (1980). Alterations in nuclear structure and function in reovirus infected cells. Clin. Invest. Med. 2:141-152.

Chang, C.-T., and Zweerink, H.J. (1971). Fate of parental reovirus in infected cell. Virology 46:544-555.

Chappell, J.D., Goral, M.I., Rodgers, S.E., dePamphilis, C.W. and Dermody, T.S. (1994). Sequence diversity within the reovirus S2 gene: reovirus genes reassort in nature, and their termini are predicted to form a panhandle motif. J. Virol. 68:750-756.

Chappell, J.D., Gunn, V.L., Wetzel, J.D., Baer, G.S. and Dermody, T.S. (1997). Mutations in type 3 reovirus that determine binding to sialic acid are contained in the fibrous tail domain of viral attachment protein σ1. J. Virol. 1834-1841.

Chow,N.-L., Shatkin, A.J. (1975). Blocked and unblocked termini in reovirus genome RNA. J. Virol. 15:1057-1064.

Cleveland, D.W., Zarbl, H., Millward, S. (1986). Reovirus guanylyltransferase is L2 gene product λ2. J. Virol. 60:307-311.

Coombs, K.M. (1996). Identification and characterization of a double stranded RNA-virus temperature-sensitive mutant defective in minor core protein μ2. J. Virol. 70:4237-4245.

Coombs, K.M. (1998a) Stoichiometry of reovirus structural proteins in virus, ISVP and core particles. Virology. 243:218-228.

Coombs, K.M. (1998b). Temperature-sensitive mutants of reovirus. Cur. Topic Microbiol. Immunol. 233:69-107.

Coombs, K.M,, Fields, B.N., and Harrison, S. (1990). Crystalization of the reovirus type 3 Dearing core: crystal packing is determined by the λ2 protein. J. Mol. Biol. 215:1-5.

Coombs, K.M., Mak, S.-C., and Petrycky-Cox, L.D. (1994). Studies of the major reovirus core proteinσ2: Reversion of the assembly-defective mutant *tsC447* is an intragenic process and involves back mutation of Asp-383 to Asn. J. Virol. 68:177-186.

Craxton, M. (1991). Linear amplification sequencing. A powerful method for sequencing DNA. Methods Companion Methods Enzymol. 3:20-26.

Creighton, T.E.(1993). Proteins: structures and molecular properties.2nd ed. Freeman and Company, New York.

Cross, R.K., and Fields, B.N. (1972). Temperature-sensitive mutants of reovirus 3: Studies on the synthesis of viral RNA. Virology 50:799-809.

Cross, R.K., and Fields, B.N., (1976a). Use of an aberrant polypeptide as a marker in three-factor crosses: Further evidence for independent reassortment as the mechanism of recombination between temperature-sensitive mutants of reovirus type 3. Virology 74:345-362.

Cross, R.K., and Fields, B.N. (1976b). Temperature-sensitive mutants of reovirus type 3: Evidence for aberrant μ1 and μ2 polypeptide species. J. Virol. 19:174-179.

Dales, S. and Gomatos, P.J. (1965). The uptake and development of reovirus in strain L cells followed with labeled viral ribonucleic acid and ferritin-antibody conjugates. Virology 25:193-211.

Danis, C., Garzon, S., and Lemay, G. (1992). Further characterization of the *ts453* mutant of mammalian orthoreovirus serotype 3 and nucleotide sequence of the mutated S4 gene. Virology 190:494-498.

Darzynkiewicz, E. and Shatkin, A.J. (1980). Assignment of reovirus mRNA ribosome binding sites to virion genome segments by nucleotide sequence analysis. Nuc. Acids Res. 8:337-350.

de Prat-Gay, G. (1997). Conformational preferences of a peptide corresponding to the major antigenic determinant of foot-and-mouth disease virus: implications for peptide-vaccine approaches. Arch. Biochem. Biophys. 341:360-369.

Dermody, T.S., Schiff, L.A, Nibert, M.L., Coombs, K.M., and Fields, B.N., (1991). The S2 gene nucleotide sequences of prototype strains of the three reovirus serotypes: Characterization of reovirus core protein σ2. J. Virol. 65:5721-5731.

Dermody, T.S., Nibert, M.L, Wetzel. K.D., Tong, X., and Fields, B.N. (1993). Cells and viruses with mutations affecting viral entry are selected during persistent infections of L cells with mammalian reoviruses. J. Virol. 67:2055-2063.

Doohan, J.P., and Samuel, C.E. (1992). Biosynthesis of reovirus-specified polypeptides: ribosome pausing during the translation of reovirus S1 mRNA. Virology. 186:409-425.

Doohan, J.P., and Samuel, C.E. (1993). Biosynthesis of reovirus-specified polypeptides. Analysis of ribosome pausing during translation of reovirus S1 and S4 mRNAs in virus-infected and vector-transfected cells. J. Biol. Chem. 268:18313-18320.

Drayna, D., and Fields, B.N. (1982a). Activation and characterization of the reovirus transcriptase: Genetic analysis. J. Virol. 41:110-118.

Drayna, D. and Fields, B.N. (1982b). Genetic studies on the mechanism of chemical and physical inactivation of reovirus. J. Gen. Virol. 63:149-160.

Dryden, K.A., Wang, G., Yeager, M., Nibert, M.L., Coombs, K.M., Furlong, D.B., Fields, B.N., and Baker, T.S. (1993). Early steps in reovirus infection are associated with dramatic changes in supramolecular structure and protein conformation: Analysis of virions and subviral particles by cryoelectron microscopy and image reconstruction. J. Cell Biol. 122:1023-1041.

Duncan, R., Horne, D., Cashdollar, L.W., Joklik, W.K. and Lee, P.W.K. (1990). Identification of conserved domains in the cell attachment proteins of the three serotypes of reovirus. Virology. 174:399-409.

Duncan, R., Horne, D., Strong, J.E., Leone, G., Pon, R.T., Yeung, M.C. and Lee, P.W.K (1991). Conformational and functional analysis of the C-terminal globular head of the reovirus cell attachment protein. Virology. 182:810-819.

Dunnebacke, T.H. and Kleinschmidt, A.K. (1967). Ribonucleic acid from reovirus as seen in protein monolayers by electron microscopy. Z. Naturforsch. 22b:159-164.

Earle, W.R. (1943). Production of malignancy *in vitro*. IV. The mouse fibroblast cultures and changes seen in the living cells. J. Nat. Cancer Inst. 4:165-211.

Ernst, G., and Shatkin, A.J. (1985) Reovirus hemagglutinin mRNA codes for two polypeptides in overlapping reading frames. Proc. Natl. Acad. Sci. USA. 82:48-52.

Esolin, L.M., Park, S., Hardwick, J.M., and Griffin, D.E. (1994). Apoptosis in measles virus - infected cells. p191. *In* American Society for Virology 13th Annual Meeting, Scientific Program and Abstracts. (1994).

Fajardo, E. and Shatkin, A.J. (1990). Expression of the two reovirus S1 gene products in transfected mammalian cells. Virology. 178:223-231.

Fane, B., and King, J. (1987). Identification of sites influencing the folding and subunit assembly of the P22 tailspike polypeptide chain using nonsense mutations. Genetics 117:157-171.

Fane, B., Villafane, R., Mitraki, A., and King, J. (1991). Identification of global suppressors for temperature-sensitive folding mutations of the P22 tailspike protein. J. Biol. Chem. 266:11640-11648.

Fausnaugh, J. and Shatkin, A.J. (1990). Active site localization in a viral mRNA capping enzyme. J. Biol. Chem. 265:7669-7672.

Fields, B.N., and Joklik, W.K. (1969). Isolation and preliminary genetic and biochemical characterization of temperature-sensitive mutants of reovirus. Virology 37:335-342.

Fields, B.N., Raine, C.S., and Baum, S.G. (1971). Temperature-sensitive mutants of reovirus type 3: Defects in viral maturation as studied by immunofluorescence and electron microscopy. Virology 43:569-578.

Fields, B.N, Laskov, R. and Scharff, M.D. (1972). Temperature-sensitive mutants of reovirus type 3: Studies on the synthesis of viral peptides. Virology 50:209-215.

Francki, R.I.B., Fauquet, C.M., Knudson, D.L. and Brown, F. eds. (1991. Classification and nomenclature of viruses. 5th report of the International Commission for the Taxonomy of Viruses. Springer-Verlag, New York.

Furlong, D.B., Nibert, M.L. and Fields, B.N. (1988). σ1 protein of mammalian reoviruses extends from the surfaces of viral particles. J. Virol. 62:246-256..

Furuichi,Y., Morgan, M., Muthukrishnan, S., and Shatkin, A.J. (1975a). Reovirus messenger RNA contains a methylated blocked 5'-terminal structure $M^7G(5')ppp(5')G^mpCp$-. Proc. Nat. Acad. Sci. USA. 72:362-366.

Furuichi, Y., Muthukrishnan, S. and Shatkin, A.J. (1975b). 5'-Terminal $m^7G(5')ppp(5')G^mp$ in vivo: Identification in Reovirus Geonme RNA. Proc. Nat. Acad. Sci. 72:742-745.

Gaillard, R.K.Jr. and Joklik, W.K. (1985). The relative translation efficiencies of reovirus messenger RNAs. Virology. 147:336-348.

Gaudin, Y., Ruigrok, R.w., Knossow, M. and Flamand, A. (1993). Low-pH conformational changes of rabies virus glycoprotein and their role in membrane fusion. J. Virol. 67:1365-1372.

Gentsch, J.R. and Hatfield, J.W. (1984). Saturable attachment sites for type 3 mammalian reovirus on murine L cells and human HeLa cells. Virus Research. 1:401-414.

Gentsch, J.R. and Pacitti, A.F., (1985). Effect of neuraminidase treatment of cells and effect of soluble glycoproteins on type 3 reovirus attachment to murine L cells. J. Virol. 56:356-364.

Gentsch, J.R. and Pacitti, A.F. (1987). Differential interaction of reovirus type 3 with

sialylated receptor components on animal cells. Virology. 161:245-248.

Geoghegan, W.D., and Ackerman, G.A. (1977). Adsorption of horseradish peroxidase, ovomucoid and anti-immunoglobulin to colloidal gold for the indirect detection of concanavalin A, wheat germ agglutinin and goat anti-human immunoglobulin G on cell surfaces at the electron microscopic level: a new method, theory and application. J. Histochem. Cytochem. 25:1187-1200.

George, C.X., Atwater, J.A. and Samuel. C.E. (1986). Biosynthesis of the reovirus-specified polypeptides. Molecular cDNA cloning and nucleotide sequences of the reovirus serotype 1 Lang strain S3 mRNA which encodes the non structural RNA binding protein σNS. Biochem. Biophys. Res. Commun. 139:845-851.

George, C.X., Crowe, A., Munemitsu, S.M., Atwater, J.A. and Samuel, C.E. (1987). Biosynthesis of the reovirus-specified polypeptides. Molecular cDNA cloning and nucleotide sequence of the reovirus serotype 1 Lang strain S2 mRNA which encodes the virion core polypeptide σ2. Biochem. Biophys. Res. Commun. 144:1153-1161.

Giantini, M., Seliger, L.S., Furuichi, Y., and Shatkin, A.J., (1984). Reovirus type 3 genome segment S4: Nucleotide sequence of the gene encoding a major virion surface protein.. J. Virol. 52:984-987.

Gilles, S., Bullivant, S., Bellamy, A.R. (1971). Viral RNA polymerases: electron microscopy of reovirus reaction cores. Science. 174:694-696.

Gilmore, R., Coffey, M.C., Leone, G., McLure, K. and Lee, P.W.K. (1996). Co-translational trimerization or reovirus cell attachment protein. EMBO J. 15:2651-2658.

Gomatos, P.J., Prakash, O, Stamatos,, N.M. (1981). Small reovirus particles composed solely of σNS with specificity for binding different nucleic acids. J. Virol. 39:115-124.

Gomatos, P.J., and Tamm, I. (1962). Animal and plant viruses with double-helical RNA. Proc. Nat. Acad. Sci. USA. 50:878-885.

Gordon, C.L., and King, J. (1993). Temperature-sensitive mutations in the phage P22 coat protein which interfere with polypeptide chain folding. J. Biol. Chem. 268:9358-9368.

Gough, J.A. and Murray, N.E. Sequency diversity among related genes for recognition of specific targets in DNA molecules. J. Mol. Biol. 166:1-19

Gottfried, D.S., and Haas, E. (1992). Nonlocal interactions stabilize compact folding intermediates in reduced unfolded bovine pancreatic trypsin inhibitor. Biochem. 31:12353-12362.

Haller, B.L., Barkon, M.L., Vogler, G.P. and Virgin, H.W. IV. (1995) genetic mapping of reovirus virulence and organ tropism in severe combined immunodeficient mice: organ-specific virulence genes. J. Virol. 69:357-364.

Hammond, G.W., Hazelton, P.R., Cheung, I., and Klisko, B. (1981). Improved detection of viruses by electron microscopy after direct ultracentrifuge preparation of specimens. J. Clin. Microbiol. 14:210-221.

Harrison, S.C. (1990), Virus Structure. *In* B.N. Fields and D.M. Knipe (ed). Fields Virology. (2nd ed). Raven Press, New York, pp. 37-61.

Harrison, S.C., Skehel, J.J. and Wiley, D.C. (1996). Virus Structure. In Fields, B.N., Knipe, D.M., Chanock, R.M., Hirsch, M.S., Melnick, J.L., Monath, T.P., and Roizman, B (eds). Fields Virology (3rd ed). Raven Press. New York. pp. 59-99.

Hassard, T.H. (1991). Understanding Biostatistics. Mosby, St. Louis.

Hayat, M.A. (1985). Basic Techniques for Transmission Electron Microscopy. Academic Press, London. p. 87-88.

Hayat, M.A, and Miller, S.E. (1990). Negative Staining. McGraw Hill, New York

Hayes, E.C., Lee, P.W.K., Miller, S.E. and Joklik, W.K. (1981). The interactions of a series of hybridoma IgGs with reovirus particles: demonstration that the core protein λ2 is exposed on the particle surface. Virology, 108:147-155.

Hazelton, P.R. and Coombs, K.M. (1995). The reovirus mutant *tsA279* has temperature-sensitive lesions in the M2 and L2 genes: The M2 gene is associated with decreased viral protein production and blockade in transmembrane transport. Virology. 207:46-58.

Hazelton, P.R. and Coombs, K.M. The reovirus mutant tsA279 L2 gene is associated with generation of a spikeless core particle: Implications for capsid assembly. In preparation.

Hazelton, P.R. and Hammond, G.W. (1983). Negative stains for electron microscopic detection of small round enteric viruses from human fecal specimens. 33rd Meeting of the Canadian Society for Microbiologists. Winnipeg, Canada.

Hewat, E.A., Booth, T.F., Loudon, P.T., and Roy, P. (1992). Three-dimensional reconstruction of baculovirus expressed bluetongue virus core-like particles by cryo-electron microscopy. Virology 189:10-20.

Hoffman, L.M., Hogan, K.T. and Cashdollar, L.W. (1996). The reovirus nonstructural protein σ1NS is recognized by murine cytotoxic T lymphocytes. J. Virol. 70:8160-8164.

Hoffman, L.M. Kuntz, I.D. and White, J.M. (1997) Structure-based identification of an inducer of the low-pH conformational change in the influenza virus hemagglutinin: irreversible inhibition of infectivity. J. Virol. 71:8808-8820.

Hogle, J.M., Chow, M., and Filman, D.J. (1985). Three-dimensional structure of poliovirus at 2.9D resolution. Science 229:1358-1365.

Hooper, J.W. and Fields, B.N. (1996a). Role of the μ1 protein in reovirus stability and capacity to cause chromium release from host cells. J. Virol. 70:459-467.

Hooper, J.W., and Fields, B.N. (1996b). Monoclonal antibodies to reovirus σ1 and μ1 proteins inhibit chromium release from mouse L cells. J. Virol. 70:672-677.

Horisberger, M. (1989). Quantitative aspects of labelling colloidal gold with proteins. p.49-61. *In* A.J. Verkleij and J.L.M. Leunissen (eds.) Immuno-gold labelling in cell biology. CRC Press, Boca Raton.

Huismans, H. and Joklik, W.K. (1976). Reovirus-coded polypeptides in infected cells: Isolation of two native monomeric polypeptides with affinity for single stranded and double stranded RNA, respectively. Virology. 70:411-424.

Hull, R.N., Minner, J.R. and Mascoli, C.C. (1958). New viral agents recovered from tissue cultures of monkey kidney cells. III. Recovery of additional agents both from cultures of monkey tissues and directly from tissues and excretia. Am. J. Hyg. 68:31-44.

Hull, R.N., Minner, J.R. and Smith, , J.W. (1956). New viral agents recovered from tissue cultures of monkey kidney cells. I. Origin and properties of cytopathic agents SV1, SV2, SV4, SV5, SV6, SV11, SV12, and SV15. Am. J. Hyg. 63:204-215

Ikegami, N., and Gomatos, P.J. (1968). Temperature-sensitive conditional-lethal mutants of reovirus 3. I. Isolation and characterization. Virology 36:447-458.

Illa, I., Nath, A., and Dalakas, M. (1991). Immunocytochemical and virological characteristics of HIV associated inflammatory myopathies: Similarities with seronegative polymyositis. Ann. Neurol. 29:474-481.

Imanaka, T., Nakae, M, Ohta, T., and Takagi, M. (1992). Design of temperature-sensitive penicillinase repressors by replacement of Pro in predicted β-turn structures. J. Bacteriol. 174:1423-1425.

Imani, F. and Jacobs, B.L. (1988). Inhibitory activity for the interferon-induced protein kinase is associated with the reovirus serotpe 1 σ3 protein. Proc. Natl. Acad. Sci. USA. 83:7887-7891.

Itakura, K., Rossi, J.J. and Wallace, R.B. (1984). Synthesis and use of synthetic oligohucleotides. Ann Rev. biochem. 53:323-356.

Jacobs, B.L., Atwater, J.A., Munemitsu, S.M. and Samuel, C.E. (1985). Biosynthesis of reovirus specified polypeptides. The S1 mRNA synthesized in vivo is structurally and funcitionally indistinguishable from in vitro-synthesized S1 mRNA and encodes two polypeptides, σ1a and σ1bNS. Virology. 147:9-18.

Jacobs, B.L and Langland, J.O. (1996). When two strands are better than one: the mediators and modulators of the cellular responses to double-stranded RNA. Virology. 219:339-349.

Jacobs, B.L. and Samuel, C.E. (1985). Biosynthesis of reovirus-specified polypeptides: the reovirus S1 mRNA encodes two primary translation products Virology. 143:63-74.

Jaenicki, R. (1991). Protein stability and molecular adaption to extreme conditions. Eur. J. Biochem. 202:715-728.

Jayasuriya, A.K., Nibert, M.L., and Fields, B.N. (1988). Complete nucleotide sequence of the M2 gene segment of reovirus type 3 Dearing and analysis of its protein product μ1. Virology 163:591-602.

Johannson, P.J., Sveger, T., Ahlfors, K., Edstrand, J. and Svensson, L. (1996). Reovirus type 1 associated with meningitis. Scand. J. Infect. Dis. 28:117-120.

Joklik, W.K. (1983). The reovirus particle, p. 9-78. *In* W.K. Joklik (ed.), The reoviridae. Plenum Publishing Corp, New York.

Kanellis, P., Romans, A.Y., Johnson, B.J., Kercret, H., Chiovetti, R.Jr., Allen, T.M., and Segrest., J.P. (1980). Studies of synthetic peptide analogues of the amphipathic helix. Effect of charged amino acid residue topography on lipid affinity. J. Biol. Chem. 255:11464-11472.

Khaustov, V.I.,. Korolev, M.B., and Reingold, V.N. (1987). The structure of the capsid inner layer of reovirus. Brief Report. Arch Virol. 93:163-167.

Klug, A., and Caspar, D.L.D. (1960). The structure of small viruses. Adv. Virus Res. 7:225-325.

Koonin, E.V. (1993). Computer assisted identification of a putative methyltransferase domain in NS5 protein of flaviviruses and λ2 protein of reovirus. J. Gen. Virol. 74:733-740.

Kozak, M., and Shatkin, A.J. (1976) Characterization of ribosome-protected fragments

from reovirus messenger RNA. J. Biol. Chem. 251:4259-4266.

Lang K., and Schmid, F.X., (1990). Role of two proline-containing turns in the folding of porcine ribonuclease. J. Mol. Biol. 212:185-196.

Lascu, I., Chafotte, A., Limbourg-Bouchon, B., and Veron, M. (1992). A Pro/Ser substitution in nucleoside diphosphate kinase of *Drosophela melanogaster* (mutation killer of prune) affects stability but not catalytic efficiency of the enzyme, J. Biol. Chem. 267:12775-12781.

Laemmli, U.K. (1970). Cleavage of structural proteins during the assembly of the head of bacteriophage T4. Nature. 227:680-685.

Lau, R..Y.,Van Alstyne, D., Berckmans, R. and Graham, A.F. (1975). Synthesis of reovirus-specific polypeptides in cells pretreated with cyclohexamide. J. Virol. 16:470-478.

Lawton, J.A., Estes, M.K. and Prasad, B.V.V. (1997). Three-dimensional visualization of mRNA release from actively transcribing rotavirus particles. Nat. Struct. Biol. 4:118-121.

Lawton, J.A., Zeng, C. Q.-Y., Mukherjee, S.K., Cohen, J., Estes, M.K. and Prasad, B.V.V. (1997). Three-dimensional structural analysis of recombinant rotavirus-like particles with intact and amino-terminal-deleted VP2: Implications for the architecture of the VP2 capsid layer. J. Virol. 71:7353-7360.

Lee, P.W.K., Hayes, E.C., and Joklik, W.K. (1981). Protein σ1 is the reovirus cell attachment protein. Virology 108: 156-163.

Lee, P.W.K. and Leone, G. (1994). Reovirus protein σ1: from cell attachment to protein of oligomerization and folding mechanisms. Bioessays. 16:199-206.

Lemay, G. and Danis, C. (1994). Reovirus λ1 protein: affinity for double-stranded nucleic acids by a small amino-terminal region of the protein independent from the zinc finger motif. J. Gen. Virol. 75:3261-3266.

Leone, G., Coffey, M.C., Gilmore, R., Duncan, R., Maybaum, L. and Lee, P.W.K. (1996). C-terminal trimerization of the reovirus cell attachment protein is a posttranslational and Hsp70/ATP-dependent process. J. Biol Chem. 271:8466-8471.

Leone, G, Duncan, R. and Lee, P.W.K. (1991a). Trimerization of the reovirus cell attachment protein (σ1)induces conformational changes in σ1 necessary for its cell-binding function. Virology. 184:758-761.

Leone, G., Duncan, R., Mah, D.C.W., Price, A. Cashdollar, L.W. and Lee, P.W.K. (1991b). The N-terminal heptad repeat region of reovirus cell attachment protein σ1 is responsible for σ1 oligomer stability and possesses intrinsic oligomerization function. Virology. 182:336-345.

Leone, G., Mah, D.C.W. and Lee, P.W.K., (1991c). The incorporation of reovirus cell attachment protein F1 into virions requires the amino-terminal hydrophobic tail and the adjacent heptad repeat region. Virology. 182:346-350.

Leone, G., Maybaum, L., Lee, P.W.K. (1992). The reovirus cell attachment protein possesses two independently active trimerizations domains: basis of dominant negative effects, Cell. 71:479-488.

Lloyd, R.M. and Shatkin, A.J. (1992). Translational stimulation by reovirus polypeptide σ3: substitution for VAI-RNA and inhibition of phosphorylation of the a-subunit of eukaryotic initiation factor-II. J. Virol. 66:6878-6884.

Lu, Y-L., Koga, Y., Tanaka, K., Sasaki,M., Kimura, G, and Nomoto, K. (1994). Apoptosis induced in $CD4^+$ cells expressing gp160 of human immunodeficiency virus type 1. J. Virol. 68:390-399.

Lubran, M.M., (1988). Bacterial toxins. Ann. Clin. Lab. Sci. 18:58-71.

Lucia-Jandris, P.A., (1990). Interaction of mammalian reovirus particles with cell membranes. PhD Thesis. Harvard University, Cambridge, MA.

Lucia-Jandris, P., Hooper, J.W., and Fields, B.N. (1993). Reovirus M2 gene is associated with chromium release from mouse L cells. J. Virol. 67:5339-5345.

Lucocq, J.M., and Baschong, W. (1986). Preparation of protein colloidal gold complexes in the presence of commonly used buffers. Eur. J. Cell Biol. 42:332-337.

Luftig, R.B., Kilham, S.S., Hay, A.J., Zweerink, H.J., and Joklik, W.K. (1972). An ultrastructure study of virions and cores of reovirus type 3. Virology 48:170-181.

Luongo, C.L., Dryden, K.A., Farsetta, D.L., Margraf, R.L., Severson, T.F., Olson, N.H., Fields, B.N., Baker, T.S. and Nibert, M.L. (1997). Localization of a C-terminal region of λ2 protein in reovirus cores. J. Virol. 71:8035-8040.

Lyubchenko, Y.L., Gall, A.A., Shlayakhtenko, L.S., Harrington, R.E., Jacobs, B.L., Oden, P.I. and Lindsay, S.M. (1992a). Atomic force microscopy of double stranded DNA and RNA. J. Biomol. Struct. Dyn. 10:589-606.

Lyubchenko, Y.L., Jacobs, B.L. and Lindsay, S.M. (1992b). Atomic force microscopy

of reovirus dsRNA - a routine technique for length measurements. Nucleic Acids Res. 20:3983-3986.

Mabrouk, T. and Lemay, G. (1994). The sequence similarity of reovirus σ3 protein to picornal viral proteases is unrelated to its role in μ1 viral protein cleavage. Virology. 202:615-620.1062.

Mao, Z.X and Joklik, W.K. (1991). Isolation and enzymatic characterization of protein λ2, the reovirus guanylyltransferase. Virology. 185:377-386.

Martin, P.E. and McCrae, M.A. 1993. Analysis of the stimulation of reporter gene expression by the σ3protein of reovirus in co-transfected cells. J. Gen. Virol. 74:1055

Matoba, Y., Sherry, B., Fields, B.N., and Smith, T.W. (1991). Identification of the viral genes responsible for the growth of strains of reovirus in cultured mouse heart cells. J. Clin. Invest. 87:1628-1633.

Matoba, Y., Colucci, W.S., Fields, B.N. and Smith, T.W. (1993). The reovirus M1 gene determines the relative capacity of growth of reovirus in cultured bovine aortic endothelial cells. J. Clin. Invest. 92:2883-2888.

Matsuhisa, T., and Joklik, W.K. (1974). Temperature-sensitive mutants of reovirus. V. Studies on the nature of the temperature-sensitive lesion of the group C mutant *ts447*. Virology, 60:380-389.

Matthews, R.E.F. (1982). Classification and nomenclature of viruses. 4th report of the International Commission on Taxonomy of Viruses. S. Karger AG, Basil

McPhillips, T.H., and Ramig, R.F. (1984). Extragenic suppression of temperature-sensitive phenotype in reovirus: Mapping suppressor mutations. Virology 135:428-439.

Metcalf, P., Cyrklaff, M., and Adrian, M. (1991). The three-dimensional structure of reovirus obtained by cryo-electron microscopy. EMBO Journal 10:3129-3136.

Middlebrook, J.L. and Dorland, R.B. (1984). Bacterial toxins: Cellular mechanisms of action. Microbiol. Rev. 48:199-221.

Miller, M.F. (1979). A universal sedimentation virus particle counting procedure, p. 56-57. *In* G.W. Bailey, (ed.), 37th Ann. Proc. Electron Microscopy Society of America.

Miller, S.E. (1995). Diagnosis of Viral Infections by Electron Microscopy. In Lennette, E.H., Lennette, D.A. Lennette, E.T., (eds.) Diagnostic Procedures for Viral, Rickettsial and Chlamydial Infections. American Public Health Association. Washington.

Miura, K.-I., Watanabe, K., Sugiura, M., and Shatkin, A.J. (1974). The 5' terminal nucleotide sequences of the double-stranded RNA of human reovirus Proc. Nat. Acad. Sci. 71:3979-3983.

Moe, G.R., and Kaiser, E.T. (1985). Design, synthesis, and characterization of a model peptide having potent calcitonin-like biological activity: Implications for calcitonin structure/activity. Biochemistry 24:1971-1976.

Monath, T.P. and Guirakhoo, F. (1996). Orbiviruses and Coltiviruses. *In* Fields, B.N., Knipe, D.M., Chanock, R.M., Hirsch, M.S., Melnick, J.L., Monath, T.P., and Roizman, B (eds). Fields Virology (3rd ed). Raven Press. New York. pp 1735-1766..

Montrose, L, Watkins, S., Moreland, R.B., Mamon, H., Caspar, D.L.D., and Garcea, R.L. (1991). Nuclear assembly of polyomavirus capsids in insect cells expressing the major capsid protein VP1. J. Virol. 65:4991-4998.

Mora, M., Partin, K., Bhatia, M., Partin, J., and Carter, C. (1987). Association of reovirus proteins with the structural matrix of infected cells, Virology 159:265-277.

Morgan, E.M., and Kingsbury, D.W. (1981). Reovirus enzymes that modify messenger RNA are inhibited by perturbation of the λ proteins. Virology 113:565-572.

Morgan, E.M., and Zweerink, H.J. (1974). Reovirus morphogenesis. Corelike particles in cells infected at 39°C with wild-type reovirus and temperature-sensitive mutants of groups B and G. Virology, 59: 556-565.

Morgan, E.M. and Zweerink, H.J. (1975). Characterization of transcriptase and replicase particles isolated from reovirus infected cells. Virology 68:455-466.

Morin, J.J., Warner, A. and Fields, B.N. (1996). Reovirus infection in rat lungs as a model to study the pathogenesis of viral pheumonia. J. Virol. 70:541-548.

Morozov, S.Y. (1989). A possible relationship of reovirus putative RNA-Polymerase to polymerases of positive-strand RNA viruses. Nucleic Acids Res. 17:5394.

Munemitsu, S.M., Atwater, J.A. and Samuel, C.E. (1986). Biosynthesis of reovirus-specified polypeptides. Molecular cDNA cloning and nucleotide sequence of the reovirus serotype 1 Lang strain bicistronic S1 mRNA which encodes the minor capsid polypeptide σ1a and the nonstructural polypeptide σ1bs. Biochem. Biophys. Res. Commun. 140:508-514.

Murray, V. (1989). Improved double-stranded DNA sequencing using the linear polymerase chain reaction. Nucleic Acids Res. 17:8889.

Mustoe, T.A., Ramig, R.F., Sharpe, A.H., and Fields, B.N. (1978). A genetic map of reovirus. III. Assignment of the double-stranded RNA mutant groups A, B, and G to genome segments. Virology 85:545-556.

Nettleship, A. (1943). Production of malignancy in tumors. VI. Pathology of tumors produced. J. Nat. Cancer Inst. 4:229-248.

Nibert, M.L., Chappell, J.D. and Dermody, T.S. (1995). Infectious subviral particles of reovirus type 3 Dearing exhibit a loss in infectivity and contain a cleaved μ1 protein. J. Virol. 69:5057-5067.

Nibert, M.L. Dermody, T.S. and Fields, B.N. (1990). Structure of the reovirus cell-attachment protein: a model for the domain organization of σ1. J. Virol. 64:2976-2989

Nibert, M.L., and Fields, B.N. (1992). A carboxy terminal fragment of protein μ1/μ1c is present in infectious subvirion particles of mammalian reoviruses and is proposed to have a role in penetration. J. Virol. 66:6408-6418.

Nibert, M.L., Furlong, D.B., and Fields, B.N. (1991a). Mechanisms of viral pathogenesis. Distinct forms of reoviruses and their roles during replication in cells and host. J. Clin. Invest. 88:727-734.

Nibert, M.L., Margraf, R.L. and Coombs, K.M. (1996a). Nonrandom segregation of parental alleles in reovirus reassortants. J. Virol. 70:7295-7300.

Nibert, M.L., Schiff, L.A., and Fields, B.N. (1991b). Mammalian reoviruses contain a myristoylated structural protein. J. Virol. 65:1960-1967.

Nibert, M.L., Schiff, L.A. and Fields, B.N. (1996b). Reoviruses and their replication. *In* Fields, B.N., Knipe, D.M., Chanock, R.M., Hirsch, M.S., Melnick, J.L., Monath, T.P., and Roizman, B (eds). Fields Virology (3rd ed). Raven Press. New York. pp 1557-1596.

Noble, S. and Nibert,M.L. (1997a). Characterization of an ATPase activity in reovirus cores and its genetic association with core-shell protein λ1. J. Virol. 71:2182-2191

Noble, S. and Nibert,M.L. (1997b). Core protein μ2 is a second determinant of nucleoside triphosphatase activities by reovirus cores. J. Virol. 71:7728-7735..

Paredes, A.M., Brown, D.T., Rothnagel, R., Chiu, W., Schoepp, R.J., Johnstone, R.E., and Prasad, B.V.V. (1993). Three-dimensional structure of a membrane-containing virus. Proc. Natl. Acad. Sci. (USA). 90:9095-9099.

Parker, M.W., Tucker, A.D., Tsernoglou, D., and Pattus, F. (1990). Insights into

membrane insertion based on studies of colicins. Trends Biochem. Sci. 15:126-129.

Peeling, R., MacLean, I., and Brunham, R.C. (1984). *In vitro* neutralization of *Chlamydia trachomatous* with monoclonal antibody to an epitope on the major outer membrane protein. Infect. Immun. 46:484-488.

Prasad, B.V.V., Rothnagel, R., Zeng, C.Q., Jakana, J., Lawton, J.A., Chiu, W. and Estes, M.K. 1996. Visualization of ordered genomic RNA and localization of transcriptional complexes in rotavirus. Nature. 382:471-473.

Prevelige, P.E. Jr., and King, J. (1993). Assembly of bacteriophage P22: A model for ds-DNA virus assembly. Prog. Med. Virol. 40:206-221.

Ralph, S.J, Harvey, J.D. and Bellamy, A.R. (1980). Subunit structure of the reovirus spike. J. Virol. 36:894-896.

Ramig, R.F., Ahmed, R., and Fields, B.N. (1983). A genetic map of reovirus: assignment of the newly defined mutant groups H, I, and J to genome segments. Virology 125:299-313.

Ramig, R.F., and Fields, B.N., (1977). Method for rapidly screening revertants of reovirus temperature-sensitive mutants for extragenic suppression. Virology 81:170-173.

Ramig, R.F., and Fields, B.N. (1979). Revertants of temperature-sensitive mutants of reovirus: Evidence for frequent extragenic suppression. Virology 92:155-167.

Ramig, R.F., Mustoe, T.A., Sharpe, A.H., and Fields, B.N. (1978). A genetic map of reovirus. II. Assignment of the double-stranded RNA-negative mutant groups C, D, and E genome segments. Virology 85:531-544.

Ramig, R.F., White, R.M., and Fields, B.N. (1977). Suppression of the temperature-sensitive phenotype of a mutant of reovirus type 3. Science 195:406-407.

Ramos-Alverez, M. and Sabin, A.B. (1954). Characteristics of poliomyelitis and other enteric viruses recovered in tissue culture from healthy American children. Proc. Soc. Exp. Biol. Med. 87:655-.

Revich, G.G., and Ripley, L.S. (1990). Effects of proflavin and photoactivated proflavin on the template function of single stranded DNA. J. Mol. Biol. 211:63-74.

Rhim, J.S., Smith, K.O., and Melnick, J.L. (1961). Complete and coreless forms of reovirus (ECHO 10). Ratio of mumber of virus particles to infective units in the one-step cycle. Virology 15:428-435.

Rhim, J.S., Jordan, L.E., and Mayor, H.D. (1962). Cytochemical, fluorescent-antibody and electron microscopic studies on the growth of reovirus (ECHO 10) in tissue culture. Virology 17:342-355.

Richardson, M.A. and Furuichi, Y. (1983). Nucleotide sequence of reovirus genome segment S3, encoding nonstructural protein σNS. Nuc. Acids Res. 11:6399-6408.

Rodgers, S.E., Barton, E.S., Oberhaus, S.M., Pike, B., Bigson, C.A., Tyler, K.L. and Dermody, T.S. (1997). Reovirus-induced apoptosis of MDCK cells is not linked to viral yield and is blocked by Bcl-2. J. Virol. 71:2540-2546.

Roner, M. R., Nepliouev, I., Sherry, B. and Joklik, WK. (1997). Construction and characterization of a reovirus double temperature-sensitive mutant. Proc. Natl. Acad. Sci. USA. 94:6826-6830.

Roner, M.R., Roner, L.A. and Joklik, W.K. (1993). Translation of reovirus RNA species M1 can initiate at either of the first two in-frame initiation codons. Proc. Nat. Acad. Sci. USA. 90:8947-8951.

Roner, M.R., Sutphin, L.A. and Joklik, W.K. (1990). Reovirus RNA is infectious. Virology. 179:845-852.

Rossmann, M.G., Arnold, E., Erickson, J.W., Frankenberger, E.A., Griffith, J.P., Hecht, H.-J., Johnson, J.E., Kamer, G., Luo, M., Mosser, A.G., Rueckert, R.R., Sherry, B., and Vriend, G. (1985). Structure of a human cold virus (rhinovirus 14) and functional relationship to other picornaviruses. Nature 317:145-153.

Rozinov, M.N. and Fields, B.N. (1994). Interference following mixed infection of reovirus isolates is linked to the M2 gene. J. Virol. 68:6667-6671.

Rozinov, M.N. and Fields, B.N. (1996). Interference of reovirus strains occurs between the stages of uncoating and dsRNA accumulation. J. Gen. Virol. 77:1425-1429.

Sabin, A.B., (1959). Reoviruses. Science. 130:1387-1389.

Schiff, L.A. and Fields, B.N. (1990). Reoviruses and their replication. *In* B.N. Fields and D.M. Knipe (ed). Fields Virology. (2nd ed). Raven Press, New York, pp1275-1306.

Schiff, L.A., Nibert, M.L., Co, H.S., Brown, E.G., and Fields, B.N. (1988). Distinct binding sites for zinc and double-stranded RNA in the reovirus outer capsid protein σ3. J. Mol. Biol. 8:273-283.

Schmechel, S., Chute, M., Sinner, P., Anderson, R. and Schiff, L. (1997). Preferential translation of reovirus mRNA by a single σ3-dependent mechanism. Virology. 232:62-

73.

Seliger, L.S., Giantini, M. and Shatkin, A.J. (1992). Translational effects and sequence comparisons of the three serotypes of the reovirus S4 gene. Virology, 187:202-210.

Seliger, L.S., Zheng, K., and Shatkin, A.J. (1987). Complete nucleotide sequence of reovirus L2 gene and deduced amino acid sequence of viral mRNA guanyltransferase. J. Biol. Chem. 262:16289-16293.

Sharpe, A.H., Ramig, R.F., Mustoe, T.A., and Fields, B.N. (1978). A genetic map of reovirus. I. Correlation of genome RNAs between Serotypes 1, 2, and 3. Virology 84, 63-74.

Sharpe, A.H., and Fields, B.N. (1981). Reovirus inhibition of cellular DNA synthesis; role of the S1 gene. J. Virol.38:389-392.

Sharpe, A.H., and Fields, B.N. (1982). Reovirus inhibition of cellular RNA and protein synthesis; role of the S4 gene. Virology 122:381-391.

Shatkin, A.J., Furuichi, Y. LaFiandra, A.J. and Yamakawa, M. (1983). Initiation of mRN A synthesis and 5'-terminal modification of reovirus transcripts. In: Compans, R.W. and Bishop, D.H.L. eds. Double stranded RNA viruses. Elsevier, New York,43-54.

Shatkin, A.J. and LaFiandra, A.J. (1972). Transcription by infectious subviral particles of reovirus. J. Virol 10:698-706.

Shatkin,A.J., Sipe, J.D. and Loh, P.C. (1968). Separation of 10 reovirus genome segments by polyacrylamide gel electrophoresis. J. Virol. 2:986-991.

Shaw, A.L., Rothnagel, R., Chen, D., Ramig, R.F., Chiu, W., and Prasad, B.V.V. (1993). Three dimensional visualization of the rotavirus hemagglutinin structure. Cell 74:693-701.

Shaw, A.L., Samal, S.K., Subramanian, K. and Prasad, B.V.V. (1996). The structure of aquareovirus shows how the different geometries of the two layers of the capsid are reconciled to provide symmetrical interactions and stabilization. Structure. 4:957-967.

Shepard, D.A., Ehnstrom, J.G. and Schiff, L.A. (1995). Association of reovirus outer capsid proteins $\sigma 3$ and $\mu 1$ causes a conformational change tha renders σ 3 protease sensitive. J. Virol. 69:8180-8184.

Shepard, D.A., Ehnstrom, J.G., Skinner, P.J. and Schiff, L.A. (1996). Mutations in the zinc-binding motif of the reovirus capsid protein $\sigma 3$ eliminate its ability to associate with

capsid protein μ1. J. Virol. 70: 2065-2068.

Sherry, B. and Blum, M.A. (1994). Multiple viral core proteins are determinants of reovirus-induced acute myocarditis. J. Virol. 68:8461-8465.

Sherry, B., Baty, C.J. and Blum, M.A. (1996). Reovirus-induced acute myocarditis in mice correlates with viral RNA synthesis rather than generation of infectious virus in cardiac myocytes. J. Virol. 70:6709-6715.

Sherry, B. and Fields, B.N. (1989). The reovirus M1 gene, encoding a viral core protein, is associated with the myocarditic phenotype of a reovirus variant. J. Virol63:4850-4856.

Shing, M. and Coombs, K.M. (1996). Assembly of the reovirus outer capsid requires μ1:σ3 interactions which are prevented by misfolded σ3 protein in temperature-sensitive mutant tsG453. Virus Res. 46:19-29.

Silverstein, S.C., Christman, J.K., and Acs, G. (1976). The reovirus replication cycle. Ann. Rev. Biochem.45:375-408.

Silverstein, S.C., and Dales, S. (1968). The penetration of reovirus RNA and initiation of its genetic function in L-strain fibroblasts. J. Cell Biol. 36:197-229.

Silverstein, S.C., Levin, D.H. Schonberg, M. and Acs, G. (1970). The reovirus replicative cycle: conservation of parental RNA and protein. Proc. Natl. Acad. Sci. USA. 1970. 67:275-281.

Silverstein, S.C. and Schur, P.H. (1970). Immunofluorescent localization of double-stranded RNA in reovirus-infected cells. Virology. 39:822-831.

Simpson, D.A. and Lamb, R.A. (1991). Influenza virus ts61s hemagglutinin is significantly defective in polypeptide folding and intracellular transport at the permissive temperature. Virology 185:477-483.

Sjöstrand, F.S. (1964). Critical evaluation of ultrastructural patterns withrespect to fixation. *In* Harris, R.J.C. (Ed). The interpretation of ultrastructure. Academic Press, New York. pp47-68.

Slot, J.W., and Geuze, H.J. (1985). A new method of preparing gold probes for multiple-labeling cytochemistry. Eur. J. Cell Biol. 38:87-93.

Smith, R.E., Zweerink, H.J., and Joklik, W.K. (1969). Polypeptide components of virions, top component and cores of reovirus type 3. Virology 39:791-810.

Sober, H.A. (ed.) 1970. Handbook of Biochemistry. Selected data for molecular biology. Chemical Rubber Company. Cleveland. p. j292.

Spandidos, D.A., Krystal, H. and Graham, A.F., (1976). Regulated transcription of the genome of defective virions and temperature sensitive mutants of reovirus. J. Virol. 18:7-19.

Spendlove, R.S., Lennette, E.H., and John, A.C. (1963). The role of the mitotic apparatus in the intracellular location of reovirus antigen. J. Immun. 90:554-560.

Spendlove, R.S., McClain, M.E. and Lennette, E.H. (1970). Enhancement of reovirus infectivity by extracellular removal or alteration of the virus capsid by proteolytic enzymes. J. Gen. Virol. 8:83-93.

Spendlove, R.S. and Schaffer, F.L. (1965). Enzymatic enhancement of infectivity of reovirus. J. Bacteriol. 89:597-602

Starnes, M.C., and Joklik, W.K. (1993). Reovirus protein λ3 is a poly(C)-dependent poly(G) polymerase. Virology 193:356-366.

Steele, M.I., Marshall, C.M., Lloyd, R.E. and Randolph, V.E. (1995). Reovirus M3 not detected by reverse transcriptase-mediated polymerase chain reaction analysis of preserved tissue from infants with cholestatic liver disease. Hepatology. 21:697-702.

Stempek, J.G., and Ward, R.T. (1964). An improved staining method for electron microscopy. J. Cell Biol. 22:697-701.

Steven, J., and Pietrowski, R.A., (1986). Bacterial toxins. p9-35. *In* Aspects of microbiology, 2nd ed. (American Society for Microbiology. Walton-on Thames, Surry.

Strong, J.E. and Lee, P.W.K. (1996). The v-erbB oncogene confers enhanced cellular susceptibility to reovirus infection. J. Virol. 70:612-616.

Strong, J.E., Leone, G., Duncan, R., Sharma, R., and Lee, P.W.K. (1991). Biochemical and biophysical characterization of the reovirus cell attachment protein σ1: Evidence that it is a homotrimer. Virology 184:23-32.

Strong, J.E., Tang, D. and Lee, P.W.K. (1993). Evidence that the epidermal growth factor receptor on host cells confers reovirus infection efficiency. Virology. 197:405-411.

Stroup, A.N., and Gierasch, L.M. (1990). Reduced tendency to form a β-turn in peptides from the P22 tailspike protein correlates with a temperature-sensitive folding defect. Biochemistry 29:9765-9771.

Sturtevant, J.M., Yu, M.H., Haase-Pettingelll, C., and King, J. (1989). Thermostability of temperature-sensitive folding mutants of the P22 tailspike protein. J. Bio. Chem. 264;10693-10698.

Sturzenbecker, L.J., Nibert, M., Furlong, D., and Fields, B.N. (1987). Intracellular digestion of reovirus particles requires a low pH and is an essential step in the viral infectious cycle. J. Virol. 61:2351-2361.

Tang, D., Strong, J.E. and Lee, P.W.K. (1993). Recognition of the epidermal growth factor receptor by reovirus. Virology. 197:412-414.

Thomas, G.J. Jr., Becka, R., Sargent, D., Yu, M.H., and King, J. (1990). Conformational stability of P22 tailspike proteins carrying temperature-sensitive folding mutations. Biochemistry. 29:4181-4189.

Tillotson, L. and Shatkin, A.J. (1992). Reovirus polypeptide σ3 and N-terminal myristoylation of polypeptide mu1 are required for site-specific cleavage to μ1C in transfected cells. J. Virol. 66:2180-2186.

Tosteson, M.T., Nibert, M.L., and Fields, B.N. (1993). Ion chanels induced in lipid bilayers by subvirions particles of the nonenveloped mammalian reoviruses. Proc. Natl. Acad. Sci. USA. 90:10549-10552.

Turner, D.L., Duncan, R., and Lee, P.W.K. (1992). Site-Directed mutagenesis of the C-terminal portion of reovirus protein σ1: Evidence for a conformation-dependent receptor binding domain. Virology 186:219-227.

Tyler, K.L., Mann, M.A., Fields, B.N. and Virgin, H.W. IV. (1993). Protective anti-reovirus monoclonal antibodies and their effects on viral pathogenesis. J. Virol. 67:3446-3453.

Tyler, K.L., McPhee, D.A., and Fields, B.N. (1996). Distinct pathways of viral spread in the host determinded by reovirus S1 gene segment. Science 233:770-774.

Tyler, K.L., Squire, M.K., Rodgers, S.E., Schneider, B.E., Oberhaus, S.M., Grdina, T.A., Cohen, J.J. and Dermody, T.S. (1995). Differences in the capacity of reovirus strains to induce apoptosis are determined by the viral attachment protein σ1. J. Virol. 69:6972-6979.

Vasquez C. and Kleinschmidt, A.K. (1968). Electron microscopy of RNA stands released from individual reovirus particles. J. Mol. Biol. 34:137-147.

Venable, J.H., and Coggeshall, R. (1965). A simplified lead citrate stain for use in electron microscopy. J. Cell Biol. 25:407-408.

Vreeswijk, J., Folkers,E., Wagenaar, F., and Kapsenberg, J.G. (1988). The use of colloidal gold immunoelectron microscopy to diagnose varicella-zoster virus (VZV) infections by rapid discrimination between VZV, HSV-1 and HSV-2. J. Virol. Meth. 22:255-271.

Wang, Q., Bergeron, J., Mabrouk, T. and Lemay, G. (1996). Site-directed mutagenesis of the double-stranded RNA binding domain of bacterially-expressed $\sigma 3$ reovirus protein. Virus Res. 41:141-151.

Ward, P.L., Ogle, W.O. and Roizman, B. (1996). Assemblons: nuclear structures defined by aggregation of immature capsids and some tegument proteins of herpes simplex virus 1. J. Virol. 70:4623.

Watanabe, Y. and Graham, A.F. (1967). Structural units of reovirus ribonucleic acid and their possible functional significance. J. Virol. 1:665-677.

Watanabe, Y., Millward, S., and Graham, A.F. (1968). The regulation of transcription of the reovirus genome. J. Mol. Biol. 36:107-123.

Weiner, H.L. and Fields, B.N. (1977). Neutralization of reovirus: the gene responsible for the neutralization antigen. J. Exp. Med. 146:1305-1310.

Weiner, H.L., McLaughlin, T. and Joklik, W.K. (1989). The sequences of the S2 genome segments of reovirus serotype 3 and of the dsRNA negative mutant ts447. Virology. 170:340-341.

Weiner, H.L., Powers, M.L., and Fields, B.N. (1980). Absolute linkage of virulence and central nervous system tropism of reovirus to viral hemagglutinin. J. Infect. Dis. 141:609-616.

Weiner, H.L., Ramig, R.F., Mustoe, T.A., and Fields, B.N. (1978). Identification of the gene coding for the hemagglutinin of reovirus. Virology 86:581-584.

Wessner, D.R., and Fields, B.N. (1993). Isolation and genetic characterization of ethanol resistant reovirus mutants. J. Virol. 67:2442-2447.

Wetzel, J. D., Chappell, J.D., Fogo, A.B. and Dermody, T.S. (1997a). Efficiency of viral entry determines the capacity of murine erythroleukemia cells to support persistent infections by mammalian reoviruses. J. Virol. 71:299-306.

Wetzel, J.D., Wilson, G.J., Baer, G.S., Dunnigan, L.R., Wright, J.P., Tang, D.S. and Dermody, T.S. (1997b). Reovirus variants selected during persistent infections of L cells contain mutations in the viral S1 and S4 genes and are altered in viral disassembly. J. Virol. 71:1362-1369.

White, C.K., and Zweerink, H.J. (1976). Studies on the structure of reovirus cores: selective removal of polypeptide λ2. Virology 70:171-180.

White, J.M. (1990). Viral and cellular membrane fusion proteins. Ann. Rev. Physiol. 52:675-697.

Wiener, J.R., and Joklik, W.K. (1987). Comparison of the reovirus serotype 1, 2, and 2 S3 genome segments encoding the nonstructural protein σNS. Virology 161:332-339.

Wiener, J.R., and Joklik, W.K. (1988). Evolution of reovirus genes: a comparison of serotype 1, 2, and 3 M2 genome segments, which encode the major structural capsid protein μ1. Virology. 163:603-613.

Wiener, J.R., and Joklik, W.K. (1989). The sequences of the reovirus serotype 1, 2, and 3 L1 genome segments and analysis of the mode of divergence of the reovirus serotypes. Virology. 169:194-203.

Wiener, J.R., Bartlett, J.A. and Joklik, W.K. (1989). The sequence of reovirus serotype 3 genome segments M1 and M3 encoding the minor protein μ2 and the major nonstructural protein μNS, respectively Virology. 169:293-304.

Wilson, G.A. Morrison, L.A. and Fields, B.N. (1994). Association of the reovirus S1 gene with serotype 3-induced biliary atresia in mice. J. Virol. 68:6458-6465.

Wilson, G.J., Wetzel, J.D., Puryear, W., Bassel-Duby, R. and Dermody, T.S. (1996). Persistent reovirus infections of L cells select mutations in viral attachment protein σ1 that alter oligomer stability. J. Virol. 70:6598-6606.

Wolf, J.L., Rubin, D.H., Finberg, R., Kauffman, R.S., Sharpe, A.H., Trier, J.S., and Fields, B.N. (1981). Intestinal M cells: a pathway for entry of reovirus into the host. Science. 212-471-472.

Wood, W.B. an Crowther, R.A. 1983. Long tail fibres: Genes, proteins, assembly and structure. p259-269. *In* C. Mathews, E.M. Kutter, G. Mosig, and P.B. Berget (eds.), Bacteriophage T4. American Society for Microbiology, Washington, D.C.

Xu, P., Miller, S.E., and Joklik, W.K. (1993). Generation of reovirus core-like particles in cells infected with hybrid Vaccinia viruses that express genome segments L1, L2, L3, and S2. Virology, 197:726-731.

Yeager, M., Berriman, J.A., Baker, T.S., and Bellamy, A.R. (1994). Three-dimensional structure of the rotavirus haemagglutinin VP4 by cryo-electron microscopy and the difference map analysis. EMBO Journal 13:1011-1018.

Yeager, M., Weiner, S.G. and Coombs, K.M. (1996). Transcriptionally active reovirus core particles visualized by electron cryo-microscopy and image reconstruction. Biophys. J. 70:A116.

Yeager, M., Weiner, S.G. and Coombs, K.M. RNA transcription in reovirus visualized by electron cryo-microscopy. In preparation.

Yeung, M.C., Lim, D., Duncan, R., Shahrabadi, M.S. Cashdollar, L.W. and Lee, P.W.K. (1989). The cell attachment proteins of type 1 and type 3 reovirus are differentially susceptible to trypsin and chymotrypsin. Virology. 170:62-70.

Yin, P., Cheang, M. and Coombs, K.M. (1996). The M1 gene is associated with differences in the temperature optimum of the transcriptase activity in reovirus core particles. J. Virol. 70:1223-1227.

Yin, P., Hazelton, P.R. and Coombs, K.M. Generation of reovirus spike-deficient core particles with functional transcriptase activity. In revision.

Yuan, L.C., and Gulyas, B.J. (1981). An improved method for processing single cells for electron microscopy utilizing agarose. Anat. Rec. 201:273-281.

Yu, M.H., and King, J. (1988). Surface amino acids as sites of temperature-sensitive folding mutations in the P22 tailspike protein. J. Biol. Chem. 263:1424-1431.

Yue, Z. and Shatkin, A.J. (1996). Regulated, stable expression and nuclear presence of reovirus double-stranded RNA-binding protein σ3 in HeLa cells. J. Virol. 70:3497-3501.

Zarbl, H., and Millward, S. (1983). The reovirus multiplication cycle. In: Joklik, W.K, ed. The Reoviridae. Plenum Press, New York, 107-196

Zou, S., and Brown, E.G. (1992). Identification of the sequence elements containing signals for replication and encapsidation of the reovirus M1 genome segment. Virology. 186:377-388.

Zou, S., and Brown, E.G. (1996a). Translation of the reovirus M1 gene initiates from the first AUG codon in both infected and transfected cells. Virus Res. 40:75-89.

Zou, S. and Brown, E.G. (1996b). Stable expression of the reovirus μ2 protein in mouse L cells complements the growth of a reovirus ts mutant with a defect in its M1 gene. Virology. 217:42-48.

Zweerink, H.J, Ito, Y. and Matsuhisa, T. (1972). Synthesis of reovirus double-stranded RNA within virion-like particles. Virology. 50:349-358.

Zweerink, H.J., Morgan, E.M. and Skyler, J.S. (1976). Reovirus morphogenesis: characterization of subviral particles in infected cells. Virology 73:442-453.

APPENDIX A

Solutions

Agar/medium 199	medium 199 in 1% agar and supplemented with 1.25%FCS, 1.25% VSP, 2mM Glutamine, 100U penicillin/ml, 100µg streptomycin sulfate/ml and 1µg amphotericin B/ml
Dialysis buffer	10mM Tris Base, pH 7.4, 150mM Sodium Chloride, 15mM Magnesium Chloride
Electrophoresis sample buffer	2.5mM Tris, pH6.8, 10% glycerol, 0.5% Sodium dodecyl sulfate, 0.4% dithiothreitol, 0.002% bromophenol blue
Elution Buffer	0.5M Phosphate Buffer, pH 8.0 with 100mM Sodium Acetate, pH 4.0, 150mM Sodium Chloride
HO Buffer	10mM Tris Base, pH 7.4, 250mM Sodium Chloride, 9.25µM 2-mercaptoethanol
Lysis buffer	50mM Tris Base pH8.0, 100mM Sodium Chloride, 0.5% NP-40
Neutral red staining overlayment	medium 199 or PBS in 1% Agar containing 0.004% filtered neutral red stain
Phosphate Buffered Saline	10mM Phosphate, pH 8.0, 750mM Sodium Chloride
PTA	2.5mM Phosphotungstic Acid, pH 7.0
Running Buffer	50mM Tris, pH 8.0, 150mM Sodium Chloride
ScMg buffer	100mM sodium cacodylate, 10mM Magnesium Chloride pH 72
Stabilizing Buffer 1	200mM Tris base, pH 8.0, 150mM Sodium Chloride, 0.05% Carbowax M20, 10% Glycerol
Stabilization Buffer 2	Stabilizing Buffer 1 with 0.2% (wt/vol) Low Bloom Gelatin

Supplemented S-MEM	MEM supplemented with 2.5% FCS, 2.5% VSP, and 2mM Glutamine

APPENDIX B

Isolation of T3D and *ts* mutant clones, and determination of culture conditions

1. Introduction.

A number of problems had to be addressed before proceeding with this project: stock T3D clones had to be isolated which demonstrated genome migration patterns distinct from serotype T1L and with EOP values similar to those previously reported; temperature sensitive clones had to be isolated from each mutant stock; and conditions had to be established which optimized expression of temperature sensitivity in order to confirm the presence and evaluate the effects of a *ts* lesion.

The clones from the Fields Panel had been stored in freezers for up to 20 years. Further, some clones had been subjected to additional plaque purification and amplification before storage. The possibility that labels may have become detached and re-attached while in storage, lids of vials exchanged accidentally, and mutation events during earlier amplification made it essential that fresh clones be isolated as the first step in this study. The next step would then be confirmation of each *ts* phenotype. Some clones were available from the original stock lysates of the Fields panel. Additional lysates of putative mutant clones were available from clones subcultured from members of the Fields' panel by K.M. Coombs during late 1989.

2. Isolation of T3D and *ts* mutant clones.

a. **Isolation of T3D.**

Stock T3D was plaque purified as described in Chapter 2, Materials and Methods. Briefly, L929 monolayers were infected with laboratory stock T3D and incubated at 37°C. 11 plaques were isolated and amplified to P2 culture. Culture lysates were titred at 32°C and 39°C, EOP values determined for each clone, and cytoplasmic extracts were prepared and electrophoresed from P3 cultures for each clone, all as described (Chapter 2.2.d and 2.3.b). The genome segments were evaluated to ensure that the migration pattern for each clone was consistent with the reported pattern for T3D and several clones were selected to be used as stock parental clones for future work on the basis of titre at 32°C (PFU/ml) and EOP at a restrictive temperature of 39°C.

b. **Isolation of temperature sensitive mutant clones.**

All isolation and amplification procedures were conducted at 32°C. Stock cultures from the Fields panel were plaque purified using the clonal isolation procedures as described (Chapter 2.2.d). To select against choosing revertant clones, or clones which may have contained further mutations, between five and seven clones were isolated from each original Fields stock clone and 3 clones were isolated from each clone which had been previously selected and amplified through third or fourth passages (P3 or P4) by K. M. Coombs.

The clones were amplified through a first passage culture (P1), titres and plaque sizes determined at permissive and restrictive temperatures of 32°C and 39°C, respectively,

and EOP values determined for each clone. After retesting, the averaged EOP values were determined and candidate clones representing each recombination group of mutants were identified as stock mutant clones on the basis of their temperature sensitivity as expressed by the EOP assay. Clones representing mutants from recombination groups A, E, H, I, and J were selected for further amplification and study (Table B.1).

c. **Amplification of *ts* clones to second passage cultures.**

Candidate *ts* clones were amplified through P2 in T75 culture flasks with 0.5ml of the P1 cultures. For most clones the resultant titres were low with the first two P2 cultures prepared. Therefore, the culture conditions were tested to determine whether it would be possible to increase the amplification of virus by modifying inoculum volume and/or by feeding the culture with fresh supplemented S-MEM during the term of infection. The titre of infectious virus in the lysates of fed infections was increased between 5 and 100 fold over the unfed samples in all thirteen clones tested. Analysis of variance indicates this increase is highly significant ($p < 0.005$) (Hassard, 1991). A subsequent round of amplification to the P2 level was then done on fresh L929 cells in T75 culture flasks. These clones were evaluated for expression of temperature sensitivity and plaque size by plaque assay at a restrictive temperature of 39°C.

d. **Amplification of *ts* clones to third passage cultures.**

Because there was continued low level amplification of several clones, especially those representing *tsA201*, and *tsI138*, some clones were amplified through a third passage as

Table B.1. Isolation of candidate *ts* mutant clones.

Reassortment Group	Clone	Source[a]	Clone	Titre[b]	EOP[c]
A	*tsA201*	KC 10/89	c†	3.1×10^6	0.015
	tsA279	BF	c†	1.94×10^6	0.16
		KC 10/89	c	8.2×10^6	0.41
	tsA329.r119	BF	a†	1.48×10^6	0.053
		KC 10/89	a	1.1×10^7	0.36
	tsA340	KC 10/89	a†	2.7×10^6	0.19
B	*tsB271*	KC 10/89	c	9.5×10^6	0.045
	tsB352	KC 10/89	a	1.8×10^7	0.0001
	tsB352	KC 10/89	b	9.1×10^6	5.6×10^{-4}
	tsB405.F54	KC 10/89	a	8.8×10^6	1.7×10^{-4}
C	*tsC447*	KC 10/89	a	3.7×10^5	$<3.7 \times 10^{-4}$
D	*tsD357.F25*	KC 10/89	c	1.9×10^6	0.25
E	*tsE320*	KC 10/89	a†	5.9×10^6	0.63
			b†	4.6×10^6	0.63
			c†	1.5×10^7	0.22
F	*tsF556A*	BF	d	1.1×10^6	0.28
	tsF556A	KC	a	2.2×10^6	0.34
G	*tsG453c*	KC 10/89	b	2.1×10^7	0.01
H	*tsH26/8-1*	KC 10/89	a	2.5×10^6	0.011
	tsH26/8-2	KC 10/89	a	4.7×10^6	0.0062
	tsH26/8-3	KC 10/89	b†	2.0×10^6	0.0026
	tsH26/8-3 P4	KC 10/89	a†	2.5×10^7	9.2×10^{-5}
	tsH26/8-3 P4	KC 10/89	c†	5.4×10^5	0.087
I	*tsI138 (1/80)*	BF	a	1.1×10^5	0.22
		KC 10/89	b†	1.6×10^5	3.13×10^{-4}
		KC 10/89	c	3.0×10^6	0.037
	tsI138 (12/82)	BF	d	1.3×10^6	0.101
		BF	f†	4.0×10^5	<0.004
		KC 10/89	a	2.0×10^5	<0.088
	tsI138 (12/82) P4	KC 10/89	b†	3.8×10^5	0.066
J	*tsJ128-1*	KC 10/89	b†	1.9×10^6	0.046
	tsJ128-2	KC 10/89	b	1.4×10^7	0.149
	tsJ128-3	BF	c	8.2×10^5	0.16
		KC 10/89	b	1.4×10^7	0.099

a. Source: BF = Original Fields' isolate; KC = Re-isolated by K. Coombs.
b. Titre: Plaque forming units per ml at 32°C.
c. 39°C EOP: Efficiency of Plating at 39°C = apparent titre at 39°C ÷ apparent titre at 32°C.
†. Clone selected for future work in this project.

previously described. A number of variables were applied in attempts to obtain high titre cultures with *tsI138*: re-amplifying with feeding the infections at 48 hours post infection and then every 3-4 days subsequent until harvest at either days 21 or 24; cultured in supplemented S-MEM containing 5% FCS without VSP; and lysates were tested after normal freeze thawing versus brief, low energy sonication with a mini probe sonicator (Branson, Danbury, CONN). All feeding supernatants were retained and evaluated for the presence of infectious virus.

The yields of the P3 amplifications normally exceeded 1 x 10^8 PFU/ml at 32°C, with the exception of the *tsI138* clones, which customarily provided infectious titres below 1 x 10^7 PFU/ml at 32°C. No appreciable levels of infectious virus were observed in the feeding supernatants from the *tsI138* cultures.

e. <u>Concentration of lysates to elevate infectious titre of amplifications.</u>

In order to further increase infectious titres, selected P2 and P3 lysates were concentrated by centrifuge filtration with Centriprep 10® filter concentration devices (molecular weight cutoff of 100,000 Daltons)(Millipore, Bedford, MA) until the samples were concentrated to a volume estimated sufficient to provide for infectious titres of 1-4 x 10^8 PFU/ml. Alternatively, samples were concentrated using Minicon® B-15 filter concentrators (Millipore). All concentrates provided apparent infectious titres in excess of 4 x 10^8 PFU/ml except where initial lysate volume was insufficient to attain that level of concentration in volumes which were 0.5 ml or more.

3. Analysis of S-MEM verses Medium 199 for conduct of plaque assays.

In order to determine whether the medium used in the plaque assays amplified any differences in titres and/or the resultant EOP values identified for the *ts* and ts^+ clones, parallel titrations of T1L, T3D, and a panel of the mutants were performed using either S-MEM or Medium 199. Fifty-one of 80 clones tested using Medium 199 showed increases in EOP between 1.5 and 22 fold over the values found with S-MEM, and 19 of the remaining 29 clones showed reduction in EOP by less than 2 fold. Average plaque size at 39°C in agar/Medium 199 was larger in 50 of 66 clones evaluated, and 11 of the remaining clones had plaque sizes which were identical in both media. These results showed that 1% Agar in Medium 199 was significantly different than 1% Agar in S-MEM by a one tailed, paired t test (Hassard, 1991) for both evaluation of EOP ($t = 3.57$; $p < 0.0005$) and size of plaque ($t = 4.539$; $p < 0.0005$).

4. Analysis of duration of culture to obtain maximum yield of virus.

Due to the apparent low yields of virus in cultures and low level cytopathic effect seen with several *ts* mutant clones, growth curves were established for selected clones. Briefly, monolayers were inoculated at an MOI of 0.2 PFU/cell. After attachment the cells were overlayed with supplemented S-MEM (with 5% FCS and no VSP) and incubated for up to 21 days post infection at 32°C. Cell lysates were titrated at 32°C by standard plaque assay as described (Chapter 2.2.f). The results indicate that maximum yield is obtained between 3 and 5 days post infection for most *ts* mutants and parental T3D. With the mutant *tsI138*, the titre of recoverable infectious virus increased

throughout the duration of the assay. The mutant *tsI138* routinely yielded between 1 and 2 x $\log_{10}$ fewer PFU/ml recoverable infectious virus than obtained with the other clones tested.

5. Determination of temperature of expression for the temperature sensitive phenotype for selected clones.

A number of clones in the Fields panel are described as leaky, exhibiting marginal temperature sensitivity at a restrictive temperature of 39°C (Fields and Joklik, 1969). To determine the temperature at which the lethal phenotype is initially, and maximally expressed, clones from each *ts* mutant were evaluated for expression of temperature sensitivity at temperatures ranging from 37°C through 40.5°C, in 0.5°C increments. Temperature control was monitored as described (Chapter 2.2.f). The relative EOP values for each clone at each temperature were determined (Table B.2).

6. Discussion.

Identification of the pedigree for each gene segment in candidate reassortant clones is necessary for successful phenotype mapping. To ensure clear differentiation between T1L and T3D stock clones a panel of T3D clones were plaque purified and their levels of inherent temperature sensitivity and electrophoretic patterns of genome segments were established. All isolates showed identical migration patterns, which clearly differed from those of the laboratory stock T1L clone. Clone $T3D_3$ was chosen as the stock parental clone on the basis of both 32°C titre (1.29×10^9 PFU/ml) and EOP_{39} (0.349). Clones

Table B.2. Efficiency of Plating of *ts* mutants at different temperatures[a,b,c].

Mutant Clone	Temperature (°C)							
	32	34	37	38	38.5	39	39.5	40
tsA201	1.00	1.14	0.364	0.37	0.230	0.073	4.6×10^{-3}	2.5×10^{-3}
tsA279	1.00	1.19	0.418	0.520	0.206	0.056	1.07×10^{-3}	1.90×10^{-4}
tsA329.r119	1.00	2.54	0.461	0.28	0.35	0.096	0.052	4.4×10^{-4}
tsA340	1.00	1.49	0.792	0.43	4.2×10^{-3}	1.9×10^{-3}	4.0×10^{-4}	6.4×10^{-6}
tsB271	1.00	4.32	0.655	0.30	2.8×10^{-3}	3.0×10^{-3}	5.1×10^{-4}	1.4×10^{-3}
tsB352	1.00	1.65	0.021	1.9×10^{-3}	1.9×10^{-3}	1.1×10^{-3}	5.1×10^{-6}	5.1×10^{-6}
tsB405	1.00	1.85	0.002	3.5×10^{-4}	3.7×10^{-3}	1.6×10^{-4}	1.6×10^{-4}	2.0×10^{-3}
tsC447	1.00	1.54	7.8×10^{-4}	7.8×10^{-4}	7.8×10^{-4}	7.8×10^{-4}	7.8×10^{-4}	7.8×10^{-4}
tsD357	1.00	3.47	0.27	0.034	1.85×10^{-4}	2.5×10^{-4}	2.5×10^{-4}	7.1×10^{-6}
tsE320	1.00	2.25	0.45	0.20	0.12	0.076	0.05	1.0×10^{-3}
tsF556	1.00	2.31	0.68	1.92	0.32	2.3×10^{-3}	2.0×10^{-3}	6.0×10^{-4}
tsG453	1.00	3.70	0.14	1.6×10^{-3}	1.6×10^{-3}	1.6×10^{-3}	1.6×10^{-3}	1.6×10^{-3}
tsH26/8-3	1.00	4.70	0.071	1.9×10^{-4}	9.7×10^{-3}	9.0×10^{-3}	1.7×10^{-4}	9.7×10^{-3}
tsI138	1.00	2.16	0.0011	4.7×10^{-4}	4.7×10^{-4}	4.7×10^{-4}	4.7×10^{-4}	3.4×10^{-4}
tsJ128	1.00	ND	0.028	5.1×10^{-3}	1.8×10^{-3}	2.9×10^{-3}	1.6×10^{-6}	2.8×10^{-7}

a. Efficiency of Plating: (Titre @ Test Temperature) ÷ (Titre @ 32°C).

b. EOP values represent the average of at least two experiments.

c. Temperatures ≥ 40.5°C caused cell death in all control and infected cultures over the prolonged time of incubation necessary for plaque assays.

$T3D_4$ ($7.4x10^8$ PFU/ml, EOP_{39} = 0.473) and $T3D_1$ ($3.8x10^8$ PFU/ml, EOP_{39} = 0.242) were also identified for use.

A number of the mutant clones were marginally temperature sensitivity under the assay conditions in use. A subgroup of the clones which were the focus of this study had been selected on the basis of the marginal EOP values (Table B.1). It was necessary to establish conditions which clearly identified the *ts* phenotype. Initially, an assay referred to as the Efficiency of Yield (EOY) assay was considered (Coombs, 1998b). While EOY assays have potential, they are very labour, materiél, and time consuming. Therefore, it was desirable to identify alternative tests for the phenotype.

The initial work was performed using S-MEM as the plaque assay medium (Fields and Joklik, 1969). Subsequently the enriched Medium 199 was introduced. The inaccuracies of plaque assays are such that differences less than 1 order of magnitude are usually considered insignificant. Since there were differences in the reported EOPs and the results obtained when mutant clones were isolated for this study, the possible effect of the different media was tested using a paired t test (Hassard, 1991). Medium 199 performed better in demonstrating EOP through plaque assays on both the basis of opening up the expression of temperature sensitivity ($p<0.001$) and plaque size ($p<0.001$). Therefore, differences between the reported EOPs (Fields and Joklik, 1969) and the levels observed in this study may be influenced by the change in media used during plaque assay.

Temperature is a factor which can affect the expression of the *ts* phenotype. Minor variations could have significant impacts upon the phenotype expression if the temperature at which the phenotype is first expressed is similar to that used for testing. Higher restrictive temperatures have been reported for assays of other systems (Barton *et al*, 1996, Simpson and Lamb, 1991). In addition, cold sensitivity (*cs*) has been reported for mutants of reovirus (Ahmed *et al*, 1982; Ikegami and Gamotos, 1968). The temperatures at which temperature sensitivity is first and optimally expressed were examined. Preliminary evaluation indicated none of the mutants were *cs*. Most strong *ts* mutants have a threshold for expression of the *ts* phenotype which is equal to or less than 38°C. Elevated restrictive temperatures improved the expression of the *ts* phenotype by several orders of magnitude for all mutants which were mildly *ts* at 39°C, (eg. clones *tsA201* and *tsE320* (Table B.2)). Some mildly *ts* mutants showed a pattern of increasing temperature sensitivity as the restrictive temperature was raised (eg. clone *tsA279*, (Table B.2)) suggesting that testing at multiple restrictive temperatures could provide additional information.

Due to consistent low titres obtained with a number of the mutant clones at various times during the study, the amplification conditions were evaluated. Size of inoculum, feeding the cultures, temperature, and duration of culture are the manipulatable parameters which could affect the amplification process. The most significant change occurred as a result of feeding the restrictive cultures, with the maximum increase in titre obtained by feeding the infection 48 hours post attachment ($p < 0.005$).

The consistently low amplifications obtained and marginal expression of cytopathic effect with the rescued pseudorevertant mutant *tsI138* justified examining growth curves for a panel of mutants. All mutants other than *tsI138* obtained maximum yield by 7 days after infection followed by declines of 1 to 3 orders in magnitude at day 21. All three *tsI138* clones demonstrated a gradual but constant increase in recoverable infectious virus from day 6 to day 21, when the maximum values were demonstrated. The yield in PFU/ml of the *tsI138* clones was consistently 1 or more orders in magnitude below the values obtained with the other clones at each level of amplification, with yields rarely exceeding 5.0×10^6. The decline in yield over time observed with the remaining clones may be explained as lysozyme degradation of virus particles during prolonged incubation.

IMAGE EVALUATION
TEST TARGET (QA-3)

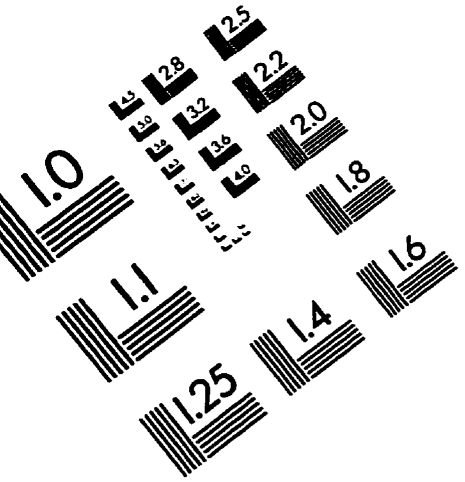

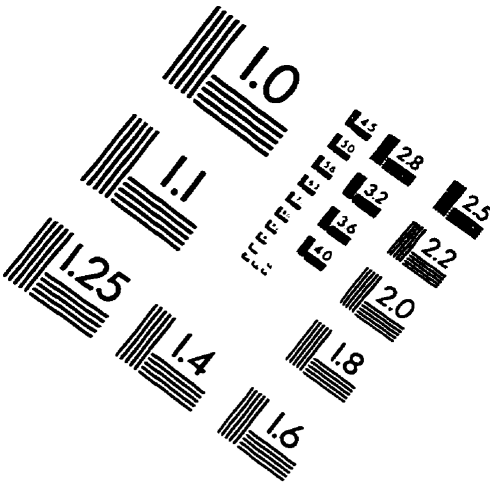

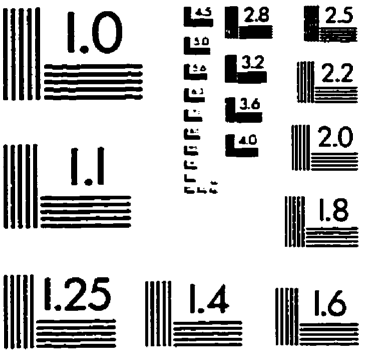

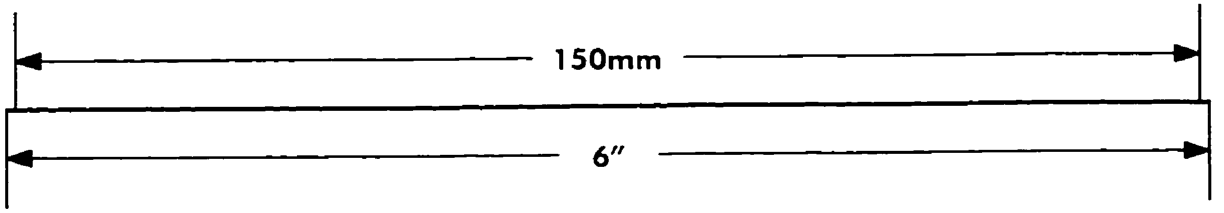

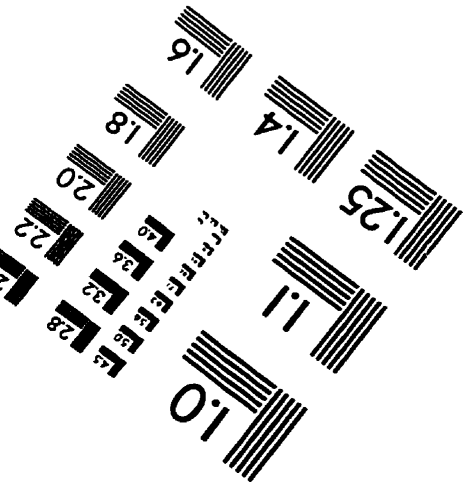

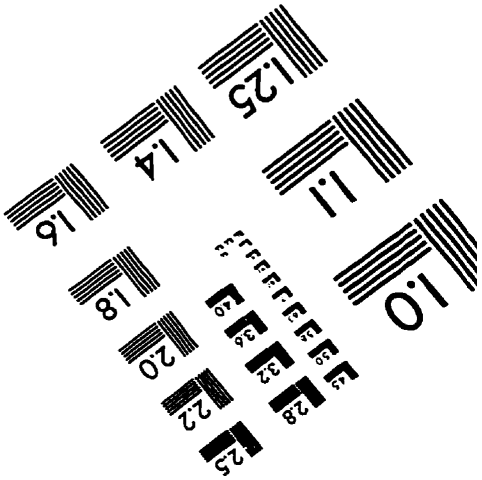

APPLIED IMAGE, Inc
1653 East Main Street
Rochester, NY 14609 USA
Phone: 716/482-0300
Fax: 716/288-5989